INVESTIGATION ON CYCLIC VARIATIONS OF A DIESEL ENGINE OPERATING WITH ALCOHOLS AND BIODIESEL BLENDS

MOHD HAFIZIL BIN MAT YASIN

Doctor of Philosophy

UNIVERSITI MALAYSIA PAHANG

UNIVERSITI MALAYSIA PAHANG

DECLARATION OF THESIS AND COPYRIGHT

Author's Full Name : MOHD HAFIZIL BIN MAT YASIN

Date of Birth : 4 JUNE 1980

Title : INVESTIGATION ON CYCLIC VARIATIONS OF A DIESEL ENGINE OPERATING WITH ALCOHOLS AND BIODIESEL BLENDS

Academic Session : SEMESTER I 2018/2019

I declare that this thesis is classified as:

☐ CONFIDENTIAL (Contains confidential information under the Official Secret Act 1997)*

☐ RESTRICTED (Contains restricted information as specified by the organization where research was done)*

☑ OPEN ACCESS I agree that my thesis to be published as online open access (Full Text)

I acknowledge that Universiti Malaysia Pahang reserves the following rights:

1. The Thesis is the Property of Universiti Malaysia Pahang
2. The Library of Universiti Malaysia Pahang has the right to make copies of the thesis for the purpose of research only.
3. The Library has the right to make copies of the thesis for academic exchange.

Certified by:

_____ _____
(Student's Signature) (Supervisor's Signature)

800604-11-5403 PROF. DR. RIZALMAN BIN MAMAT
Date: Date:

NOTE : * If the thesis is CONFIDENTIAL or RESTRICTED, please attach a thesis declaration letter.

SUPERVISOR'S DECLARATIONS

We hereby declare that We have checked this thesis and in our opinion, this thesis is adequate in terms of scope and quality for the award of the degree of Doctor of Philosophy.

_____
(Supervisor's Signature)
Full Name   : PROF. DR. RIZALMAN BIN MAMAT
Position   : PROFESSOR
Date   :

_____
(Co-supervisor's Signature)
Full Name   : DR. AHMAD FITRI BIN YUSOP
Position   : SENIOR LECTURER
Date   :

INVESTIGATION ON CYCLIC VARIATIONS OF A DIESEL
ENGINE OPERATING WITH ALCOHOLS AND BIODIESEL BLENDS

MOHD HAFIZIL BIN MAT YASIN

Thesis submitted in fulfillment of the requirements
for the award of the degree of
Doctor of Philosophy

Faculty of Mechanical Engineering
UNIVERSITI MALAYSIA Pahang

DECEMBER 2018

ACKNOWLEDGEMENTS

ABSTRAK

Butanol dan etanol merupakan bahan api bio generasi kedua yang mendapat perhatian utama sejak beberapa tahun kebelakangan ini. Butanol dan etanol merupakan bahan api bio generasi kedua yang mendapat perhatian utama sejak beberapa tahun kebelakangan ini. Alkohol dihasilkan daripada sumber biojisim dan digunakan untuk meningkatkan ciri-ciri dan prestasi bahan api terdahulu. Namun, terdapat kekaburan dalam sifat pembakaran bagi campuran butanol dan etanol dalam pengoperasian kelajuan enjin dan bebanan berbeza menggunakan analisis keragaman kitar pembakaran yang perlu dikaji secara lebih mendalam. Bahan api diesel galian (D), biodiesel minyak kelapa sawit (B), butanol (10%)-diesel (90%) (berdasarkan isipadu) (DBu10), butanol (10%)-biodiesel kelapa sawit (90%) (BBu10), etanol (10%)-diesel (90%) (DE10), and etanol (10%) - biodiesel kelapa sawit (90%) (BE10) telah digunakan dalam kajian ini. Antara objektif kajian ini adalah mengenalpasti sifat fizikal-kimia, untuk menyiasat kesan beban dan kelajuan enjin berbeza serta menganalisis kestabilan pembakaran silinder tekanan menggunakan *recurrence plot* (RP) dan *recurrence quantification analysis* (RQA) pada bahan api tersebut. Kajian eksperimental menggunakan enjin diesel suntikan terus silinder tunggaluntuk mengkaji sifat keragaman kitar pembakaran bagi profil tekanan silinder dan tekanan puncak silinder, P_{max}. Perekodan kitar pembakaran sebanyak 200 kitar dilakukan untuk menganalisis secara statistik keragaman kitar pembakaran bagi setiap bahan api pada setiap keadaan pengoperasian. bagi mendapatkan pekali variasi (COV) untuk P_{max}. Sebagai tambahan, pendekatan baru menggunakan *recurrence plot* (RP) dan *recurrence quantification analysis* (RQA) bagi menilai ketidakragaman pembakaran bagi setiap bahan api pada kelajuan dan bebanan berbeza secara kualitatif dan kuantitatif. Keputusan menunjukkan campuran butanol dan ethanol mempunyai purata profil tekanan silinder yang hampir sama dengan D dan B. Terdapat peningkatan tekanan puncak silinder yang berlaku bagi campuran butanol dan etanol dengan peningkatan kelajuan enjin, namun penurunan dikesan pada 2300 rpm. Kebanyakan puncak HRR direkodkan berlaku pada 7-10 deg.CA bagi kesemua bahan api tersebut dengan perbezaan 8-10%. Berkenaan dengan keragaman kitar pembakaran, khususnya silinder tekanan, kenaikan keragaman kitar ke kitar bagi silinder tekanan berlaku pada bebanan dan kelajuan tinggi bagi kesemua bahan api, terutamanya DE10 yang mempunyai nilai COV_{Pmax} yang tinggi bagi 200 kitar berterusan. Dengan RP dan RQA, kajian terhadap ciri-ciri pembakaran dinamik dalam enjin diesel melalui keragaman kitar P_{max} dapat dilakukan. Bagi kesemua bahan api, keseluruhan proses pembakaran dalam pengoperasian berbeza menunjukkan banyak sifat kacau-bilau dan kelakuan tertumpu dikaitkan corak pada RP dan RQA. DE10 menghasilkan paling banyak ketidakragaman pembakaran bersifat kacau-bilau dan keragaman kitar lebih tinggi bagi siri masa pada pengoperasian berbeza. Kesimpulannya, keragaman silinder tekanan pada siri masa adalah disebabkan oleh komposisi bahan api dan jenis bahan api yang digunakan dalam pengoperasian enjin. Secara keseluruhan, dapatan ini menyumbangkan kefahaman asas berkenaan campuran alkohol beroperasi dengan enjin dan menyediakan maklumat yang lengkap untuk mencapai pengoperasian pembakaranyang efisien dengan teknologi suntikan bahan api terkini.

ABSTRACT

Butanol and ethanol are second-generation biofuels that have received great attention in recent years. These alcohols obtained from the biomass feedstock sources to improve the fuel properties and performance of the recent fuels. However, there are certain grey aspects in the combustion characteristics of butanol and ethanol blends in various operating speeds and loads using combustion cyclic variation analysis to be further investigated. This previous work investigated the use of commercially available mineral diesel (D), palm biodiesel (B), butanol (10%)-diesel (90%) (DBu10), butanol (10%)-palm biodiesel (90%) (BBu10), ethanol (10%)-diesel (90%) (DE10), and ethanol (10%)-palm biodiesel (90%) (BE10) fuels. The objectives of this study are to characterise the *physico-chemical* properties, to investigate the effects of loads and speeds, and to analyse the combustion stabilities in cylinder pressure using recurrence plot (RP) and recurrence quantification analysis (RQA) on tested fuels. Experimental works were conducted on a single cylinder, direct injection diesel engine to investigate the cyclic combustion variations of cylinder pressure profiles and peak cylinder pressure, P_{max}. The recorded 200 consecutive cycles were recorded to analyse the cyclic combustion variations for each fuel at the different operating condition. Those parameters were statistically analysed to obtain the coefficient of variation (COV) for P_{max}. Also, the novel approaches, recurrence plot (RP) and recurrence quantification analysis (RQA) are introduced to evaluate qualitatively and quantitatively the combustion instabilities for each fuel at different speeds and load rates. The results showed that butanol and ethanol blends have comparable averaged cylinder pressure profiles with D and B. Also, higher peak cylinder pressures were observed for butanol and ethanol blends with the increase in engine loads but gradually decreased at 2300 rpm. For all six fuels, most of the peak HRR occurred at 7-10 deg.CA with differences between 8-10%. Regarding cyclic combustion variability, particularly cylinder pressure, higher cylinder pressure cyclic variability occurred at high load and speed for all test fuels, especially DE10 with higher COV_{Pmax} values obtained for 200 consecutive cycles. By using RP and RQA, the dynamical characteristics of combustion in diesel engine through P_{max} cyclic variations were investigated. For all fuels, most combustion processes in different operating conditions exhibit many chaotic features and deterministic nature that can be easily related to patterns in RPs and RQAs. Thus, in this case, DE10 produced the most chaotic combustion irregularities and higher cyclic variations for the time series in those conditions. In conclusion, cylinder pressure variations in the time series were found to be affected by the fuel composition of butanol and ethanol in the blends and types of fuel in engine operation. Overall, these findings have contributed to the fundamental understanding of the alcohol blends operating with engines and provide further information to achieve the most efficient fuel combustion of engine with advanced fuel injection technologies.

TABLE OF CONTENT

vi

LIST OF TABLES

LIST OF FIGURES

LIST OF SYMBOLS

A	Area (m^2)
f_a	Atmospheric factor
f_c	Factor
f_m	Engine factor
n	Number of engine cycle
N	Engine speed (rpm)
P	Engine brake power (kW)
P_o	Observed power (kW)
P_c	Corrected power (kW)
Q_f	Heating value of the test fuel (MJ/kg)
Q_{gross}	Gross heat release rate (J/deg.CA)
HRR	Net heat release rate (J/deg.CA)
R	Characteristic gas constant
t	Time (s)
T	Engine brake torque (Nm)

LIST OF ABBREVIATIONS

ASTM	American Society for Testing and Materials
BTE	Brake thermal efficiency
BSFC	Brake specific fuel consumption
CO	Carbon monoxide
COV	Coefficient of variation
COV_{IMEP}	Coefficient of variation of IMEP
COV_{Pmax}	Coefficient of variation of P_{max}
CV	Cyclic variability
DET	Determinism
deg.CA	Crank angle degree
DTBP	*Di-tert-butyl peroxide*
EGR	Exhaust gas recirculation
EGT	Exhaust gas temperature
ENTR	Entropy
EPA	Environmental Protection Agency
EU	European Union
FAME	Fatty acid methyl ester
FIP	Fuel injection pressure
HC	Unburned hydrocarbons
HCN	Hydrogen cyanide
HVO	Hydrotreated vegetable oil
IMEP	Indicated mean effective pressure
J/deg.CA	Joule/crank angle degree

LAM	Laminarity
MFB	Mass fraction burned
MTBE	Methyl tertyl butyl ether
NO	Nitric oxide
NO_2	Nitrogen dioxide
NO_X	Nitrogen oxides
O_2	Oxygen
P_{max}	Peak cylinder pressure
PAHs	Polycyclic aromatic hydrocarbons
PM	Particulate matter
PRR	Pressure rise rate
RP	Recurrence plot
RQA	Recurrence quantification analysis
RR	Recurrence rate
RSD	Relative standard deviation
SCR	Selective catalytic reduction
TREND	Recurrence trend
TT	Trapping time
ULSD	Ultra-low sulphur diesel
VSD10	Volvo Standard Diesel. (*VSD10*<10ppm)

CHAPTER 1

INTRODUCTION

1.1   Introduction

Internal combustion engines produce mechanical work by converting chemical energy which is stored in the fuel. These internal combustion engines use the reciprocating concept in which the conversion of the energy occurs continuously, in the closed chamber, on a constant supply of fuel-air charge. The mechanical work in the engines is produced from the constant piston movements through the action of gas pressure which occurs during the intake, compression, power and exhaust strokes. Therefore, outputs from the in-cylinder pressure and its cyclic variations are most related to the engine to produce a certain amount of work. In-cylinder pressure has always been considered an important experimental diagnostic parameter in engine research and development due to its direct relation to the fuel combustion process (Ding et al., 2015). The analysis of thermodynamic for the measured in-cylinder pressure data is a significant tool to quantify the combustion parameters of both compression and spark ignition engines. Furthermore, the in-cylinder pressure measurement could provide useful information regarding cylinder torque variability, cyclic fueling variability, thermal efficiency, intake and exhaust tuning, combustion phasing, cylinder balance, detonation and structural loading (Bueno, Velásquez, & Milanez, 2012; Chiatti et al., 2015; D'Ambrosio, Ferrari, & Galleani, 2015; Guardiola et al., 2017)

Other than that, measured in-cylinder pressure data is also providing a significant presence in the validation of the cylinder pressure data generated from the cycle simulation models of the engine cycle which are categorised as zero, multi-zone andmulti-dimensional models. A simulation model is used to simulate a mean cycle, which is derived from a collective of average pressure trace for a specific engine. Some in-cylinder pressure cycle simulation models has been discussed in further details (Suneel & Kumar, 2013; Mansor, Abbood, & Mohamad, 2017; Sindhu et al., 2014). These simulation models could provide great assistance to the engine designers regarding economic values which reduce the time and costs for new engines development as well as the technical knowledge in the identification of areas which require specific attention as the design study evolves. Also, the cycle simulation models can be used to predict the in-cylinder pressure and determine the characteristics of engine performance without conducting any experimental work (An, Yang, & Li, 2015; Choi, Song, & Park, 2016; Huang et al., 2016). Regarding the studies for the purposes described above, in-cylinder pressure data is averaged at each crank angle to obtain the mean at desired accuracy and used to obtain average indicated engine performance characteristics including indicated work, indicated power and indicated mean effective pressure (IMEP) (D'Ambrosio et al., 2015; Phuong et al., 2014).

In-cylinder pressure cyclic variations can easily be seen by plotting the pressure data for each cycle on one figure. However, the mean measured in-cylinder pressure in the experimental work is computed averagely from the numbers of the cyclic variation at a certain period. The existence of cyclic combustion variations in internal combustion (IC) engines have long been recognised (Yaopeng et al., 2016; Najafabadi & Dynamics, 2017; Dimitrios et al., 2016; Reyes et al., 2013; Zhang et al., 2013). Through the measurements of the pressure-time history of consecutive cycles in the combustion chamber in the engines, the variations from one cycle to another do exist and can be easily seen. Since the in-cylinder pressure rate is exclusively related to the combustion, the pressure variations are caused by both chemical and physical phenomena variations that occur cyclically in the combustion process. Those chemical and physical phenomena are considered as the fuel composition, the fuel-air ratio, the changes in the residual gas fraction and the motion of unburned gas in the closed cylinder. Three identified sources that contribute to the development of cyclic variations in the cylinder are mixture composition (Dimitrios et al., 2016; Reyes et al., 2013), cyclic cylinder charging

(Gürbüz, Akçay, & Buran, 2014) and in-cylinder mixture motion (Yang et al., 2016). The factors which belong to the mixture composition and cyclic cylinder charging influence mostly the main stage of the combustion, while the other sources play a regular role at any stage of the combustion.

1.2   Project Overview

The interest of using alternative fuels in compression ignition engines has increased recently due to the rapid depletion in global fossil oil reserve. The increasing oil prices and higher restrictions on exhaust emission limits from transportation and industrial applications have been initiated due to environmental concerns. Therefore, several European Union (EU) countries currently have implemented the use of renewable fuels to replace the fossil fuels due to fuel security, environmental sustainability and economic growth stability. For that reason, first and second generation of biofuels were vastly produced to meet the global demand from other countries. At this time, the demand for alcohols which are second-generation biofuels to be used as a blend or an additive in diesel and gasoline engines is greatly increased. Furthermore, the addition of alcohols to diesel and biodiesel fuels has been discovered to influence some physicochemical properties with specific reference to fuel density, viscosity, heating value, cetane number, and oxygen values, hence, causing significant dissimilar effects to the characterization of engine combustion, performance and emissions. As examples of an engine parameter, extensive prolong ignition delay phase of the combustion was found due to the use of alcohol blends in compression ignition engines, whereas this use is dependable on which type of alcohol and the increasing amount of alcohols in the fuel blends. At times, the fuel blends with alcohols could serve fuel properties improvement, thus providing superior engine performance and emissions.

Combustion cyclic variations is an undesirable characteristic of compression ignition engines due to fluctuations in both early flame kernel development and turbulent flame propagation. Combustion in engines evolves differently in each combustion cycle at normal steady-state operating conditions due to some parameters. Cycle-to-cycle or cyclic variations are best observed by plotting to scatter points of the measured experimental cylinder pressure data compared to the mean pressure curve. Furthermore, such developed fluctuations of the cylinder pressure consistently exert an adverse effect

on engine performance, fuel consumption and pollutant emission, whereas in some cases such as highly diluted lean mixtures or too large level of variations could result in misfiring or knocking. This thesis would, therefore, contribute towards understanding the correlation between different biofuel blends and combustion cyclic variations on different engine loads and speeds from low to high inhomogeneous combustion; hence from a literature review, this belongs to a detailed research area. For this purpose, an experimental investigation of cylinder pressure cyclic variations of different alcohol blends on a single cylinder diesel engine was among the objectives of this thesis.

1.3 The Hypothesis of the Study

In this study, few hypotheses have been developed on the use of butanol and ethanol with mineral diesel (D) and palm biodiesel (B) as blend fuels in the diesel engine which is described in detail as below:

a) Biodiesel can be directly blended with butanol and ethanol in small proportion.

b) The presence of oxygen in biodiesel and butanol and ethanol could increase the cylinder pressure and combustion temperature with the improvement in combustion.

c) Further chaotic and instabilities occur in the cyclic variations of both butanol and ethanol blends due to inconsistent combustion.

1.4 Problem Statement

Combustion instabilities are the core of much present research works in compression ignition engines when running with different kinds of fuel. These combustion instabilities produce cycle-to-cycle or cyclic variations in cylinder pressure in compression ignition engines which are undesirable in term of combustion efficiency and are thus essential to understand and control in an attempt to further optimise overall engine efficiency. The difficulty is that many different parameters which originate from various sources can lead to engine cyclic variations, and that their importance and interactions can be studied using cylinder pressure analysis recorded from the standard engine experiments (Ball, 1999; Ceviz et al., 2011; Maurya, Saxena, & Akhil, 2016; Rakopoulos, Rakopoulos, & Giakoumis, 2010a). Cyclic variation in compression

ignition engines is identified as a fundamental combustion problem which increases the idle speed operation and limits the use of lean mixtures and the amount of recycled exhaust. By eliminating the cylic variation, the engine power output could be increased for the same fuel consumption. Also, the repeatability of cyclic variations leads to torque fluctuations and poor vehicle drivability as well as higher engine noise and vibration (Dong et al., 2016; Kyrtatos et al.,2017; Yaopeng et al., 2016).

One of the sources that could affect the engine cyclic variations is different types of fuel running on the engine. Different types of fuel produce different combustion rate and patterns. Therefore, a higher possibility of producing different cyclic variations could be found based on the feedstock sources of the fuel. Diesel engines commonly used mineral diesel for operation in different applications. Thus, their characteristics with pure diesel are commonly recognized and well-understood. However, a new generation of fuels from different feedstock sources are introduced to fuel the engine which produces a different range of characteristic outputs. As a result, a diverse possibility of research areas is proposed to determine and assess the engine characteristics when fueled with different types of fuel including biodiesel and alcohol fuels such as butanol and ethanol. Most of the previous engine testings mainly focused on the performance, combustion and emission characteristics of the engine running with biodiesel and alcohol blends (Imdadul et al., 2016; Rajesh Kumar & Saravanan, 2016; Yilmaz & Atmanli, 2017). However, there are also studies on the cyclic variations and its parameters where such a relationship has not been found which mainly attributed to the limitation for the combustion data which requires an advanced combustion analyser that can interpret innumerable cylinder pressure data. One reason might be that the measure on the cylinder pressure cyclic variations that have been used to assess the engine stability when operating with different test fuels has typically a combination of data complexity and larger data storage.

1.5   The Objective of the Study

The overall aim of this research focuses on the investigation of the cylinder pressure cyclic variations with butanol and ethanol blends, mixed with mineral diesel (D) and palm biodiesel (B) in a single cylinder diesel engine. The objectives of this research are listed as follows:

a) To characterise the fuel physicochemical properties of butanol and ethanol blends with mineral diesel (D) and palm biodiesel (B) on combustion characteristics with regards average cylinder pressure and heat release rate (HRR) profiles.

b) To investigate the effects of various loads and speeds on the cylinder pressure cyclic variations and coefficient of variations (COV).

c) To analyse the combustion stabilities with regards to peak cylinder pressure, P_{max} using data analysis of recurrence plot (RP) and recurrence quantification analysis (RQA).

1.6 The Scope of the Study

The purpose of this study is to investigate the combustion cyclic variations about average cylinder pressure, heat release rate (HRR), cylinder pressure cyclic variations, the coefficient of variations (COV) and variations of peak cylinder pressure, P_{max} of butanol and ethanol blends as fuels for a single cylinder unmodified diesel engine. To achieve the objectives of this study, several points are listed here to elucidate the scope of the study as follows.

a) An experimental study is conducted to measure the physiochemical properties such as kinematic viscosity, density, Cetane number, calorific value and flash point of mineral diesel (D), palm biodiesel (B), butanol (BBu10 palm biodiesel-90% + butanol-10% and DBu10 mineral diesel-90% + butanol-10%) and ethanol (BE10 palm biodiesel-90% + ethanol-10% and DE10 mineral diesel - 90% + ethanol-10%) blends.

b) A series of engine testing is conducted with a single cylinder diesel engine at different engine speeds of 1100 rpm, 1700 rpm and 2300 rpm under zero (0%), partial (50%) and full (100%) loads fuelled with all six fuels.

c) The required consecutive cycle numbers are determined for analysing the coefficient of variation (COV) for the cylinder pressure time series.

d) The combustion characteristics with regards average cylinder pressure and heat release rate (HRR) and cyclic variation characteristics of all six fuels are analysed during the engine test series.

e)   Two hundred (200) consecutive cycles are used for analysing the peak cylinder pressure, Pmax, and $COVP_{max}$ with zero (0%), partial (50%) and full (100%) engine loads at engine speeds of 1100 rpm, 1700 rpm and 2300 rpm.

f)   The recurrence plot (RP) and recurrence quantification analysis (RQA) is used to analyse the peak cylinder pressure, Pmax cyclic variations for butanol and ethanol blends over 200 consecutive cycles with different engine loads and speeds using the Matlab software.

g)   The engine test results with butanol and ethanol blends with regards to base fuels namely; mineral diesel (D) and palm biodiesel (B) are considered to evaluate the effects of various engine loads and speeds on combustion characteristics and cyclic variations of the engine.

1.7   Thesis Outline

This thesis is divided into five chapters to describe details throughout the study. A brief description of the thesis is presented in this section. The general introduction to the study, which includes the project overview, problem statement, objective, scopes of the development of internal combustion engines. Then, discussions on basic chemical contents of the study, research methodology and outline report of the study are presented in Chapter 1.

A brief description of a literature review on the internal combustion (IC) engine and biodiesel fuels are presented in Chapter 2. An overview of using alcohols in diesel engines is also presented, including alcohol effects on fuel properties, engine performance and regulated exhaust emissions. The literature suggests that ethanol is a viable fuel additive in diesel engines. However, research on butanol is infrequent, but is novel and potentially challenging. Consequently, butanol is used in this chapter for further study on the effect of the molecular structure of biodiesel-alcohol and alcohol-diesel blends. Palm biodiesel (B) is selected to study the effect of the hydroxyl group in biodiesel, on fuel properties and combustion of biodiesel-butanol and diesel-butanol blends. Therefore, the performance of the hydroxyl group in biodiesel is assessed. Finally, a brief review of the use of recurrence plot (RP) and recurrence quantification analysis (RQA) as a combustion cyclic variation analysis tool for diesel engines is given.

Chapter 3 provides the research methodology of this experimental study. A description of the test fuels including methods used to investigate fuel properties is also described. The details of the experimental engine, instrumentation and exhaust gas analysers are also given. This chapter briefly explains on how the diesel engine test cell was set up according to the known standard, SAE J1349 - Engine Power Test Code-Spark Ignition and Compression Ignition-Net Power Rating and SAE J1312 - Procedure for Mapping Performance - Compression Ignition and Spark Ignition Engines. Exhaust measurement apparatus used in this study are briefly explained in this chapter. Overall, Chapter 3 discusses the test cycles and fuel test operating conditions for the engine testing to make the objective of the study clear and understandable.

Chapter 4 presents three main sections; firstly, chemical properties data for the test fuels, secondly engine combustion analysis and, thirdly engine cyclic variation (CV) analysis. In the first section, results on chemical properties including density, viscosity, heating value and cetane number of the test fuels used in the engine testing are presented. In the second section, the results presented the combustion analysis of the engine including the in-cylinder pressures and heat release rate (HRR) as evaluated according to the test fuels. Chapter 4 also presents and discusses the results for cyclic variations of test fuels using peak cylinder pressure, P_{max} values and COV_{Pmax} values. This follows with the use of recurrence plot (RP) and recurrence quantification analysis (RQA) to quantify and in evaluating the dynamic behaviours of the P_{max} time series for 200 consecutive cycles for each test fuel. Overall conclusions from Chapter 4 are discussed along with the recommendations of the potential areas for future research Chapter 5.

8

CHAPTER 2

LITERATURE REVIEW

2.1 Introduction

This chapter presents a brief description of diesel engines and various fuel types from biodiesel fuel to alcohol fuels. Next, the use of alcohol and biodiesel as blend fuels with diesel is briefly covered and systematically reviewed. Past research studies on the use of alcohol regarding combustion and cyclic variations are also outlined and concisely presented. This chapter also covers engine cyclic variations that affect the various fuels in diesel engines. The review is organised chronologically to offer an insight into how past research efforts have laid the groundwork for subsequent studies, including the present research effort. The present research effort can be adequately tailored to add to the present body of literature as well as justifies the scope and direction of the current research effort.

2.2 Biofuels in Diesel Engines

Diesel engines deliver mechanical work as a result of fuel chemical reaction during combustion in the cylinder. Therefore, the knowledge of fuel properties is required to verify the exact fuel before fuelling the engine. This section describes the details of the specific fuels that been used in the diesel engines with previous research works.

2.2.1 Biodiesel Fuel

Fossil fuels have been widely used for many years in the power generation and transportation sectors due to its higher thermal efficiencies, reliability, the higher torque generated and better fuel economy. However, much responsible scientific governments and university reports have concluded that the exhaust emissions from fossil fuels especially diesel fuel have produced harmful toxic gas emissions NOx, carbon dioxide (CO_2), sulphur dioxide (SO_2), particulate matters (PMs) and soot formation. These adverse effects have caused severe environmental problems including global climate change, lower ozone layer concentration, denser smog (a mixture of smoke and fog) and acid rain (Baklanov, Molina, & Gauss, 2016). Since mineral fuels are formed from hydrocarbon molecules, these hydrocarbon substances are completely dissolved and combined with other new elements to create new components when the fuels are completely burnt (Johnson, 2015). These hydrocarbon emissions possibly have both toxic (alkanes and alkenes) and carcinogenic (polycyclic aromatic hydrocarbons) effects (He, 2016; Yilmaz & Davis, 2016). Polycyclic aromatic hydrocarbons (PAHs) are formed when acetylene is polymerised and absorbed on soot which includes large numbers of separate compounds which contain two or more aromatic rings. These noxious PAHs are often found in the environment and possibly cause carcinogenic diseases and hematic system disorders (Vojtisek-Lom et al., 2015; Yilmaz & Davis, 2016).

Since the negative impacts of mineral fuels severely affect the environment, there is an increasing interest in finding a new type of fuels that are more environmental-friendly and domestic produced in the current years. Most of the new fuels are targeted to be used directly in the motor vehicles without any modification. One of the substantial alternative ecological fuel sources is vegetable oils which possess similar physical and chemical (physicochemical) properties and combustion characteristics to the petroleum diesel. The use of vegetable oils as workable fuels in internal combustion engines is not new and had been extensively introduced by Rudolf Diesel that runs the diesel engine with peanut oil in early 1900. However, the popularity of the vegetable oils at that time had been obliterated with the introduction of petroleum fuels to the engines after the discovery of petroleum rigs and massive petroleum production. Nowadays, the current condition on the use of fuel type sources is turning back to the early introduction of

engines with the introduction of sustainable edible and non-edible oils as biodiesel and biofuels for better efficiency and serving lower emissions and better fuel economy. The selection of edible and non-edible oils are mainly based on geographical and climate conditions where soybean, corn, peanut, rapeseed, canola and olive are mostly planted and harvested in the European continent and the United States, while palm oil, coconut, jatropha and rubber seeds are primarily found in hot and warm climatic countries including Asia, Africa and South America (Ciriminna et al., 2014). These edible and non-edible oils have several advantages including higher oxygenated content, low sulphur, higher cetane number and producing lower harmful exhaust gases (Issariyakul & Dalai, 2014; Martínez et al., 2014).

Moreover, these edible and non-edible oils possess improved lubrication and higher ignition temperature which does not tend to flame easily. Many types of research have been performed to determine and evaluate the effect of edible and non-edible oils including soybean, rapeseed, jatropha, canola, karanja, jojoba, palm oil and others to be used as alternative engine fuels without engine modification. Interestingly, there are significant potentials to be explored regarding engine efficiency and emissions using the edible and non-edible oils with new and improved engine technology. Biodiesel feedstock sources from edible and non-edible of plant oils and animal fats are processed through a transesterification process to produce methyl or ethyl esters of fatty acids (FFAs). Transesterification process can be defined as a chemical reaction of a triglyceride with the presence of alcohol as a catalyst to produce methyl esters and glycerol (Maity, 2015; Sun et al., 2015). Since the triglyceride has three long-chain fatty acids including a glycerine molecule, a catalyst or alcohol is required to break the fatty acids or triglyceride into methyl esters and glycerol (Bharathiraja et al., 2014). As a result, biodiesel production commonly generates glycerol as its main by-product by about 10% (w/w). This means for every gallon of biodiesel produced, approximately 1.05 pounds of glycerol is produced. Biodiesel or fatty acids of methyl ester (FAME) is a sustainable alternative fuel produced from vegetable oils, animal fats and waste oils that can be used in diesel engines (Alptekin, Canakci, & Sanli, 2014). Biodiesel owns certain significant environmental benefits. For example, it approaches the neutrality of carbon dioxide and therefore contributes less to global warming and environmental degradation throughout its life cycle (Bhuiya et al., 2015). Many studies on biodiesel have concluded that when

biodiesel possibly displaces petroleum diesel, the greenhouse gases (GHGs) will be significantly reduced (D'Agosto, Ribeiro, & de Souza, 2013; Mofijur et al., 2016).

Biodiesel significantly reduces the hydrocarbon (HC), particulate matters (PMs), soot formation and carbon monoxide (CO) emissions in diesel engines (Imdadul et al., 2016; Suh & Lee, 2016; Tosun et al., 2014). Most of these benefits owe to the higher oxygenated content in biodiesel which permits the complete burning of fuel when mixing with the inlet charge that significantly produces lower emissions (Lahane & Subramanian, 2015; Suh & Lee, 2016; Zare et al., 2016; Zhu et al., 2016). This similar characteristic potentially reduces harmful air pollution which is associated with the unburned or partially burned hydrocarbon (HC) matters and PM emissions. Many studies show evidence that the reductions in PM, HC and CO emissions are considered independent of the biodiesel feedstock. EPA had reviewed eighty biodiesel emission tests on diesel engines and from these test results, EPA had concluded that the benefits in reducing emissions were actual and foreseeable over a wide range of biodiesel blends from different feedstock sources (EPA, 2016). Confirmation on the hypothesis that B20 produces positive impacts on HC, PM and CO emissions have been proved by the detailed analysis examined by EPA and by high impact published results (Lahane & Subramanian, 2014; Mirzajanzadeh et al., 2015; Ramalingam et al., 2016; Serrano et al., 2015). However, further investigation on NOx results indicated that the effect of biodiesel is varying with the engine design, calibration and specific test cycle (Bär et al., 2016; Fathi, Jahanian, & Shahbakhti, 2017; Maroteaux & Saad, 2015; Yu et al., 2017). Also, data on the average effects of B20 on NOx emission are insufficient and lack detailed knowledge.

Further studies concluded that edible and non-edible oils used in diesel engines at lower concentration of 20% possibly causes long-term engine deposits to ring sticking, lubricating oil waxing and other maintenance difficulties as well as lessen engine life (Knothe & Razon, 2017; Kumar & Sharma, 2016; Shahir, Jawahar, & Suresh, 2015). Furthermore, raw edible and non-edible oils also reduce power output and thermal efficiency as well as leaving unburned carbon deposits inside the cylinder. Most of these problems with raw edible, non-edible oils and animal fats are due to high viscosity, low cetane number, low flash point, and resulting incomplete combustion (Bhuiya et al., 2016a; Ibrahim, 2016; Sakthivel et al., 2018; Yuan et al., 2017). These problems are

mostly instigated by the higher viscosity of the edible and non-edible oils than the mineral diesel fuel since the engines and fuel injectors are designed to receive fuel viscosity in a range between 1.3 to 4.1 mm^2/s. Viscosity of the fuel could be reduced through a transesterification process, which converts the edible and non-edible oils or fats into biodiesel using alcohol as a catalyst (Geacai, Iulian, & Nita, 2015). This method helps biodiesel to achieve closer characteristics such as density and viscosity (typically 4 to 5 mm^2/s for biodiesel) as compared to mineral diesel.

Since biodiesel possesses higher viscosity and density than mineral diesel, generally biodiesel blends up to 20 per cent with mineral diesel to make them completely soluble (Nalgundwar, Paul, & Sharma, 2016). Several research works have reported that biodiesel blends tend to reduce CO, PM and HC emissions with a slight increase in NOx emission for all operating engine conditions (Aurélio et al., 2017). However, the effect of NOx emission is contradictory to the current experimental works that reported NOx emissions of biodiesel were similar or possibly lower than that of ULSD fuels depending on the operating engine strategy. Moreover, a number of studies on biodiesel have found an average of 20% reduction of PM emissions with the use of 20% biodiesel blending with mineral diesel (B20) (Cheung et al., 2015; Gülüm & Bilgin, 2015; Lim et al., 2014; Tang et al., 2016).

2.2.2 Alcohols

Alcohols belong to a family of oxygenates. The general chemical formula for alcohol fuel is $C_nH_{2n+1}OH$. Each alcohol molecule has one or more oxygen molecules, which contributes to superior combustion. Therefore, the alcohols are named accordingly to the basic molecules of hydrocarbon including ethanol (C_2H_5OH), butanol (C_4H_9OH), methanol (CH_3OH) and propanol (C_3H_7OH). Since the alcohols own the hydrocarbon and oxygen molecules, theoretically, the alcohols are suitable as a fuel. Also, alcohols can be synthesised chemically or biologically, and they have similar characteristics to current fuels to be used in diesel engines (Chauhan et al., 2016; Kumar & Saravanan, 2016). Although the list of alcohols is extensive for fuel combustion, however, only three different alcohols are technically and economically feasible for internal combustion engines. These listed alcohols are known with the simplest molecular structure namely ethanol, butanol, and methanol (Ghadikolaei, 2016).

Octane number can be defined as an index of quality that shows the ability of the fuel to resist and burn evenly when subjected to high pressures and temperatures inside the engine and therefore reduces knocking (abnormal combustion in the cylinder). Additional tetramethyl lead and tetraethyl lead increase the octane number. However, these octane improvers had been prohibited due to hazardous emissions containing lead. A fuel requires higher Cetane number or ability to self-ignite at high temperatures and pressures. There is a significant difference between diesel, gasoline and alcohol regarding Cetane number and autoignition. Higher Cetane number fuel leads to shorter ignition delay period, whereas lower Cetane number results in more extended ignition delay period (Atmanli, 2016b; Fayyazbakhsh & Pirouzfar, 2016; Li et al., 2014a). Literature works exhibit that alcohols have lower Cetane number than that of mineral diesel (Ghadikolaei, 2016; Kumar & Saravanan, 2016). However, some substances, an example of which is nitrate glycol, can improve the Cetane number of alcohols. This means that the ignition delay period will become shorter, which tends to reduce diesel knocking. Also, the inadequate lower rate of heat release would result with poor ignition delay period (Moxey, Cairns, & Zhao, 2016).

Many advantages could describe the alcohols as a possible fuel for engines. Alcohols can be produced from the organic materials such as biomass and municipal waste. Also, alcohols also can be made out from solid hydrocarbons such as coal (Renó et al., 2014; Sarathy et al. 2014). Alcohol combustion produces higher combustion pressure inside the cylinder due to the higher molar products to reactant ratio, compared to gasoline, which improves power output and thermal efficiency. Alcohols have a higher average octane rating ((RON+MON)/2=104) as compared to gasoline (Lapuerta et al., 2015). This variable increases the compression ratio of the engine to 12:1 with increasing power and fuel efficiency by 20% and 15% respectively (Khandal et al., 2015). Alcohols also have better performance and combustion characteristics due to the increased volumetric efficiency of alcohol fuels; for example, methanol is widely used for racing fuel (Datta & Mandal, 2016b; Gurgen, Unver, & Altin, 2017; Sarathy et al., 2014). Engine power increases with the decrease in acceleration time. Other than that, alcohols have a lower evaporative emission with less harmful by-products released in the atmosphere. Theoretically, since the hydrocarbon molecules content in alcohols is small, a negligible amount of soot is formed and released to the atmosphere when burnt in the engines (Gómez, Soriano, & Armas, 2016; Zhang et al., 2016).

There are few disadvantages of alcohols when used in the engines that can be described in this section. One of them is the economics of the production of alcohols which play a significant role limiting its use as an alternative fuel in diesel engines, which highly depends on the mineral fuels (Bae & Kim, 2017). The possibility of higher utilisation of alcohols as future fuels is minimal unless the cost of alcohol production from renewable feedstock sources is cost-effective. These alcohols could be produced from coal, biomass, crude oil and natural gas. The second disadvantage of alcohol is related to the cold start ability problem. Alcohols especially ethanol with lower vapour pressure, the higher latent heat of vaporisation and single boiling point have difficulty in meeting the industry standards for starting in cold weather (Mofijur, Rasul, & Hyde, 2015; Yilmaz & Atmanli, 2017). However, this cold start problem could be solved by adding a small amount of gasoline to the alcohol blends and complying with the industry standards (Galloni et al., 2016).

Although these alcohols, when reached near their stoichiometric air-fuel ratios, produce more power, more fuel is required to produce a specified power output. For example, in an automobile, more fuel is consumed for each kilometre driven. As the prices of alcohol and mineral diesel both vary according to the market situations, the kilometre-per-dollar factor is the most crucial consideration which fuel type or blend percentage to use. In general, the use of alcohol or gasoline-alcohol blends tend to reduce fuel economy (kilometre per litre), however, if the price of alcohol is lower, the economics (kilometre per dollar) may still be considered. Other disadvantages that relate to alcohol properties are relatively low boiling point and high vapour pressure of methyl and ethyl alcohol that lead to the rapid vapourisation of the alcohol fuel known as vapour lock (Sarathy et al., 2014). This condition occurs due to the interruption in the fuel delivery system when the liquid fuel changes its state from liquid to gas. Reduction or delay in engine power could be the adverse effects due to the vapour lock. Other than that, the relative high latent heat of vaporisation of methyl and ethyl alcohols also causes problems in mixing these alcohols with air and delivering them through the intake manifold of the engine. Therefore, it is necessary to heat the intake manifold first during the cold weather or before the engine reaches operating temperatures. Therefore, the engine requires an external heat source to vaporise the fuel more completely to prevent the starting difficulty and sluggish performance after starting the engine. Apart from other disadvantages, flammability is also associated with the problems of alcohol. During

alcohol combustion, the flame visibility of alcohol is difficult to be detected which creates a possible hazard to the user (Kumar et al., 2013). This lack of visibility state is possibly associated with the small number of carbon atoms present in the alcohol content. Since there are very slight carbon molecules, no soot formation is observed to give the flame colour (Moon et al., 2013; Zhang et al., 2016).

2.2.2.1 Alcohol Blends

Alcohol fuels can be used in different blending ratios with diesel and gasoline fuels which can be operated in unmodified diesel and SI engines. Some alcohol fuels including methanol and ethanol have been used commercially, blending with gasoline for transportation up to 20% blending ratios (Chauhan et al., 2016; Imran et al., 2013). Many countries including Brazil, Germany, South Africa and few regions in the United States have amended and regulated the use of alcohols (ethanol and methanol) up to 20% by volume content, blending with gasoline for transportation fuel. Fuel properties contribute significant impacts on the engine characteristics regarding performance, combustion and exhaust emissions (Obed et al., 2016; Corach, Sorichetti, & Romano, 2015; Krutof & Hawboldt, 2016; Dimitrios et al., 2015). Blending alcohols with diesel and gasoline at different proportions provide substantial modifications regarding properties including density, viscosity, Cetane number, heating value and, octane rating (Datta & Mandal, 2016b; Kumar & Saravanan, 2016; López et al., 2015a). Therefore, newly designated fuels have been developed through the blending methods that provide improved different characteristics. However, there are particular adverse effects from the alcohol blends that could cause major defect to the engine parts. Few adverse effects that could be listed are material incompatibility and corrosiveness which possibly damage the engine components and fuel lines because of the presence of higher water content and acidity in alcohols. Consideration of fuel selection is mainly prioritized on the properties that possibly affect the engine for fuel evaluation. Previous research works have concluded that fuel properties for experimental works have proportionally changed to increasing alcohol proportions in the fuel blends (Atmanli, 2016b; Chauhan et al., 2016; Ramírez et al., 2014; Sarathy et al., 2014).

For years, the continued global use of mineral fuel has contributed to the shortage in fuel supply while exacerbating environmental problems. These factors continue

making it critical points for engine manufacturers to develop engines with better fuel efficiency and emitting less pollution. Also, many research has been conducted through the years for searching superior fuels to adapt to advanced engines. Alternative fuels including biodiesel are a fundamental subject to study since biodiesel is originated from domestic feedstock sources, which are sustainable and of continuous supply. Many kinds of literature have discovered that alternative fuels including biodiesel can fuel the engines without any modifications since their properties are similar to mineral fuel (Barrios et al., 2014; Bharathiraja et al., 2015; Shahir et al., 2015; Wan Ghazali et al., 2015). However, similar literature also concludes that engine performance including brake power and brake specific fuel consumption (BSFC) when fuelled with biodiesel is significantly lower than mineral diesel with the same amount of air and fuel injected within the cylinder (Abu-Hamdeh & Alnefaie, 2015; Obed et al., 2016; Lahane & Subramanian, 2015; Yilmaz & Atmanli, 2017).

Alternative fuels such as biodiesel are made of methyl esters of vegetable oils and fats, which are characterised by their properties, including density, viscosity, cetane number, calorific value, flash point, as well as cloud and pour points (Knothe & Razon, 2017). These properties are technically similar to mineral diesel and can be used to fuel the engines. However, biodiesel possesses higher density and viscosity than mineral diesel in most cited literature. In general, biodiesel is conventionally diluted with mineral diesel at different properties to reduce the density and viscosity for diesel engines without any engine modification (Abu-Hamdeh & Alnefaie, 2015; Imdadul et al., 2016; Kumar & Saravanan, 2016). Biodiesel-alcohol blend fuels are considered as alternatives to current mineral fuels. Their physical fuel characteristics are among the most critical parameters to determine the quality of each fuel. Strict procedures are used in observation and measurement to obtain the flash point, viscosity, density, acid value and cetane number to define the actual properties of biodiesel and its alcohol blend fuels. These obtained properties are beneficial to be used in any mathematical simulation for further findings. These properties provide good explanations of how the engine operates with those fuels regarding performance, combustion and emission characteristics.

Biodiesel is an alkyl monoester subtracted from edible and non-edible plant oils, waste cooking oils and animal fats through a transesterification process with the presence of a catalyst. The transesterification process is functional to remove the unnecessary

constituents, for example, dirt and water from the produced biodiesel. Biodiesel is regulated technically under EN14214 (European Standards, 2013) and ASTM D6751 (ASTM International, 2015). There is a large volume of published studies describing the potential of the biodiesel as a substitute for conventional mineral diesel and at the same time significantly reducing the emissions. Also, with the current practicality of biofuels including bio-alcohols, for example, bio-ethanol and bio-butanol as additives are successfully mixing with the biodiesel to reach the similar objectives. Moreover, in recent years, there has been an increasing amount of literature on different proportions of biodiesel-alcohol blends at different operating engine conditions and with varying engine parameters (Atmanli, 2016a; Awad et al., 2016; Imdadul et al., 2016; Yilmaz & Vigil, 2014). Therefore, results from previous experimental works were discussed and compared with the current works. For example, different properties of biodiesel from palm oil were observed as compared to other biodiesel made from other feedstock sources when mixed with alcohols at different proportions. Therefore, a comprehensive data of varying biodiesel and alcohols with their respective fuel properties are essential in analysing the engine characteristics because the fuel properties are important parameters in fuel atomization process in the engine cylinder (Knothe & Razon, 2017; Sakthivel et al., 2018).

Viscosity plays a vital role in the quality of atomization when the fuel is injected in the cylinder, followed by formation of fuel droplet sizes and uniformity of the mixture (Geacai et al., 2015; Lapuerta, Rodríguez-Fernández, & García-Contreras, 2015). Higher viscosity fuel can result in larger surface tension which affects the dissolution of a liquid jet into smaller fuel droplets (poor atomization) and inaccurate fuel injection timing. The viscosity of biodiesel is significantly higher than that of mineral diesel but approximately lower than neat vegetable oils (Paiva et al., 2015; Dimitrios et al., 2015). Therefore, the viscosity of the fuel can be significantly reduced through transesterification process. Also, viscosity could also be reduced with an increase in temperature in the storage tank and the tubing before delivering the fuel into the engine. In addition, prior studies have noted the importance of alcohols that significantly reduce the viscosity of biodiesel when blending with alcohols since the viscosity of alcohols is much lower than that of biodiesel (Bae & Kim, 2017; Imdadul et al., 2016; Yilmaz & Atmanli, 2017; Zhu et al., 2016).

Cetane number defines the ignition quality indicator for the specified fuel. It indicates the ignition delay either shorter or longer during the combustion period. The Cetane number of the fuel increases with the increase in the length of the carbon chain. The longer the fatty acid of carbon chains and the more saturated the molecules, the higher the Cetane number is (Angelovi, Tká, & Jablonický, 2014; Jose & Anand, 2016). Diesel engines generally accept the range of Cetane number between 40 and 55, but if the Cetane number is below 38, a rapid increase in ignition delay occurs accompanied by engine noise. In general, alcohols have lower Cetane number as compared to that of mineral diesel and biodiesel. For example, the Cetane number of neat alcohols is as low as 3 for methanol and 8 for ethanol which clearly defines them as poor internal combustion engine fuels. However, the Cetane number of biodiesel is significantly higher than mineral diesel due to the presence of fatty acids in the neat biodiesel (Atmanli, 2016b; Naser, Yang et al., 2017). The Cetane number for biodiesel-diesel blends also increases with the increases of biodiesel percentage in the biodiesel-diesel blends (Adewale, Dumont, & Ngadi, 2015; Suh & Lee, 2016).

Mineral fuels have been significantly associated with global warming issues, greenhouse gas emissions (GHG), scarcity in oil reserve, price volatility and political instability throughout the regions (British Petroleum, 2016; ENVIRON, 2014). Therefore, sustainable alternative biofuels from the organic feedstock sources are possible choices to counter those problems. In recent years, some studies have found that those alternative biofuels produce lower or no sulphur, less toxic, biodegradable and comparable combustion characteristics with the conventional diesel fuels (Nor et al., 2015; Žaglinskis, Lukács, & Bereczky, 2016). Moreover, the properties of biofuel including biodiesel are relatively similar with mineral diesel, which can be used directly in neat form or blend in the diesel engines without any modification. However, there are some dissimilarities in chemical composition for the biofuels which contribute to the differences in basic properties, affecting engine performance, combustion and emission characteristics. Thus, for a reason to move forward with the increasing demand in biodiesel industry and technology, up to now some studies on biodiesel have been conducted to evaluate the effects of biodiesel from different feedstock sources in diesel engines, taking account mineral diesel as a baseline fuel.

However, there are some aspects in the biodiesel properties that could be possibly improved as higher viscosity, and low volatility of biodiesel can lead to the problems in long-term engine operation. Higher viscosity in biodiesel may cause inconsistency of fuel droplet size, poor atomization qualities and deficiency in fuel penetration in the cylinder which highly affects the combustion qualities. The presence of free fatty acid (FFA) in the chemical bonding of the biodiesel contributes to the higher viscosity that can result in injector coking, ring sticking and gumming in diesel engines (Suh & Lee, 2016). Therefore, few methods have been proposed including transesterification (Adewale et al., 2015), micro-emulsification (co-solvent bonding) (Badday et al., 2012) and pyrolysis (Liu et al., 2018) in order to reduce the viscosity of the biodiesel and vegetable oils which are currently associated with higher price in production and extensive production time required. However, simpler approaches are feasible to reduce the density and viscosity of the biodiesel, for example, through blending with mineral diesel and alcohols at different proportions (Gomez et al., 2016; Imdadul et al., 2016; Yilmaz & Atmanli, 2017).

2.2.2.2   Ethanol Blends with Diesel and Biodiesel

Ethanol (C_2H_5OH) is an alcohol-based alternative transportation fuel that can be produced from sustainable feedstock resources. This alcohol fuel is applied as a fuel extender, octane enhancer, and oxygen additive or in pure form to substitute gasoline fuel (Obed et al., 2015; López et al., 2015b; Shaafi & Velraj, 2015). Also, ethanol is secure with its potential as a hydrogen carrier for fuel cell applications. Ethanol is mainly produced by fermenting and distilling starch crops that have been converted into simple sugars (Garcia & Sperling, 2017). Main cellulose feedstock sources for ethanol include corn, wheat, barley and sugar cane which contain sugar. While most ethanol production is currently from applied grain fermentation, recent ethanol development proposes the possibility of ethanol to be produced more efficiently from other biomass feedstock sources, thus offering much potential to be explored and reducing further current fossil fuel dependency (Garcia & Sperling, 2017; Diederichs et al., 2016; Suganya et al., 2016). As ethanol is mainly produced from agricultural grains, the production cost for this alternative transportation fuel is much lower in regions where their economy is primarily based on the agriculture sectors (Datta & Mandal, 2016b). Thus, the current dependency

on fossil fuels could be reduced in these regions. The most straightforward yet low-cost approach of alcohols in engines is by blending the alcohols at a moderate amount with base fuels. However, the second and more technically challenging option is to use alcohols in pure form as engine fuel. Furthermore, ethanol offers some advantages include carbon monoxide (CO) and unburnt HC emissions reduction, as well as improved anti-knocking characteristics, which are suitable to be used in engines of higher compression ratio (Khandal et al., 2015). The presence of wide flammability and oxygenated characteristics in ethanol influences the reduction of CO emission. Therefore, some significant improvements are found in power output, efficiency and emissions (Chuepeng et al., 2016; Ghadikolaei, 2016; Gurgen et al., 2017). Also, ethanol possesses a higher flash point and auto-ignition temperature than gasoline with low Reid evaporation pressure which is safer to handle and store, and causing lower evaporative losses (Morone & Pandey, 2014). Since ethanol is a liquid fuel, the storage and dispensing method of ethanol are similar to gasoline. Other than that, the latent heat of evaporation for ethanol is approximately 3 to 5 times higher than gasoline which delivers lower temperature intake manifold and increases volumetric efficiency (Serras-Pereira et al., 2013).

Ethanol is produced mainly from agricultural products including corn, sugar cane, potatoes, wood, barley, sugar beets, cassava and waste biomass feedstock sources through a fermentation process (Antunes et al., 2017; Crago et al., 2010; Diederichs et al., 2016; Kurkijärvi et al., 2014). This kind of ethanol is known as bioethanol. It can also be produced from crude oil and natural gas. This alcohol can be considered as non-toxic soluble in water and biodegradable. It is more flammable than gasoline, however neat ethanol is rarely used as fuel due to its higher price in production. Usually, it acted as an oxygen enhancer and mixed with gasoline to meet clean fuel requirements (Giakoumis et al., 2013; Schifter, González, & González-Macías, 2016). The use of ethanol for engines is well proven as seen from its wide applications and established technologies. As a result, ethanol has been globally applied as a neat fuel or fuel blend, particularly in Brazil with up to 20% blend from bioethanol (made from sugar cane), and in USA and Canada for the gasoline additive and combustion enhancer (Alonso-Pippo et al., 2013; Johnson & Silveira, 2014).

Ethanol blends well with gasoline to form stable solutions at any blend ratio, however in the case of mineral diesel, ethanol does not blend well with mineral diesel, becoming less stable at larger blend ratio. Anhydrous ethanol effortlessly blends with mineral diesel to form stable solutions having up to a tenth of percent ethanol at warm ambient temperature. However, in contrast, the ethanol and diesel blends start to split into dual phases for ethanol content at 20% or higher. Therefore, there are alternative additive-based methodologies for maintaining the stable blends at a low temperature. Firstly, the use of surfactants or emulsifiers to preserve stable emulsions or microemulsions, and secondly, the application of co-solvents that possibly develop the stable blending (Kumar et al., 2013; Parthasarathi, Gowri, & Saravanan, 2014; Wu et al., 2015). The use of emulsifiers for ethanol blends have been used extensively since the 1980s which successfully produce stable blends for diesel engines. However, extensive application of ethanol as a fuel blend with mineral diesel was hindered due to the higher price of ethanol production at that time.

Current development of technology in recent years have driven researchers to investigate ethanol-diesel blend used in diesel engines (Ghadikolaei, 2016; López et al., 2015c; Schifter et al., 2016; Storch et al., 2015). Several engine performance variables including brake specific fuel consumption (BSFC), cylinder pressure data, exhaust emissions of NOx, CO, CO_2, HC and smoke number were measured at different operating engine conditions with diesel-ethanol blends and compared to the reference line fuel, mineral diesel. Since ethanol contains approximately 60% of the energy content of gasoline, the vehicle consumes more ethanol to get the same mileage as similar gasoline fuel. Because of the current technology and production price structures, the price of ethanol is higher than the same volume of gasoline. However, neat ethanol does not mix well with gasoline and diesel fuel when the mixing proportion is over 10%. Neat ethanol is a low cost oxygenate with a 35% oxygen content used for ethanol blends with mineral diesel. Higher oxygen content in the blends theoretically improves the combustion characteristics with higher gas temperature and cylinder pressure. Therefore, the use of ethanol in diesel blends may cause significant reduction of particulate matter (PM) emissions for diesel-powered vehicles (Mofijur et al., 2016). On the other hand, there are many technical barriers and limitations to the direct use of ethanol in diesel blends because of

the properties of ethanol, for example, low cetane number, high latent heat of vaporization and poor solubility of ethanol with diesel fuel in low temperature (Kuszewski et al., 2017; Dimitrios et al., 2015; Schifter et al., 2016; Yu et al., 2017).

2.2.2.3   Butanol Blends with Diesel and Biodiesel

First generation biofuel, biodiesel from different feedstock sources, producing edible and non-edible oils have been an important subject for many years since the development of diesel engines. Then, came second-generation biofuels including alcohols, with feedstock sources originating from sustainable feedstocks that could be planted and harvested throughout the year. Alcohol forms including ethanol, methanol, butanol and propanol have been utilised intensively as transportation fuels for light and small vehicles. However, a promising and sustainable replacement fuel that has been overshadowed by ethanol and methanol for many years is butanol and bio-butanol. This fuel is a type of alcohol forms that possess lower water miscibility, similar energy content and rating octane number (RON) with gasoline which can be used directly in gasoline engines. Also, butanol offers identical characteristics with other principal alcohols when blended with gasoline and diesel into different blending ratios. Interestingly, similar to second generation biofuels including bio-ethanol, butanol or bio-butanol originates from lignocellulose biomass that has been processed through fermentation of acetone butanol ethanol (ABE). Other than that, butanol has the following advantages and disadvantages compared to ethanol as listed in Table 2.1 and Table 2.2.

The number of previous experimental works on the use of alcohols including butanol in the diesel and biodiesel blends is comparatively few. This requires more research to determine the potential behaviour of alcohols as a neat form or fuel blends in diesel engines. The selection of butanol as a fuel oxygenate in the diesel and biodiesel blends due to the miscibility and reduce the viscosity and density of the biodiesel (Atmanli, 2016a; Feng et al., 2017; Babu et al., 2017) In addition, butanol could improve the combustion efficiency and reduce the particular emission when operating with diesel engines. Butanol has approximately 35% oxygen content that could improve the fuel burning and combustion quality (Zhang et al., 2016). Higher oxygenated fuels in the engines result in complete combustion being achieved (An et al., 2015; Barrios et al., 2014; Nithyanandan et al., 2016).

A study conducted by Tüccar et al. (Tüccar, Özgür, & Aydın, 2014) on the performance and combustion characteristics of butanol-microalgae biodiesel-diesel blends on a four-stroke, four-cylinder Mitsubishi Canter diesel engine under full loads with the increasing engine speeds from 1200 to 2800 rpm. Butanol of 10% and 20% were blended with microalgae biodiesel and diesel to form three fuel blends of D70B20But10 (70% diesel, 20% microalgae biodiesel, 10% butanol), D60B20But20 (60% diesel, 20% microalgae biodiesel, 20% butanol) and D80B20 (80% diesel and 20% microalgae biodiesel). Overall results showed that the addition of butanol in fuel blends caused a slight reduction in torque and brake power values, whereas significant improvement in the engine emissions was observed.

Table 2.1   Advantages of butanol as a fuel

Advantages	Ref.
Butanol and bio-butanol can be blended in any ratio with gasoline or pure form, while ethanol is suitable for blending ratio up to 85% or in pure form using special designated engines.	(Fournier et al., 2016; E. Galloni et al., 2016; Yuqiang Li et al., 2016, Nithyanandan et al., 2016)
No need to modify the existing engine when using a pure form bio-butanol or gasoline-butanol blends.	(Acharya et al., 2016; Fournier et al., 2016; E. Galloni et al., 2016; Yuqiang Li et al., 2016; Senthil et al.,2015)
Butanol possesses lower vapour pressure which safer to handle compared to bio-ethanol.	Bergthorson & Thomson, 2015; Kumar & Saravanan, 2016; Ndaba et al., 2015)
Butanol can be blended with gasoline at the refinery before storage and distribution because it is not absorptive.	(Kujawska et al., 2015; Ndaba et al., 2015)
Since butanol is incapable of mixing with water, it less contaminates the groundwater if it spills; while ethanol is miscible with water thus contaminating the water.	(Hönig et al., 2014; Jiang et al., 2015; Kujawska et al., 2015; Morone & Pandey, 2014; Szulczyk, 2010)
Butanol is less corrosive which is suitable to be stored in pipelines, tanks, filling stations and others.	(Ndaba et al., 2015; Srirangan et al., 2012)

Table 2.1 Continued

Advantages	Ref.
Butanol has a higher energy content which is more suitable to be blended at higher blending ratio with gasoline.	(Kumar & Saravanan, 2016; Kumar et al., 2013; Morone & Pandey, 2014; Szulczyk, 2010)

Table 2.2 Disadvantages of butanol as a fuel

Disadvantages	Ref.
Butanol production is quite low compared to ethanol since the production rate of butanol yield from ABE fermentation is 10% to 30% lower than ethanol which produced from the yeast ethanol fermentation process.	(Barros et al., 2013; Li et al., 2014)
Butanol has higher fuel consumption since its heating value is still lower than diesel or gasoline fuel, even though it retains higher energy density compared to other alcohols.	(Dimitrios et al., 2015; Şahin et al., 2015; Zhang & Balasubramanian, 2014)
Since butanol is an alcohol-based fuel, it possibly creates trouble with specific fuel system components such as fuel meter reading errors.	(Acharya et al., 2016; Atmanli, Ileri, & Yilmaz, 2016; Dimitrios et al., 2016)
Butanol tends to produce higher exhaust emission due to its lower octane number. Higher octane number means better compression ratio and efficiency, which lean towards achieving fewer exhaust emissions.	(Liu et al., 2013; Şahin et al., 2015; Zhang & Balasubramanian, 2014)
A potential corrosive or aggradation problem possibly to occur since butanol has a higher viscosity when directly used in SI engines.	(Bergthorson & Thomson, 2015; Giakoumis et al., 2013; Nithyanandan et al., 2016)

Dimitrios et al. (2015) examined the impact of cottonseed oil, cottonseed biodiesel, butanol and ethanol as fuel additives in the diesel blends on a four-stroke, 6-cylinder, heavy-duty direct injection (HDDI) diesel engine under steady and transient condition. Combustion and emissions of these fuel blends were compared with the base fuel, diesel. Results indicated that the ignition delay for the cottonseed oil-diesel blend and cottonseed biodiesel-diesel blend were not significantly changed, whereas the significant increases for ignition delay were observed for the ethanol-diesel and butanol-diesel blends. Moreover, a slight decrease in maximum cylinder pressure for cottonseed

and its biodiesel blends were observed, which was higher than that of ethanol and butanol diesel blends. Interestingly, a significant reduction in smoke opacity and NOx emissions were observed for ethanol and butanol diesel blends, with butanol diesel blends performing better.

The experimental investigation on n-butanol, iso-butanol and octanol as additives in diesel blends was conducted by Zhang et al. (2015) to determine and evaluate the performance and emissions on an AVL 501 single cylinder, heavy-duty diesel engine with a common rail injection. These n-butanol, iso-butanol and octanol were blended with VSD10 diesel and mixed with either HVO or DTBP to increase the Cetane number. The results showed that the alcohol blends had comparable engine performance and similar brake thermal efficiencies. However, higher brake specific fuel consumption for the alcohol blends was observed concerning diesel which was mainly attributed to the lower calorific value of butanol. As for emission values, soot emission and CO emissions were found to decrease for the alcohol blends, whereas higher NOx emissions were observed for similar blends.

Valentino and Iannuzzi (2014) conducted one study that focused on the use of butanol and gasoline as fuel blends with diesel on a Euro 5 light-duty cylinder engine tested under 0.8 MPa of BMEP with an engine speed of 2500 rpm. Test fuel blends for volume ratio were gasoline-(20%)-diesel (80%) and butanol (20%)-diesel (80%). The study focused on the management injection strategy for different combustion phasing for these fuel blends. Results showed that longer ignition delay and better volatility were provided by the gasoline and butanol blends, which simultaneously caused a reduction in smoke and NOx emissions. Also, lower HC (unburned hydrocarbon) emissions were observed due to the reduction of local fuel-rich regions and oxidation which mainly attributed to the complete combustion.

In summary of the literature review based on the study of butanol as fuel blends, soot emissions were reduced significantly while some of the literature works had contradictory results for CO and NOx emissions. Similar inconsistent results also occurred to CO emissions, in which some literary works found reduction in CO emissions whereas others observed increase in CO emissions. However, it can be concluded that butanol is feasible to be used as fuel blend for base fuels including diesel and biodiesel

and positively producing significant results for performance, combustion and emission characteristics.

2.3   Diesel Engines

The fundamental in internal combustion engines has been sustained until today even though continuous engine improvements have been introduced. Advancement in internal combustion engine development is evolving at present with pioneering knowledge in engine operation, cutting-edge engine technology and constant demand on new engines that produce less emission and yet with higher performance efficiency (Heywood, 1988). The fundamental concept of the internal combustion engine is the generation of mechanical power due to the fuel that is injected under high pressure into the engine cylinder, where the fuel mixes with the swirling air causing combustion, converting chemical energy into heat energy (Atkins, 2009).

Automobiles are one of the internal combustion engine applications, where the engine is the prime mover for the powertrain. Reciprocating engine type is used in most automobiles, using fuel derived from the mineral oil distillation (Reitz, 1997). Other applications include machinery, stationary engines in generators and portable engine in equipment such as chainsaws and lawn mowers. Other than the reciprocating engine, rotary or Wankel engine is another type of internal combustion engine. This type of engine uses the rotor to deliver mechanical power for automobiles, small aircraft, go-karts and auxiliary power units for the airplane. A similar concept of the internal combustion engine can be discovered in rocket engines, jet engines and gas turbine engines which require different types of combustion process but burn fuels in confined spaces. The concept of a reciprocating engine is introduced in diesel engines where diesel engines are categorized into particular classifications including cycles, cylinder arrangement and displacement, fuel input method, cooling systems and specific applications Diesel engine applications employ two-stroke cycles for large engines and four-stroke cycles for medium and small engines.

Different sizes are available in diesel engines corresponding to the engine arrangements and engine block shapes. Various engine arrangements employ single cylinder and multi-cylinder from two to eight cylinders for small and medium engines

and a maximum of 32 cylinders for large engines. In-line engine cylinder arrangement is the most common cylinder arrangement, where cylinders are vertically arranged in a linear position corresponding to the crankshaft position. While for V-type cylinder arrangement, this type employs two linear rows at an angle of 15° - 120° with each row mounted along a single crankshaft. V6 and V8 engines are the most common V-type engines for automobiles inclined at an angle of 60° to -90°. Besides engine type arrangement, diesel engines can be characterised by the displacement volume in the engine cylinder. Engine displacement is defined as the inlet air volume displaced from the piston moves from the bottom dead centre (BDC) to the top dead centre (TDC) during the compression stroke. Engine parameters including piston stroke length, cylinder bore size and numbers of involved cylinders govern the engine displacement volume.

Diesel engines are also characterised corresponding to the different types of fuel delivery method namely; indirect injection (IDI) and direct injection (DI). Indirect injection (IDI) fuel method possesses two sections in the combustion chamber, where the fuel is injected in small precipitations into the pre-combustion chamber located at the upper section of the engine block and linked to the main combustion chamber. While for direct injection (DI) fuel method, this method employs the fuel to be injected into small droplets and mixes with the compressed hot air inside the cylinder during the compression stroke. Besides those explained conventional fuel delivery methods, there is an advanced concept of homogeneous charge compression ignition (HCCI) being introduced at present, where some smaller fuel droplets are injected during the intake stroke (Chen et al., 2016; Maurya & Akhil, 2016; Wang et al., 2015).

Diesel engines are widely utilised as power systems in the transportation sector and power generation in electricity sector due to their higher thermal efficiency, long proven record in reliability, higher power delivery, better fuel economy and maintenance cost and more straightforward arrangement in design (Breeze, 2014; Kegl & Pehan, 2013). The importance of diesel engines to generate power mechanisms are found mostly in on-road and off-road vehicles especially in the agriculture sector and heavy-loading trucks. Diesel engines are feasible to be repaired, extremely durable in all terrain condition and economical to operate. Diesel engine applications are characterised into different generated speed and torque from the engines. High-speed engines that generate speed from 1200 rpm and above are utilized in the vehicles include trucks, cars, buses

and locomotives. Diesel engines are mostly utilized in the automobile for producing higher torque and robustness with superior fuel efficiency and lower maintenance cost. Diesel engine-powered automobiles include SUV and 4-WD which can reach maximum engine speed of 5500 rpm with higher torque output of 400 Nm (Karavalakis et al., 2010).

Features of a diesel engine are defined by its characteristics which can be classified into six groups as follows:

i.   Fuel injection characteristics
ii.   Fuel spray characteristics
iii. Engine performance characteristics
iv.   Economy characteristics
v.   Combustion characteristics
v.   Emission characteristics
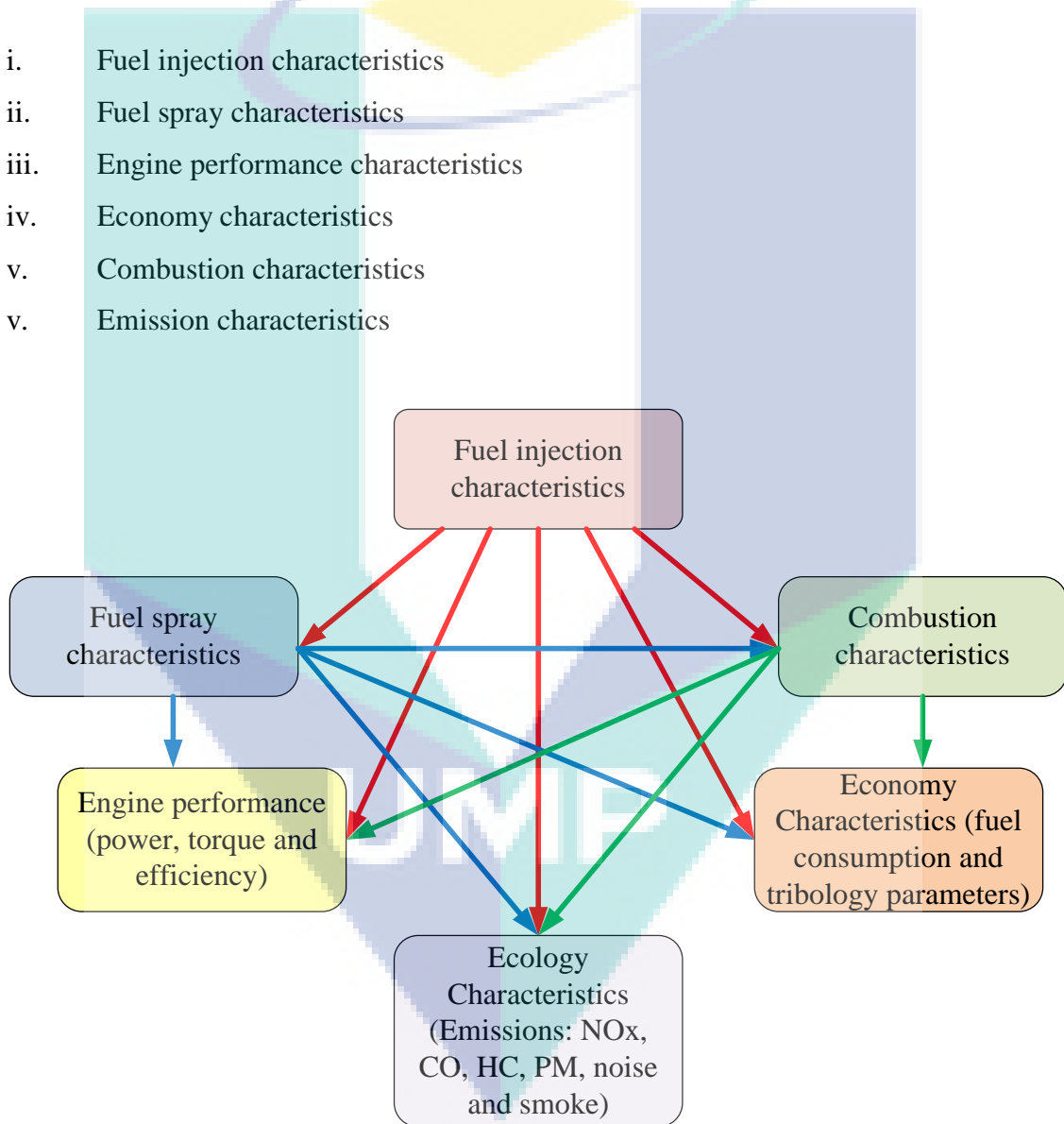
Figure 2.1   Diesel engine characteristics
Source: Karvountzis-Kontakiotis, (2015)

29

The significant relations between the six groups of diesel engine characteristics is illustrated in Figure 2.1. Those engine characteristics depend on the most essential parameters including fuel type and type of injection system as well as various process characteristics such as fuel spray development, injection formation process, atomization, the formation of fuel/air, ignition quality and combustion characteristics. Also, various geometrical and set up parameters for a fixed engine type could influence the aspects of a diesel engine with fuel injection system which is controlled mechanically or electronically. The geometrical parameters signify the most critical role for the mechanical controlled injection systems that involve in-line, single, and distributor injection pumps, unit pumps or unit injectors. In the meantime, common rails systems, engine behaviour and performance in the electronic-controlled injection system are determined by setting up parameters. The most important fuel injection parameters that influence the characterisation of diesel engines are injection pressure, injection duration, injection timing, and injection rate profiles. These listed parameters affect the formation of fuel spray, combustion characteristics, engine performance as well as fuel consumption and pollutant emission characteristics. Also, those injection parameters also can be influenced by the rest of the fuel line from the fuel tank to the fuel injector including the granulated fuel filter, fine fuel filter and low-pressure pump.

2.4 Combustion in Diesel Engines

In internal combustion engines, combustion analysis is considered as part of critical parameters, which characterise the behaviour of the engine under specific engine speeds and loads. This becomes clearer when the diesel engine runs on different types of fuel. There is a strong correlation between combustion analysis, types of fuel and engine parameters (including AFR, cooling system and loads). Eq. (2.1) shows a typical engine combustion reaction:

$$\text{Fuel} + \text{Air} (N_2 + O_2) \rightarrow CO_2 + CO + H_2O + O_2 + HC + O_3 + NO_2 + SO_2 \qquad 2.1$$
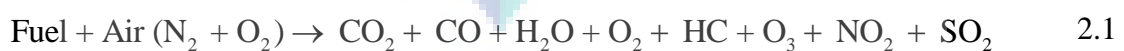
Eq. (2.1) mainly shows the outer surface reaction of the engine combustion since there is a crucial need to understand the inner surface reaction of the combustion. There are four phases in the combustion process of diesel fuel in a diesel engine as follows:

i.   Ignition delay duration

ii.   Premixed burning duration

iii.   Diffusion burning duration

iv.   After burning duration

Each of the stated phases will be further discussed in the next four subsections. The ignition delay is a significant variable in the engine operation that contributes to the production of NOx and hydrocarbon (HC) emissions (Barik & Murugan, 2014; Palash et al., 2013). This variation occurs between the start of fuel injection (SOI) and the start of detectable combustion (SOC) in the engine cylinder. The fuel is injected at high pressure through the nozzle, which is being subjected to physical processes such as fuel atomization, evaporation, mixing and initial chemical reactions. Thus, an auto-accelerating response simultaneously occurs where the evaporated combusted fuel influences the pressure to rise as well as the cylinder temperature. This event causes more fuel to turn rapidly into smaller droplets and burn. This event continues rapidly until it reaches the auto-ignition period which defines the end of the ignition delay. The significant increase in cylinder pressure exhibits the end of the ignition phase in the combustion process.

Premixed burning duration is defined as the preliminary stage of fuel-air mixed burning that causes the rapid increase in the in-cylinder pressure. This significant phase is justified by the heat release rate of the burning fuel to be vaporised, where the fuel droplets turn to vapour forms and mix with a specific amount of air charge to allow the combustion to occur. The premix burning duration is completed after all evaporated fuels are burnt. The length of the ignition delay duration generally influences the amount of fuel to be burnt, as the longer the ignition delay duration, the higher the potential for fuel to mix with air and consequently the more fuel will burn spontaneously in this phase thereby increasing the heat release rate. The diffusion-burning duration occurs after the

premixed burning duration and the complete burning of all vaporised fuels. When the fuel-air mixture combusts and causes a significant increase in the cylinder pressure as well as the cylinder temperature, the sudden change in the increased cylinder pressure pushes the piston descending to the bottom dead centre (BDC). After the burning duration indicates the condition when the fuel injection phase has finished the combustion period, there is remaining fuel and soot that continues to burn. There is also excess oxygen available ready for the next combustion since not all oxygen has been used entirely for the main diffusion burning duration. In this phase, the in-cylinder pressure and temperature start to decrease, and the piston moves gradually for the expansion stroke. Combustion by-products including residual solid particles such as unburned soot and exhaust gaseous (NOx, CO_2 and CO) remain circulating in the cylinder until the exhaust valve opens. These unwanted regulated emissions are released to the atmosphere affecting living forms and the environment.

Indicated combustion parameters including in-cylinder pressure, heat release rate (HRR), pressure rise rate (PRR), mass fraction burn (MFB) and combustion temperatures are measured and collected using a combustion analysis software tool. Those combustion parameters for the combustion analysis are calculated using in-cylinder pressure data and crank angle degree (deg.CA) and saved in Microsoft Excel as a database. Measured in-cylinder pressure in the cylinder provides the significant contribution to the combustion analysis. In-Cylinder pressure is defined in which the chemical energy is transformed into useful work (Heywood, 1988). This parameter determines specific event occurring for each stroke from one cycle to another. Therefore, quantifying the in-cylinder pressure provides closer insight of the engine ability to perform useful work (Bueno et al., 2012; Kaimal & Vijayabalan, 2015; Pan, Shu, & Wei, 2014).

Cylinder pressure is measured using a piezoelectric pressure transducer in which the signal conditioner/amplifier converts the signal before being analysed by the combustion analyser or data acquisition (DAQ) system as shown in Figure 2.2. To obtain detailed combustion characteristics, a full assessment is required to measure and record the cylinder pressure and crank angle degree (deg.CA), which are the most essential tools in combustion analysis. This is because the maximum rate of change of pressure occurs near the top dead centre (TDC), of the piston's motion, where the lowest velocity of piston is achieved during combustion period. In-cylinder pressure increases to the

maximum when the piston travels to the top dead centre (TDC) from the intake stroke to compression stroke. Then, the in-cylinder pressure decreases at the expansion stroke when the piston rapidly travels down to the bottom dead centre (BDC). The cycles continue until the engine stops running. Moreover, a delay occurs before the combustion takes place, signifying the fuel is injected which gives lower in-cylinder pressure before the peak combustion is achieved. Variabilities of in-cylinder pressure represent different engine input variables including fuels, fuel injection spray patterns, the air-fuel ratio (AFR) and engines (Heywood, 1988).
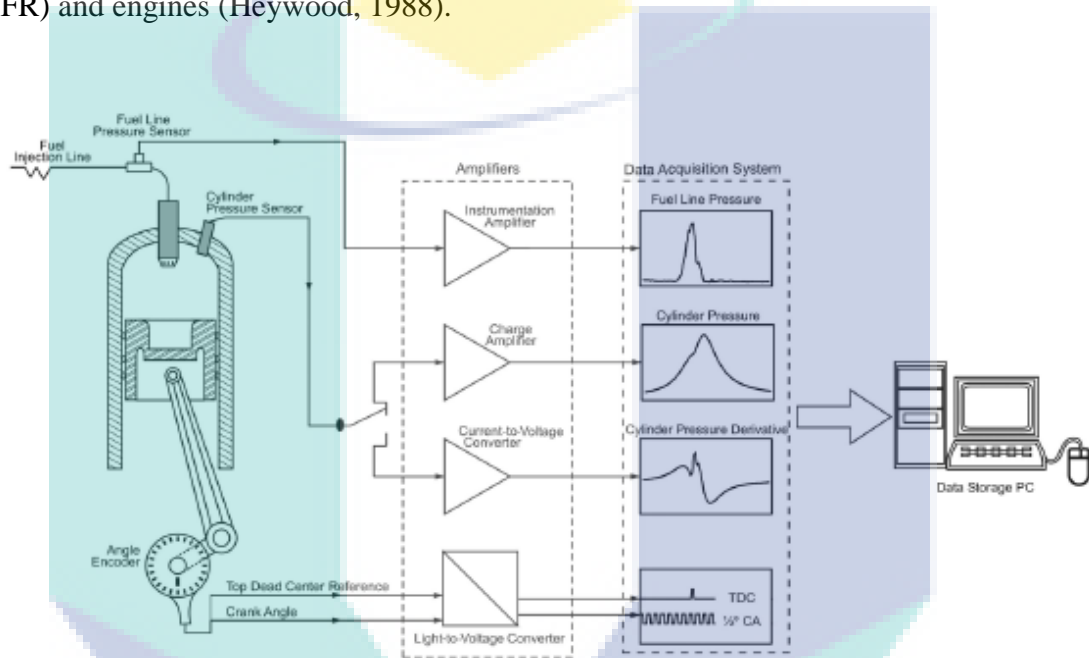
Figure 2.2   A typical engine indicating measurement system

Source: Bueno et al., (2012)

The measured in-cylinder pressure change per crank angle is a significant parameter for combustion characteristics besides IMEP and the peak cylinder pressure, P_{max} indicated by the combustion analyser. These specified combustion parameters are used to describe and evaluate the combustion process and characteristics within the engine cylinder, running with different types of fuel at the same engine operating condition and the engine cycle. For example, the coefficient of variation (COV) is extensively used for in-cylinder pressure time series to study and evaluate the engine cyclic variations within specific cycle numbers (Heywood, 1988).

$$\text{Coefficient of variation, COV} = \frac{s}{P} \times 100\% \qquad \qquad 2.2$$

where *s* is the standard deviation calculated from Equation (2.3);

$$\text{Standard deviation, s} = \sqrt{\frac{\sum\left(p - \bar{p}\right)^2}{x - 1}} \qquad \qquad 2.3$$

where x is the number of samples and $\bar{p}$ is the average value of the relevant parameter, p.

2.5   Cyclic Variations (CV) in Diesel Engines

The cyclic variability phenomenon in the cylinder is generally known and not well understood in internal combustion engines primarily in the case of diesel engines. Even under similar constant conditions such as the same load, similar speed, same controlled fuel and air temperatures, consecutive cycles are not similar; since the combustion process of the individual cycle does not fully possess similar pattern, resulting in slight differences in-cylinder pressure curve patterns. Combustion in internal combustion engines varies significantly from cycle-to-cycle in peak cylinder pressure, P_{max} as well as combustion period and flame speed. Also, cycle-resolved measurements including IMEP and total heat release (THR) can provide useful measures of combustion characteristics for large numbers of cycles. Therefore, whether these sets of data are treated as continuous or discrete, these similar data sets are arranged into time series since current data acquisition systems can generally record those crank angle data and cycle-resolved measurements from thousands of consecutive engine cycles (Finney et al., 2015).
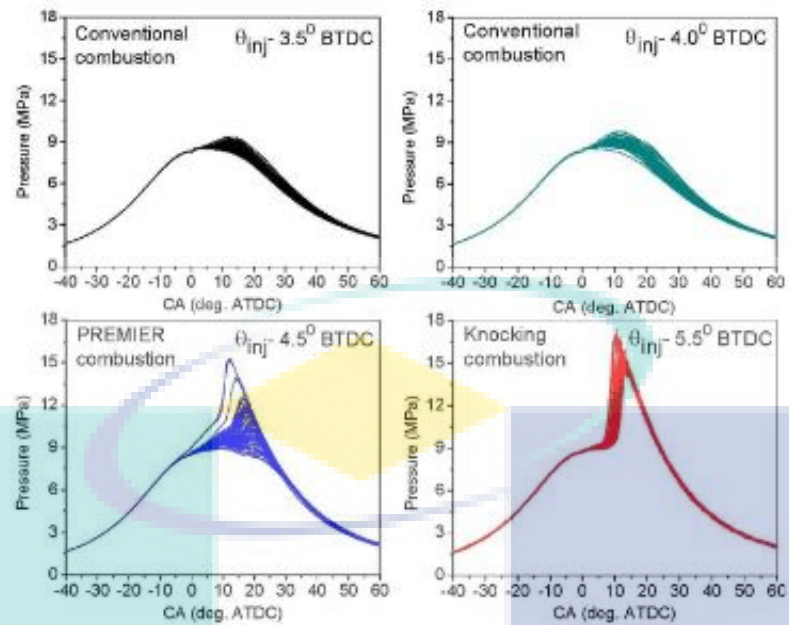
Figure 2.3　　　An example of the cyclic variations in-cylinder pressure

Source: Azimov, Tomita, & Kawahara, (2013)

CV is among important indication for internal combustion engines, especially in spark ignition (SI) engines. However, diesel engines also possess similar problem as SI engines as observed and discussed for over 30 years (Ceviz et al., 2012; Maurya & Agarwal, 2012; Rakopoulos et al., 2010a; Reyes et al., 2013; Yusri et al., 2016). Abundant proposed explanations for the causes have encompassed fuel variations, in-cylinder mixing and turbulent fluctuations as well as leading effects of late residual gas from the previous combustion cycle. Also, the argument on the cyclic variability topic continues significantly as these combustion irregularities are producing higher emissions which constrain the possible practical levels of lean-fuelling and NOx reduction methods including EGR. Consideration about cyclic variations in engines is highly significant for engine manufacturers to be included in designing more economical yet environmentally friendly engines since fuel economy and current environmental regulation trends are the main issues to be achieved. As an example, in the present case, the directions for engine manufacturers to optimise fuel economy with lower NOx emissions are continuous to be achieved with the adaptation on lean-fuelling and NOx reduction methods (Johnson, 2015; Maunula, 2013; Tadano et al., 2014). However, in many cases, cyclic variations occur continuously even with employment of lean-fuelling and EGR which reduces the operational efficiency at those operating conditions.

Figure 2.3 presents the example of in-cylinder pressure cyclic variations for consecutive cycles during the engine operation. Recent research works have discovered that the engine combustion cyclic variations under lean-fuelling demonstrate irregularity patterns as the result of noise nonlinear combustion instabilities (Janakiraman, Nguyen, & Assanis, 2013; Rakopoulos, Rakopoulos, & Giakoumis, 2010b; Wendeker et al., 2003; Yang et al., 2016). These irregularities are much influenced by the effects of late residual gas and noise agitations to the engine parameters. Since these dynamical noises are ambiguous underlying behind these irregular patterns, it is quite difficult to determine the pattern changes when the minimal changes of the engine parameters occur significantly.
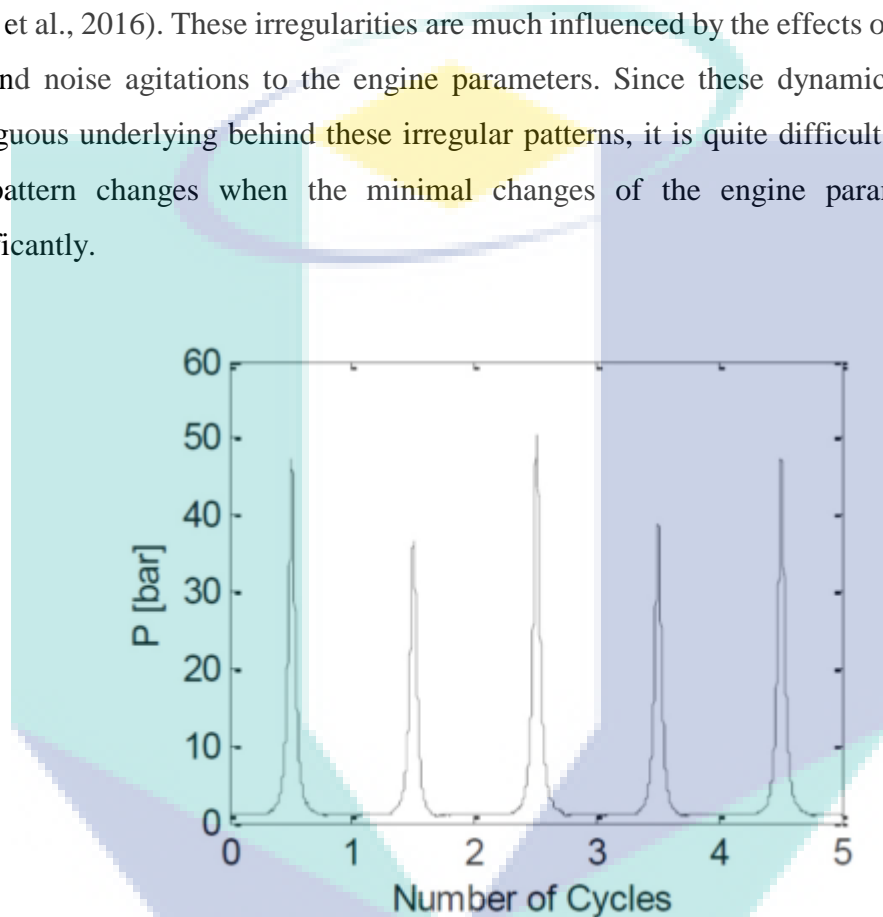
Figure 2.4   The n-cylinder pressure cyclic variations

Source: Ding et al., (2015)

Previous studies had been conducted to assess and reduce or exclude the cyclic variation from taking place. It is necessary that when controlling the cyclic variations, particular aspects could be improved including engine drivability as well as fuel consumption and harmful gas emissions level. Noise due to engine irregularity patterns could also be reduced. The most interesting analysis of engine parameters is cylinder pressure-time history from one cycle to another, completing 720° of crankshaft rotation) as shown in Figure 2.4 which provides a practical and direct measure of combustion, in addition, to characterise the first movement of the engine crankshaft corresponding to the

measured cylinder pressure. In most cases including under steady-state condition, actual cylinder pressure data demonstrates overall cyclic variability significantly. The flame advance and constant propagation obviously vary, cycle by cycle, since the differences in cycle to cycle occur considerably corresponding to the cylinder pressure shape, mass fraction burned (MFB) curves and volume fraction enflamed. Most of the flame growth tendency highly depends on the original mixture motion and fuel-air composition during combustion. These varying parameters are most responsible in influencing the cyclic variability in consecutive cycles either in any given cylinder or from cylinder to cylinder.
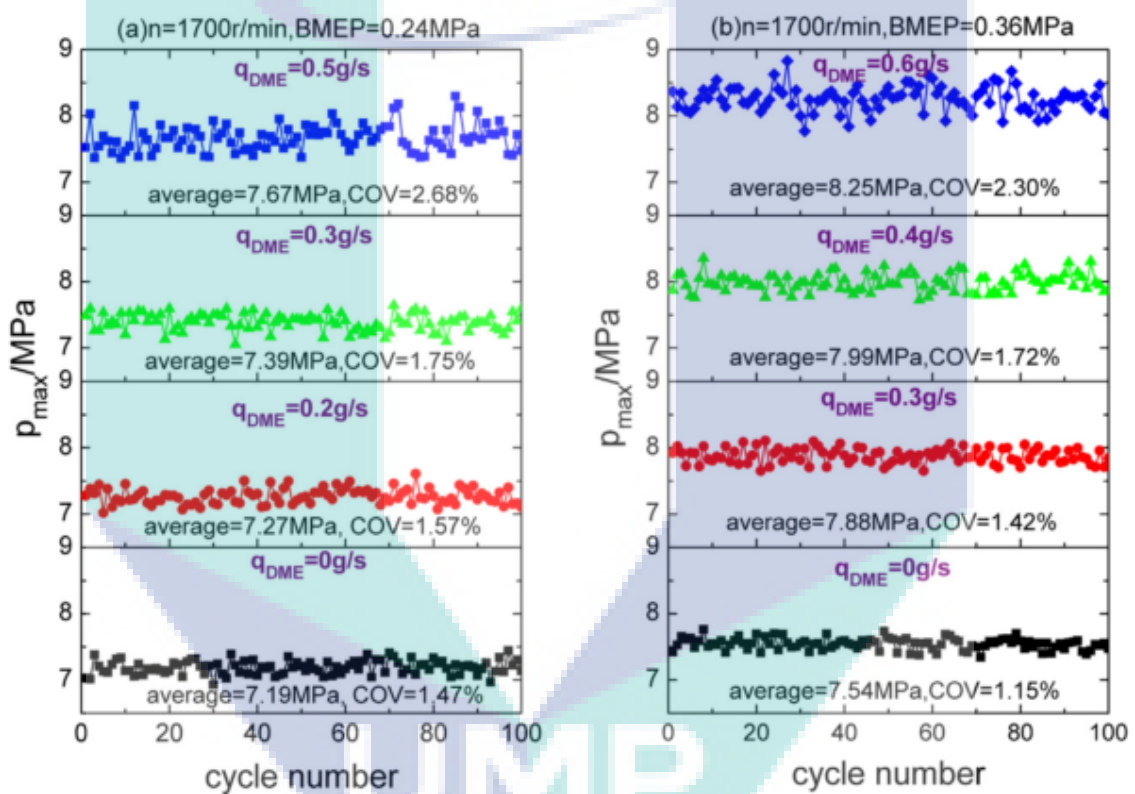
Figure 2.5   Peak cylinder pressure during 100 consecutive cycles

Source: Wang et al. (2015)

Those important parameters govern the early stages of flame development after the fuel is injected into the combustion chamber and mixed with the air homogenously. This represents how important is the cycle-to-cycle and cylinder-to-cylinder variability influencing combustion characteristics which may prevent the exceeding limit cycles in engine operating condition.

37

Observation on peak cylinder pressure, P_{max} versus cycle number as shown in Figure 2.5 during consecutive operating cycles from a diesel engine, exhibits meaningful existence of cyclic variability. Since the pressure advance from the start of combustion (SOC) until the end of combustion (EOC) is highly associated with the combustion process, cycle-to-cycle variations in individual cylinders is definitely occurring in the combustion process (Obed et al., 2016; Maurya, Saxena, & Akhil, 2016; Dimitrios et al., 2016). Besides these cyclic variabilities occurring in each cylinder, there can be substantial differences in the pressure advance during the combustion process between the cylinders in a multi-cylinder engine. When the mixture composition variability of fuel and air is self-ignited within the cylinder, cyclic variations is formed during the combustion process (Reyes et al., 2013). The profile of cycle-to-cycle variations is exactly transformed from the amounts of air and fuel delivered to the cylinder.

2.5.1   Parameters of Cyclic Variations in Diesel Engines

Cyclic variations (CV) are developed from the combustion process in the compression-ignition and spark-ignition engines when the engine operating conditions achieve the fundamental limits including lean flammability (Heywood, 1988). These parameters could indicate the actual engine behaviours for the output characteristics such as output power and exhaust emissions. There were many studies conducted on the cycle-to-cycle variations of pressure in spark-ignition and diesel engines operating with neat gasoline (Xin et al., 2013), neat diesel (Ng, Kiat, & Gan, 2012), neat biodiesel, biodiesel blends (Obed et al., 2016), and alcohol blends including butanol (Dimitrios et al., 2016), ethanol (Sen et al., 2014) and methanol (Yaopeng et al., 2016). Those studies were important to enhance a better understanding of the various parameters that could relate to the combustion process and develop some effective control strategies for combustion enhancement. Among essential factors that could much influence the average in-cylinder pressure level and cycle-to-cycle variations include types of fuel, fuel-air ratio during combustion, amount of recycled gases drawn to the engine cylinder and aerodynamic engine designs (Chen et al., 2015; Heywood, 1988; Yusri et al., 2016).

One of the important parameters to indicate the cyclic variations is in-cylinder pressure during fuel combustion (Finney et al., 2015). The cylinder pressure is measured

by mounting a pressure sensor to the cylinder for the individual cycle at each crank angle degree (deg.CA) interval. For the crank angle, the crank angle sensor is attached to the flywheel of the engine. Considerable cylinder pressure related parameters could be retrieved from the measured cylinder pressure history, which could indicate the cyclic variations with certainty. Some important measured cylinder pressure related variables include:

i.   In-cylinder peak pressure, P_{max}
ii.   In-cylinder peak pressure is occurring at the crank angle interval for the individual cycles.
iii. Crank angle degree (CAD) in which in-cylinder peak pressure occurs for individual cycles.
iv.   Maximum pressure rise rate (PRR_{max}), dP/d max.
v.   Indicated mean effective pressure (IMEP) for each cycle.
vi.   Combustion duration

Other than that, the heat release rate (HRR) and the mass fraction burned (MFB) rate related variables are also retrieved to indicate cyclic variations. Various significant combustion related parameters include:

i.   Mass fraction burned occurrence of 5%, MFB5
ii.   Mass fraction burned occurrence of 10%, MFB10
iii. Mass fraction burned occurrence of 50%, MFB50
iv.   Mass fraction burned occurrence of 90%, MFB90

Pressure related parameters are the simplest yet achievable form to measure and indicate the straightforward effect of the cyclic variations from input associated parameters such as fuel variations. On the other hand, the cylinder pressure pertaining parameters are most influenced by changing volume, crevice effect and blow-by gas (Heywood, 1988). Also, the heat release analysis produces the heat release related parameters which indicates the fuel burning history of the individual cycles. However, more attention is required on the variables analysis involving the complex correlation between combustion rate variations and cylinder pressure variations. Many previous research works have used IMEP as the cyclic variation indicator to measure and evaluate

the level of variation experience by an engine at a specific engine speed and load (Maurya et al., 2016; Pham et al., 2014; Wang et al., 2015). The IMEP for 4-stroke engine indicates work output related to the cylinder pressure in the cycles. Also, use of pressure related variables is the modest choice and easy to measure for evaluating the cyclic variations occurring in the cylinder (Obed et al., 2016; Dimitrios et al., 2016). Other than that, a coefficient of variation (COV) of IMEP from the cyclic variations which achieved greater than 10% is perceptible to a driver as a sign of descent in vehicle drivability.

2.5.2 Effects of Engine Variables on Cyclic Variations

Cyclic variations in combustion occur during the early stages of the combustion process. Influence of engine variables on combustion variations have been investigated in many previous studies (Ding et al., 2015; Guardiola et al., 2017; Jung & Iida, 2017; Najafabadi & Dynamics, 2017; You-cheng et al., 2015). There are two main factor groups of engines operating and design variables, namely chemical and physical factors that can be divided into four areas;

i.   Mixture composition;
ii.   Spark and spark plug;
iii.   In-cylinder mixture motion;
iv.   Cyclic cylinder is charging related issues.

Chemical factors including mixture composition and in-cylinder mixture motion determine the composition of trapped cylinder charge with related variables such as the type of fuel, equivalence ratio, overall fraction of diluents, mean flow velocity and flow patterns. Those listed factors were justified to influence the cyclic variations by affecting the laminar flame speeds and expansion velocity. Equivalence ratio and a fraction of diluents are factors that mainly relate with the deterministic nature of cyclic variation; therefore, their control is of the primary objective as it gives the potential opportunity to improve fuel economy and engine-out emissions.

Cyclic variations occur from the time of spark to the establishment of a fully developed flame (Soltau, 1960). This is the period in which the developing flame kernel is susceptible to factors that cause cyclic variations. Cyclic variations of the turbulence

level constitute a significant cause for cycle-to-cycle variations in combustion. Moreover, incomplete mixing of fuel/air and residual contribute to cyclic variations in combustion (Jaat et al., 2016). Also, the increase of residuals results in increased cyclic pressure variability. Engine speed also contributes to cyclic variations in combustion, where increasing the engine speed results in an increase in flame speeds and cyclic flame speed variations. Increase in turbulence has also been attributed to engine speed, and higher turbulence is the main reason for the increase in flame speed variations. Panagiotis et al. (2016) in his paper obtained experimental results from 145 consecutive individual cycles (Kyrtatos, Brückner, & Boulouchos, 2016). His findings included mass fraction burn durations, peak cylinder pressures, crank angles of peak pressure as well as heat release rate and ignition delay. He determined the mean and standard deviation for each of the above quantities. For the most part, the results were consistent with a normal distribution. On the other hand, physical factors are related with the physical conditions under which combustion proceeds and can also affect the cycle-to-cycle combustion variations. Note that some factors such as the spark plug design and the type of ignition system may affect the level of cyclic variations. However, those variables do not vary from one cycle to another. These factors are combustion chamber geometry, ignition system, compression ratio, engine speed, mixture preparation and motion. The factors that influence cyclic variability are reviewed in the next section. In this thesis, there are two main areas of interest including the cyclic variations of the different type of fuels and cyclic in-cylinder motion and charging for 200 cycles. Therefore, the following discussion focuses on the factors included in those two areas.

2.5.2.1 Mixture composition

Mixture composition of fuel is characterised by its excess air coefficient, which is the ratio of air supplied to the quantity required at different engine speeds and loads to produce engine power. Therefore, a constant volume of air supply and fuel injected mix homogeneously in the combustion chamber are required to maintain engine power output (Atkins, 2009). This will reduce the possibility of the higher cyclic variations of cylinder pressure occur in engine operation. Some of the mixture composition parameters are described in details:

2.5.2.2 Different types of fuel

Different types of fuel either in liquid or gaseous phase can be injected in diesel and SI engines. Diesel, biodiesel, gasoline, methane, hydrogen and liquid petroleum gas (LPG) are the most extensively used fuels in the literature. Each of these fuels has different chemical and physical properties that affect different combustion process, emission characteristics as well as the variations (Datta & Mandal, 2016a; Park & Lee, 2013). However, it is acknowledged that fuels with richer oxygen and hydrogen content possess faster burning rate and lower combustion variability due to the high flame velocity of O_2 and H_2 (Labeckas, Slavinskas, & Mažeika, 2014b). The investigation on the impact of fuel type on cyclic variations using a variety of liquid fuels from gasoline, benzene to methanol are compared with gaseous fuels including coal gas, butane and methane using a single cylinder diesel engine (Gurgen et al., 2017; Ji, Zhang, & Wang, 2013; Sen et al., 2014). The results exhibited that town gas with higher hydrogen content produced lower combustion variations as there was no significant difference in combustion variation observed among other fuels (Montoya, Amell, & Olsen, 2016; Sehatpour et al., 2017).

2.5.2.3 Equivalence Ratio

Equivalence ratio can be defined as the ratio of the actual air-fuel ratio to the stoichiometric air-fuel ratio, which characterises the leaner or, the richer mixture ratio for the engine. Therefore, equivalence ratio value less than 1 represents a lean mixture, and the value greater than 1 represents a rich mixture. Homogeneous air-fuel mixtures that achieve closer to stoichiometric may self-ignited instantaneously when the mixture temperature exceeds the auto-ignition temperature. Hence, when the mixture achieves stoichiometric with a higher temperature than auto-ignition temperature, the period of delay of time interval known as the ignition delay or ignition lag will occur. This variable highly depends on the fuel characteristics and the equivalence ratio and normally decreases with the increasing temperature in the cylinder. Regarding air-fuel ratio, the value of equivalence ration can be calculated using Eq. (2.4).

$$\text{Equivalence ratio, ER} = \frac{\left(A/F\right)_{\text{stoichiometric}}}{\left(A/F\right)} \qquad 2.4$$

Equivalence ratio is justified as the mixture parameter that strongly contributes to the development of cyclic variations. A series of research on the engine cyclic variations mostly have shown the relation of the significant impact of equivalence ratio to the cyclic variations (Bedoya et al., 2012; Porpatham, Ramesh, & Nagalingam, 2012; Shivapuji & Dasappa, 2014). Richer mixtures of fuel-air produce higher burning rates, higher peak cylinder pressure and the minimum heat release variations (Labeckas et al., 2014b).

2.5.2.4 In-cylinder Mixture Motion

Other engine physical factors such as intake manifolds connected to the engine also suffer the stochastic variations from one cycle to the next. The mixture motion related factors contribute to significant impact on the development of the cyclic variations in the engine performance. Since the presence of turbulence is unavoidable in the cylinder motion, cyclic variation in the engine cannot be considerably eliminated. Therefore, various engine flow controls and flow geometries have been introduced to minimise and control the effect of turbulence. Inevitable turbulence occurring in the cylinder has two major impacts. Firstly, the turbulence accelerates the premixed combustion by increasing the flame front area and transports the heat and fuel mass rapidly between the burned and unburned charge. Secondly, the arbitrary flow patterns in the turbulence cause fluctuations in the magnitude and direction of the charge velocity in the spark gap region. These effects highly depend on other factors including combustion chamber geometry and the location of spark plug for SI engines. The optimum in-cylinder flow pattern is based on the engine geometry; therefore, there is a commonality between engines operating with similar combustion systems with regards to cyclic variations.

2.5.2.5 Cyclic Cylinder Charging

Fluctuations in low-frequency velocity contribute to the variation in the mean or bulk flow between individual cycles, whereas turbulence is often defined as fluctuations

in high frequency. The cyclic variation in the in-cylinder flow fields is mainly attributed to the combustion variations. Therefore, these identified factors include dissipation in turbulence, residual gaseous motion, intake port flow separations, fuel injection and pressure wave variations in the intake and exhaust ports contributing to the development of flow variation in the intake and the dynamical structures of in-cylinder flows (Ge, Reitz, & Willems, 2008). However, some of these identified factors may have affected the flow variations at the inlet valve closure (IVC), as beyond this point, only in-cylinder phenomenon affects the dynamical flow structures since no further external factors have influenced the cylinder. The combustion process may decrease with the increase in its cyclic variations due to the increase in the fraction of excess air as well as the exhaust gas residuals when using exhaust gas recirculation (EGR) (Heywood, 1988). As a result, the limitation in the amount of charge dilution that can be received by the engine occurs when the combustion stability is decreasing simultaneously. Moreover, engine induction systems with EGR have exhibited a distribution of residual gaseous variations when entering separable cylinders and therefore, not only suffer from cyclic variations in EGR fraction but from the variability of cylinder to cylinder (Andwari et al., 2014)

2.6   Time Series Analysis on Diesel Engine Cyclic Variations

The time series analysis involves a range of data into various disciplines, from finance to engineering and earth sciences, and its development covers different aspects namely; the assumption of a stochastic or deterministic process, and analysis in the time and frequency domain (Kugiumtzis & Tsimpiris, 2010). In many applications, specifically climate, seismology, physiology and economic involving higher complexity data in the systems, the development of data modelling can be a challenging task. Therefore it is necessary to interpret or compress a series of complex data into some extracted features or measures that can be explained into simple descriptive statistics. Also, the results may involve the vast number of time series data, as examples, consecutive segments from the fragmented of a long physiological signal, such as heartbeat signals from an electrocardiogram (ECG) and electroencephalogram (EEG) as well as multiple stock indices in stock exchanges. Since analysis on combustion characteristics including peak cylinder pressure, IMEP and total heat release provide a global measure of combustion performance for a large number of cycles, those data are treated as continuous or discrete which been arranged into a time series (Finney et al.,

2015). Therefore, these arrangements provide immense opportunities for statistical and time series analysis to be further studied. Several conventional time-series analysis methods have been applied to the analysis of engine measurements including autocorrelation and Fourier analysis (Rakopoulos, Giakoumis, & Rakopoulos, 2008; Shehata, 2010; Tily & Brace, 2011).

There are many challenges in handling these data sources including processes to determine to characterise, discriminate or cluster the time series by the assessed measures (Kugiumtzis & Tsimpiris, 2010). For example, fragmented heart rate variability (HRV) signals from ECG, EEG and spatial vectorcardiogram (VCG) in order to assess overall cardiac health with the further dynamical analysis, including non linear HRV (Vandeput, 2010), neural network (Chen & Yang, 2012c), recurrence plot (RP) (Mohebbi, Ghassemian, & Asl, 2011) and multiscale RQA (Yang, 2011). Also, different types of measures have been applied to economic and financial time series in order to compare currency exchange rates at different periods or to each other, including non-linear time series analysis (NLTSA) (Strozzi, Zaldívar, & Zbilut, 2002), and in chaos analytical of gross domestic product (GDP) (Kříž, 2014). This approves that none of the existing commercial software or open source packages are in line to those problems and generally they provide partial access, as an example, computing some specific measures, and the user has to write additional code to complete the detailed analysis.

Recently, previous studies on time series analysis have been introduced into analysis on diesel engines involves cyclic variations and determinism results (Obed et al., 2016; Ding et al., 2015; Keskinen, Vuorinen, & Kaario, 2016; Litak & Longwic, 2009b; Longwic, Litak, & Sen, 2009a). Typically, time series of in-cylinder pressure, peak cylinder pressure (P_{max}), indicated mean effective pressure (IMEP) or heat release rate (HRR) is feasible to describe the various rules of combustion systems in internal combustion engines (Yang et al., 2016). For examples, wavelet analysis also was used to characterise the dynamics of cyclic variations (CV) in diesel engines (Obed et al., 2016) and SI engines (Sen, Zheng, & Huang, 2011; Tily & Brace, 2011; Yusri et al., 2016). Also, calculated statistical analysis of combustion fluctuations is performed regarding the kurtosis of the probability density functions (Sen, Litak, Yao, & Li, 2010). The dynamic state and its advancement process of combustion system attractor in high

dimensional phase space can only be visualised into projected views of two or three-dimensional plotting.

2.6.1 Time Series Visualisation

The time series visualisation is feasible to provide one, two and three-dimensional views of the time series, including histograms. Time history plots (1D plot) are generated using some selected time series by gathering them all in one panel or plotting them separately in one figure (arranging them horizontally in one plot or subplots). This approach can be practically suitable to understand all fragments of a time series together or substitute time series and original time series together. Besides, scatter plots in two and three dimensions (2D/3D plots) can be arranged for one time series at a time. This arrangement is practicable to investigate the fundamental deterministic dynamics and able to visualise a projected view in 2D and 3D of the theorised primary attractor. Also, histogram plots are either generated into superimposed lines in one panel for the given time series or as subplots in a matrix plot of given size which displayed one histogram per time series.

2.6.2 Dynamical Invariants

Dynamical invariants can be defined as an operator whose expectation value is a constant. Among the function of the analysis in the dynamical systems is to determine the system invariants which are not sensitive to the initial conditions (Bradley & Kantz, 2015). Invariants provide the information regarding the structure of the system which executes the order on the dynamics or the signal-in-the-noise. Therefore, quantification of system variants is feasible for the physical insights corresponding to the process dynamics (Sandeep et al., 2016; Xu, Shang, & Lin, 2017).

2.6.3 Dimension

The important first step in constructing a viable phase-space representation of the dynamics is establishing the dimension of the dynamical process. There are several methods for achieving this establishment in which each method has its advantages and disadvantages. The listed methods for estimating the dimension include False Nearest

Neighbours (FNN) and dimensional saturation of a system invariant. The FNN method is feasible due to the computationally efficient and robust algorithm to establish an upper-bound on the set dimensionality. However, this method does not deliver the non-integer estimates of dimension. Also, further analysis on the slope of attractor inter-point correlation integrals can provide an estimate of the dimension. Both methods depend on access to a phase-space data representation at an arbitrary dimension, which is a particular level of dimensionality corresponding to a phase-space reconstruction defined as the embedding dimension. If the observed data is given as a single dimension (a scalar time-series measured at a single spatial location), hence the suitable option for reconstruction of phase space is time-delay embedding.

2.6.4   Time Delay Embedding

Time-delay embedding was first introduced to convert a discrete scalar time-series, s(n) into a d-dimensional vector time-series given in Eq. (2.5),

$$\mu(n) = \left[s(n) s(n+\tau) s(n+2\tau) \ldots\ldots s(n+(d-1)\tau) \right]$$ 2.5

For selecting a sensible time-delay, t for the embedding, this can be done by computing the autocorrelation of the scalar dataset and use of the value of the first zero-crossing of the autocorrelation. While this obviously cannot account for any nonlinearities in the statistical description of the interrelation between points in the time-series, it nonetheless provides a surprisingly robust initial estimate for an appropriate embedding delay as it prescribes on average the delay at which two points become statistically independent. An alternative approach for establishing a time-delay is to estimate the mutual information, M(t), between an observation at a time t and one at some later time.

This method offers an advantage by considering the nonlinearities in the data when providing the amount of information that has been added by the current observation after a previous observation. Then, when new information is not applicable, the observation data are completely independent as M(t)=0. According to Gallagher (1968), the mutual information can be represented by Eq. (2.6).

$$\text{Mutual info, } M(\tau) = \sum_{n-1}^{N} P(s(n), s(n+\tau)) \log \left[\frac{p(s(n), s(n+\tau))}{P(s(n)) P(s(n+\tau))} \right] \qquad 2.6$$

2.6.5 False Nearest Neighbour (FNN)

The method of false nearest neighbour (FNN) is used to determine the exact embedding time which is sufficient to eliminate the false crossings of an orbit (phase-space trajectory) with itself representing the result of having projected the attractor into too low a dimensional space (Keskinen et al., 2016). Therefore, the procedure in this method is to define a function of the closeness between the adjacent points which depends mainly on the geometrical arrangements that been carried out by the coordinate dimensions, and then iteratively increasing the number of dimensions until there are no false nearest neighbours (FNNs).

2.6.6 Recurrence Plot (RP)

The significance of recurrent or frequent behaviours, including heart rate and seasonality, in natural processes, has been studied and presented for decades (Aceves-Fernandez et al., 2014; Josiński et al., 2016; Marwan et al., 2010). However, these recurrent behaviours are hardly visualised in time domain analysis. Thus, to solve this restraint, recurrence plot (RP) was first introduced into the dynamical system study by Eckman et al. in their distinguished 1987 paper which its function as an experimental time-series data analysing tool (Eckmann, Kamphorst, & Ruelle, 1987). However, this method was first proposed by Maizel and Lenk in the year 1981 for visualising the substantial array patterns of genetic nucleotides (Maizel & Lenk, 1981). Recurrence plots (RP) were used to visualise the quantification of recurrence patterns in a time series or sequence into a graphical presentation form to analyse the experimental data (Eckmann et al., 1987; Marwan et al., 2007).
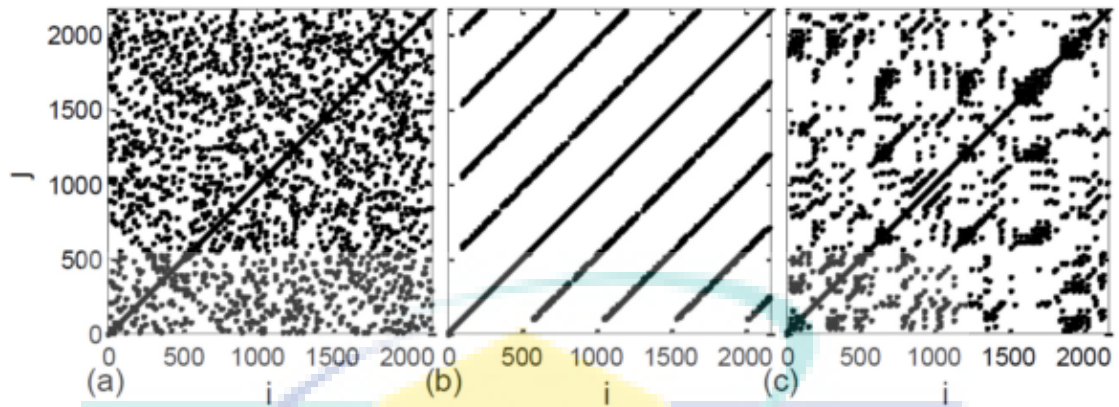
Figure 2.6   The RPs for different systems or functions; (a) the RP of white noise, (b) the RP of the sine function, (b) the RP of the Lorenz system.

Source: Yun Chen & Yang, (2012a)

An RP is a two-dimensional representation of a single trajectory as illustrated in Figure 2.6. Interestingly, these recurrence plots often reveal the correlations between the data which are not readily determined by the standard time series methods. Then, based on the RP proposal by Eckmann et al. (1987), considerable efforts have been taken to develop quantification schemes for the plots and for the patterns within them from that time. At present, there are substantial accessible quantitative recurrence plot (RP) approaches that have been applied successfully into different fields, e.g., climate variation, earth sciences (Brady, 2013; Sparavigna, 2014), cardiovascular variability (Marwan et al., 2010; Singh & Bharti, 2015), economy, neuroscience (Tošić et al., 2015), video recognition (Ouyang et al., 2014), as well as engine cyclic variations (Mhalsekar, Rao, & Gangadharan, 2010; Sen et al., 2008). Other than that, recurrence plot (RP) has the following advantages and disadvantages as listed in Table 2.3 and Table 2.4.

Table 2.3   Advantages of recurrence plot (RP) as a time series analysis tool

Advantages	Ref.
Applicable to short and nonstationary data	(Jie et al., 2013; Yang & Liu, 2013)
Recurrence plot visualise the recurrent behaviour of dynamical systems	(Yun Chen & Yang, 2012b)
Allows more efficient interpretation of the rare events	(Uribe et al., 2014)
Obtain qualitative information from RPs	(Ding et al., 2015)

49

Table 2.4   Disadvantages of recurrence plot (RP) as a time series analysis tool

Disadvantages	Ref.
Requires sufficient resolution to display the graphical patterns	(Constantin-Ovidiu et al., 2017)
More profound knowledge to detect and interpret the pattern and structures	(Uribe et al., 2014)

This recurrence plot (RP) tool allows the above assumptions are testing which gives substantial useful information and describes whether the assumptions are satisfactory or otherwise. According to Eckmann et al. (1987), recurrence plots were used to visualise time-dependent behaviour of orbits x_i in phase space, which represent the recurrence of the phase space trajectory to a state. The recurrence of states is a fundamental property of deterministic dynamical systems. Deterministic dynamical models mean the substantial mathematical objects involving larger population size that been used to model the physical phenomenon whose state changes over time. In the case of visualisation, the primary step is computing the $N \times N$- matrix by defining it as in Eq. (2.7).

$$R_{i,j} = \theta\left(\varepsilon \left\|\vec{x}(i) - \vec{x}(j)\right\|\right) \vec{x}(.) \in R^m, i, j = 1.......N \qquad 2.7$$

where N is the number of states, $\vec{x}_i$ and $\vec{x}_j$ are the subsequence observed at the position i and j, correspondingly, $\|\cdot\|$ is the norm (e.g. Euclidean norm) between the observations, ϵ is a threshold for closeness and θ is the Heaviside function.

2.6.7   Recurrence Quantification Analysis (RQA) on Diesel Engines

Recurrence quantification analysis (RQA) was developed by Zbilut and Webber (Zbilut, Thomasson, & Webber, 2002) and then a further study was conducted by Marwan et al. (Marwan, 2006; Marwan, 2011; Marwan & Kurths, 2005; Marwan & Meinke, 2002) to provide quantitative and statistical measures of recurrence plot (RP) analysis. Several RQA parameters include recurrence rate (RR), the maximal length of

the diagonal or vertical lines (L_{MAX} or V_{MAX}), determinism (DET), laminarity (LAM), trapping time (TT), entropy (ENTR) and the recurrence trend (TREND) used for analyzing quantitatively the in-cylinder pressure time series. This approach is paralleled with several literatures on the cycle-to-cycle variations in the engine operation (Alexa et al., 2015; Constantin-Ovidiu et al., 2017; Ding et al., 2015; Litak & Longwic, 2009b; Sen et al., 2008; Yang et al., 2016).

2.6.7.1 Recurrence rate (RR)

The recurrence rate (RR) is a measure of recurrences or density of recurrence points in the recurrence plot analysis. This rate provides the mean probability of recurrences concerning the total number of possible recurrences in the detailed system. The recurrence rate, RR is calculated using Eq (2.8).

The recurrence rate (RR) is a measure of recurrences or density of recurrence points in the recurrence plot analysis. This rate provides the mean probability of recurrences concerning the total number of possible recurrences in the detailed system. The recurrence rate, RR is calculated using Eq (2.8).

$$\text{Recurrence rate, RR} = \frac{1}{N^2} \sum_{i,j=1}^{N} R_{i,j} \qquad 2.8$$

This value corresponds to the probability that a specific state will recur.

2.6.7.2 Determinism (DET)

Determinism is a measure of the percentage of recurrence points which forms diagonal lines or line segments which are parallel to the Line of Identity (LOI). This quantitative parameter also can be described as the measure for predictability of the specific system. The characteristics of determinism are briefly described by Gao et al. (2009) and is presented in Eq. (2.9).

$$\text{Determinism, DET} = \frac{\sum_{l=l_{\min}}^{N} lP(l)}{\sum_{i,j}^{N} R_{i,j}} \qquad 2.9$$

where $P(l)$ represents the probability of finding a diagonal line of length, l in the recurrence plot analysis. Thus, this variables quantify the predictability of a designed

system, which ranges from 0 to 1. Randomness is represented by numbers close to zero while the presence of a strong signal component is indicated by those approaching the value of one. The average diagonal line length, L_{MEAN} is represented by Eq. (2.10). This variable indicates the average time corresponding to the trajectory that present close to each other, and is associated with the mean predictability time.

$$\text{Average diagonal line length, } L_{mean} = \frac{\sum_{l=l_{min}}^{N} lP(l)}{\sum_{l=l_{min}}^{N} P(l)} \quad\quad 2.10$$

2.6.7.3 Laminarity (LAM)

Laminarity (LAM) can be defined as the number of recurrence points which develop the vertical lines. This variable is related to the number of laminar states and is presented in Eq. (2.11).

$$\text{Laminarity, } LAM = \frac{\sum_{v=v_{min}}^{N} vP(v)}{\sum_{v=1}^{N} vP(v)} \qu\quad 2.11$$

where $P(v)$ is the histogram of the lengths v of the vertical lines and $P(v)$ is the frequency distribution of the lengths v of the vertical lines, which have at least a length of v min. It is noteworthy that LAM is evidence of chaotic transitions and is related to the number of laminar phases in the system (intermittency).

2.7   Conclusion

The significant progress in alcohol blends research has been reviewed and discussed. Also, the effect of each alcohol type with mineral diesel and biodiesel fuel on combustion characteristics has been revealed. Although alcohol has become more sustainable as an alternative fuel for diesel engines, there is limited usage in Malaysia and many other countries. It can be concluded that alcohols will become another potential fuel to be developed for ensuring the feasibility of the fuel in the domestic sectors as well as achieving advanced standard emissions. The alcohol technical specifications not only cover various technical aspects but also most of the aspects are interdependent.

Therefore, manufacturers are required to overcome the critical issues behind the alternative fuels including alcohols in the global trade of unconventional fuels. It is likely that, as energy sources become sustainable and renewable for the current years, more technical issues arose and needed to be systematically solved. The present review findings are summarised as follows:

i.   The blending of alcohols; butanol and ethanol with palm biodiesel is an effective method to improve the properties of B, and this blend can be used up to 20% of alcohols directly in a standard diesel engine.

ii.   It can be concluded from the literature that most alcohols are suitable for biodiesel at different blending ratios.

iii.   Most of the studies have focused on the effect of alcohols on combustion characteristics. However, the relation between the fuel properties change with alcohols, and the influence on combustion characteristics remains unclear.

iv.   In general, the alcohols can be classified as sustainable and renewable fuels.

v.   Most studies reveal that the alcohols are potentially in improving the physical properties of biodiesel fuels which are less favourable than the mineral diesel fuel.

vi.   The alcohol usages are effective to improve engine combustion.

vii.   There are few studies conducted to indicate the effect of alcohols; butanol and ethanol with D and B fuels on the cyclic variation of the diesel engine at different loads and engine speeds.

viii.   It can be concluded from the literature that there are no studies conducted to analyse the P_{max} cyclic variations of the butanol and ethanol blends using recurrence plot (RP) and recurrence quantification analysis (RQA) at different loads and engine speeds.

CHAPTER 3

METHODOLOGY

3.1   Introduction

This chapter presents the employed methods and procedures in this study. Experimental works were performed to determine and evaluate the test fuels properties, different engine characteristics running with test fuels regarding performance, combustion and cyclic variations. The experimental setup and facilities for fuel properties determination, engine testing, data acquisition (DAQ) system are presented in this chapter. The computation of the cyclic variation is presented in the numerical work method. Also, the engine cyclic variation analysis based on the in-cylinder pressure time series using the coefficient of variations (COVs) is also presented.

3.2   Strategy of Framework

There are two main components of the experimental work—engine testing and engine cyclic variation analysis. According to this framework, the results are presented in a consistent sequence. Figure 3.1 presents the flowchart of the framework strategy for the current research methodology.

54
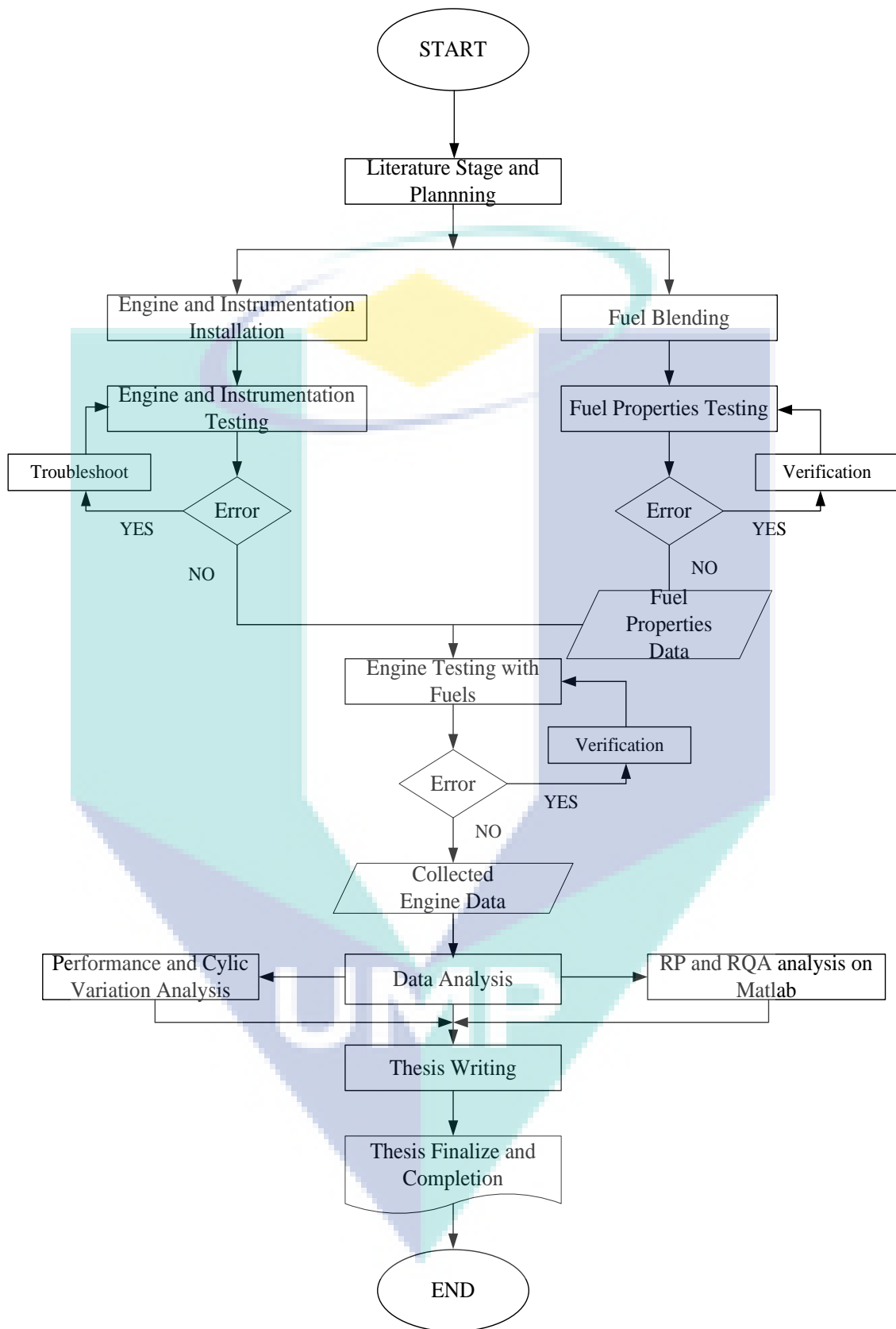
Figure 3.1   Flow chart of the framework strategy

3.3   Base Fuels

Two base fuels had been used in the engine testing. In Figure 3.2, the first reference fuel was pure mineral diesel (100% diesel) denoted as "D" which was procured from a local supplier and the second reference fuel was pure palm biodiesel (100% biodiesel) or palm oil methyl ester biodiesel designed as "B", purchased from Mission Biotechnologies Sdn. Bhd. Both fuels provided by the respective company were complying with EN 14214. During the experimental study, mineral diesel-alcohol and palm biodiesel-alcohol blends were labelled as DXYY and BXYY, where D and B represent mineral diesel and palm biodiesel, X represents the type of alcohol (butanol=Bu/ethanol=E) and YY signifies the volumetric blending percentage of alcohol base content, mixed with mineral diesel (D) and palm biodiesel (B).
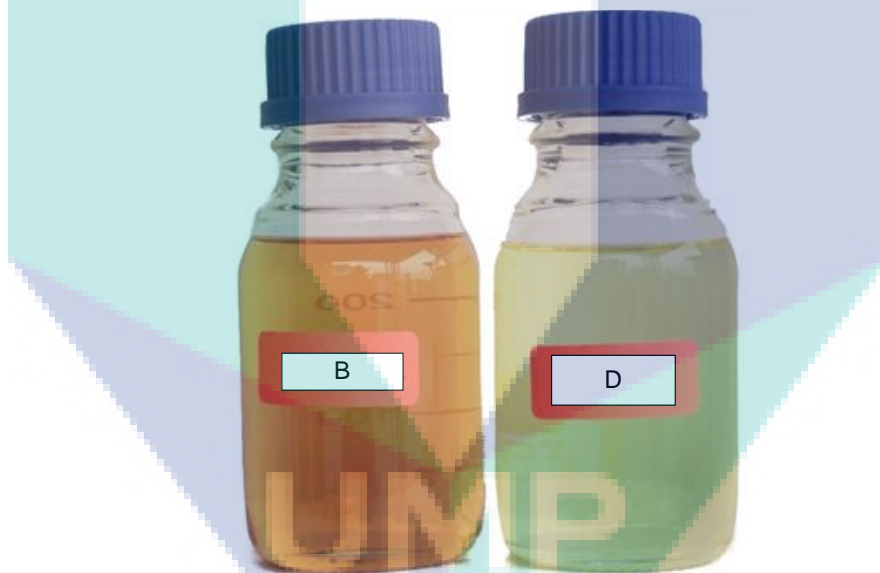
Figure 3.2   Palm biodiesel (B) and mineral diesel (D)

Table 3.1 lists the fuel properties measured of base fuels including D and B fuels. As an example, DBu10 represents the volumetric blend of 10% butanol with 90% mineral diesel for diesel-butanol blends. Then, butanol and ethanol, alcohol-based additives in 10% by volume were diluted homogeneously with D and B using a homogeniser. Thesetest fuel samples were tested in the laboratory to determine their physicochemical properties to conform to ASTM standards.

Table 3.1   Base fuels properties measured

Properties	Testing Method	Mineral diesel (D)	Palm biodiesel (B)
Density (g/cm^3)	ASTM D287	0.8264	0.8671
Viscosity (mm^2/s)	ASTM D445	5.144	7.495
Energy Content (MJ/kg)	ASTM D240.	44.8	38.6
Cetane Number	ASTM D613	47.8	52.8
Flash Point (°C)	ASTM D93	60	80

3.4   Base Alcohols

There were two alcohol-based fuels, butanol and ethanol used in the study to be diluted in 10% by volume with two base fuels; D and B fuels in a diesel engine. The selection of the two alcohol-based fuels provides a significant part to prior studies including the engine performance, fuel combustion characteristics and the emission reduction as well as engine cyclic variations during combustion. The properties of butanol and ethanol are described in Table 3.2.

Table 3.2   Base alcohols properties

Physical Properties	Unit of Measurement	Standard/ method	Butanol*	Ethanol**
Chemical name	-		Methyl alcohol	Ethyl alcohol
Chemical formula	-		$(CH_2)_3OH\ CH_3$	C_2H_5OH
Molar mass	g/mol		74.12	46.07
Density	g/cm^3 at 20 °C		0.81	0.790 – 0.793
Viscosity, dynamic	mPa.s at 20 °C		2.95	1.2
Flash Point	°C	DIN 51755	34	12
Boiling point	°C at 1,013 hPa	DIN 53171	116- 118	78.3
Vapour pressure	hPa at 20 °C		6.7	59

Table 3.2   Continued

Physical Properties	Unit of Measurement	Standard/ method	Butanol*	Ethanol**
Water solubility	g/l at 20 °C	OECD Test guideline 105	66	(20 °C) soluble
Ignition temperature	°C	DIN 51794	340	425

Source: *http://www.merckmillipore.com/malaysia/chemicals/methanol
         **http://www.merckmillipore.com/MY/en/product/Ethanol

3.5   Test Fuels Preparation of the Fuel Blends and Analysis of Basic Parameters

In this study, the neat palm oil methyl ester (POME) was purchased from local industry in Pahang, Malaysia, while a commercial fuel supplier supplied the neat mineral diesel. Whereas, both butanol and ethanol were purchased from Merck through local agent company in Pahang. Both butanol and ethanol blends were prepared by pouring anhydrous (99.9% purity) butanol and ethanol into the neat D and B beaker in 10/90 proportions by volume and mixing them to ensure the fuel blends were inhomogeneous conditions. During the mixing process, the fuel blends were stirred using an electric, magnetic stirrer at 200 rpm for 20 minutes. Then, the fuel blends were stirred continuously for an additional 20 minutes and left for 30 minutes to ensure the fuel blends reached an equilibrium state at room temperature before the fuel blends were subjected to further fuel testing. The use of butanol and ethanol also have some limitations, such as lower lubricity, reduction in ignitability, low cetane number and miscibility but higher in volatility and cooling effects which may lead to increased unburned hydrocarbon emissions. Therefore, butanol and ethanol were added separately in small concentrations of 10% ±0.1% by volume to fuel blends, designated by DBu10 (90 % diesel + 10% butanol), BBu10 (90 % palm biodiesel + 10% butanol), DE10 (90 % diesel + 10% ethanol), and BE10 (90 % palm biodiesel + 10% ethanol) fuels as shown in Figure 3.3.

Figure 3.3   Mineral diesel (D), palm biodiesel (B), DBu10 (90 % diesel + 10% butanol), BBu10 (90 % palm biodiesel + 10% butanol), DE10 (90 % diesel + 10% ethanol), and BE10 (90 % palm biodiesel + 10% ethanol)

The density, viscosity, net calorific values and Cetane number of the test fuel blends were determined by taking into account the mixing percentage of each component and respective data of anhydrous butanol and ethanol, mineral diesel (D) and palm biodiesel (B) as listed in Table 4.1. In this study, the density of the fuel samples was measured at 15 °C using a KEM Portable Density/Specific Gravity Meter (model DA-130N), while the determination of viscosity for each fuel was carried out using a digital constant temperature kinematic viscosity bath (model K23376 KV1000) at a temperature of 40±0.1 °C. Also, analysis on the energy content is primarily needed since it related directly to the engine power. Therefore, an Oxygen Bomb Calorimeter, model 6772 (Parr instrument company, USA), was used to determine the fuel heating/calorific value.

3.6   Engine Testing Experimental Details

This section is dedicated to describing the engine testing experimental setups and the included important facilities. Experimental setups describe the engine test bench and eddy-current dynamometer as well as the main components for measurement, including the cylinder pressure, fuel flow, engine torque and speed. Detailed descriptions of the data acquisition (DAQ) system and sensor attachment are also provided in this section. Fuel engine testing was conducted at Automotive Engine Centre (AEC) laboratory located in Universiti Malaysia Pahang. Figure 3.4 shows the picture of engine testing bench in AEC lab. Figure 3.5 shows the schematic diagram of the test bench including

a Yanmar TF120M single cylinder, horizontal diesel engine with water cooling system, a 10 kW eddy current dynamometer equipped with dump load, two fuel beakers which can accommodate up to 1 litre, a Meriam laminar flow element (LFE) for air intake system and TFX data acquisition (DAQ) system.
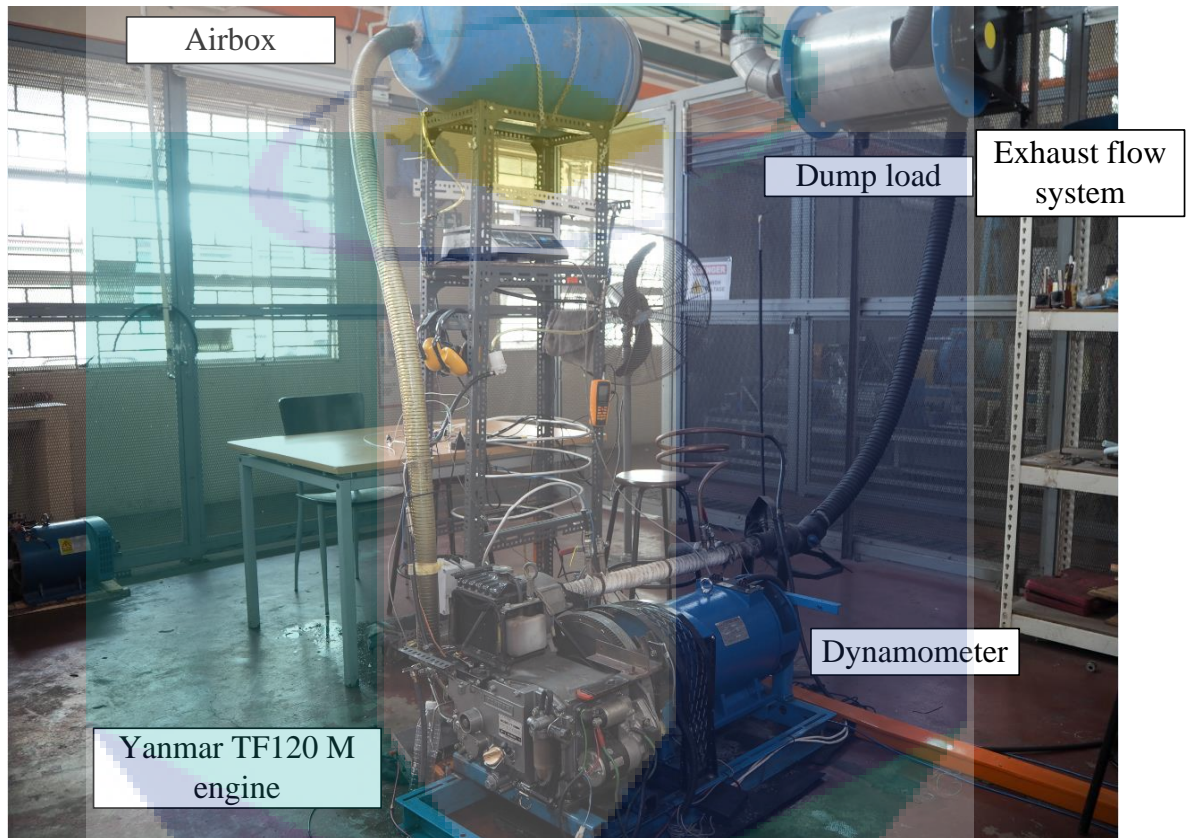
Figure 3.4   Engine test bench
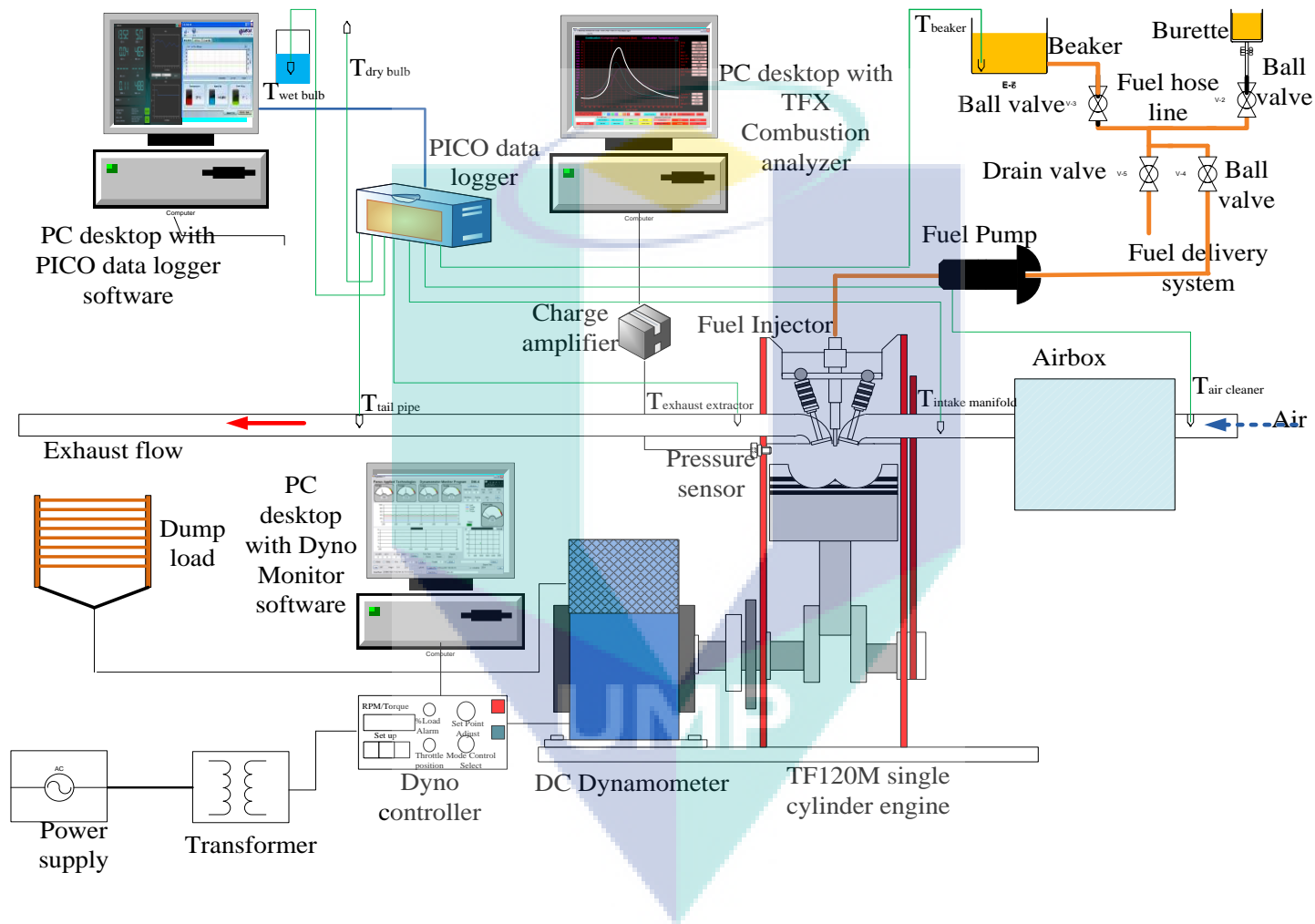
Figure 3.5   Engine testing facilities schematic diagram

3.6.1 Test Engine

The experimental studies were primarily conducted using a Yanmar TF120M diesel engine, which was naturally aspirated, water-cooled, and equipped with a fuel injection system. The engine specifications are listed in Table 3.3.

Table 3.3   Engine specifications

Parameter	Value
Type	Horizontal, water-cooled 4 stroke diesel engine diesel
Combustion system	Direct injection
Number of cylinders	1
Bore (mm)	92
Stroke (mm)	96
Compression ratio	17.7
Displacement (ℓ)	0.638
Connecting rod length (mm)	150
Rated continuous output, hp / rpm (kW)	10.5 / 2400 (7.8)
Maximum torque, kgf.m / rpm	4.42 /1800
Injection timing, deg	bTDC 17.0
Injection pressure, kg/cm^2	200
Injection hole diameter (mm) x number of holes	0.26 x 4

Source: Yanmar (2014)

3.6.2 Dynamometer and Drive Trains

A 15 kW eddy-current, generator dynamometer model BD-15kW from Focus Applied Technologies Sdn Bhd. with a universal controller model DC5 was used to load the engine as shown in Figure 3.5. The generator in this dynamometer is nominally rated at 7.5 kW electrical at 1500 rpm and 15 kW mechanical at 2000 rpm. Main specifications for the dynamometer are listed in Table 3.4. Also, the engine speed is controlled by the throttle engine position lever to increase or decrease the engine speed when operating the dynamometer. Before experimenting, the dynamometer was calibrateded in March 2016 using levers and weights that allow clear and precise adjustment. The torque measuring

chain had been checked regardless of whether the brake was at a standstill or rotating at the same time.

Table 3.4   Specifications for a 15 kW dynamometer model BD-15 kW

Parameter	Value
Model	AC synchronous generator
Type	ST-7.5
Power	7.5 kW
Rated voltage	230/115 V
Current	65.2
Frequency	50 Hz

Source:Focus Applied Technologies, (2017)

3.6.3   Engine and Dynamometer Controller

A dynamometer controller model DC5-10 as depicted in Figure 3.5 with torque, load and speed indication was used to control the dynamometer system, and cables wired the engine itself which was positioned in the control test room to the dynamometer. Main specifications of the dynamometer controller are listed in Table 3.5.

By loading the dynamometer electrically, the control achieved was reliable at different load and speed of the engine (torque/ speed characteristics of the engine). As for torque indication, the dynamometer stator assembly was mounted with a universal precision grade load cell transducer to give an input signal to the torque indication circuitry. When an excitation current was passed through the dynamometer coil, the engine was decelerated, and as a result, an equal and opposite reaction was exerted on the dynamometer stator assembly. This reaction torque is displayed on the torque indication display in the desired unit of torque measurements such as Nm or kgm. As for the engine, the controller uses a throttle servo motor which can directly drive the engine throttle for the speed control.

A hundred per cent (100%) load is expected to achieve 65 Nm above 1500 rpm. The dynamometer sizing is chosen to cover the full-load engine operation for the whole range of engine speeds as the characteristic parts of the engine curve must fall within the characteristic curve of the dynamometer. While for rpm indication, a magnetic pick-up

sensor is mounted 0.5 ~ 1 mm from the face of 30 teeth gear wheel which attached to the shaft on the non-driving end of the dynamometer. As the prime mover starts, the dynamometer shaft starts rotating, the sensor senses the passing teeth of the gear wheel and displays the speed of dynamometer, similar to engine speed in rpm. As for computer communications (displaying and recording the logging data) between the computer and dynamometer controller, serial ports are employed for the connection. The serial port communications are via RS232 which automatically sends data out in the format of speed and torque at approximately 4 Hz.

Table 3.5   A DC5-10kW dynamometer controller specification

Parameters	Value
Model	DC5-10kW
Voltage	120 VAC
Frequency	50 to 60 Hz
Current Draw	13 A max
Controller output	Resistance: 10 Ω minimum
	Power: 1000 W maximum
	Voltage: 50 or 100 V nominal
	Current: 3A to 10 A maximum
Inputs	Speed: 1 to 60 pulse per revolution
	24,000 rpm maximum
	Load Cell: 100 to 500 Ω
	5 or 10 V excitation
Operating temperature	10 to 40 °C

Source: Focus Applied Technologies, (2017)

3.6.4   Cooling Systems for Engine and Dynamometer

Most of the test benches were provided with two type of cooling systems; engine cooling and dynamometer cooling systems to cool the engine parts and the instrumentation parts. The specific engine operating conditions rely on variable engine parameters which are controlled by the cooling systems, providing a well-balanced energy condition (Martyr & Plint, 2007). The engine cooling system employs a radiator system with a 2.3-liter water tank to cool down the hot engine surface by dissipating the heat from the engine. The hot water is shifted from the engine into other parts of the engine cooling system and is cooled by using a fan. This process runs continuously with the engine running with or without load from the dynamometer.
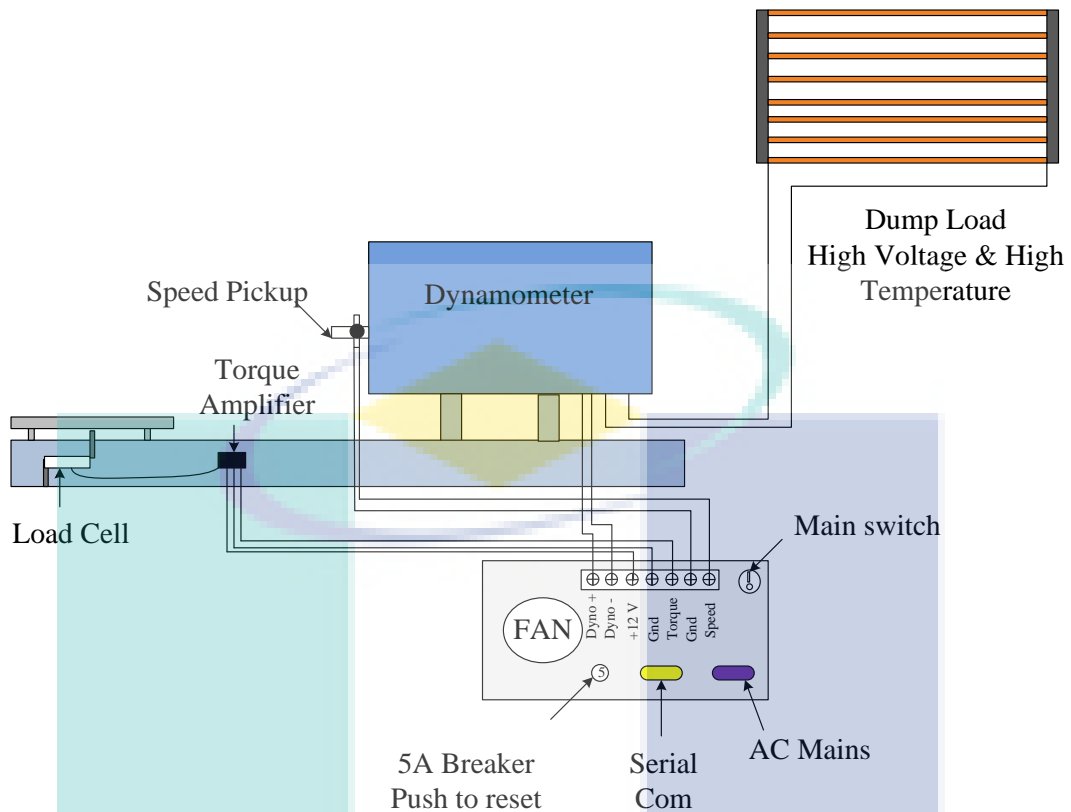
Figure 3.6   A dump load for the dynamometer

Source:Focus Applied Technologies, (2017)

For safety reasons, the dynamometer had been equipped with a dump load heater system as presented in Figure 3.6. This system diverts the dump load power which turns into electricity from the engine and heats the surrounding air. The dump load heater system for the dynamometer is fabricated from high-quality industrial heater which operates at relatively high temperatures (more than 100 °C) and voltages (up to 400 VAC). Since the dump load system or heater produces high voltage, this dump load is rigidly mounted to the wall in the test rig cell.

3.6.5   Fuel Delivery and Measurement System

The fuel delivery system for the engine which starts from the beaker and burette (fuel consumption measurement), are linked to the engine with a rubber hose tubing as presented in Figure 3.5. The test fuels were stored in two 1-litre glass beakers, and a burette is located side by side and was labelled according to its content. With proper adjustment using ball valves, the fuel flowed by gravity through 3/8" diameter rubber

hose tubing and a 10-micrometre filter before entering the fuel pump. The fuel flow measurement was taken for each testing data to determine the fuel consumption by the engine for different modes and parameters. The fuel consumption for each test condition was made by controlling the ball valves at the beaker and the burette using a stopwatch. This procedure was repeatedly measured for each fuel for ten times to ensure reliability and accuracy of the results. As previously mentioned, the return fuel from the engine was at a sufficiently high temperature, as it expanded after high compression in fuel injection line; mixing with fresh fuel in the fuel line and flow again back into the engine. Two K-type thermocouples had been attached to the beaker and return fuel line to measure the fuel temperature before and after it flowed through the heat exchanger.

3.6.6 Air Intake Measurement System

Air intake measurement is one of the key elements for the engine when operating in different condition and using different fuels. As air intake properties depend on ambient pressure, relative humidity and temperature surrounding the engine, the correction factors must be considered during calculation of the actual brake power. Meriam model 50MY15-6F from Scott Peter Company was used to create laminar airflow as shown in Figure 3.4. The pressure drop across the element was measured by an airflow manometer and corrected to standard conditions when the diesel engine was operating in different engine speeds and loads.

3.6.7 Temperature Monitoring and Measuring

The engine was instrumented with six K-type thermocouple probes to measure the engine temperatures as well as exhaust extractor, fuel beaker, fuel hose tubing, air intake piping, dry bulb and wet bulb temperatures as shown in Figure 3.5. The location of these thermocouples was purposefully selected to ensure the accuracy of the measurements since these measurements were used for the combustion model and real-time monitoring to stay within testing constraints and engine limitations. An exhaust extractor and the tailpipe were insulated using Billion super-thermo 70 bandage exhaust wrap with a temperature limit of 1650 °C to keep the heat inside the exhaust extractor and tailpipe for temperature monitoring and measurement. Modifications on the engine

and components were prepared necessarily to provide the engine with all the thermocouples, without compromising the functionality of the engine.

3.6.8   Cylinder Pressure Data Acquisition (DAQ) system

Engine combustion characteristics are the main subject of this work with much of them related to engine cyclic variations with different fuels. Thus, careful selection of reliable cylinder pressure data acquisition (DAQ) system must be considered and taken into account. In this work, the cylinder pressure data acquisition (DAQ) system is supplied by TFX Engineering from the USA. The system consists an Optrand AutoPSI-S model C22294-Q pressure sensor, a magnetic type crank angle sensor, sensor interface, transfer cable and LCS data logger.
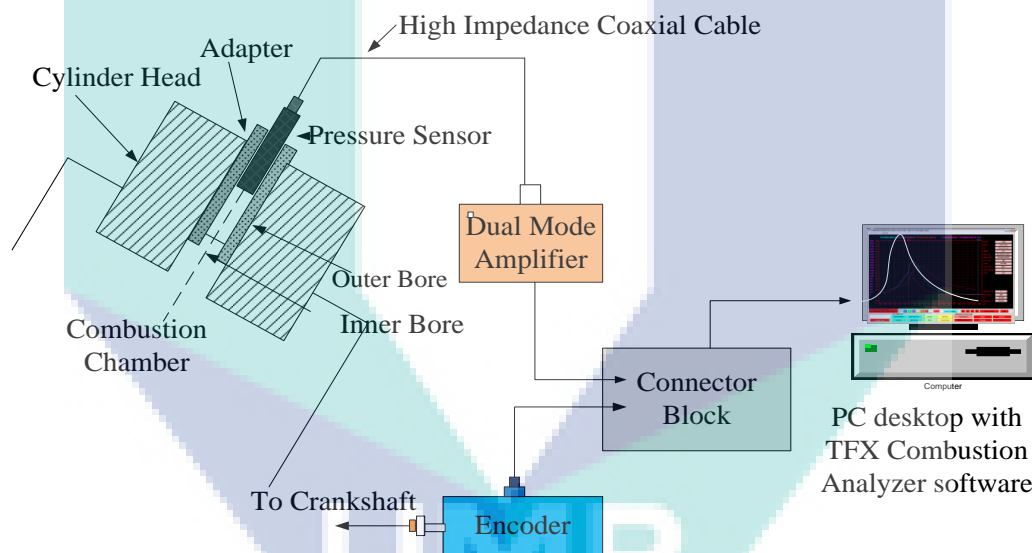
Figure 3.7   A schematic diagram for an in-cylinder pressure measurement system

Figure 3.7 illustrates a schematic diagram of the engine test bed with the instrumentations. Engine combustion characteristics were measured and computed with the use of the cylinder pressure data acquisition (DAQ) system. The cylinder pressure was mounted onto the combustion chamber incorporated with a magnetic type crank angle sensor to give the timing in crank angle degree (deg.CA) when the combustion occurred as shown in Figure 3.7.
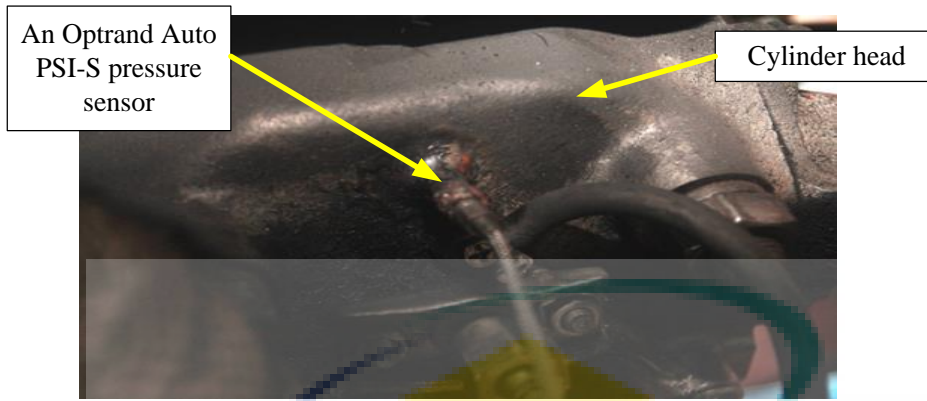
Figure 3.8   An OPTRAND AUTOPSI-S pressure sensor attached to the engine head

In this work, an Optrand AutoPSI-S model C22294-Q cylinder pressure sensor was mounted using a custom adapter attached to the cylinder head as shown in Figure 3.8. The cylinder pressure sensor specifications are listed in Table 3.6. This custom adapter was a stud bolt with a dimension of M8 x 1.25 which had been modified to accommodate the pressure sensor. The engine head was modified by drilling and tapping a hole with an M8 x 1.25 size thread from the top of the engine head to the combustion chamber. This pressure sensor was connected via a 2 m optical fibre cable to the AutoPSI signal conditioner to convert the analogue signal into digital signal.

Table 3.6   Optrand AutoPSI-S cylinder pressure sensor specification

Description	Specification
Pressure range	0 – 5000 psi
Input voltage	5V DC
Sensor output signal	Analog, 0.5 – 4.5V DC
Sensitivity	1.55 mV/psi @ 200 °C
Non-Linearity & Hysteresis	± 1% FSO (combustion), ± 0.5% FSO (non-combustion)
Operating temperature range	-40 °C to 350 °C (~660 °F)
Natural frequency	0.1Hz to 15 kHz

Source: Optrand Inc., (2017)
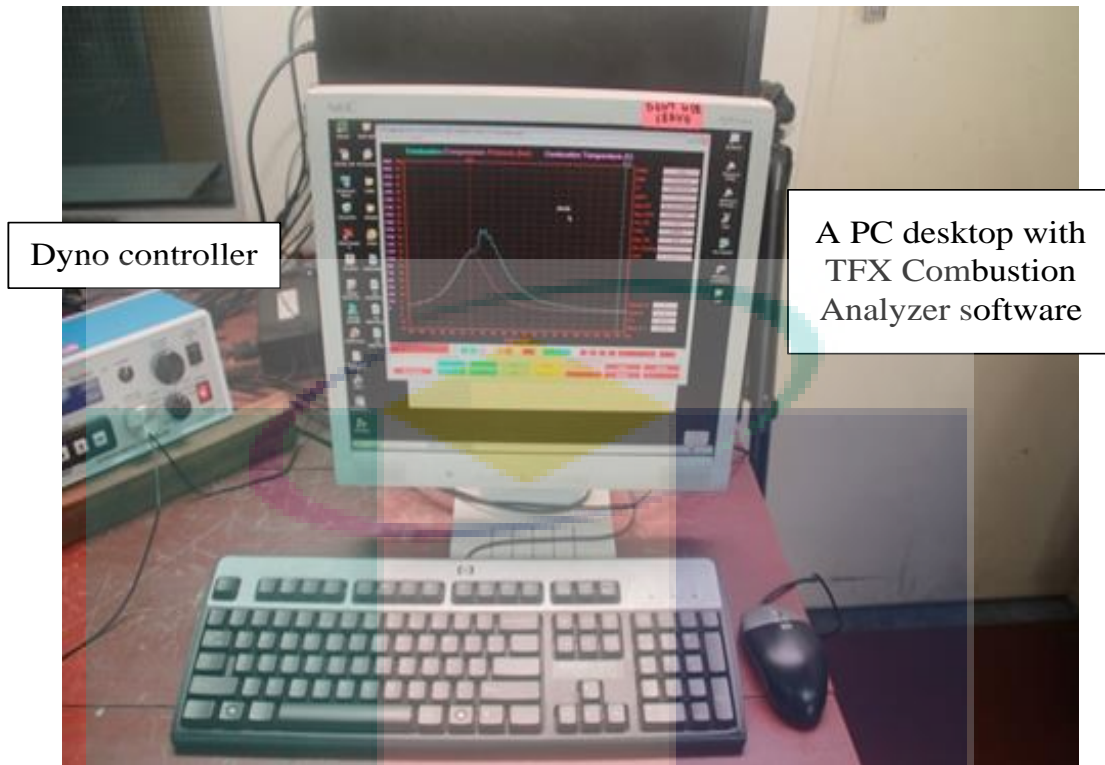
Figure 3.9   A PC desktop with TFX combustion analysis software

Figure 3.9 shows a PC desktop with TFX combustion analysis software provided by a US-based company, TFX Engine Technology Inc. This software was used to obtain the cylinder pressure data from the engine and used to calculate and analyse the combustion characteristics. In this application, the input channels, crank angle degree, pressure transducers characteristics and engine parameters were modified to suit with the single cylinder diesel engine. The conditioned in-cylinder pressure signals from the channel of the charge amplifier corresponding to the engine crankshaft position signal from the shaft encoder signal were simultaneously collected by wiring to a signal conditioning amplifier model AutoPSI-S static pressure interface.

3.7   Test Operating Conditions

The test cycles were manually controlled using engine speeds and engine loads as variable parameters. The engine was operated during the first test condition with the test fuels at a constant partial engine load with increasing engine speeds from 1100 rpm to 2300 rpm. A two-minute time interval was set for each engine speed point until completion. The measured engine parameters included torque, fuel consumption, exhaust

temperatures, ambient temperature, and cylinder pressure. They were measured and recorded simultaneously at each point for the first test condition, mineral diesel (D) was scheduled to be the first fuel to be operated with the diesel engine, followed by palm biodiesel (B) with the next test fuels being BBu10, DBu10, BE10 and DE10 respectively.

These base and blend fuels were employed on the agricultural diesel engine, which was a Yanmar TF120M four-stroke, one cylinder natural aspirated. Alcohol-based fuels represented as a density reducer and oxygenated enhancer for the studied test fuel due to the need for improvement of their performance on engine performance, combustion and cyclic variations characteristics. The test fuels were investigated with the engine which operated at increasing engine speeds ranging from 1100 rpm to 2300 rpm with three different engine loads, zero (0%), partial (50%) and full (100%) load. As for the time interval, 3 minutes were chosen for the engine load transition until completion to the final point. The sequence of the test fuels for the second test condition followed similar to the sequence of the first test condition. The performance curve tests were carried out conforming to the SAE J1349-Engine Power Test Code for Diesel Engines (SAE International, 2004). As described in the SAE J1349 documentation, the following parameters were measured including engine torque, engine speed, cooling water, oil and ambient temperatures.

To define the power curve, the data were recorded for five operating speeds, approximately evenly spaced, between the lowest stable speed and the maximum speed as recommended by the manufacturer. The following data were recorded during the engine testing (SAE International, 2004):

i.   Engine speed;

ii.   Ambient air temperature, pressure, humidity;

iii.   Inlet air pressure, temperature;

iv.   Exhaust system pressure;

v.   Fuel supply temperature;

vi.   Oil and coolant temperature; oil pressure;

vii.   Intake manifold temperature, pressure;

viii.   Exhaust manifold temperature and, pressure;

Torque, fuel consumption, exhaust temperatures, relative humidity, ambient temperature and cylinder pressure were measured and recorded instantaneously. At the start of both test-operating conditions, the engine was idled at an average of 30 minutes to ensure the temperature of the engine oil had reached approximately 80 °C. On the other hand, continuous cylinder pressure measurements were conducted at the average of 200 consecutive cycles. Furthermore, both test-operating conditions for each test fuels were repeated five times to ensure accuracy and reliability of the measurement.
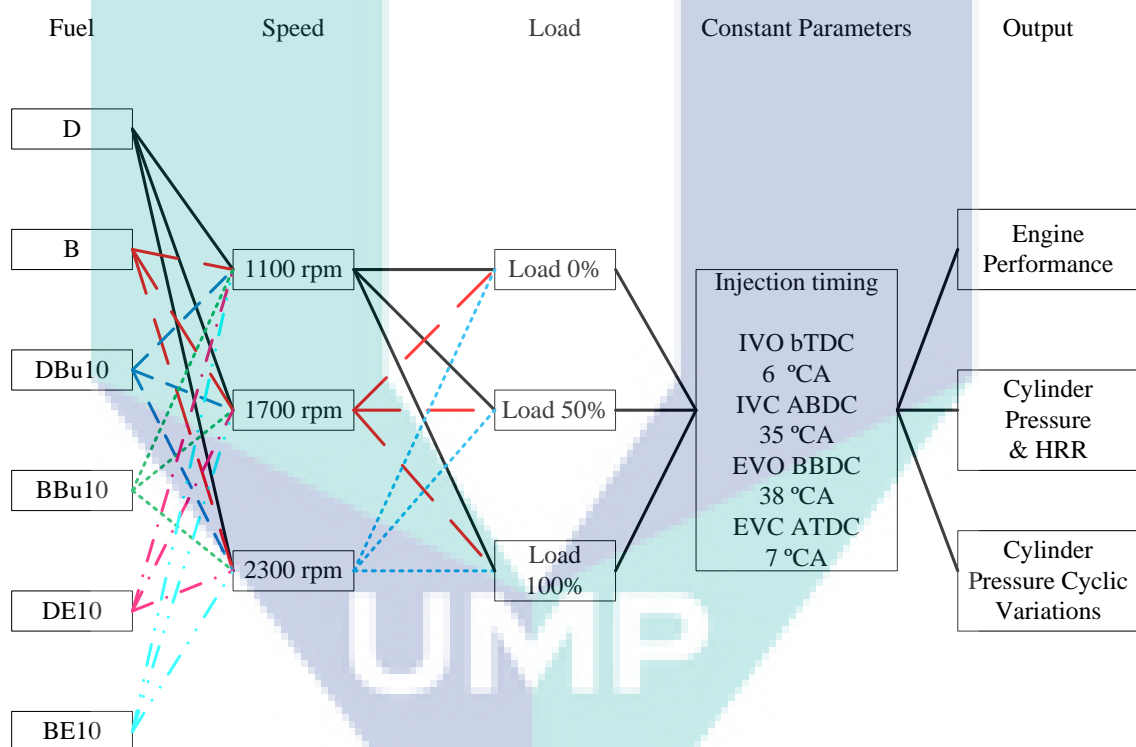
Figure 3.10   Arrangement of data collection in the experimental work

The differences in the measured cylinder pressures for the engine using each test fuels and the reference operation of the engine when operating with mineral diesel were evaluated and compared as illustrated in Figure 3.10. Since mineral diesel (D) is the reference fuel for the study, this fuel was first tested and assessed to determine the engine performance, combustion and emission characteristics, then followed by palm biodiesel (B). The same procedure was repeated for each test fuel at the same operating conditions.

The test fuel line for each fuel was cleaned for each fuel change to provide higher accuracy and more reliable results. The engine was left idling for about 20 minutes to stabilise the engine condition before starting the new test according to the SAE J3149 standard. This procedure was repeated for the next fuel change.

The measurements were again taken after, allowing the engine to stabilise and data collection for this mode were repeated up to five times to ensure consistency and reliability of the testing data. Three corresponding engine speeds targeted were 1100 rpm, 1700 rpm and 2300 rpm. These three engine speeds were selected with an equally spaced range of 600 rpm, providing an apparent justification based on the different engine testing modes with different measure and calculated parameters, especially for the engine performance. As for the second strategy, the engine testing was conducted at three different engine loads; zero (0%), partial (50%) and full (100%) load rates with increasing engine speeds ranging from 1100 rpm to 2300 rpm with the test fuels as presented in Figure 3.10. Each operating condition was repeated for five times to ensure reliability and accuracy of the measured parameters. The methodology involved in analysing the cyclic variations is summarised as follows:

i.   In-cylinder pressures for 200 continuous cycles were measured at each operating point.

ii.   The cyclic variations in cylinder pressures and related parameters were analysed.

iii.   Cyclic variations in crank angles of heat release were investigated.

iv.   Results focused on the in-cylinder pressure variations along the 200 consecutive cycles include statistical analysis (maximum, average, COV) and study of the cycle-to-cycle variations using recurrence plot for the test fuels.

Prior cycle effects were identified.

i.   The entire sample is separated into three groups based on their mode of combustion.

ii.   The cyclic variations of baseline fuels; D and B as well as butanol and ethanol blends on the engine were individually compared.

The cyclic variations were analysed using the above methodology, and the results are presented in the following Section 3.8 and Section 3.9.

3.8   Cyclic Variation Data Collection and Analysis

The piezoelectric pressure transducer used in this engine was specifically designed for measuring the change of pressure in the cylinder when the engine operates. This pressure transducer uses a quartz piezoelectric crystal which response to a change in force applied to the sensor, generating a voltage corresponding to the change in pressure. Most of the pressure transducers use 0 to 5 volts to quantify the applied force which the transducer measures in the cylinder (Bueno et al., 2012). Thus, if there were no change in pressure, the pressure transducer will read zero volts. This type of sensor is needed to be performed in a highly dynamic and robust environment and, therefore highly applicable to internal combustion engines. The preparation for the cylinder pressure data recording strictly followed the operation sequence to ensure high accuracy of the data (Bueno et al., 2012).

To facilitate the operation, the calibration data was required first and must be collected for further details. The magnetic crank angle sensor was rigidly mounted to the opposite of the engine flywheel and connected to the signal conditioner which signifies the signal to the DAQ system. The in-cylinder pressure data from the charge amplifier and crank angle degree data from the crank angle sensor were collected by TFX high-speed data logger in an Intel Quad, 4.00 GHz personal desktop. Data were collected using a software package TFX engine pressure analysis software obtained from TFX Engine Technology Inc. Analysis of combustion parameters was performed by using a software named CATOOL which was developed in Matlab. Peak in-cylinder pressure, P_{max} and coefficient of variation (COV) for cylinder pressure were used to investigate the cyclic variation.

There is no requirement for the specific number for the consecutive cycles to evaluate the ecyclic variations. There were a different number of consecutive cycles being used in the previous studies for the cyclic variations. For example, some researchers provided 100 consecutive cycles for the studies (Obed et al., 2015), whereas other researchers used the samples of 1000 consecutive cycles (Saxena & Maurya, 2016).

The cycle data depends on the operation conditions, different test fuels, method of data analysis, and data storage for the consecutive cycles (Ceviz et al., 2011). Therefore, the more accurate analysis could be achieved with the increasing number of cycles that had been observed. However, insufficient data storage could pose a threat to the ineffectiveness of the data processing and calculation. In this study, the samples of 200 consecutive cycles were recorded and used for the test fuels to analyse the cyclic variability.

3.9 Statistical Analysis for Sufficient Number of Cycles

A statistical evaluation is required to determine the number of cycles from the engine combustion to correctly represent the covariance (COV) value. The recorded combustion data belonged to the 200 consecutive cycles for each test fuel at different condition. Initially, data of the combustion cycles were grouped as bundles of first 50, first 100, 150 and so on, then the statistical properties of P_{max} data across these groups were evaluated. Since the COV_{Pmax} value is the ratio of P_{max} standard deviation, σ_{Pmax} to mean P_{max}, μ_{Pmax}, both statistical parameters were examined. The mean values from the combustion results across groups indicated higher variations. Thus, the mean values could be considered as significant compared to the variation in standard deviation. Hence, it was sufficient to analyse only mean P_{max} to make a correct determination. Therefore, to inform whether there were enough cycle for COV_{Pmax}, it was necessary to determine the data that, if added after some point, there would be not any significant change in the statistics of σ_{Pmax}. If the data showed that the standard deviation of P_{max} stayed the same as the cycles added, then it could be concluded that there was no necessity to include more cycles to reach the correct value of COV_{Pmax}.

3.10 Data Uncertainties

The accuracy of the measurements and the uncertainties in the calculated results were performed according to the method described by Holman (Holman, 1994) and are listed in Table 3.7. The measured and calculated results are obtained from the engine testing operating with three different engine loads; namely zero (0%), partial (50%) and full (100%).

Table 3.7   Measurement accuracies and data uncertainties of the calculated results

Measurements	Sensor type	Accuracy
Torque	Load cell	± 1 Nm
Speed	Photoelectric sensor	± 1 rpm
Crank angle	Magnetic crank angle sensor	
Temperature of injected fuel	K type	± 1.5 °C
Temperature of exhaust gas	K type	± 1.5 °C
Temperature of ambient air	K type	± 1.5 °C
Cylinder pressure	Piezo electric an Optrand AutoPSI-S model C22294-Q	± 1 bar
Liquid fuel mass flow rate	Burette	± 1 ml/min
Intake air flow rate		± 0.5 l/min
HC	Infrared	± 12 ppm
CO	Infrared	± 0.06 % volume
CO_2	Infrared	± 0.5 % volume
NO	Fuel cell	± 5 %
O_2	Fuel cell	± 0.1 %
Calculated results		Uncertainty range (%)
Brake power		0.4 -1.9
BSFC		0.6 – 2.0

In addition, the measurement error of the data collections for peak cylinder pressure, P_{max}, 200-cylinder pressure variations was calculated based on the percentage of the relative standard error (RSE) as follows in Eq. (3.1).

$$RSE \ (\%) = \left(\frac{S_{Error}}{\overline{X}} \right) \times 100\%$$

3.1

where S_{Error} is the standard error, and X is the mean of the data collections. The standard error, S_{Error} was calculated based on the following equation, Eq. (3.2):

$$S_{Error} = \frac{\sigma}{\sqrt{n}}$$

3.2

where σ is the standard deviation, and n is the number of the data collections. Data on the percentage of relative standard errors were calculated for five repeatable readings

during the engine combustion data collection. The percentage of the relative standard error is calculated by dividing the standard error of the peak cylinder pressure, P_{max} of each tested fuel with the mean of the combustion profiles. Therefore, based upon the percentage of relative standard error calculations for each tested fuel, these results featured errors of less than 10%.

3.11   Peak Cylinder (P_{max}) Pressure Cyclic Variation Analysis

A schematic diagram of the experimental set up is shown in Figure 3.5. This single cylinder, direct injection diesel engine was fueled by six test fuels including reference fuels; D and B along with butanol (BBu10 and DBu10) and ethanol (BE10 and DE10) blends. The pressure sensor was attached to the cylinder head (Section 3.6.8) to measure the cylinder pressure for all six fuels under steady-state conditions. The signal from the pressure sensor was transferred over connecting cables to a charge amplifier and then analysed by a combustion analyser software, TFX combustion analyser in the computer. A 15 kW eddy current dynamometer was used to control the loading to the engine through a connecting shaft. The cylinder pressure data were collected over 200 consecutive cycles for three different engine loads; zero (0%), partial (50%) and full (100%) load rates with three specific engine speeds; 1100 rpm, 1700 rpm and 2300 rpm. According to Longwic et al. (2009) and Sen et al. (2008), the most common parameter to investigate the cyclic variations is the peak cylinder pressure values for the specific number of cycles.

Therefore, in this study, the peak pressure value was identified in each of the 200 cycles from the time series for all six fuels, forming a peak-pressure time series for further analysis at different operating conditions. The CATOOL combustion analysis software was used to determine these peak cylinder pressure values in detail. Then, the Matlab coding of RPs and RQA from Hui Yang (Chen & Yang, 2012a) was modified in the Matlab software and being employed to examine the peak cylinder pressure, P_{max} time series for each of the three loads; zero (0%), partial (50%) and full (100%) load at each engine speeds; 1100 rpm, 1700 rpm and 2300 rpm as presented in Appendix A and Appendix G. For this reason, each time series is embedded in a high-dimensional space using time-delay coordinates (as shown in Appendix F) with the following equation by Longwic et al. (2009b):

$$\text{Pmax}(i) = [Pmax(i), Pmax(i - \delta i), Pmax(i - 2\delta i), \ldots., Pmax(i \qquad\qquad 3.3$$
$$- (m - 1)\delta i)]$$

where *m* is the embedding dimension and *δi* is the time delay. The values of *m* and *δi* were estimated by calculating the average mutual information and the fraction of false nearest neighbours (FNNs) as shown in Appendix C. For further detail, the smallest value of δi is 1, and the largest value of m, m = 1 being used for all time series of cylinder pressure in the study. The recurrence plot (RP) is formed from the matrix of $R^{m,\varepsilon}$ with its elements $R_{ij}^{m,\varepsilon}$ based on previous works:

$$R_{ij}^{m.\varepsilon} = \left(\varepsilon - \|P\max(i)\| - P\max(j)\right) \qquad\qquad 3.4$$

The features of empty space and a black dot are represented by values of 0 and 1 into recurrence plot, and *ε* is a threshold value. As a result, the developed vertical and horizontal lines in recurrence plot graphs can categorise the dynamics of the time series or system into a more quantifiable designation known as recurrence quantification analysis (RQA).

As for recurrence quantification analysis (RQA) in Section 0, several parameters can be defined in detail such as recurrence rate, RR that determined the segment of black dots in an RP. On the other hand, parameters such as determinism, DET is a measure of the proportion of recurrence points forming diagonal line segments and reveals the deterministic structures in the time series which further explains the existence of deterministic structures in the time series. While as for laminarity, LAM is based on vertical line segments which represent the extent of laminar phase or intermittency. Also, trapping time (TT) describes how long the system remains in a laminar phase. These listed parameters are determined in the Matlab software using the distributions P (l) and P (v) of the lengths of diagonal and vertical lines which formed the RP

CHAPTER 4

RESULTS AND DISCUSSION

4.1   Introduction

This chapter presents the experimental results of the test fuels on the fuel properties, performance, combustion and cyclic variations at three different engine loads; zero (0%), partial (50%) and full (100%) load conditions with increasing engine speeds ranging from 1100 rpm to 2300 rpm. The results in this chapter are divided into four main sections including fuel properties analysis, engine combustion analysis, cyclic variations, recurrence plot (RP) and recurrence quantification analysis (RQA). The test fuels were measured and compared for fuel properties by conforming to the ASTM D7647 Standard to ensure suitability of the test fuels for diesel engines. Different types of blends were used, and the trends of change in the fuel properties are briefly discussed in this section. Comparison between mineral diesel (D) and palm biodiesel (B) as reference fuels with butanol (DBu10 and BBu10) and ethanol (DE10 and BE10) blends at specific engine loads and speeds are discussed in detail.

The last section of this chapter focuses on the cyclic variation, which is analysed based on the maximum cylinder pressure, P_{max} as an important parameter used to indicate the engine cyclic variations. The recurrence plot method and coefficient of variation (COV) are used to analyse the cyclic variations. The results are compared to those of mineral diesel (D) as a baseline to reveal the trend of cyclic variation under different engine test conditions.

4.2 Effects of Butanol and Ethanol on Diesel and Biodiesel Blend Fuel Properties

The properties of base and alcohol blend fuels are investigated in this study. These properties are significantly important to understand the character of each test fuel before relating them to any result including engine performance, combustion and emission characteristics as well as cyclic variations. Measurement and estimation are two indicating points for fuel characterisation trends when involving blend fuels. Thus, D and B fuels were blended with alcohol base fuels; butanol and ethanol at 10% by volume, resulting in four fuel samples (Bu10, DBu10, BE10 and DE10). The properties of the butanol and ethanol blends are discussed in this section, which aims to provide a brief understanding of those test fuel characteristics. The tested properties include density, kinematic viscosity, energy content and cetane number. All fuel property tests were conducted according to the standard methods of ASTM D7647. The measured properties of test fuels are listed in Table 4.1. Furthermore, the trend of change for each investigated fuel property is highly relative to D, B, butanol and ethanol change trends. Figure 3.3 shows a photo of the test fuels which were used in this study. It is noticed from the picture that different fuels represented different characteristics during engine operation in various operating condition.

Table 4.1   Fuel properties for the test fuels

| Properties | Testing Standard | Test Method | Types of fuel | | | | | | | |
| | | | Reference fuels | | | | Butanol Blends | | Ethanol Blends | |
			Ethanol	Butanol	D*	B	BBu10	DBu10	BE10	DE10
Formula	-	-	C_2H_5OH	$CH_3CH(OH)CH_2CH_3$ / C_4H_9OH	$C_{10}H_{20}$	Methyl esters of C12 to C22 fatty acids	N/A	N/A	N/A	N/A
Viscosity (mm²/s) (cSt)	D 445	KV1000 Koehler Digital constant Temp. Kinematic Viscosity Bath KEM Portable Density/ Specific Gravity Meter [DA-130N]	1.2	4.21	5.144	7.495	6.026	3.576	4.311	3.674
Density (g/cm³) @ 25 °C	D4052		0.79	0.81	0.826	0.867	0.858	0.824	0.862	0.823

Table 4.1   Continued

Properties	Testing Standard	Test Method	Ethanol	Butanol	D*	B	BBu10	DBu10	BE10	DE10
					Reference fuels		Butanol Blends		Ethanol Blends	
Cetane number	D613	Shatox Cetane Number SX-300	8	25	47.8	55.5	52.4	51	52.8	43.82
Calorific value (MJ/kg)	D240	A Parr B41 calorimeter with a Oxygen Comb. Bomb and a Model 6772 Digital Thermometer	26.8	32.5	44.8	38.6	37.99	43.57	37.42	43
Flash point (°C)	D93	Pensky-Martens Closed Tester	12	24	60	80	74.4	56.4	73.2	55.2

4.2.1 Variations in Density for Test Fuels

The density of the fuel is a function of the fuel chemical composition. Density increases with carbon chain number with a class of compounds. In general, D and B fuels have different densities, with B fuel having a higher density as compared to D fuel. This result is similar to the previous results from Chong et al. (2015a) and Phoon et al. (2016). The density of test fuels varies in the range of 0.826-0.867 g/cm^3 for both D and B fuels. The density of B fuel is moderately higher than D fuel as listed in Table 4.1. Moreover, as a comparison, the difference in density is approximately a 4.8% increase when compared B fuel to D fuel. The density of biodiesel is influenced by different feedstock sources used in the biodiesel production process (Bhuiya et al., 2016b; Verma & Sharma, 2016). This requires the addition of density reducer including alcohol to reduce the biodiesel density. Thus, it is obvious that the decrease in the density of the biodiesel blends is due to the additional butanol and ethanol content in the palm biodiesel.

The use of alcohols was significantly diluted with the biodiesel as mineral diesel was diluted with biodiesel at different proportions (Chauhan et al., 2016; Kumar & Saravanan, 2016; Sarathy et al., 2014). The analysis shows that B achieved the highest density with 0.867 g/cm^3, higher compared to that of other test fuels, namely BBu10 (1.02%), DBu10 (4.50%), BE10 (0.60%) and DE10 (5.30%) respectively, lower than that of B as listed in Table 4.1. Moreover, adopting butanol and ethanol with D and B blends further reduce the densities of the fuel blends since butanol and ethanol have a lower density than D and B, respectively. These results provide further support for the hypothesis that various alcohol could reduce the density of the higher density fuels including biodiesel. Moreover, these results match those observed in earlier studies of butanol (Dimitrios et al., 2015; Zhang, Chua, & Balasubramanian, 2016; Zheng et al., 2015), ethanol (Fayyazbakhsh & Pirouzfar, 2016; Lee & Kim, 2015; Murcak et al., 2013), methanol (Chen et al., 2017) and propanol (Atmanli, 2016a; Man et al., 2014). The present study contributes to existing knowledge of different fuel densities by providing significant findings on butanol and ethanol mixing with base fuels including palm biodiesel.

4.2.2   Variation in Calorific Value for Test Fuels

Calorific value or heating value is one of the most significant parameters to characterise fuel due to its energy content. Calorific value is the amount of heat energy released through combustion of the unit value of fuel per mass. Higher calorific value of the fuel is desirable for a combustion engine regarding fuel economy (Bhuiya et al., 2016b). Previous studies have found that the calorific values of biodiesel fuel from different feedstock sources are lower than that of diesel fuel (Chong et al., 2015b; Gandure, Ketlogetswe, & Temu, 2014; Tarabet et al., 2014). A possible explanation for this might be that higher oxygen content (about 10 to 11%) is obtained for biodiesel as compared to that of mineral diesel. For the record, the calorific value is not specified in ASTM D6751 and EN 14214 biodiesel standards, but it is stated in EN 14213 (biodiesel for the heating purpose) standard with a minimum value of 35 MJ/kg.

Different feedstock sources of biodiesel possess different calorific value as well as use different alcohol-based fuels blending with base fuels. Table 4.1 presents the calorific values for D, B, butanol (BBu10 and DBu10) and ethanol (DE10 and BE10) blends. The results in Table 4.1 clearly show that the measured calorific value for D fuel is 14.9% higher than B fuel. Moreover, the measured calorific value for both DBu10 and DE10 blends are higher than BBu10 and BE10 blends by 13.7% and 13.8%, respectively due to the presence of the D fuel in the blends. This result may be explained by the fact that a higher volume of D fuel improves the calorific values of the blends. It seems possible that these results are due to the observed decrease in calorific value could be attributed to the mixing of alcohol fraction in the blend fuels since alcohol has higher oxygen content than D fuel, reduces the carbon and hydrogen content (Kumar et al., 2013; Tosun et al., 2014; Zhang et al., 2016). Therefore, the analysis of calorific value undertaken here has extended the knowledge on the critical fuel properties in developing various combustion characteristics of different fuels with different operating conditions.

4.2.3 Variation in Cetane Number for Test Fuels

Cetane number mainly indicates the quality of the fuel which significantly affects the fuel ignition time delay upon injection within the combustion chamber. Higher Cetane number produces a shorter ignition delay period that results in the easy cold start and low idling noise (Bhuiya et al., 2016b). Conversely, when more extended ignition delay period occurs in the expansion process, this event produces incomplete combustion, reduces in power output, creates fuel economic inefficiency and increases the engine noise slightly. In general, most biodiesel fuel studies have found that biodiesel has a higher Cetane number than mineral diesel as biodiesel is mainly composed from the groups of long-chain hydrocarbon (Atmanli, 2016b; Fayyazbakhsh & Pirouzfar, 2016; Jose & Anand, 2016; Li et al., 2014b; Suh & Lee, 2016). Interestingly, palm biodiesel has higher Cetane number compared to biodiesel from other feedstock sources due to the higher saturated fatty acid acting as the main component in the fuel composition (Mosarof et al., 2015) and its higher oxygen content which results in higher combustion efficiency (Bhuiya et al., 2016b).

The Cetane number of test fuels varies in the range between 47 – 52.8 for both D and B fuels. In consequence, the Cetane number of the test fuels decreases as an increase in alcohol amount dilutes with D and B fuels as listed in Table 4.1. The Cetane number for B fuel is 55.5, which is a 23.5% higher than that of D fuel, and surpassed the test fuels with 8.5% (DBu10), 5.7% (BBu10), 14.9% (DE10) and 4.9% (BE10), correspondingly. The observed correlation between Cetane number and oxygen content might be explained in this way with different results between D and B fuels. Also, the addition of butanol and ethanol in D and B blends have reduced the Cetane number of the butanol and ethanol blends. It seems possible that these results are due to butanol and ethanol possessing lower Cetane number than B fuel. These measured results are similar to the previous alcohol fuel studies involving butanol (Atmanli et al., 2015; Liu et al., 2013), ethanol (Labeckas, Slavinskas, & Mažeika, 2014a; Lee & Kim, 2015) and methanol (Li et al., 2014b; Yaopeng et al., 2013). The following conclusions can be drawn from the present study that the blending of butanol and ethanol in the base fuels could significantly reduce the Cetane number values of biodiesel and diesel blends, hence various combustion characteristics and cyclic variations are developed.

4.3 Effects of Engine Loads and Speeds on Average Cylinder Pressure and Heat Release Rate (HRR)

In a compression ignition engine, the peak cylinder pressure reflects on the combustion rate during the early stages, air-fuel mixture compression stage that is influenced by the amount of fuel to be burned in the unrestrained combustion duration, which corresponds to delay duration (Heywood, 1988). Moreover, cylinder pressure is significantly influenced by the types of fuel operating in the engine, as well as fuel properties, and different types of the engine and air-fuel ratio (AFR). The first law of thermodynamics is applied to calculate the nett heat release rate (HRR) using the measured in-cylinder pressure data at the closed part of the engine cycle. This parameter is considerably related to the sensible enthalpy corresponding to the unit time in which the chemical energy of the fuel converses into heat within the combustion period.

Combustion period is the time interval from the start of combustion (SOC) to the end of combustion (EOC) along the crank angle degrees (deg.CA) of a combustion cycle. Start of combustion (SOC) is described as the start of the heat release rate (HRR), while the end of combustion (EOC) indicates the heat release rate achieved over 95% of the total HRR at the specific degree of crank angle degree (deg.CA). Since the fuel starts to vaporise during the ignition delay, a negative heat release is observed at the beginning, before the SOC and then, the heat release rate turns positive. The ignition time indicates the start of the heat release within the combustion period. Total combustion period can best be described as the time interval from the initial of the heat release to the end of heat release.

This section presented experimental results on the measured and calculated combustion characteristics for D, B, BBu10, DBu10, BE10 and DE10 blends using a Yanmar TF120M single cylinder, horizontal-type diesel engine (with the engine specifications as detailed in Section 3.6.1. This section describes the effects of engine loads from zero load to partial load and full load conditions using the measured cylinder pressure data and crank angle degree (deg.CA) to compute the instantaneous HRR. The measured in-cylinder pressure data and the crank angle degree (deg.CA) were measured and collected at 200 consecutive engine cycles. An Optrand in-cylinder pressure transducer (refer Section 0) was attached to the cylinder at the corresponding diesel

engine; then the cylinder pressure data was recorded and displayed using a TFX combustion analyser DAQ system. Data measurement and recording were conducted for the in-cylinder pressure within the 200 consecutive cycles with a sampling rate corresponding to 1 deg.CA. The measured cylinder pressures for the test fuels were averaged by calculating the mean value of cylinder pressure from the 200 consecutive cycles. Further analysis of the measured and calculated combustion parameters of the test fuels are briefly described and discussed at Section 4.3 and 4.4.

4.3.1 Average Cylinder Pressure and Heat Release Rate (HRR) at Engine Speed, N=1100 rpm

Determination of cylinder pressure and heat release rate (HRR) is standard practice in engine research. Cylinder pressure data is measured corresponding to the crank angle degree (deg.CA) as the net heat release rate (NHRR) is normally calculated from the in-cylinder data based on the first law of thermodynamics. These combustion data including in-cylinder pressure and heat release rate (HRR) provide valuable insight into the combustion process.
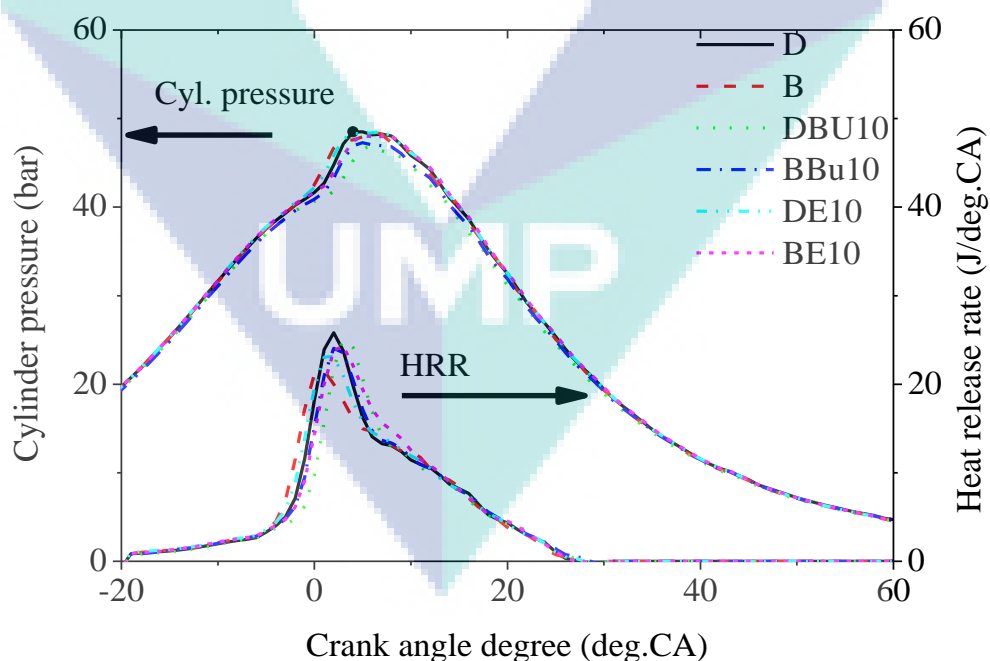
Figure 4.1 Cylinder pressure profiles and HRR curves with zero load, 0% at 1100 rpm

Cylinder pressure and heat release rate (HRR) resulted as a function of crank angle degree at a constant engine speed of 1100 rpm are presented in Figure 4.1 Cylinder pressure profiles and HRR curves with zero load, 0% at 1100 rpm. These parameters were averaged from the 200 consecutive cycles for each test fuel. Measured cylinder pressures are used to determine the average combustion pressure when running with different kinds of fuel and characterise the whole combustion characteristic for each cycle. It can be seen from Figure 4.1 and Figure 4.2 that the results for measured parameters, cylinder pressure and HRR, are comparable with each test fuel especially at zero and partial engine loads. However, there is a significant trend observed at full engine load for the test fuels whereas higher cylinder pressure is considerably achieved at specific engine speed. These results agree with the findings of other studies, in which slight differences are observed for cylinder pressure when compared with different test fuels at low load and speed condition (Can et al., 2016; Fahd et al., 2013; Uyumaz, 2018; Zhou, Cheung, & Leung, 2013). Thus, the observed increase in the cylinder pressure at higher engine load could be attributed to the more fuel-air mixture with more fuel injected into the cylinder and richer oxygenated inlet charge (Gharehghani, 2017; Lahane & Subramanian, 2015; Turkcan, 2018).

An example of a heat release rate (HRR) diagram can be seen in Figure 4.1. This figure shows HRR profiles for D, B, BBu10, DBu10, BE10 and DE10 at zero load condition. It is also noted that the maximum HRR for BBu10 and DBu10 are higher than BE10 and DE10, concerning D fuel. The maximum HRR for BBu10 and DBu10 were found to be 24.1 J/deg.CA and 25.2 J/deg.CA, which were higher than the maximum HRR of BE10 and DE10 with 23.8 J/deg.CA and 23.1 J/deg.CA respectively, while as for D and B, the values for maximum HRR were 23.9 J/deg.CA and 21 J/deg.CA. These findings are rather slight differences between each test fuel and could not provide clear justification on the current findings. There are similarities between the attitudes expressed by cylinder pressure and HRR traces of these test fuels in this operating condition and those described by (Dimitrios et al., 2016; Wood et al., 2015; Zheng et al., 2015).

Interestingly, this approach is used to determine the start of combustion (SOC) occurring at which crank angle degree (deg.CA) during the combustion as can be seen in Figure 4.1. However, this approach has a few limitations including the effect of crevice

regions in the combustion chamber (Heywood, 1988), difficulty in quantifying the mixture non-uniformity in the air-fuel ratio and the burned and unburned gas non-uniformity. Also, the limitations also cover the assumption on the incorrect heat transfer rate between the cylinder charge and the combustion chamber walls with the addition of a cooling additive such as alcohol or water (Heywood, 1988).
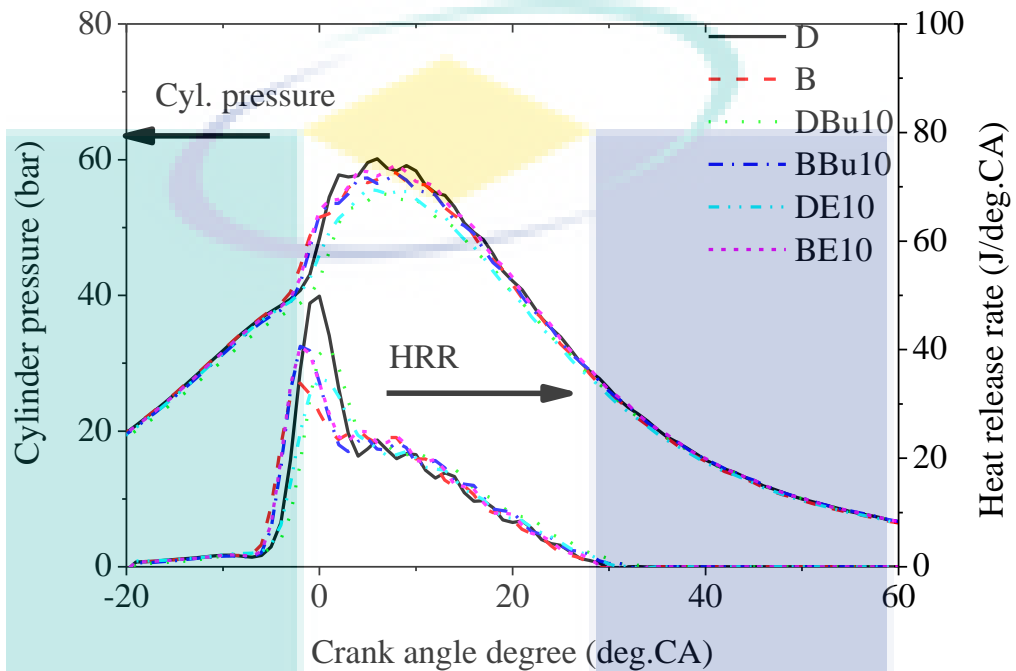
Figure 4.2   Cylinder pressure profiles and HRR curves with partial load, 50% at 1100 rpm

The variations of average cylinder pressure and HRR curves for the test fuels at partial engine load with a constant speed of N=1100 rpm are compared in Figure 4.2. It can be seen from the figure that there is a clear trend in increasing cylinder pressure for all test fuels. Reference fuels; namely D and B, achieve their peak cylinder pressure with 59.6 bar at 5 deg.CA and 58.2 bar at 7 deg.CA respectively, a 2.4% percentage difference. At partial load, the peak cylinder pressure, P_{max} was found to be 57.1 bar, 55.1 bar, 58.5 bar and 56.5 bar at 7 deg.CA after TDC for BBu10, BE10, DBu10 and DE10, respectively against 59.6 bar at 5 deg.CA after TDC for D fuel. It is noted that the peak pressure, P_{max} for test fuels and loading condition falls between 5 deg.CA to 7 deg.CA which ensures safer engine operation. If the maximum pressure lies close to TDC which is 1 deg.CA, it may result in diesel knock and vibration (Ipci & Karabulut, 2016; Lounici et al., 2017; Taghizadeh-Alisaraei & Rezaei-Asl, 2016).

As for the heat release rate (HRR) curves shown in the figure, the maximum HRR for D and B are higher than butanol and ethanol blends at zero load condition. The maximum HRR for D and B are found to be 48.6 J/deg.CA and 31.4 J/deg.CA respectively, higher than BBu10, DBu10, BE10 and DE10 occurring at 40.7 J/deg.CA, 40.6 J/deg.CA, 40.6 J/deg.CA and 34.5 J/deg.CA, respectively. The findings observed in this section mirror those of the previous studies that have examined the effect of alcohol fuels regarding heat release rate (HRR) (Ogunkoya et al., 2015; Şahin et al., 2015; Sathiyamoorthi & Sankaranarayanan, 2017; Wang et al., 2013).
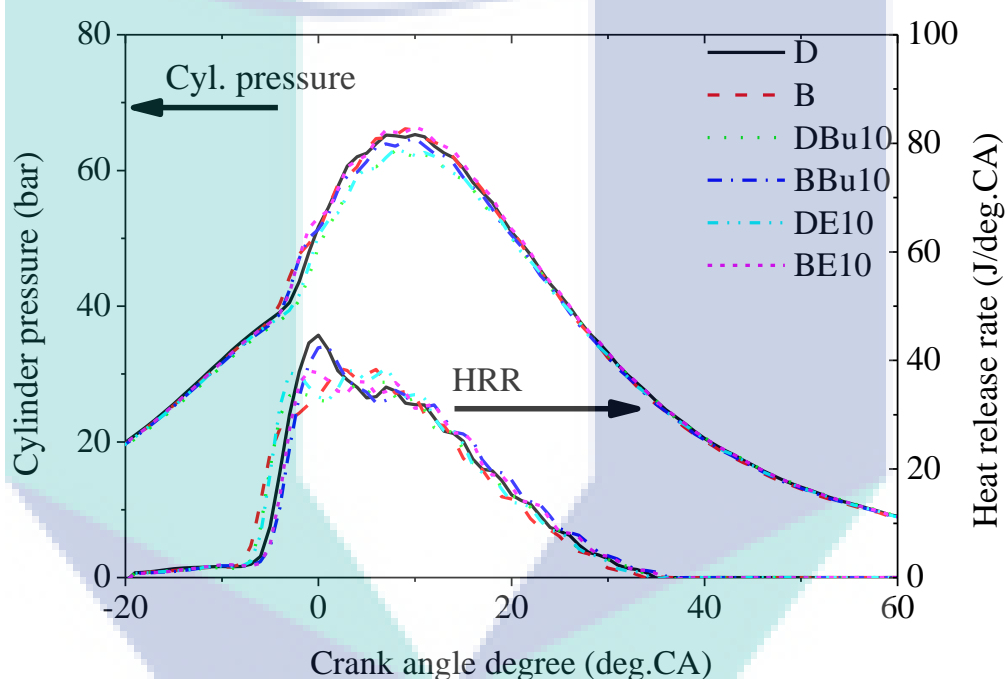
Figure 4.3   Cylinder pressure profiles and HRR curves with full load, 100% at 1100 rpm

The results obtained from the preliminary analysis of cylinder pressure and heat release rate (HRR) with full engine load at similar engine speed (N= 1100 rpm) can be compared in Figure 4.3. It is apparent from this figure that there are comparable results for all test fuels at the respective point, which shows significant increasing trends from the previous partial engine load to full engine load. The peak cylinder pressure was found to be 64.3 bar, 61.8 bar, 66.4 bar (10 deg.CA) and 62.7 bar (9 deg.CA) after TDC for BBu10, BE10, DBu10 and DE10 against 65.3 bar at 10 deg.CA after TDC for D fuel at

full load condition. However, the peak cylinder pressure value for B was higher than that of D fuel and both butanol and ethanol blends with 66.2 bar at 9 deg.CA, respectively. In fact, to ensure safer engine operation, the range between 7 deg.CA to 10 deg.CA for the peak pressure of the test fuels and loading condition are necessarily achieved. This is because there is a possibility for diesel knocks to occur when the maximum pressure is closer to TDC. Under normal circumstances, 62% to 85% of the fuel is at the vaporised stage during the start of combustion (SOC). However, during combustion, the percentage of vaporisation increases to more than 92% in a shorter period. From Table 4.1, it is noticeable that the Cetane number of the test fuels directly affects the ignition delay period and causes a rise in P_{max} and HRR to a certain extent.

Concerning the traces of heat release rate (HRR), the figure shows a comparison of HRR for the test fuels at full load condition. It is noticed that the maximum HRR for D and B are higher than butanol and ethanol blends for that specific loading. The maximum HRR for D and B fuels were found to be 43.2 J/deg.CA and 38.6 J/deg.CA (respectively, which are higher than BBu10, DBu10, BE10 and DE10 occurring at 34.5 J/deg.CA, 42.4 J/deg.CA, 38.2 J/deg.CA and 38.1 J/deg.CA separately. The ignition delay occurs when more quantity of blends is accumulated (collected) before combustion and also resulting in a maximum HRR for B. This section has demonstrated the effects of engine loads namely; 0%, 50% and 100% load conditions with an engine speed of 1100 rpm on average cylinder pressure and HRR for D, B, butanol and ethanol blend fuels. The next part of this study discusses the similar observations at an engine speed of 1700 rpm.

4.3.2 Average Cylinder Pressure and Heat Release Rate (HRR) at Engine Speed, N=1700 rpm

The issues addressed in this section are the measured cylinder pressure and HRR of the test fuels from various engine loads applied to the engine running on a constant engine speed, 1700 rpm. The first part of this section examines the results of cylinder pressure variations when operating with butanol and ethanol blends. The final section describes the HRR for the test fuels in details and discusses the influence of butanol and ethanol in the presence of D and B blends.
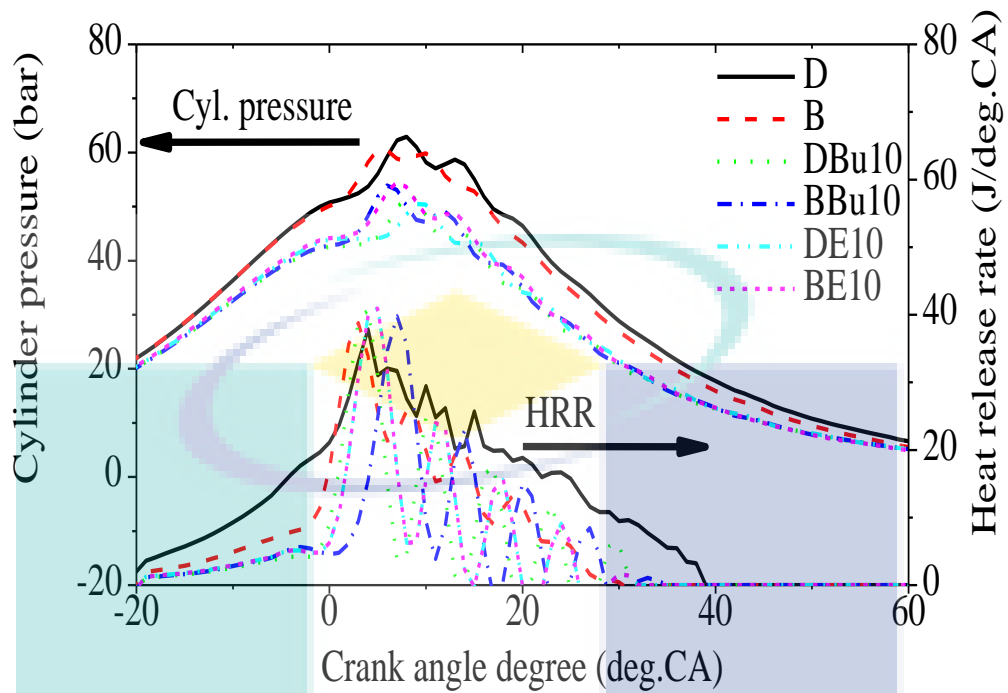
Figure 4.4   Cylinder pressure profiles and HRR curves with zero load, 0% at 1700 rpm

The average in-cylinder pressure and HRR profiles over 200 consecutive cycles for the test fuels are compared in Figure 4.5 for zero load at 1700 rpm respectively. It can be seen from the figure that in-cylinder pressure for D fuel, the highest of all comparable test fuels at all operating loads. There is a significant difference between D and B fuels as presented in the figure. Since the engine speed increases with the applied loads, more extended combustion periods are achieved when running with B. This condition is strongly supported by evidence of the in-cylinder pressure and HRR as shown by the figure. Figure 4.5 compares the experimental data on cylinder pressure and HRR profiles with zero engine load for the average of 200 consecutive cycles at a constant engine speed of 1700 rpm. It can be seen from the figure that premixed combustion of D and B fuels are significantly higher than butanol and ethanol blends, which lead to a significant peak pressure for these reference fuels. At this zero load condition, the peak cylinder pressure for D and B were found to be higher than other butanol and ethanol blends with 62.9 bar and 60.2 bar at 8 deg.CA and 12 deg.CA, respectively. While as for BBu10, DBu10, BE10 and DE10 blends, the peak cylinder pressure was obtained at 54 bar (6 deg.CA), 51.9 bar (8 deg.CA), 54.5 bar (7 deg.CA), and 50.5 bar (9 deg.CA) after TDC,

respectively. By the present results, previous studies have demonstrated that an increase in engine load significantly increased the cylinder pressure (Attia & Hassaneen, 2016; Chong et al., 2015b; Prakash, Singh, & Murugan, 2013; Saleh & Selim, 2017).
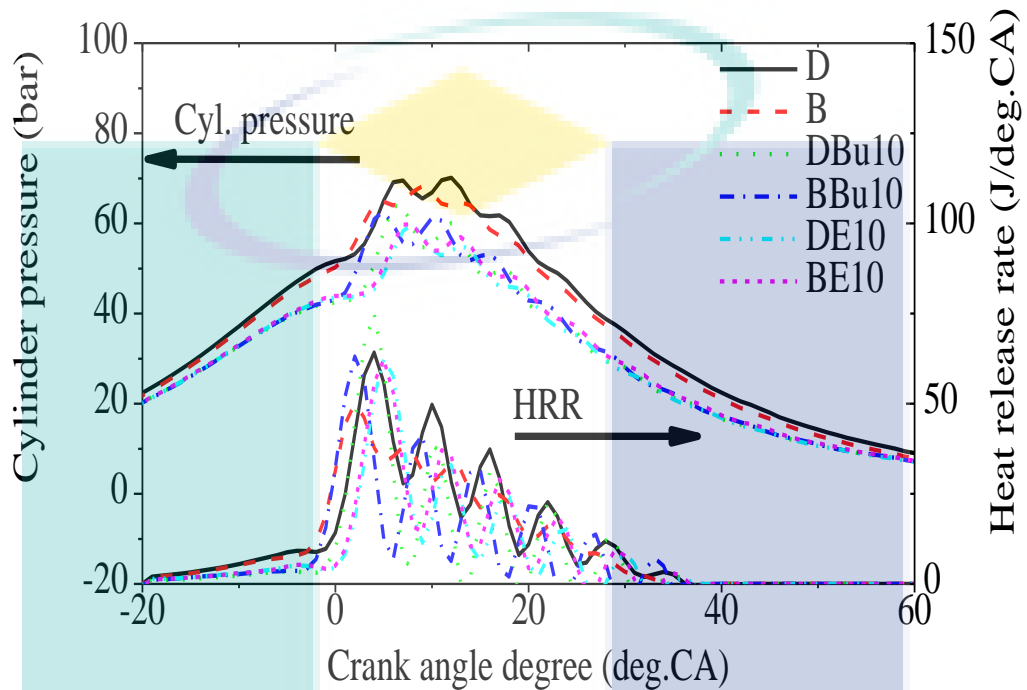
Figure 4.5   Cylinder pressure profiles and HRR curves with partial load, 50% at 1700 rpm

Moreover, most HRR profiles for the test fuels started at -20 deg.CA and ended at 35 deg.CA. However, as for B fuel, the HRR began at -22 deg.CA similar to other test fuels but ended beyond 35 deg.CA which was 70 deg.CA with maximum HRR being 44 J/deg.CA (10 deg.CA). Since palm biodiesel (B) fuel has possession of higher density and viscosity than other test fuels as described in Table 4.1, palm biodiesel (B) fuel exhibits more extended combustion period from other test fuels of lower density and viscosity. It is understandable that when delaying in the start of combustion (SOC) occurs with longer combustion period; these conditions cause more fuel to be consumed resulting in higher maximum cylinder temperature. With respect to D fuel with the maximum HRR obtained at 48.9 J/deg.CA, the maximum HRR for both butanol and ethanol blends were found to decrease with BBu10 (40.7 J/deg.CA at 4 deg.CA), DBu1

(42.4 J/deg.CA at 6 deg.CA), BE10 (40.9 J/deg.CA at 5 deg.CA) and DE10 (39.8 J/deg.CA at 7 deg.CA), correspondingly. These findings confirm that fuel properties are significantly associated with the combustion characteristics and seem to be consistent with the results of previous studies on alcohol (Kumar & Saravanan, 2016; Tutak et al., 2015; Zaharin et al., 2017; Zhang & Wu, 2016).

Figure 4.6 shows the experimental data on cylinder pressure and HRR profiles concerning crank angle degree (deg.CA) at partial engine load, running with a constant engine speed of 1700 rpm. It could be interpreted from the figure that with the increase in engine load and speed, the peak cylinder pressure increases, and maximum peak cylinder pressure are observed for D and B fuels, respectively. The fuel properties significantly contribute to the characteristics of the combustion duration and combustion by-product (Yaopeng et al., 2016; Sakthivel et al., 2014; Vallinayagam et al., 2013). Since D is less viscous as compared to B, better combustion and fuel evaporation for D is achieved in this study. Several literatures acknowledged the low viscosity of the fuel as a decisive factor for better combustion because of the higher evaporation rate (Atmanli, 2016b; Vallinayagam et al., 2014). At partial load condition, the peak cylinder pressure was obtained at 70.1 bar and 61.1 bar at 12 deg.CA and 16 deg.CA, respectively, after TDC for D and B fuels, which are higher than other butanol and ethanol blends. While for these fuels, the resulting peak cylinder pressure was found to be at 62.6 bar (BBu10), 63.9 bar (DBu10) at 7 deg.CA, 59.7 bar (BE10) at 7 deg.CA and 59.7 bar (DE10) at 8 deg.CA after TDC, respectively. These results agree with the findings of other studies, in which lower peak HRR are observed when alcohol is blended with base fuels (Khandal et al., 2015; Zaharin et al., 2017).

Also, the HRRs for all test fuels have similar shape except D and B fuels. Compared with D as a reference fuel, butanol and ethanol blends develop almost identical levels of peak pressure. Besides, the peak HRR for the test fuels at the main combustion phase is slightly lower than that of D and B fuels. At partial load condition, the maximum HRR for D and B are found to be 64.2 J/deg.CA and 63.9 J/deg.CA respectively, which are higher than BBu10, DBu10, BE10 and DE10 occur at 54 J/deg.CA, 75 J/deg.CA, 62.3 J/deg.CA and 62.3 J/deg.CA correspondingly. The lower peak HRR with the addition of butanol and ethanol in D and B blends can be attributed to the cooling effect of the butanol and ethanol, leading to lower in maximum HRR. Hence, the cooling effect

of butanol and ethanol are associated with lower calorific value and higher latent heat of vaporization of these alcohols (Bae & Kim, 2017; Imdadul et al., 2016; Khandal et al., 2015; Lapuerta et al., 2015; Liu, Hu, & Jin, 2016).
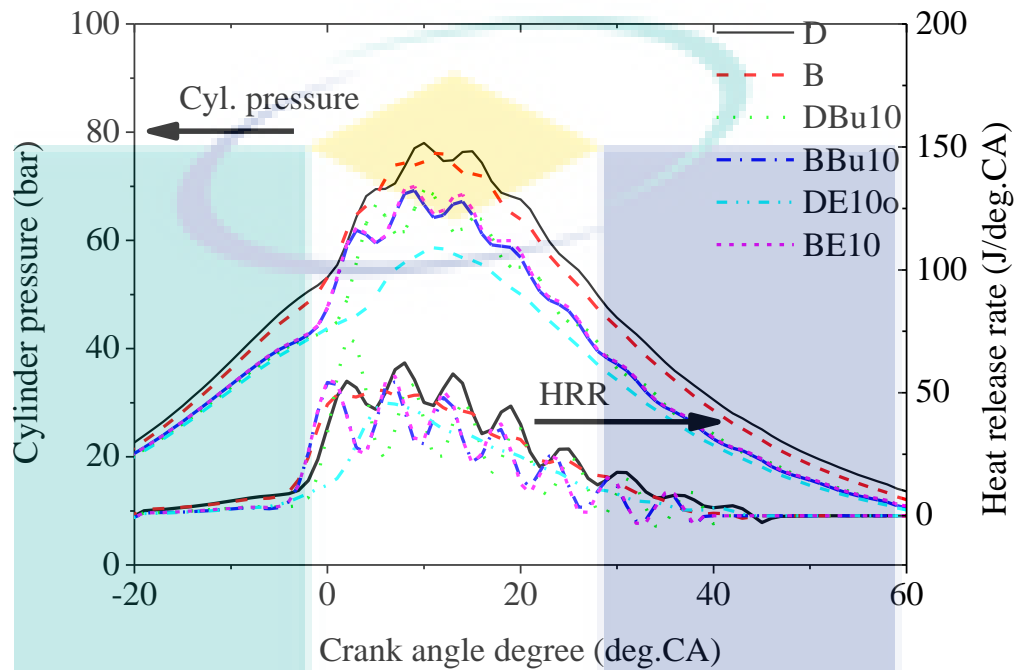
Figure 4.6   Cylinder pressure profiles and HRR curves with full load, 100% at 1700 rpm

Figure 4.6 compares the correlations among the six test fuels of cylinder pressure and HRR profiles corresponding to the crank angle degree (deg.CA) when the full load is applied to the engine running at 1700 rpm. It can be seen from the figure that the averaged cylinder pressure and HRR for all test fuels increase corresponding to the increase in engine load and speed. Compared with D and B, lower maximum peak cylinder pressure and heat release rate were achieved for the fuel blends with 10% of butanol and ethanol as D (78 bar at 10 deg.CA) and B (71.5 bar at 17 deg.CA). The peak pressure profiles for BBu10, DBu10, BE10 and DE10 were found to be at 69.2 bar at 9 deg.CA, 69.3 bar at 10 deg.CA, 70 bar at 9 deg.CA and 58.6 bar at 11 deg.CA after TDC, respectively. This was because butanol and ethanol have lower Cetane number with the higher latent heat of vaporisation that prolongs the ignition delay period and provide a cooling effect during the premixed combustion phase (Atmanli, 2016a; Moxey et al.,

2016; T. Zhang et al., 2016). However, the engine tends to exhibit more vibration due to the increase in peak pressure and pressure rise rate when more load is applied at higher engine speed.

The plot of HRR profiles, averaged over 200 consecutive cycles, for all test fuels at a full operating load and 1700 rpm is presented in Figure 4.6. Generally, it can be seen that the HRR profiles for butanol and ethanol blends are slightly lower than that of D and B. Also the maximum HRR for D and B are significantly higher than butanol and ethanol blends at this condition. The maximum HRR for D and B are found to be 62.1 J/deg.CA and 81.9 J/deg.CA, respectively, which are higher than BBu10, DBu10, BE10 and DE10 occurring at 54.5 J/deg.CA, 72.3 J/deg.CA, 55.2 J/deg.CA and 45.8 J/deg.CA, correspondingly. Lower peak HRR of butanol and ethanol blends due to lower Cetane number values in this section seem to be consistent with the findings of previous studies (Rajesh & Saravanan, 2016; Zaharin et al., 2017). The most apparent outcome to emerge from this section is that the influence of Cetane number on the peak HRR of the test fuels, specifically butanol and ethanol blends. The current findings add to a growing body of literature on the effects of engine loads and speeds as well as fuel properties regarding combustion characteristics in the diesel engine. This section has analysed the impact of engine loads namely; 0%, 50% and 100% load conditions with an engine speed of 1700 rpm on average cylinder pressure and HRR for D, B, butanol and ethanol blend fuels. The next section of this study discusses the similar observations at an engine speed of 2300 rpm.

4.3.3 Average Cylinder Pressure and Heat Release Rate (HRR) at Engine Speed, N=2300 rpm

This section describes in detail the combustion characteristics including cylinder pressure variations and HRR from the engine operating at three different loads under a constant speed of 2300 rpm. This section aims to evaluate the combustion characteristics of test fuels and validate the presence of both alcohols; butanol and ethanol in D and palm B blends.
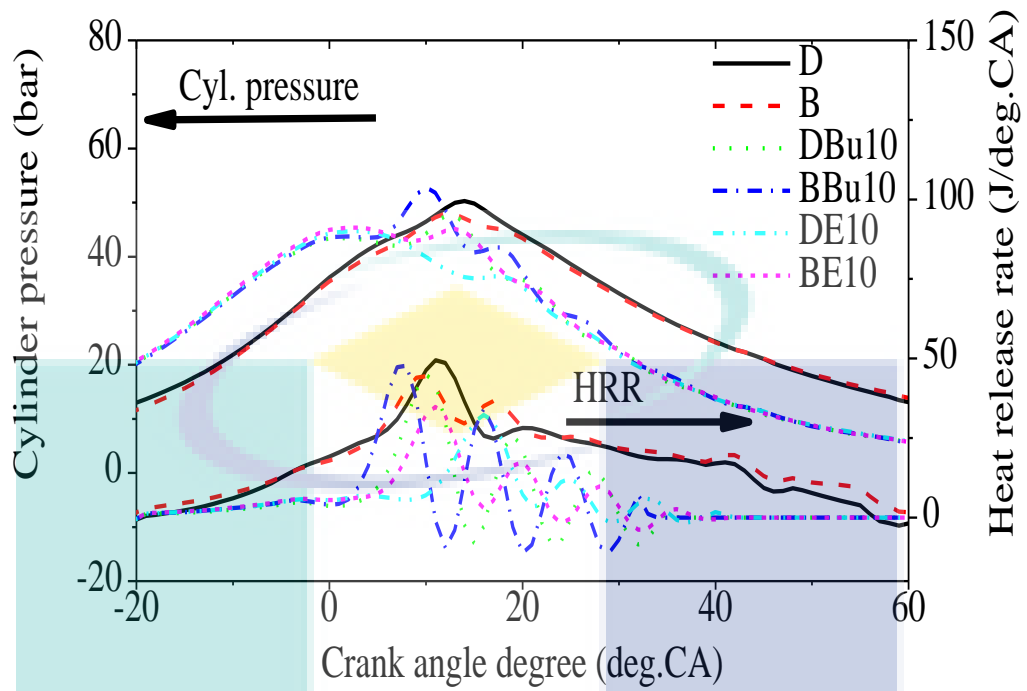
Figure 4.7   Cylinder pressure profiles and HRR curves with zero load, 0% at 2300 rpm
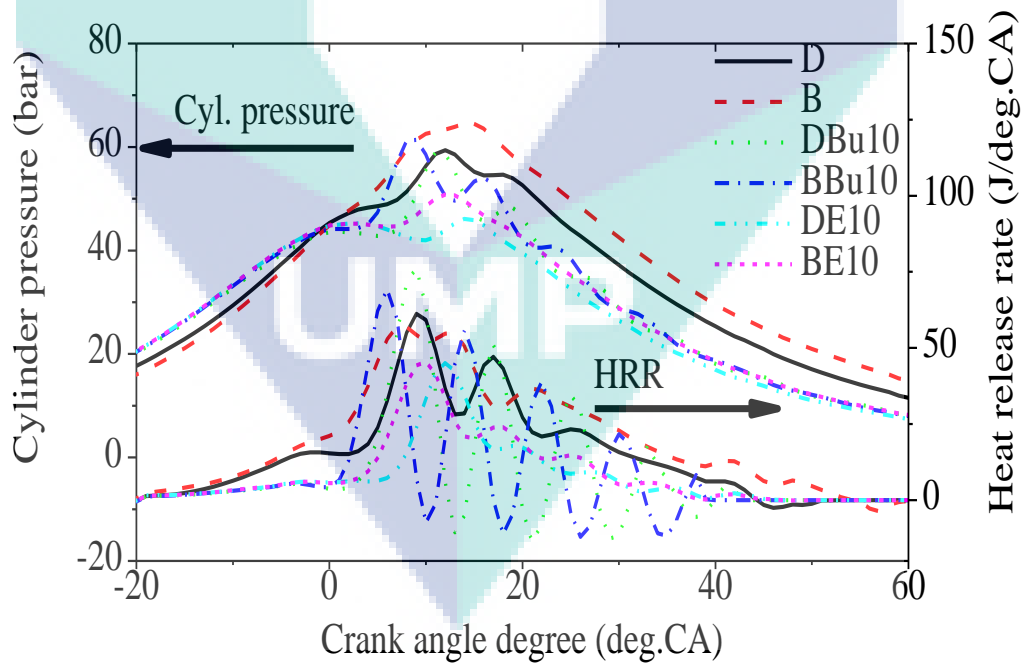
Figure 4.8   Cylinder pressure profiles and HRR curves with partial load, 50% at 2300 rpm

Figure 4.7 shows the results of cylinder pressure and HRR curves as functions of the crank angle degree obtained from the test fuels when operated at zero load (10%) at the specific engine speed of 2300 rpm. For analysis of the combustion, the peak cylinder pressure is closely associated with the fuel heating values and ignition delays. Generally, biodiesel produces a higher peak cylinder pressure than diesel fuel due to the longer ignition delay with lower calorific value (Aydin et al., 2015; Pham et al., 2014; Zare et al., 2016). Surprisingly, it is apparent from Figure 4.7 that D displays the highest peak cylinder pressure of 50.3 bar at 14 deg.CA after TDC, whereas minimum peak cylinder pressure was 44.7 bar at 3 deg.CA ATDC with a DE10 blend. Also, the figure shows that B, BBu10, DBu10 and BE10 obtained a lower peak cylinder pressure of 47.8 bar (13 deg.CA), 52.8 bar (10 deg.CA), 47.8 bar (13 deg.CA), and 45.1 bar (13 deg.CA), respectively, than that of D. The properties of B, butanol and ethanol in the blends, such as high Cetane number, low volatility are the main factors for the differences in peak cylinder pressure among the test fuels. Adopting butanol and ethanol in the biodiesel and diesel blends could decrease the peak cylinder pressure in the combustion process (Ghadikolaei, 2016; Şahin et al., 2015; Tse, Leung, & Cheung, 2015; Vinod et al., 2017; Zhang & Balasubramanian, 2014).

The averaged HRR results of 200 consecutive cycles as a function of crank angle degree (deg.CA) for the test fuels with zero engine load are compared in Figure 4.7. It can be seen from the figure that there are significant increases in HRR for the test fuels when the engine load is increased to partial load and full load from zero engine load. From the HRR analysis at zero load condition, maximum HRR for D is observed at 11 deg.CA with 49.4 J/deg.CA, while as for B, the peak HRR is determined at 44.4 J/deg.CA at 10 deg.CA respectively. Moreover, it is apparent in the figure that there is a significant ignition delay, more extended combustion period and greater expansion in power stroke observed with B in comparison with D. Since B possesses higher density and viscosity, vaporisation occurs more slowly during injection resulting in the lesser air-fuel mixture for the combustion. Figure 4.7 shows that DBu10 and DE10 blends exhibit peak HRRs of 45.1 J/deg.CA and 32.3 J/deg.CA, respectively; these rates are approximately 8.7 % and 34.6% lower, correspondingly than that of the reference higher cylinder pressure of D. Thus, the recorded peak HRRs were obtained at 47.7 J/deg.CA and 34.8 J/deg.CA with BBu10 and BE10, respectively; these resulted rates are approximately 2.3% and 23% lower, correspondingly than that of the reference B fuel. These findings also accord

with previous studies, which showed that there is a strong correlation between fuel properties of the test fuels and engine combustion characteristics.

Figure 4.8 provides the experimental data on cylinder pressure and HRR at a function of crank angle degree (deg.CA) for the engine running at 2300 rpm with partial load condition. A strong relationship between the increase in engine load and speed with the increases in-cylinder pressure and HRR has been reported in the literature works (Attia & Hassaneen, 2016; Balamurugan & Nalini, 2014; Vallinayagam et al., 2013). From this figure, it is noticed that the peak pressure depends mainly on the engine load. As the engine load increase, the peak pressure also increases. Peak pressure for D is usually higher than or equal to the corresponding one for blends. As observed at partial load condition, the first reference fuel, D exhibits the maximum peak cylinder pressure of 59.4 bar at 12 deg.CA after top dead centre (ATDC), whereas the second reference fuel, B displayed 61.7 bar at 18 deg.CA for peak cylinder pressure. These figures also show that BE10 achieves lower peak cylinder pressure of 50.6 bar (12 deg.CA) than that of the reference B, except BBu10 with 61.4 bar at (9 deg.CA). Also, the peak cylinder pressure of DBu10 and DE10 attained are 57.6 bar and 46.1 bar, respectively, both occurring at 11 deg.CA and 14 deg.CA. These differences can be explained in part by the proximity of fuel properties including Cetane number and engine operating conditions.

Further analysis of the averaged HRR profiles for the test fuels is also presented in Figure 4.8. From the HRR analysis, the peak HRR is achieved at 61.2 J/deg.CA and 64.3 J/deg.CA with the reference fuels, D and B. Figure 4.7 (b) shows that BBu10 and DBu10 demonstrate higher peak HRR (69.2 J/deg.CA and 68.9 J/deg.CA) than those of other ethanol blends, also higher than that of the reference fuels. This result may be explained by the fact that higher cetane number values of butanol blends compared to that of ethanol blends. Also, BE10 and DE10 exhibit peak HRRs of 45.4 J/deg.CA and 41.6 J/deg.CA, respectively; these rates are approximately 25.8% and 32% lower, respectively that of the reference fuel, D.
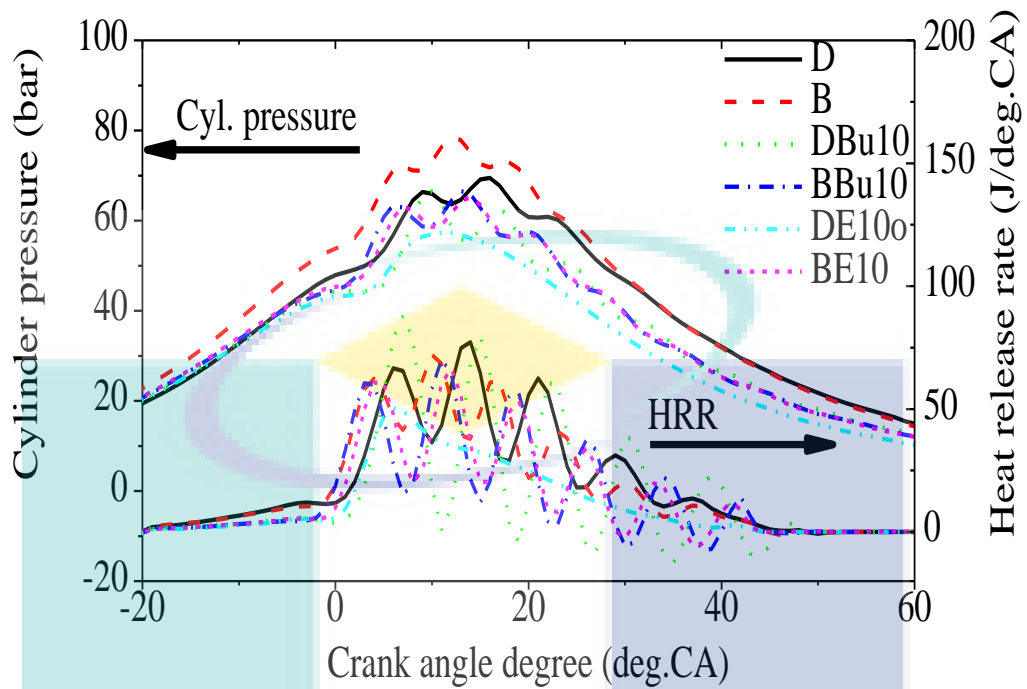
Figure 4.9   Cylinder pressure profiles and HRR curves with full load, 100% at 2300 rpm

The experimental data obtained from the analysis of cylinder pressure and HRR profiles under an operating condition of full load at 2300 rpm are shown in Figure 4.9. In this graph, higher engine load is found to cause a significant increase in cylinder pressure and HRR for all test fuels. Prior studies have noted that the effect of engine load applied to the engine can result in the rise of peak cylinder pressure as well as heat release rate (Attia & Hassaneen, 2016; Kaimal & Vijayabalan, 2015; Maghbouli et al., 2015; Monirul et al., 2016; Sakthivel et al., 2014). These figures indicate that the first reference fuel, D exhibits the peak cylinder pressure of 69.5 bar at 16 deg.CA ATDC, whereas DE10 obtained the peak cylinder pressure of 57.3 bar at 11 deg.CA, respectively. As for the second reference fuel, B, the peak cylinder pressure is found to be 64 bar at 21 deg.CA, which are 3.9% and 1.8% lower than that of BBu10 and BE10 with 66.6 bar at 13 deg.CA and 65.2 bar at 14 deg.CA, correspondingly. Surprisingly, average peak cylinder pressure for BBu10 and BE10 blends were found to be increased compared to B.

These figures also show that DBu10 and DE10 obtain lower peak cylinder pressures of 66.4 bar (10 deg.CA) and 57.3 bar (11 deg.CA), respectively than that of the first reference fuel, D. Since a 10% by volume of butanol and ethanol is added to each D and B blend, as shown in the figure, there are no significant differences between those test fuels except D and B which own greater expansion in power stroke for all engine loads. However, the findings of the current study do not support the previous research from the last research works concluded that when a small proportion of alcohol is added to the reference fuel such as D, there is a significant influence resulting an increase in maximum heat release rate and cylinder pressure (Imdadul et al., 2016; Liu et al., 2016). Also, the mixture of alcohol possibly causes the prolonged ignition delay, higher fuel consumption and shorter combustion duration due to the higher latent heat of vaporisation.

Figure 4.10 shows a detailed analysis of the averaged HRR for the test fuel under an operating condition of the full load with a constant engine speed of 2300 rpm. From the HRR analysis, the peak HRR is determined at 77.2 J/deg.CA and 79.6 J/deg.CA with the reference fuels, D and B, respectively. It can be seen from Figure 4.10 that BBu10 and BE10 demonstrate higher peak HRR (70.3 J/deg.CA and 66.4 J/deg.CA) than those DBu10 and DE10 blends, but lower than that of the reference fuels. Also, DBu10 and DE10 blends exhibit peak HRRs of 88.2 J/deg.CA and 50.3 J/deg.CA, respectively; these rates are approximately a 14.3% increase and a 34.8% decrease, respectively, compared to that of the reference fuel, D. The results of this study indicate that average peak HRR for all test fuels increases with the increase in engine loads and speeds. There are similarities between the attitudes expressed by average HRR for the test fuels in this study and those described by Liu et al. (2018) and Ma et al. (2015).

The primary goal of the current study was to determine the effects of various engine loads and speeds with regards different test fuels with fuel properties regarding averaged cylinder pressure and HRR profiles. The investigation of average cylinder pressure and HRR profiles has shown that lower averaged cylinder pressure and HRR profiles were observed for butanol and ethanol blends for most operating conditions compared to that of base fuels namely; D and B. The evidence from this study suggests that the Cetane number values influence the values of average cylinder pressure and HRR profiles for the test fuels. Also, The present study provides additional evidence with

respect to the combustion characteristics of alcohol specifically; butanol and ethanol. So far this section has focused on the effects of three different engine loads namely; 0%, 50% and 100% loads with three engine speeds (1100 rpm, 1700 rpm and 2300 rpm) operating D, B, butanol and ethanol blends in terms of average cylinder pressure and HRR. The following section discusses the effects of similar engine loads and speeds on the cylinder pressure cyclic variations and coefficient of variations (COVs) for those test fuels.

4.4 Effects of Engine Loads and Engine Speeds on Cylinder Pressure Cyclic Variations and Coefficient of Variation (COV)

Cylinder pressure cyclic variations (CV) or cylinder pressure cycle-to-cycle variation (CCV) is among essential engine parameters that characterise the engine performance. The variation in cylinder pressure from cycle-to-cycle which originates from many sources is identified as a fundamental combustion problem (Heywood, 1988; Dimitrios et al., 2010a; Sun, Bittle, & Jacobs, 2013). It limits the use of lean mixtures, increases levels of pollutant emissions and increases idle speed operation. Therefore, an increase in engine power output and a reduction in engine noise and vibration could be achieved by eliminating or reducing the cyclic variation effect (Galloni, 2009a; Ghazimirsaied & Koch, 2012).

Moreover, cyclic variation also causes torque fluctuations and poor vehicle drivability (Dimitrios et al., 2016; Zhang et al., 2013). The study on cyclic variations of the engine provides a single statistical measure for a regular specific time series, which characterises the periodical variability of the data values (Heywood, 1988). Also, the cyclic variation study can also measure and indicate the repetitiveness of the mean values during the cycles. This section provides and discusses the results of cylinder pressure cyclic variations of 200 consecutive cycles and the COV from the effects of zero, partial and full loads on cylinder pressure cyclic variations at three different engine speeds (N=1100 rpm, 1700 rpm and 2300 rpm). In this section, further details are provided on the influence of butanol and ethanol in the blends with regards to the engine cyclic variations.

4.4.1 Cylinder Pressure Cyclic Variations and Coefficient of Variation (COV) of Test Fuels at Engine Speed, N=1100 rpm

Another most important factor with regards to engine performance characteristics is the cyclic variations in the consecutive engine combustion cycles which is mostly defined by the COV. Previous studies have been conducted using the COV values to analyse the cyclic variations in diesel and SI engines (Gürgen, Ünver, & Altın, 2018; Ji et al., 2016; Pham et al., 2014; Dimitrios et al., 2016; Sen et al., 2014). Cyclic variation approach is a practical statistic method to compare the degree of variation between two-time series even if their mean values are entirely different (Obed et al., 2016; Galloni, 2009b). This approach provides a single numerical measure for a given time series which characterises the temporal variability in the data, as the standard deviation of the data is divided by the mean value of the given time series data.

This section presents the results of the cylinder pressure cyclic variations and the COVs from the effects of varying loads namely; 0%, 50% and 100% at a constant engine speed of 1100 rpm. These cylinder pressure cyclic variations results are based on the different test fuels operated at the similar controlled condition. This section aims to determine and evaluate the 200 consecutive combustion cyclic variations for each test fuel when the engine is applied to a specific condition. Also, the significance of the butanol and ethanol in the test fuels for cylinder pressure cyclic variations are briefly discussed.

Figure 4.10 shows the variations of the cyclic cylinder pressure and mean cylinder pressure with a function of crank angle degree (deg.CA) for the test fuels, obtained at constant engine speed, 1100 rpm with zero engine load. The cylinder pressure cyclic variations are recorded for 200 consecutive cycles. The comparisons are made based on the mean cylinder pressure (red line), and all 200 cycles of the cylinder pressure (cyan line) are plotted for each test fuel to determine the cyclic variability under a specific condition. It can be observed from the figure that the cylinder variations for all test fuels are comparable with each other except DE10. There are more substantial cylinder pressure fluctuations and instabilities with DE10 occurring at the power and expansion stroke. This observation is mainly attributed from the effect of different chemical

compositions, low flash point and high volatility of DE10 on the combustion process of the mixture which leads to developing more engine cyclic variations (Obed et al., 2016).
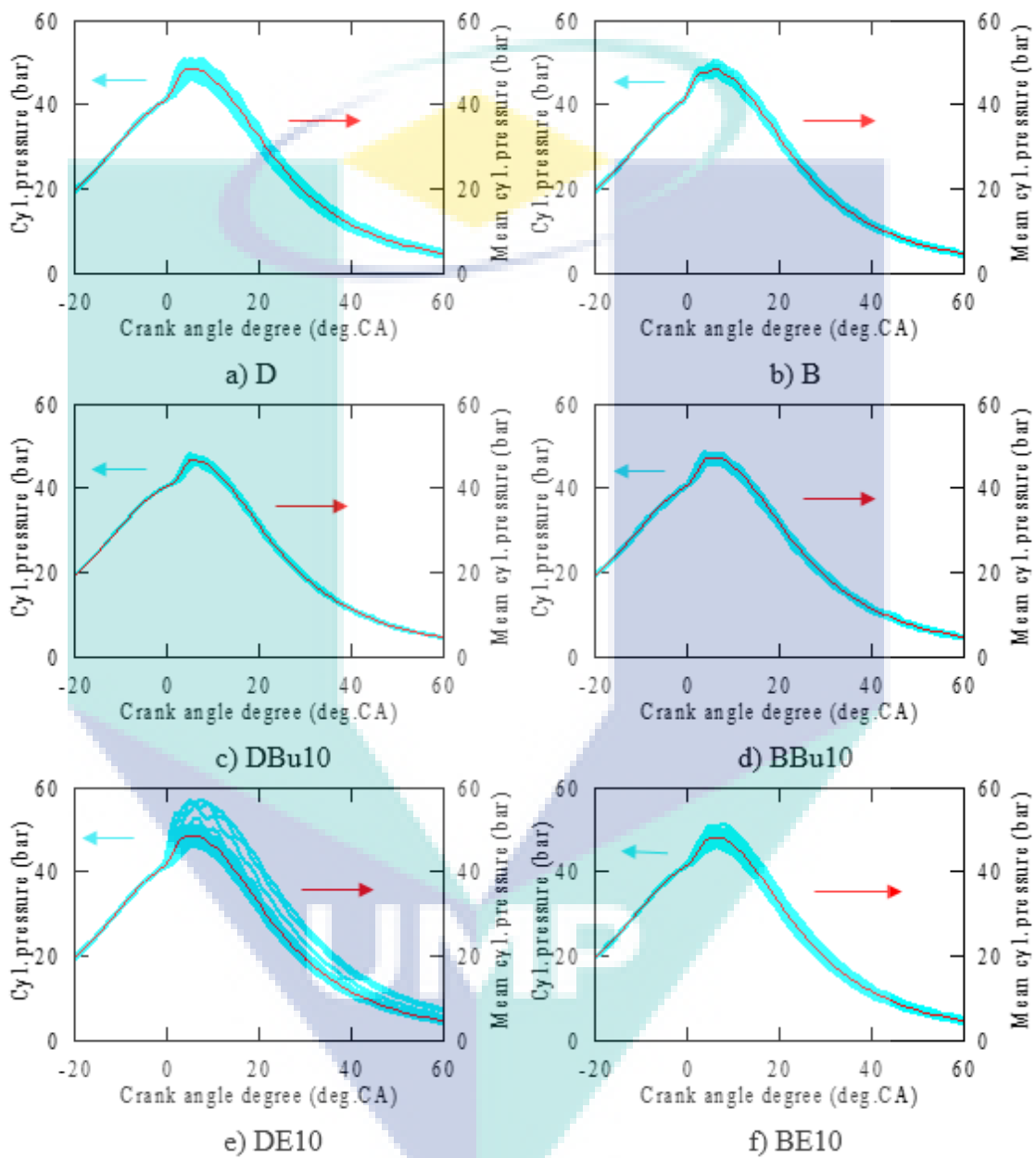
Figure 4.10   Comparison of cylinder pressure cyclic variations and mean cylinder pressure with zero load, 0% at 1100 rpm

Table 4.2   Statistical results and percentage of relative standard error, RSE% on cylinder pressure cyclic variations at zero load, 0% (N=1100 rpm)

Test fuels	Cylinder pressure, bar			Std Dev, σ	COV	RSE, %
	Mean	Max	Min			
D	48.7	50.9	46.0	0.92	0.019	0.133
B	48.5	50.4	47.0	0.62	0.013	0.090
BBu10	47.3	48.5	45.7	0.54	0.012	0.081
DBu10	46.9	48.5	45.3	0.52	0.011	0.130
BE10	48.2	51.3	45.8	0.89	0.019	0.079
DE10	48.7	57.0	46.0	1.47	0.030	0.213

Statistical results, COVs and the percentage of relative standard error (RSE%) as listed in Table 4.2 for the peak cylinder pressure cyclic variations for all test fuels in Figure 4.10. It is observed from the table that the mean cylinder pressures for D and DE10 are comparable with other test fuels with the lowest point being DBu10. On average, the minimum scores for the test values are relative. However, the maximum value for DE10 is significantly higher than other test fuels at this condition. The standard deviation and COV obtained for DE10 are correspondingly higher than other test fuels. Higher standard deviation, σ obtained by DE10 indicates higher instabilities of the cylinder pressure cyclic variations within the 200 consecutive cycles. The results revealed that at low engine load, the lower combustion temperature is observed due to the smaller amount of fuel burnt in the cylinder which leads to lower the temperature of the residual gas and the cylinder wall. Then the ignition delay simultaneously increases to produce higher cyclic variations (Maurya et al., 2016).
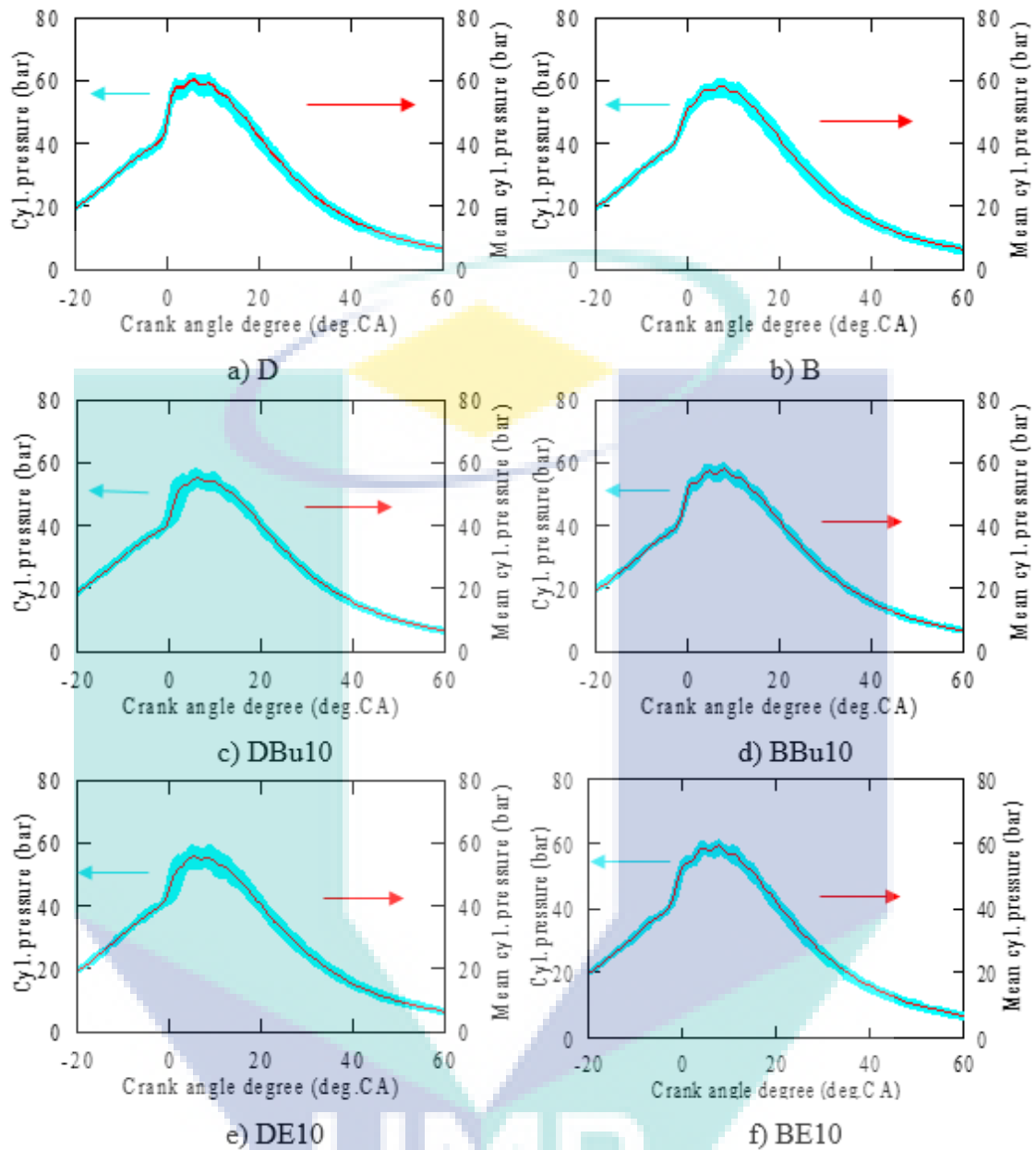
Figure 4.11   Comparison of cylinder pressure cyclic variations and mean cylinder pressure with partial load, 50% at 1100 rpm

The effect of butanol and ethanol blends with D and B on cylinder pressure cyclic variations and mean cylinder pressure is shown in Figure 4.11 for partial load, 50% and 1100 rpm. As expected, the cylinder pressure variations are comparable with D and B and almost identical with other fuels. It is evident that an increase in load causes lowering of the cyclic variation of the cylinder pressure. Again in Figure 4.11, it is seen that most of the cylinder pressure practically starts at the same point for butanol and ethanol blends

and the corresponding D and B case (for the same load). This is attributed to similar fuel injection condition, as there is no significant difference in their ignition delay values due to similar Cetane number values except DE10. However, as expected, all butanol and ethanol blends diagrams show slightly lower maximum pressures compared with both D and B fuels. The explanation for this behaviour is mainly attributed to the fuel spray characteristics containing butanol and ethanol droplets of smaller size and higher cooling effect of alcohols, lowering the combustion temperature.

Table 4.3   Statistical results and percentage of relative standard error, RSE% on cylinder pressure cyclic variations at partial load, 50% (N=1100 rpm)

Test fuels	Cylinder pressure, bar			Std Dev, σ	COV	RSE, %
	Mean	Max	Min			
D	60.2	61.9	57.2	0.82	0.014	0.095
B	58.3	60.3	55.3	0.94	0.016	0.113
BBu10	58.0	59.6	55.6	0.64	0.011	0.078
DBu10	55.2	57.8	52.5	1.14	0.021	0.078
BE10	59.3	60.7	57.6	0.67	0.011	0.082
DE10	55.9	59.1	52.6	1.40	0.025	0.176

Table 4.3 lists the statistical results, COVs and percentage of relative standard error, RSE% for the test fuels at the specific condition in Figure 4.11. Data from this table can be compared with the data in Table 4.2 which shows a significant increase in mean cylinder pressure when the higher load is applied with the engine rotating at the same speed. It is noticeable that DBu10 and DE10 blends achieve lower mean and minimum values than other test fuels, a fact attributed to the delayed combustion with these blends. This is attributed to their lower Cetane number (Cetane numbers in Table 4.1) which leads to higher ignition delay values and delayed dynamic injection timing. In addition, the standard deviation and COV values for DBu10 and DE10 are significantly higher compared to those of the test fuels.

Figure 4.12   Comparison of cylinder pressure cyclic variations and mean cylinder pressure with a full load, 100% at 1100 rpm

The analysis of test fuels comparison involving 200 cycles of cylinder pressure data and mean cylinder pressure are shown in Figure 4.12 for full load and 1100 rpm. It can be seen from the figure that the 200-cylinder pressure cycles and mean cylinder pressure diagrams do not show any appreciable difference in profile between D, B, butanol (BBu10 and DBu10) and ethanol (BE10 and DE10) blends. However, as expected, the pressures increase with load for all fuels at similar engine speed. The results reveal that higher combustion temperature is observed at high engine load for all fuels

due to larger amount of fuel burnt in the cylinder which is mainly attributed to the increase in temperature for the residual gas and the cylinder wall. Also, lower cyclic variations in cylinder pressure are observed with the decrease in the ignition delay (Dimitrios et al., 2016).

Table 4.4   Statistical results and percentage of relative standard error, RSE% on cylinder pressure cyclic variations at full load, 100% (N=1100 rpm)

Test fuels	Cylinder pressure, bar			Std Dev, σ	COV	RSE, %
	Mean	Max	Min			
D	65.5	68.0	63.3	0.92	0.014	0.099
B	66.2	69.2	63.5	1.08	0.016	0.115
BBu10	64.8	68.1	62.6	0.89	0.014	0.096
DBu10	63.0	64.6	61.0	0.70	0.011	0.078
BE10	66.5	69.5	63.3	1.26	0.019	0.133
DE10	63.3	65.6	60.5	0.85	0.013	0.094

The D fuel combustion in a diesel engine is nearly steady with minimal cyclic variations existing for all loads at similar engine speed. However, when alcohols including butanol and ethanol with lower Cetane number are combusted in a diesel engine, the combustion variations still exist and cause problems at low load condition. In Table 4., it is observed that higher applied load significantly increases the mean cylinder pressure for all test fuels at constant engine speed. More fuel is delivered and burnt at this point; the hence higher combustion temperature is achieved as well as cylinder pressure. Therefore, most of the test fuels achieve higher mean cylinder pressure at this point. Consequently, peak cylinder pressure, P_{max} for all fuels elevates with an increase in engine load. Also, it can be observed from Table 4. that addition of ethanol leads to a relatively higher COV of cylinder pressure cyclic variations, and as ethanol is absent, the COV of cylinder pressure cyclic variations decreases. This is because ethanol tends to knock which can result in higher cylinder pressure cyclic differences (Taghizadeh-Alisaraei & Rezaei-Asl, 2016).

4.4.2   Cylinder Pressure Cyclic Variations and Coefficient of Variation (COV) of Test Fuels at Engine Speed, N=1700 rpm

The effects of different engine loads applied to the engine when operating with the test fuels at 1700 rpm regarding cyclic cylinder pressure variations are briefly described and discussed in this section. The aim of Section 4.4.2 is to determine and evaluate statistically the cyclic variations of the fuels when different engine loads are applied to the engine at constant engine speed. Also, the results were statistically analysed and summarised in the listed tables. Also, the influence of butanol and ethanol in the biodiesel and diesel blends using the cylinder pressure cyclic variations are also evaluated and discussed in this section.

Further analysis results involving 200 cycles of cylinder pressure data and mean cylinder pressure acquired concerning the crank angle degree (deg.CA) at zero load, 0% and 1700 rpm are shown in Figure 4.13. First, it can be seen that the cylinder pressure cyclic variations do not show any significant difference in shape between the corresponding fuels; D, B, butanol and ethanol blends. Increasing the engine speed from 1100 rpm to 1700 rpm, the maximum combustion pressure for all fuels rises slightly. However, it is noticeable that B, BBu10 and BE10 have an apparent longer ignition delay due to the significant decrease in Cetane number. It is found that maximum cylinder pressure has no considerable rise with butanol and ethanol blends. Other than that, interestingly, it is found that more significant differences in expansion stroke are exhibited by BE10 and DE10 blends. These results indicate that instabilities occur during the expansion stroke which may lead to the high noise and vibrations in the engine.

Table 4.5   Statistical results and percentage of relative standard error, RSE% on cylinder pressure cyclic variations at zero load, 0% (N=1700 rpm)

| Test fuels	Cylinder pressure, bar			Std Dev, σ	COV	RSE, %
	Mean	Max	Min			
D	62.9	65.2	60.7	0.86	0.014	0.097
B	60.7	62.7	58.9	0.61	0.001	0.052
BBu10	54.0	56.3	52.1	0.81	0.015	0.105
DBu10	51.9	54.6	49.2	0.96	0.019	0.130
BE10	54.6	59.9	46.3	2.31	0.042	0.298
DE10	50.8	56.6	44.3	2.68	0.053	0.372

Figure 4.13   Comparison of cylinder pressure cyclic variations and mean cylinder pressure with zero load, 0% at 1700 rpm

Statistical results and percentage of relative standard error, RSE% for the test fuels in Table 4.5 are obtained and calculated from Figure 4.13. Also, it is apparent that the mean values for the test fuels are significantly increased with the increase in engine speed. Mineral diesel (D) achieves the highest mean value for cylinder pressure compared to that of other fuels. There is a significant increase in the mean value when

the engine speed is increased from 1100 rpm to 1700 rpm. One can observe that with increasing engine speed, increases in maximum and minimum cylinder pressure values for the fuels are obtained.

Figure 4.14   Comparison of cylinder pressure cyclic variations and mean cylinder pressure with partial load, 50% at 1700 rpm

Variations of cylinder pressure data and the corresponding mean cylinder pressure are plotted against crank angle degree (deg.CA) in Figure 4.14, for all six fuels

at 1700 rpm with partial engine load. It can be seen from the figure that the mean values of maximum combustion pressure are highest for D and lowest for DE10 and BE10; this is being consistent with the heating value of the fuel. However, the cyclic variation is similar for all fuels except DE10 and BE10. It is important to note that at the same load, the trends in the mean combustion maximum pressure are similar to those reported earlier. For example, an increase in carbon chain length results in an increase in the mean of maximum combustion pressure, however, this value will be reduced with the rise in unsaturation degree (Pham et al., 2014; Pinzi et al., 2013). It is noticeable that biodiesels have higher flash points compared to D and this may degrade their ignition; therefore it is useful to measure the laminar ignition delays of these fuels.

Table 4.6   Statistical results and percentage of relative standard error, RSE% on cylinder pressure cyclic variability at partial load, 50% (N=1700 rpm)

Test fuels	Cylinder pressure, bar			Std Dev, σ	COV	RSE, %
	Mean	Max	Min			
D	70.2	71.8	68.6	0.55	0.008	0.056
B	68.2	69.9	66.7	0.65	0.010	0.113
BBu10	62.6	64.0	61.1	0.51	0.008	0.057
DBu10	64.4	66.3	63.0	0.68	0.011	0.074
BE10	61.3	65.4	52.5	2.05	0.033	0.236
DE10	61.3	68.0	44.3	4.49	0.073	0.517

Cyclic variations and percentage of relative standard error, RSE% of the cylinder pressure over 200 consecutive cycles for the test fuels are calculated statistically and compared in Table 4.6. From the data presented in this table, it is apparent that the mean values for all test fuels are significantly increased when the higher load is applied to the engine which rotates at constant engine speed. At this point, D has dominated the highest mean value for the cylinder pressure as B, BE10 and DE10 achieve the lowest point for the mean values, correspondingly. Since the mean cylinder pressure values for the test fuels are increased at this point, the maximum and minimum cylinder pressure values correspondingly increase.
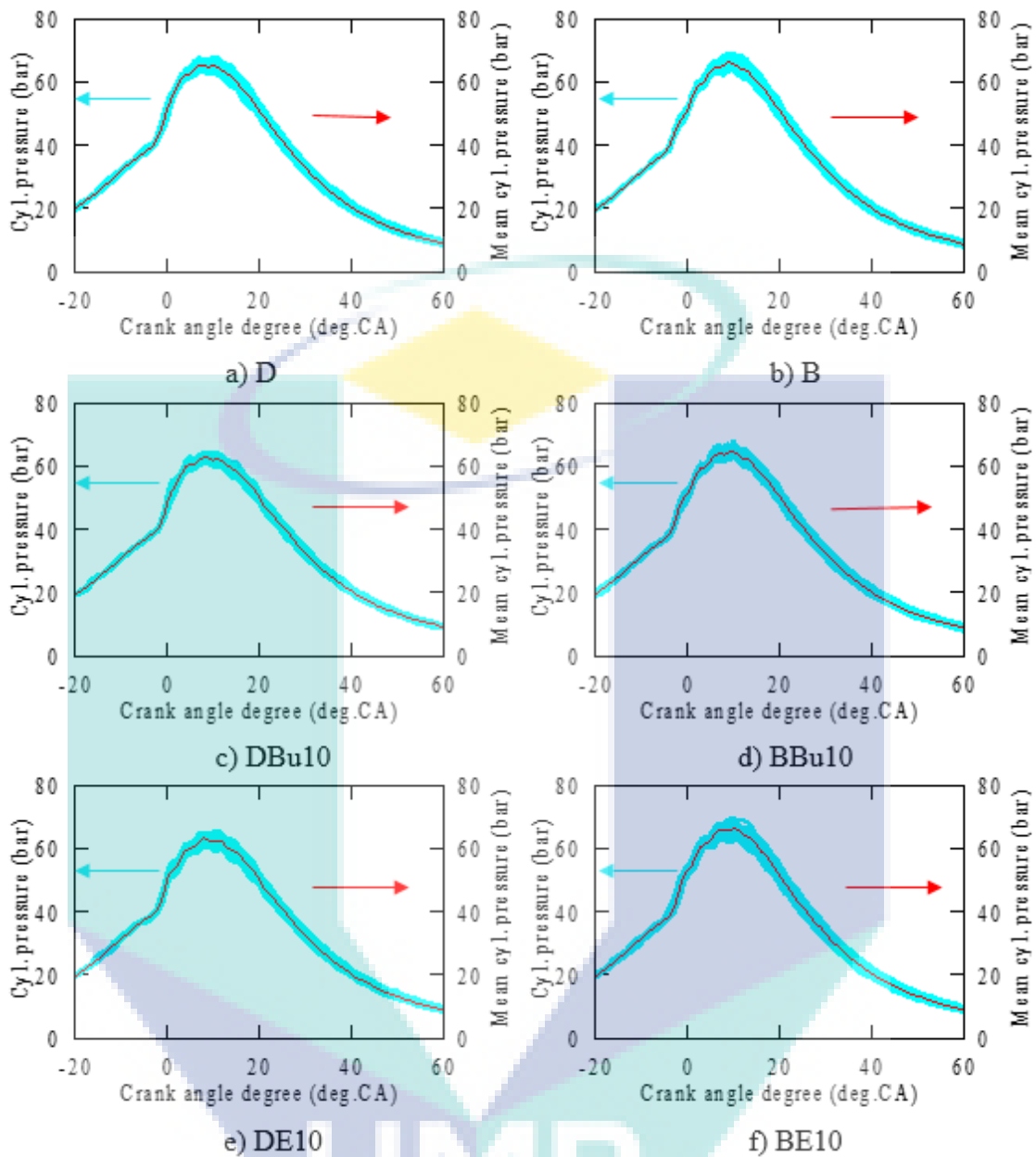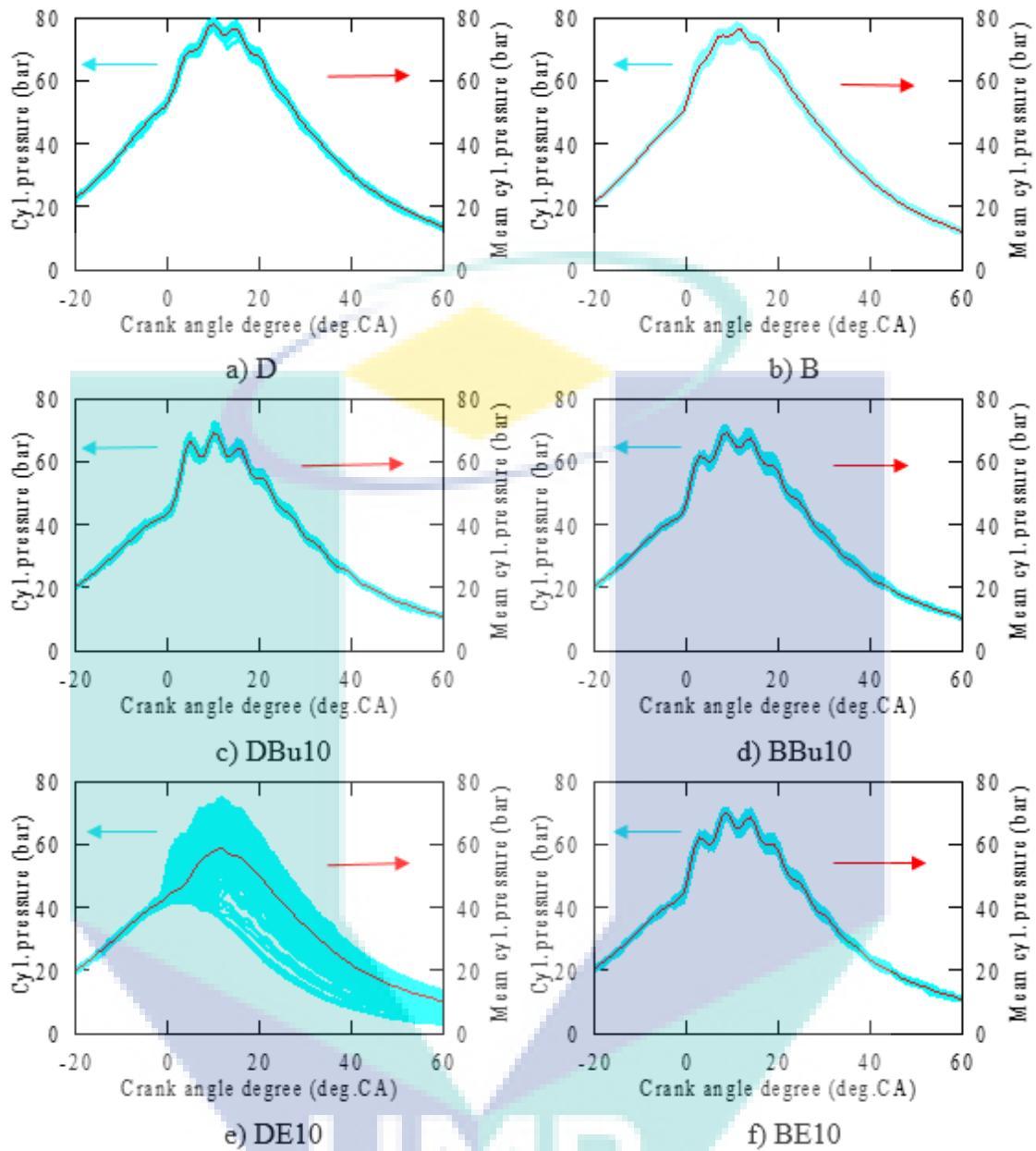
Figure 4.15　Comparison of cylinder pressure cyclic variations and mean cylinder pressure with a full load, 100% at 1700 rpm

Variations of 200 cylinder pressure cycles and the mean cylinder pressure plotted against crank angle degree (deg.CA) are shown in Figure 4.15 for all test fuels at 1700 rpm with partial engine load, respectively. The maximum combustion timing occurs around 15 - 20 deg.CA after TDC regardless of fuel types. The inter-cyclic variations revealed by the shape of the cylinder pressure traces are similar for all fuels except DE10, which shows higher combustion variations. This is understandable as DE10 has the lowest Cetane number and viscosity; hence, resulting in higher combustion variations.

A statistical analysis was used to compute the statistical results and percentage of relative standard error, RSE% of the cylinder pressure cyclic variations shown in Figure 4.15 and presented in Table 4.7. From the table, it can be seen that there is a positive correlation between the partial load condition and full load condition in which the mean, maximum and minimum cylinder pressure values are significantly increased when the higher load is increased. Interestingly, D fuel still leads the highest mean cylinder pressure value when compared to other test fuels, followed by both B and BE10. However, DE10 has achieved the lowest point for the mean and minimum values for cylinder pressure with the highest value in standard deviation.

Table 4.7   Statistical results and percentage of relative standard error, RSE% on cylinder pressure cyclic variations at full load, 100% (N=1700 rpm)

Test fuels	Cylinder pressure, bar			Std Dev, σ	COV	RSE, %
	Mean	Max	Min			
D	78.0	79.8	76.0	0.65	0.008	0.058
B	76.2	78.3	73.9	0.80	0.011	0.072
BBu10	69.3	71.1	67.9	0.55	0.008	0.055
DBu10	69.3	72.5	67.4	0.76	0.011	0.077
BE10	70.1	71.5	68.5	0.58	0.008	0.059
DE10	60.5	75.0	42.6	6.55	0.108	0.763

4.4.3   Cylinder Pressure Cyclic Variations and Coefficient of Variation (COV) of Test Fuels at Engine Speed, N=2300 rpm

This section focuses on the effects of zero, partial and full engine loads applied to the engine operating with all six fuels at 2300 rpm. This section aims to determine and evaluate statistically the cylinder pressure cyclic variations of all fuels when the engine is running at a specific test condition. Besides, the influence of the butanol and ethanol in the biodiesel and diesel blends on the cylinder pressure cyclic variations are also discussed in this section.
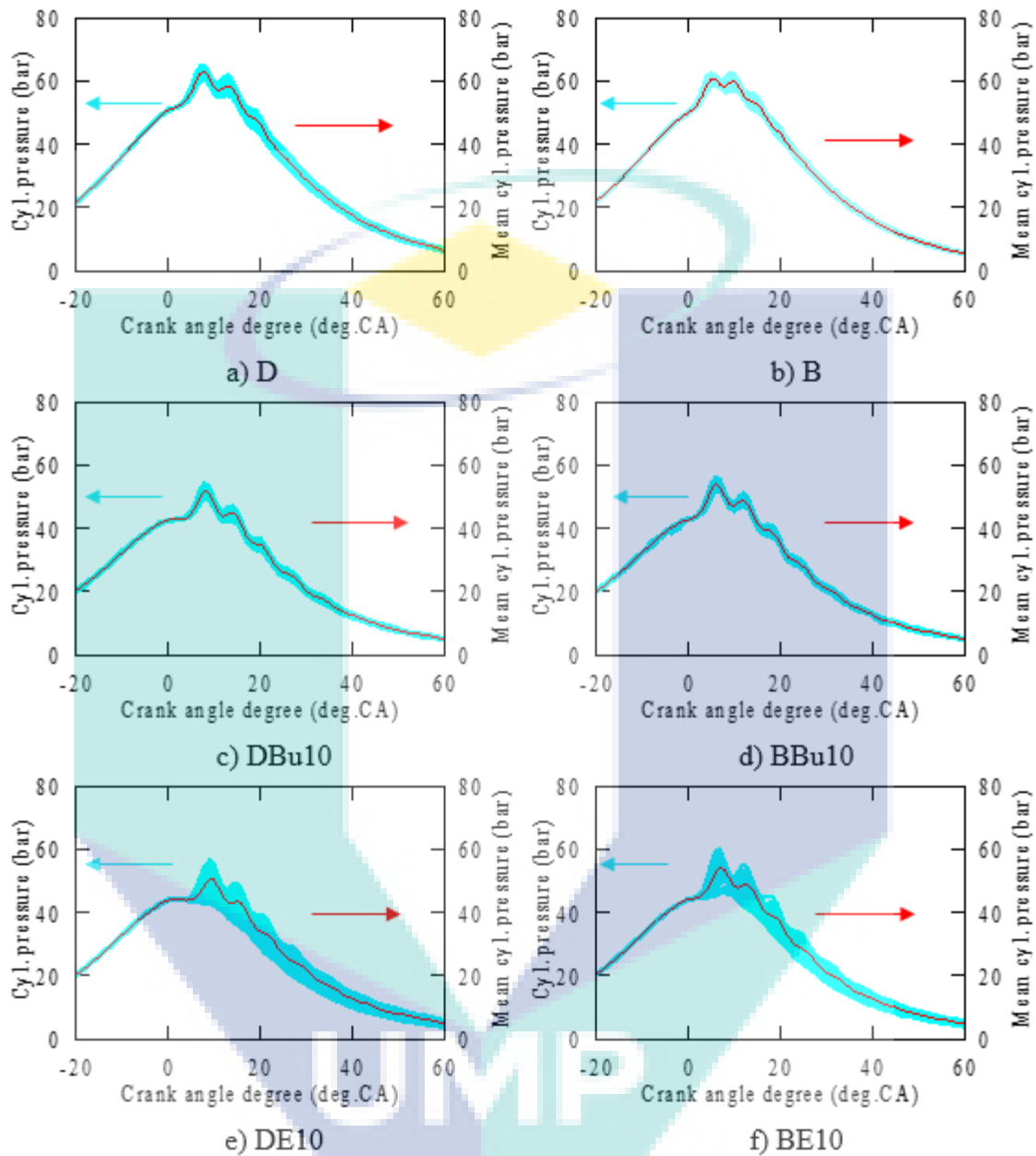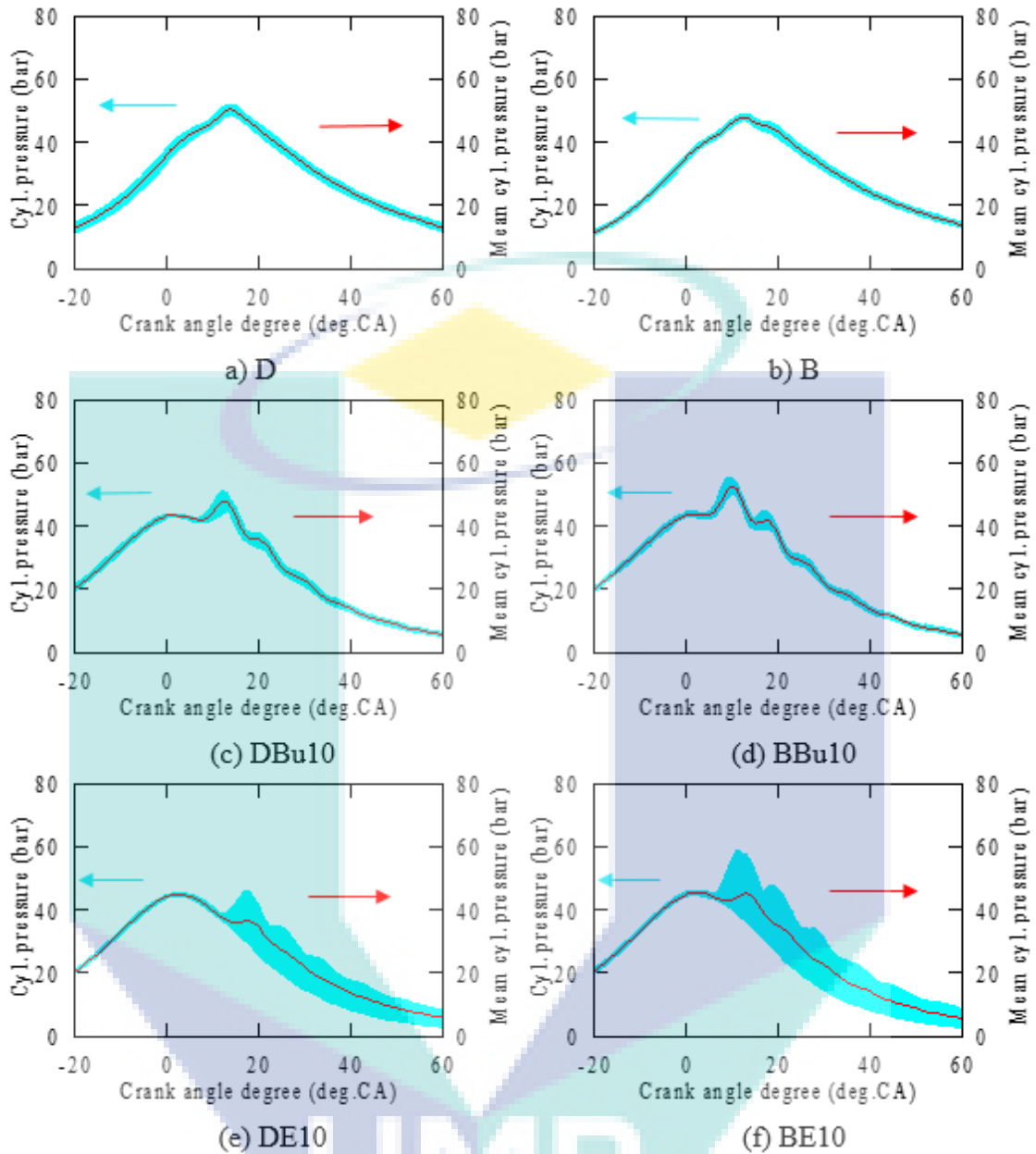
Figure 4.16   Comparison of cylinder pressure cyclic variations and mean cylinder pressure with zero load, 0% at 2300 rpm

Consider Figure 4.16 (a) – (f), which plot variations of 200 cylinder pressures and mean cylinder pressure plotted against the crank angle degree (deg.CA) when the zero load is applied to the engine at 2300 rpm for all six fuels. One can observe that with the increasing engine speed from 1700 to 2300 rpm, the maximum peak cylinder pressure increases. This is probably due to more fuel injected in the cylinder as more fuel is burned and the mean temperature in the cylinder increases simultaneously. As expected, the variability increases gradually with increased engine, so that all fuels are almost identical

except DE10 and BE10, as seen from the variations of cyclic cylinder pressure traces shown in Figure 4.16. It is evident that higher engine speeds lead to higher cyclic variations of the cylinder pressure. With the zero load the increase in variability is significant as reflected by the relevant cylinder pressure traces shown in Figure 4.16 which are broader and have much lower peaks than those obtained at full load. As expected, the lower average peak pressure and higher combustion variations are observed for DE10 and BE10 concerning both D and B fuels. This is an expected behaviour due to the lower heating value and lower Cetane number of butanol and ethanol concerning D.

Statistical results and percentage of relative standard error, RSE% for the cylinder pressure values obtained from all six fuels in Figure 4.16 are listed in Table 4.8. This table is quite revealing in several ways. Unlike other tables that list the mean cylinder pressure values, this table lists low mean values for the cylinder pressure at similar load with the highest engine speed. There is a clear trend of decreasing for the mean cylinder pressure values at this point due to the engine having achieved its maximum torque at 1800 rpm. Therefore, lower performance and combustion characteristics are achieved when the engine rotates at this engine speed. Interestingly, the mean cylinder pressure value for BBu10 is significantly higher than that of D and other test fuels. BE10 and DE10 achieve the highest in maximum and minimum values. Also, BE10 achieves the highest value in standard deviation which indicates higher instabilities in the engine.

Table 4.8   Statistical results and percentage of relative standard error, RSE% on cylinder pressure cyclic variations at zero load, 0% (N=2300 rpm)

Test fuels	Cylinder pressure, bar			Std Dev, σ	COV	RSE, %
	Mean	Max	Min			
D	50.3	51.7	49.0	0.54	0.011	0.076
B	48.0	48.7	47.2	0.28	0.006	0.041
BBu10	52.8	55.4	50.7	0.81	0.015	0.108
DBu10	47.9	50.8	44.8	1.06	0.022	0.156
BE10	48.2	58.7	45.1	3.54	0.074	0.518
DE10	44.7	45.5	44.5	0.10	0.002	0.016

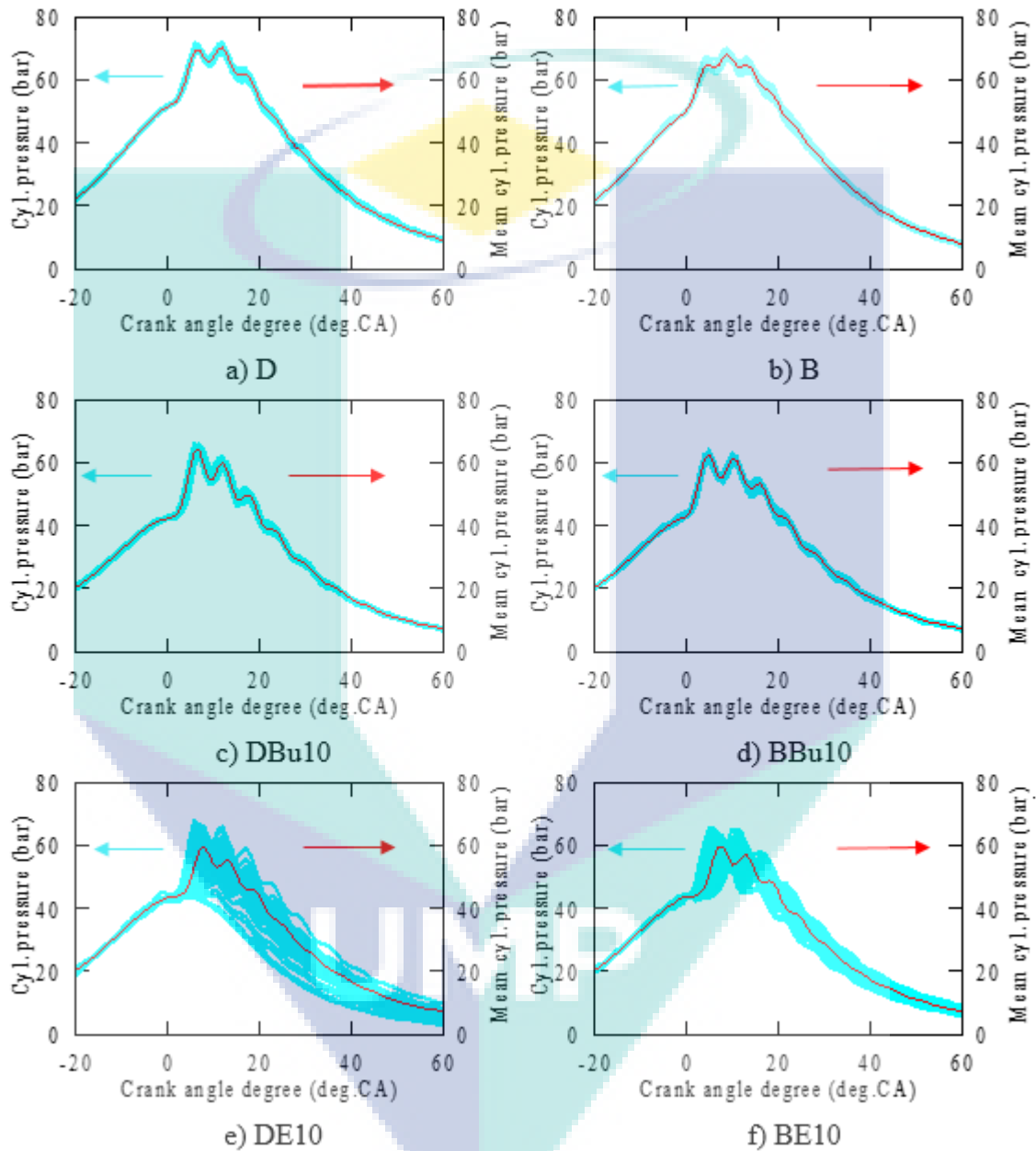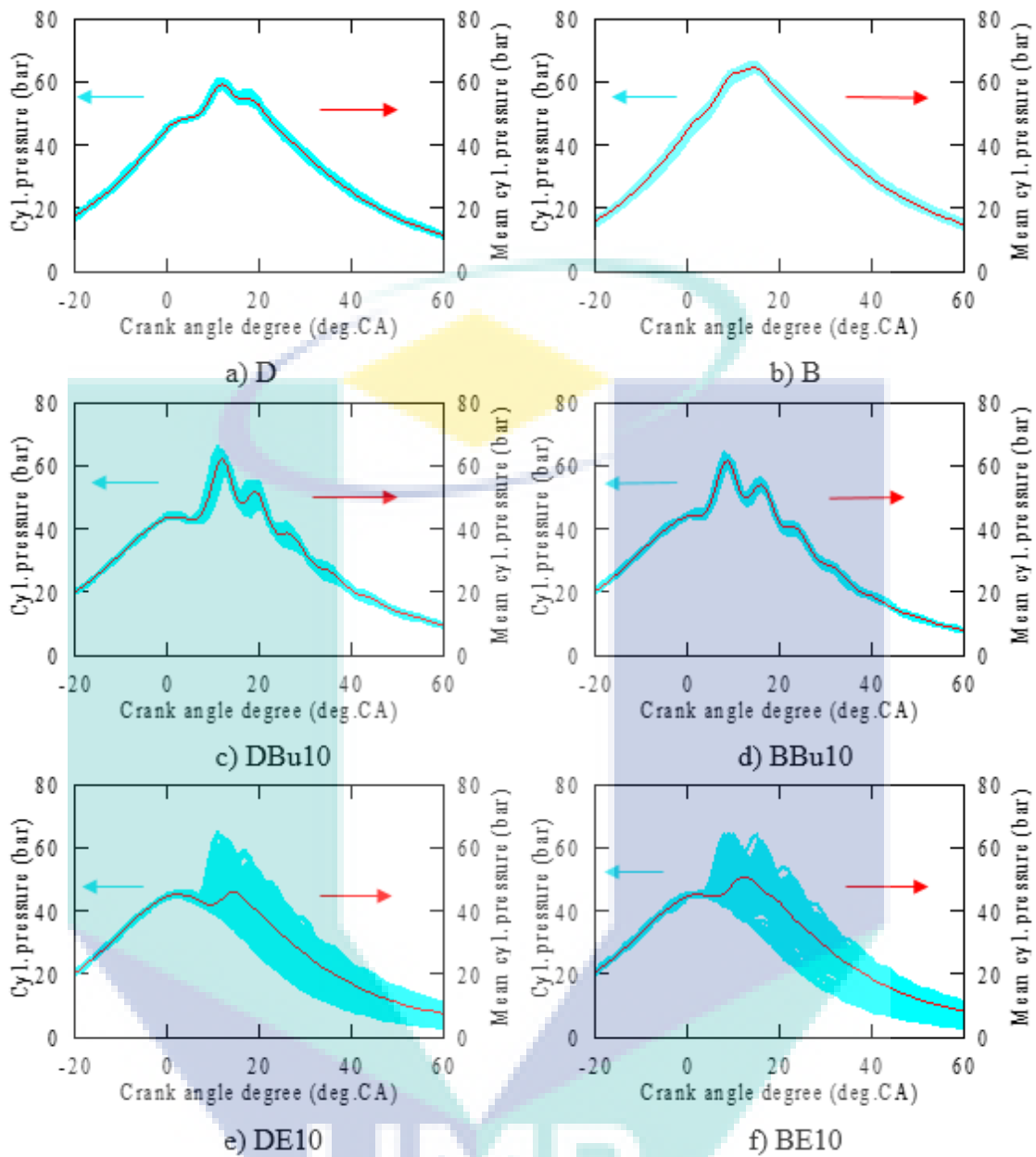Figure 4.17   Comparison of cylinder pressure cyclic variations and mean cylinder pressure with partial load, 50% at 2300 rpm

Figure 4.17 provides the experimental data on the 200 cylinder pressure cycles and mean cylinder pressure concerning crank angle degree (deg.CA) for the test fuels at partial load and constant engine speed, 2300 rpm. It could be interpreted from the graphs that with the increase in engine load and speed, the gap for expansion stroke increase is found for the ethanol blends; BE10 and DE10. The attributes of the fuel contribute a significant part on the combustion characteristics. Since ethanol and butanol, unlike other fuels, have low Cetane numbers, they have the tendencies to extend ignition delay and

provide a cooling effect that occurs during the expansion stroke. Moreover, for better fuel evaporation, less viscous fuels tend to produce a higher evaporation rate (Vallinayagam et al., 2014). In parallel with this, lower viscosities of butanol and ethanol are likely to reduce the viscosity of D and increase the evaporation rate when blending them by 10% volume. Therefore, the fuel spray formation is projected to be improved with superior evaporation with the BBu10 and BE10 blends. Meanwhile, it can be observed from Figure 4.17 (e) and Figure 4.17 (f) that BE10 and DE10 blends have an apparent larger redundancies in expansion stroke due to the increases in knocking pressure at similar conditions.

The statistical results and percentage of relative standard error, RSE% obtained from the graphs in Figure 4.17 can be compared in Table 4.9. It can be seen from the data in the table that the highest and lowest mean cylinder pressure values are achieved by BBu10 and DE10 respectively, with a percentage difference of 19.2%. Interestingly, also DE10 has reached the highest maximum and lowest minimum values for cylinder pressure correspondingly with a percentage difference between them being 36.6%. These maximum and minimum values also increase the standard deviation which indicates that the engine experiences more instabilities regarding cylinder pressure profiles

Table 4.9   Statistical results and percentage of relative standard error, RSE% on cylinder pressure cyclic variations at partial load, 50% (N=2300 rpm)

Test fuels	Cylinder pressure, bar			Std Dev, σ	COV	RSE, %
	Mean	Max	Min			
D	59.4	60.9	58.3	0.48	0.008	0.056
B	64.6	66.1	63.0	0.59	0.009	0.058
BBu10	61.6	64.0	59.5	0.73	0.012	0.084
DBu10	60.5	62.9	56.7	1.11	0.019	0.153
BE10	54.0	64.5	45.2	5.68	0.105	0.740
DE10	50.8	64.9	44.8	5.72	0.112	0.792
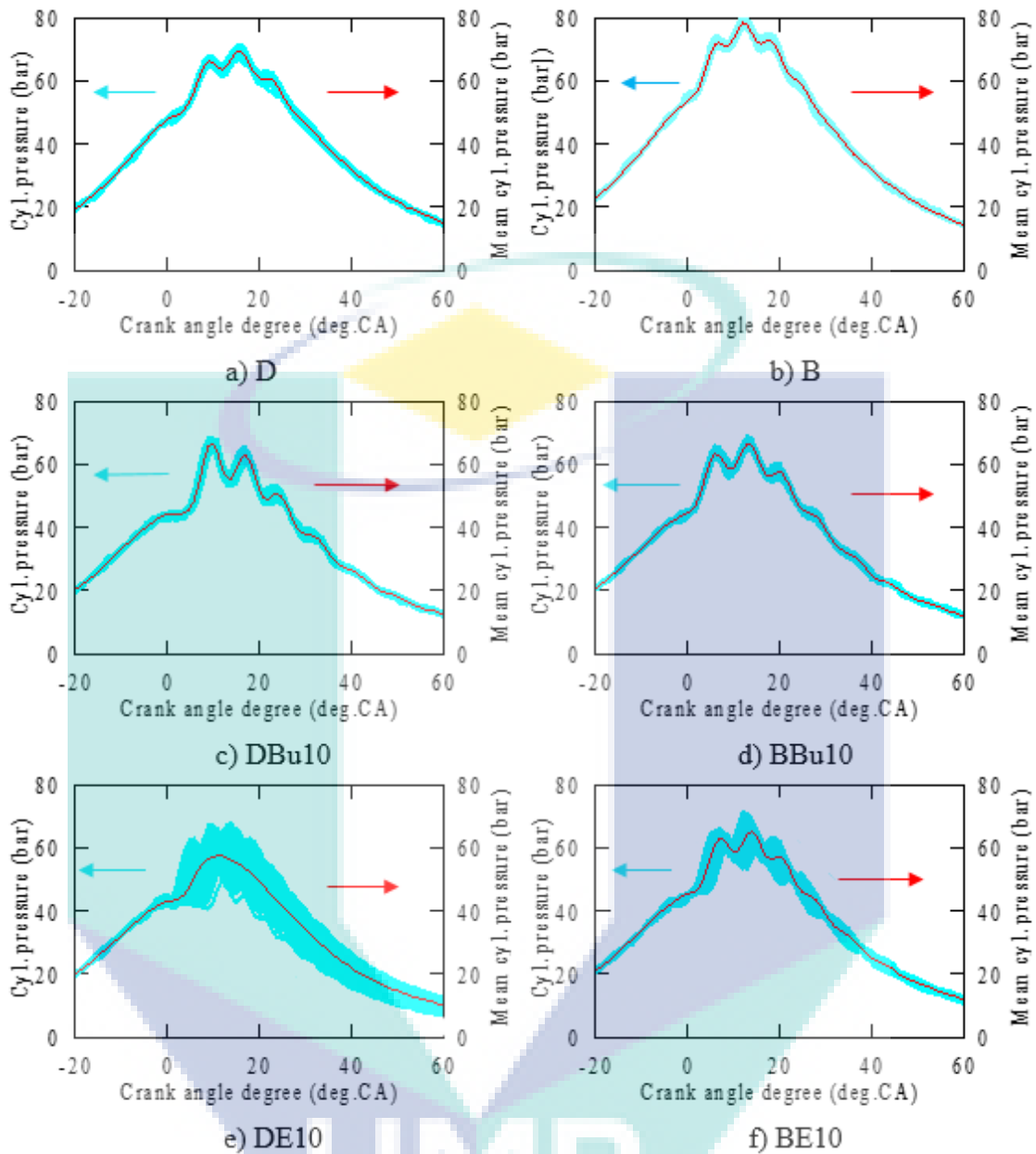
Figure 4.18   Cylinder pressure cyclic variations and mean cylinder pressure with a full load, 100% at 2300 rpm

To evaluate the engine cyclic variation, cylinder pressure for 200 cycles was recorded and stored corresponding to the crank angle degree (deg.CA) for each test fuel. As a comparison, mean cylinder pressure was used as a reference to compare the value of measured cylinder pressure cyclic variations. Figure 4.18 shows the variations of cylinder pressure data and mean cylinder pressure concerning crank angle degree (deg.CA) for all test fuels operating with a speed of 2300 rpm under full engine load. From the graphs, it can be observed that in-cylinder pressure for diesel-butanol and

diesel-ethanol blends are lower than D for 200 consecutive cycles and mean cylinder pressure. Interestingly, butanol and ethanol develop the peak cylinder at longer crank angles, which is evident at similar conditions. This was because butanol and ethanol have a lower flash point than D. Thus lower flash point for the alcohol blends was also observed. Also, because of the higher flash point in butanol and ethanol with diesel blends, larger amount of D in DBu10 and DE10 blends ignite at the start of combustion with lower cylinder temperature. Therefore, this event increases the cylinder temperature simultaneously during the premixed combustion period and the cylinder temperature tends to reach higher when the cylinder temperature extends the flash point of butanol and ethanol. However, those effects lead to a longer combustion period with the pressure releases corresponding to the extended crank angle degree (deg.CA). With the combination of the attributes of the butanol and ethanol, for example, the lower energy density and low Cetane number are likely to reduce the cumulative energy density of the DBu10 and DE10 blends which simultaneously decrease the cylinder pressure.

Table 4.10   Statistical results and percentage of relative standard error, RSE% on cylinder pressure cyclic variations at full load condition (N=2300 rpm)

Test fuels	Cylinder pressure, bar			Std Dev, σ	COV	RSE, %
	Mean	Max	Min			
D	69.5	71.2	66.7	0.73	0.011	0.074
B	78.5	80.8	76.7	0.70	0.009	0.068
BBu10	66.6	68.8	64.9	0.68	0.010	0.072
DBu10	66.7	68.5	64.2	0.85	0.013	0.090
BE10	65.9	73.2	61.2	2.15	0.033	0.222
DE10	59.7	67.7	44.0	3.43	0.057	0.405

Table 4.10 provides the statistical results and percentage of relative standard error, RSE% obtained from Figure 4.18. It can be seen from the table that D achieves the highest mean cylinder pressure value compared to that of other test fuels at this condition as DE10 has reached the lowest mean value with a percentage difference of 15.1%. Moreover, the percentage difference is obtained at 49.8% for the difference between the highest maximum and lowest minimum values of the cylinder pressure by BE10 and DE10, correspondingly. Also, the values of the standard deviation for the cylinder pressure cyclic variations are obtained at this point with DE10 reaching the highest value (3.43) while B achieving the lowest value (0.6). The correlation between the values of

maximum, minimum and standard deviation is interesting because the higher gap between the maximum and minimum values indicates higher standard deviation values of the cylinder pressure. Therefore, a DE10 blend possesses a higher gap between the maximum and minimum values with a percentage difference of 42.4% as compared to that of D (6.5%), B (6.4%), BBu10 (5.83%), DBu10 (6.5%) and BE10 (17.8%).

In this investigation, the aim was to assess the effects of varying engine loads and speeds with regards different fuel properties of the test fuels to the cylinder pressure cyclic variations and COV of P_{max}. One of the more significant findings to emerge from this study, higher COVs were observed for ethanol blends for all operating conditions compared to that of butanol blends and base fuels. This is mainly attributed to lower Cetane number and calorific values of ethanol blends. This work contributes to existing knowledge of alcohol combustion characteristics by providing further findings of the engine combustion cyclic variations when operating with butanol and ethanol blends. The results in this section indicate that there are strong correlations between three different engine loads namely; 0%, 50% and 100% loads with three engine speeds (1100 rpm, 1700 rpm and 2300 rpm) operating D, B, butanol and ethanol blends in terms of cylinder pressure cyclic variations and COVs. The next section, therefore, moves on to discuss the effects of similar engine operating conditions on the analysis of peak cylinder pressure, P_{max} using recurrence plot (RP) and recurrence quantification analysis (RQA) for those test fuels.

4.5 Recurrence Plot (RP) and Recurrence Quantification Analysis (RQA) of the Peak Cylinder Pressure, P_{max}

The fuel burning processes in a diesel engine are attributed by many parameters that lead to complex dynamics. These parameters include different physicochemical properties in the fuel, the composition of the fuel-air mixture, amount of air charge and inlet temperature delivered to the engine as well as different engine design (Sen et al., 2008). Different parameters in the engine operation affect the combustion variables including in-cylinder pressure, cylinder temperature and HRR, resulting in variations in engine power output and emission characteristics (Deb et al., 2015; Wei et al., 2015). Hence, understanding the subject of cyclic variations in the fuel combustion process during engine operation has been among substantial topics of research for recent years.

Earlier research works in the dynamical behaviour of cyclic variations focused mainly on gasoline engines (Chandrashekar & Antony, 2005; Johansson et al., 1995; Sen et al., 2011; Wu, 2013), however further studies in cyclic variations have also recently focused on diesel engines (Maurya et al., 2016; Dimitrios et al., 2016; Yasin et al., 2013). Therefore, it is essential to develop a good understanding of the dynamical behaviour of the combustion variables to develop effective control strategies for more reliable and efficient engine performance with lower emissions. Hence, there were many efforts in research works to analyse the cyclic variations particularly in-cylinder pressure using deterministic methods from nonlinear dynamical systems and chaos theory (Alexa et al., 2015; Litak & Longwic, 2009a; Wendeker et al., 2003).

A nonlinear system is fundamentally complex and difficult to predict for the next cycle and often delivers the behavioural pattern include engine cyclic variation. Therefore, these cyclic variations are represented with the RP to detect dynamical patterns and nonlinearities in the specific data. The variability in engine cyclic combustion variables is particularly cylinder pressure and heat release. Therefore, this section attempts to evaluate the P_{max} fluctuation values for each test in a diesel engine at three different engine loads with varying engine speeds from the results presented in Section 4.6 and present further results using the methods of RP and RQA in order to assess their dynamical behaviours over the entire engine cycles. In this study, the whole pressure signals of each cycle are acquired and collected with a chosen sampling resolution of 1 crank angle degree (deg.CA). Note that an engine cycle consists of two rotations, therefore there are 720 sample points for each cycle. Each cycle is composed of intake process, compression process, combustion process and exhaust process.

4.5.1 Effects of Engine Loads on P_{max} at Engine Speed, N=1100 rpm

This study focuses the use of RP on the measured P_{max} for 200 consecutive cycles to determine the dynamical behaviour of all six fuels when three different engine loads are applied to the engine at the rotational engine speed of 1100 rpm.

Figure 4.19   Time series of peak cylinder pressure cyclic variation values, P_{max} (i) and recurrence plot (RP) with zero load, 0% at 1100 rpm

To recap, the three different engine loads in the study are zero, partial and full engine load respectively. Recurrence plot (RP) is an effective and qualitative two-dimensional graphical method which has been designed to determine and analyze the dynamical system/time series for qualitative results (Yang et al., 2016). To compare the results of dynamical behaviour or nonlinear dynamical systems for all six fuels, both RP and the measured P_{max} values are shown in Figure 4.19. It can be seen from the figure that different trends of dynamical behaviour characterised by different colour codes (red,

yellow, green, blue) are plotted in the RPs for all fuels. Note that the blue colour code represents the points closer to each other in the state space, while the red colour code characterises the points that are located far between each other. In the case of DE10, the RP pattern consists mainly of blue regions except for the coordinate i=50 with three visible vertical lines indicating irregular oscillations. Irregular behaviours are also observed in D and DBu10 with visible vertical lines at i-coordinate. Conversely, there are extensive blue regions on the lower-left and upper-left corners in BE10 and DE10. These blue regions indicate the presence of a trend or other less periodic in the time series.

Table 4.11   RQA parameter values for test fuels at zero load, 0% (N=1100 rpm)

Test fuels	RQA Parameters Values	
	DET	LAM
D	3.576	0
B	7.757	0
BBu10	12.058	2.315
DBu10	3.124	0
BE10	16.821	3.072
DE10	1.616	0

Next, the results of RQA for Figure 4.19 are listed in Table 4.11. The same fixed recurrence rate, RR= 0.5 is used in all six fuels. Note that the values of DET and LAM for BE10 and BBu10 are the largest among all the fuels. These parameters confirm the deterministic nature of the periodic fluctuations. In contrast, the other periodic fuels; D and DBu10 are characterised by smaller values of DET and LAM, which point to less regular dynamics. This could also be related to the effect of a curved structure. Curved structures can significantly appear in RP when the amplitude and frequency are modulated. The intermittency is also reflected in the RQA parameters. Note that in all the fuels LAM is smaller than DET which implies a delicate vertical structure and is far related to the appearance of laminarity and intermittency. In particular, the RQA parameters can be used to quantify the peak cylinder pressure, Pmax variations that are represented by relatively short time series.

Figure 4.20   Time series of peak cylinder pressure cyclic variation values, Pmax (i) and RP with partial load, 50% at 1100 rpm

RP patterns were used to evaluate various nonlinear dynamical systems through two-dimensional patterns (i, j) for D, B, butanol and ethanol blends as shown in Figure 4.20. The P_{max} values were obtained from the cylinder pressure data over 200 cycles at 1100 rpm with partial engine load. It is apparent from the figure that those RP have plotted different trends or behaviours which most been influenced by how the engine operates based on the fuel combustion characteristics and properties. These RP show patterns with diagonal and vertical or horizontal structures of the line composed of different colour codes from blue to red. These structures can easily classify the dynamics

of the studied system based on the colour code differences. Notice that in Figure 4.20, there are several red/yellow regions at upper-centre and left-centre of RP pattern for DE10 that identify the presence of intermittency in the P_{max} time series. Smaller intermittencies or irregularities are also observed for DBu10 and BE10 with the presence of red/yellow vertical lines at i=100. Conversely, in the similar figure which applies to the fuels of D and BBu10, it is noticeable that a series of less red/yellow vertical lines is present. These structures indicate a more regular oscillatory behaviour. Interestingly, the RP for B and BBu10 have checkerboard structures indicating a regular oscillatory behaviour.

Table 4.12　　RQA parameter values for test fuels at partial load, 50% (N=1100 rpm)

| Test fuels | RQA Parameters Values | |
	DET	LAM
D	4.806	0.367
B	2.938	0
BBu10	8.461	1.458
DBu10	1.410	0
BE10	6.839	0.516
DE10	0.823	0

Since RP provides only a qualitative description of the dynamics of a time series, Webber and Zbilut (Zbilut et al., 2002) provided the solution called recurrence quantification analysis (RQA) that quantified the various parameters based on the line structure and point density in an RP. The following results for RQA parameters include DET, and LAM are presented iin Table 4.12 for analysis of the peak cylinder pressure, P_{max} time series. It is observed that the values of DET and LAM for BBu10 and BE10 blends are larger for a more stable work of the engine at similar operating conditions. These quantities are significantly connected to the deterministic recurrence structure. On the other hand, a smaller value of DET is observed for DE10 which indicates less determinism of the P_{max} values in the engine operation. In addition, this parameter also relates to higher cyclic variations of peak-to-peak cylinder pressure due to the combustion inconsistencies at a specific controlled condition.
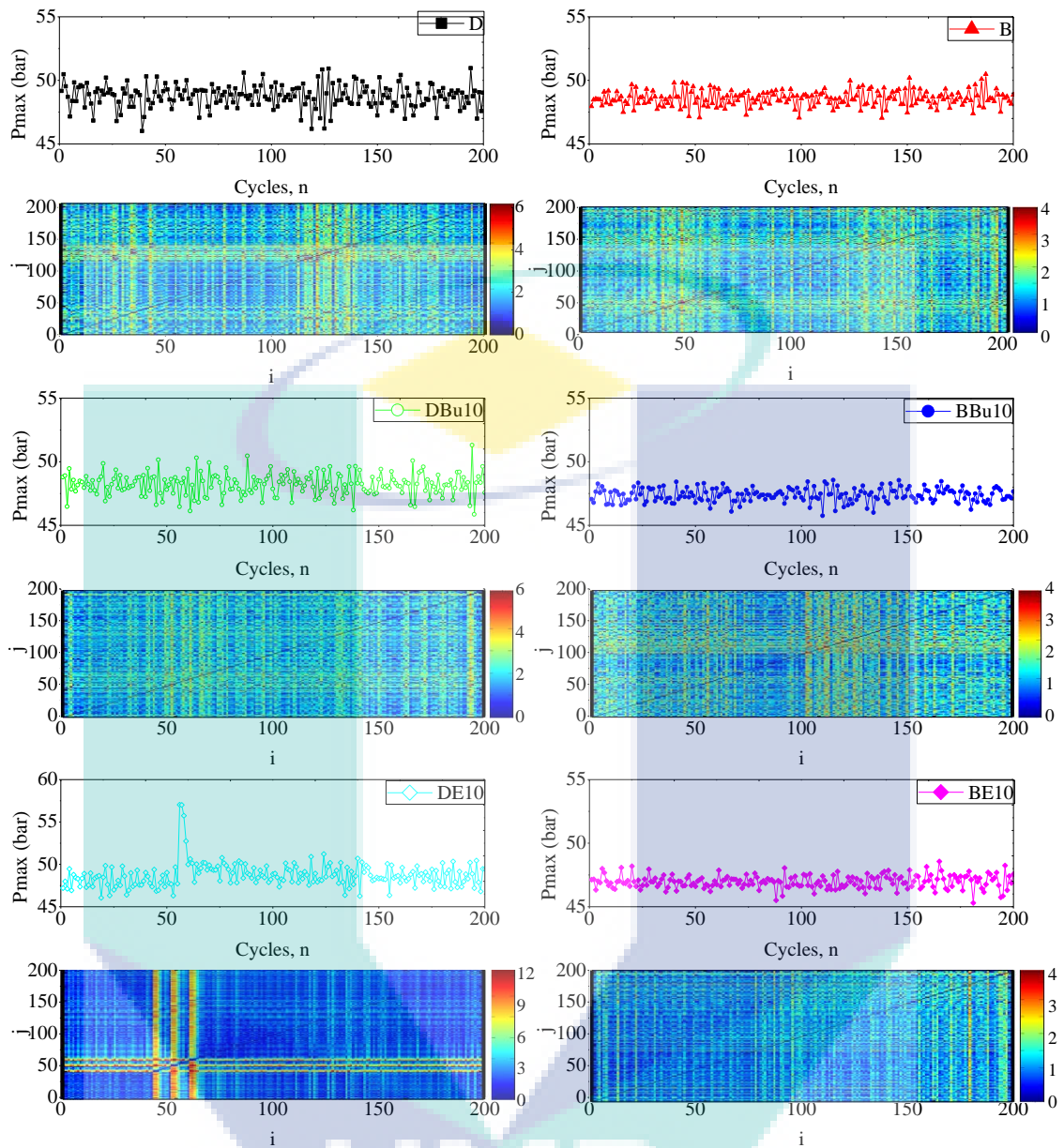
Figure 4.21   Time series of peak cylinder pressure cyclic variation values, P_{max} (i) and RP with a full load, 100% at 1100 rpm

Two-dimensional dynamical graphic patterns of the P_{max} values from the RP are compared in Figure 4.21. It is observed from the figure that different graphical patterns are found corresponding to the magnitude of the P_{max} data values representing all six fuels. As shown in the figure the points in the state space are represented by the colour codes at the coordinates from blue to red. In RP, the points that are close to each other in the state space are represented by blue colour, whereas the red colour code represents the points that are located far from other points (Yang, Bukkapatnam, & Barajas, 2011). Note

that the RPs of peak cylinder pressure, P_{max} time series are inconsistent with that of a pure random process whose RP describes a uniform distribution (all blue regions). The RP patterns for all fuels are more similar to the chaotic processes whose RPs are composed of red, yellow and blue regions. Analysing Figure 4.21, larger irregularities are observed in case of B and BE10, while for other fuels D, BBu10, DBu10 and DE10, smaller irregularities are found in the RPs. Note that at high load with constant engine speed, more fuel is delivered and burned at high temperature which leads to higher pressure in the cylinder. Also, more chaotic combustion process are observed at this state with different fuel composition.

The summary of the corresponding RQA is listed in Table 4.13. Note that DET and LAM are the corresponding ratios of points in diagonal and vertical lines. It is observed that larger DET and LAM values are observed for DBu10 and DE10 at this operating condition which significantly leads to more deterministic structures. These quantities are connected to the stability of the engine operation in which lower cyclic variations are observed. On the other hand, other fuels; BE10 and B are characterised by smaller values of DET and LAM which point to the more regular dynamics or irregularities.

Table 4.13   RQA parameter values for test fuels at full load, 100% (N=1100 rpm)

| Test fuels | RQA parameters values | |
	DET	LAM
D	2.720	0
B	1.604	0
BBu10	3.671	0
DBu10	6.462	2.206
BE10	1.188	0
DE10	4.490	1.72

4.5.2 Effects of Engine Loads on P_{max} at Engine Speed, N=1700 rpm

This study uses measured P_{max} values of 200 consecutive cycles at the rotational engine speed of 1700 rpm under zero, partial and full engine load, to determine the engine dynamical behaviour using the recurrence plot (RP) analysis. Therefore, a sampling frequency of 1024 times per combustion cycle was measured to ensure the reliability of the results.
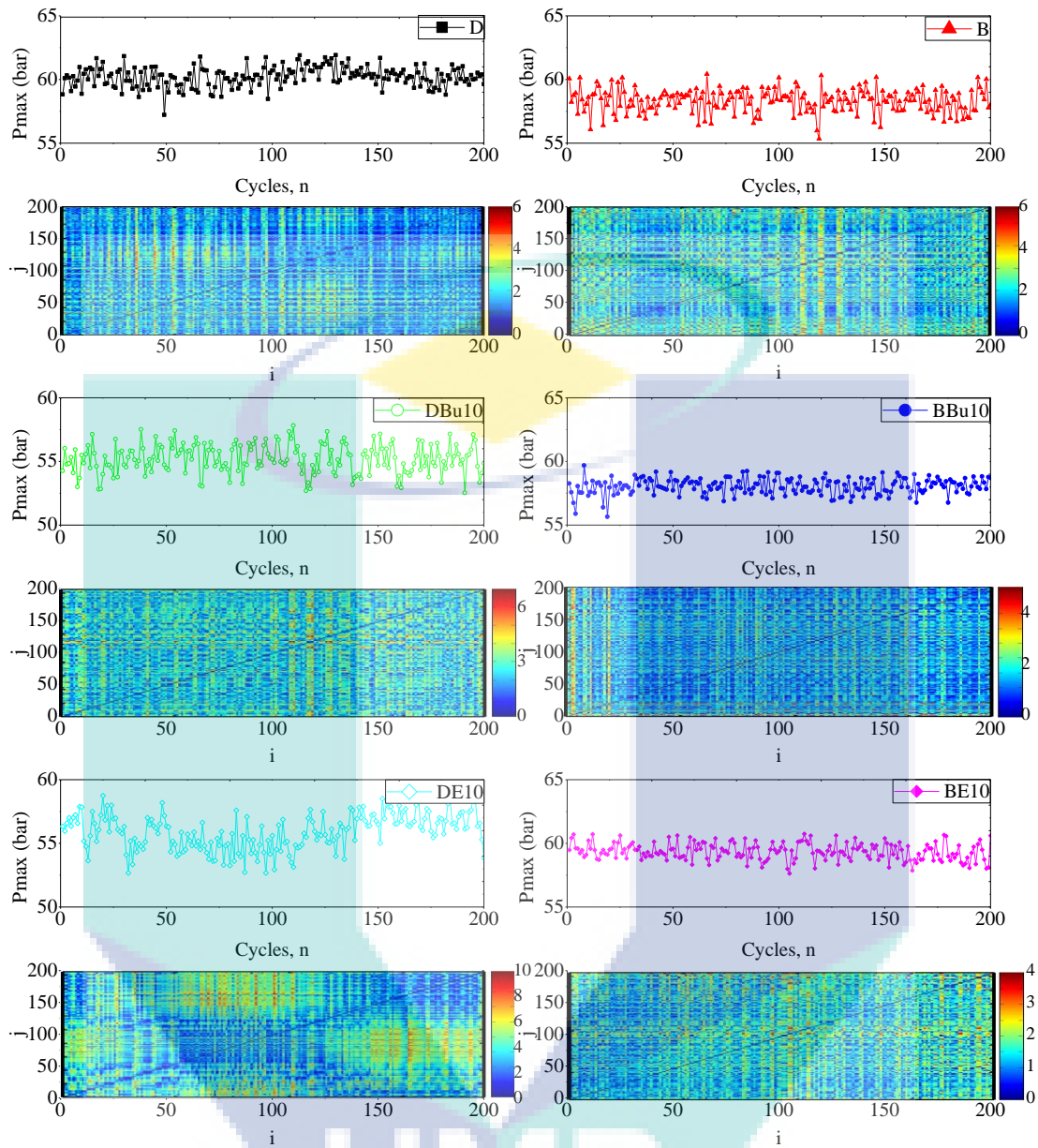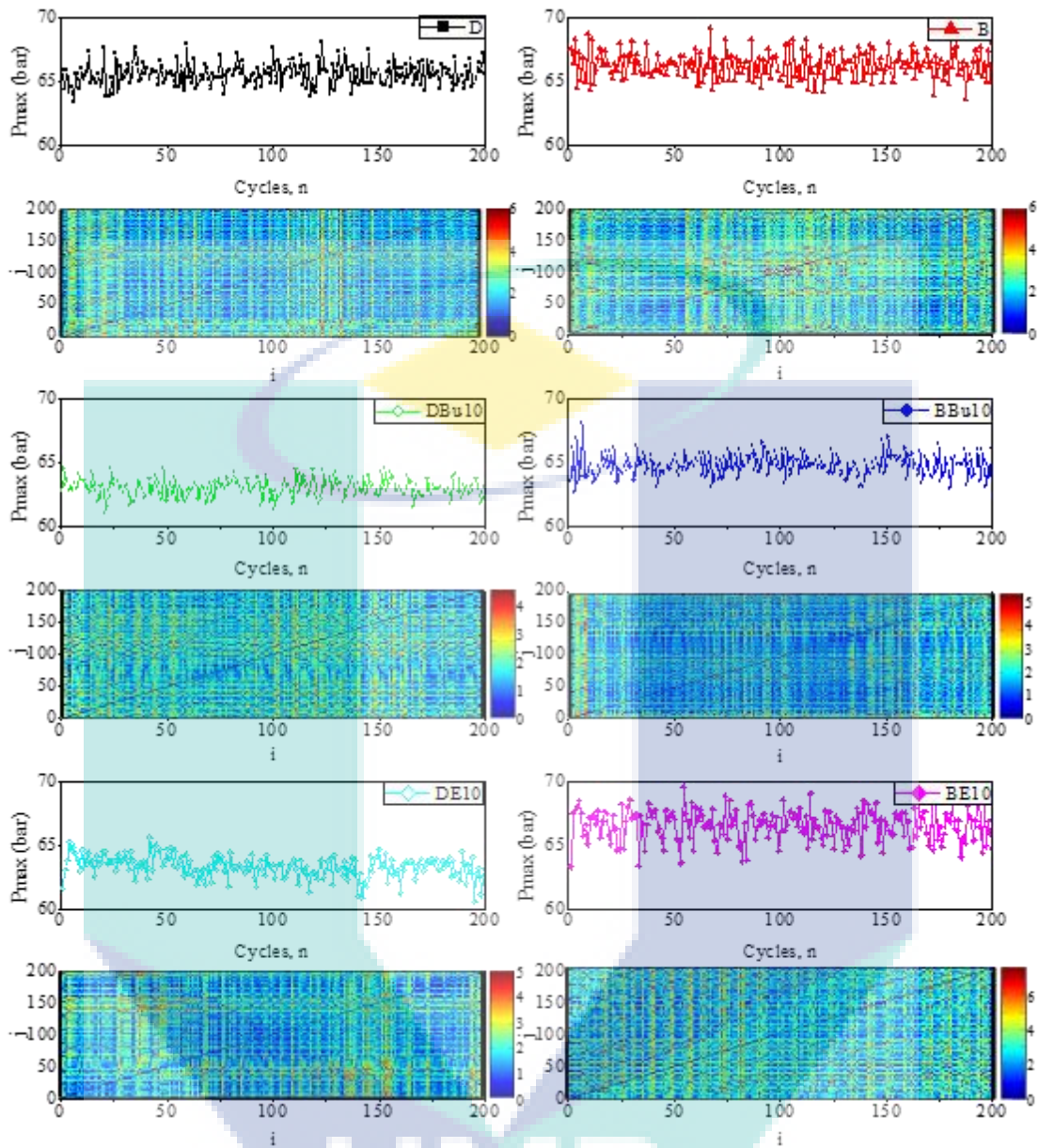

Figure 4.22 Time series of peak cylinder pressure cyclic variation values, Pmax (i) and RP with zero load, 0% at 1700 rpm

Figure 4.22 shows the different magnitude of the P_{max} data values influencing the recurrence plot patterns into presenting a variegated graphical rectangular plot in a two-dimensional array. The colour codes from blue to red at the coordinates in the figure are representing the points in the state space. Note that in RP pattern, the blue colour code specifies the points that are close to each other in the state space, while the red colour code characterises the points that are located far from other points. Thus, the RPs of peak cylinder pressure, P_{max} time series for all fuels which are inconsistent with a uniform distribution is characterised with all blue regions. In Figure 4.22, by visual observation, it is noticeable that the red, yellow and blue regions that composed the chaotic processes are shown in the RP patterns for all fuels. From the RPs for all fuels, the number of red regions are more in the case of DE10 as compared to that other fuels, followed by BE10, which indicates larger irregularities in cases of both fuels. Larger irregularities in the system or the time series characterise less deterministic and higher variations of the cycle-to-cycle or peak-to-peak. On the other hand, smaller irregularities are observed for B and BBu10 which indicate more deterministic with superior combustion characteristics. This is a good indication to understand that combustion characteristics of biodiesel with butanol blends are better than biodiesel with ethanol blends. This may be attributed to fuel injection quality of biodiesel and butanol which leads to better combustion characteristics at low engine speed.

Table 4.14   RQA parameter values for test fuels at zero load, 0% (N=1700 rpm)

Test fuels	RQA Parameters values	Values
	DET	LAM
D	4.48	1.206
B	25.113	10.67
BBu10	3.79	0.470
DBu10	2.910	0
BE10	0.368	0
DE10	0.119	0

Cylinder pressure values were collected to determine the P_{max} data and computed in RQA. From the RQA, the DET was calculated and used to asses the combustion characteristics of all six fuels given irregularity and the expected values of the variable. In all the six RP plots, recurrence rate RR was kept at 0.5 so that more recurrence points

will be visible in the RPs, and such that the horizontal and vertical line structures are visible. In Table 4.14, the value of DET is highest for palm biodiesel compared to that of other fuels at the similar operating condition. This indicates that the combustion characteristics evaluated regarding peak cylinder pressure, P_{max} values regularity is better for B followed by D and BBu10.
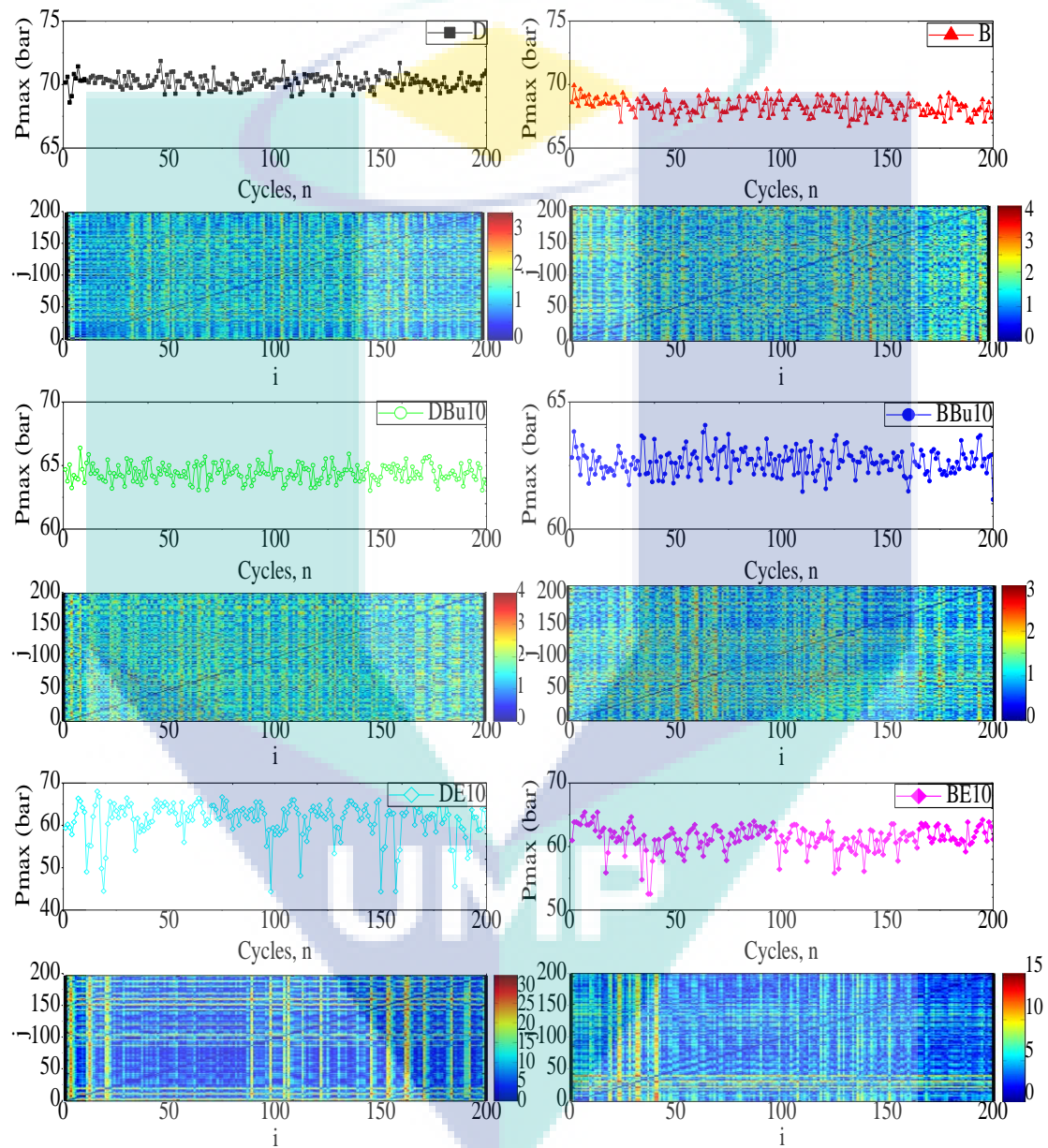
Figure 4.23 Time series of peak cylinder pressure cyclic variation values, P_{max} (i) and recurrence plot (RP) with partial load, 50% at 1700 rpm

Figure 4.23 shows the effects of partial (50%) load at 1700 rpm on the engine cyclic variations of the P_{max} values for all fuels using recurrence plot (*RP*). Compared with both *RPs* for D and B, the *RPs* of peak cylinder pressure time series for DE10 and BE10 are inconsistent with that of the pure random process whose RP describes as a uniform distribution. These patterns are more similar to chaotic processes whose RP is composed of blue, cyan, yellow and red regions with the characteristics of pure periodic oscillation. These RP patterns are composed with only diagonal lines. Note that by visual inspection, RP patterns in DE10 and BE10 change rapidly with the increase in cycle number. Under the lower load, the line structures of RP are almost the same. There are composed of the similar density of the colours and some diagonal lines. With increasing load in constant engine speed, a higher density of yellow and red regions in the RP have observed as well as the blue region with the presence of diagonal lines. These diagonal lines in the RP indicate that some periodic fluctuations exist in the system of the magnitude of the P_{max} data values for each fuel.

Table 4.15   RQA parameter values for test fuels at partial load, 50% (N=1700 rpm)

Test fuels	RQA Parameters val-	Values
	DET	LAM
D	11.82	1.055
B	2.400	0
BBu10	14.861	4.077
DBu10	6.070	0
BE10	0.570	0
DE10	0.048	0

Table 4.15 lists the summary results for RQA parameters. Note that when the engine speed is held constant, by changing the engine operating conditions from zero (0%) to partial load (50%), it affects changes to all the RQA parameters. It is noticeable that almost the same tendencies of all RQA parameters are observed when the engine load is held constant when changing the engine speeds from 1100 rpm to 1700 rpm. Note that the diagonal line structures based measures of DET and LAM for BBu10 and D have their maximal values at 1700 rpm and partial (50%) load compared to other fuels. Hence, higher DET and LAM values indicate more regularity in the pattern which means more stable engine operation is achieved. Conversely, the value of DET for DE10, in this case,

is the smallest among all the fuels. This parameter affirms the less deterministic nature of the periodic oscillations in the time series.
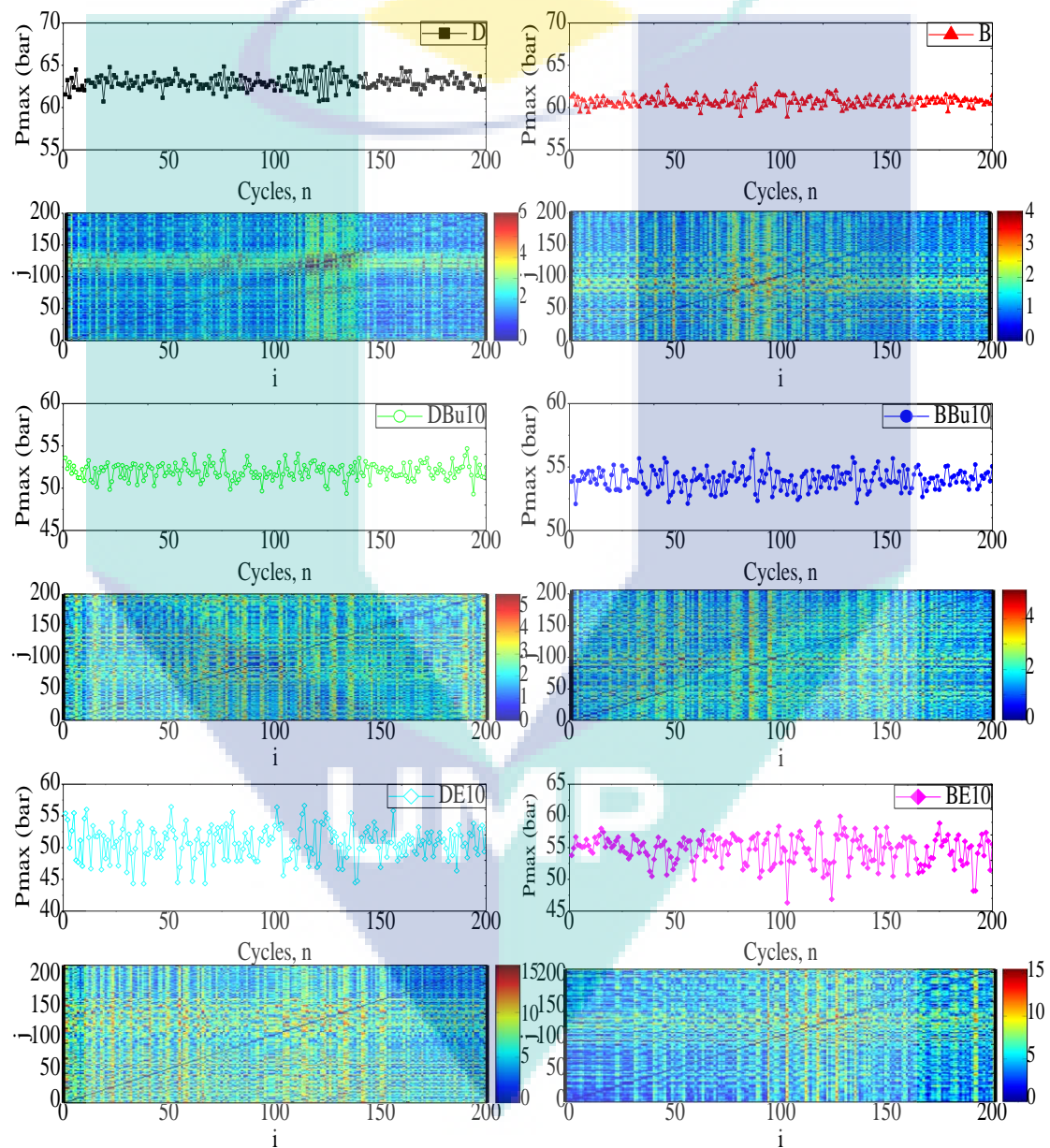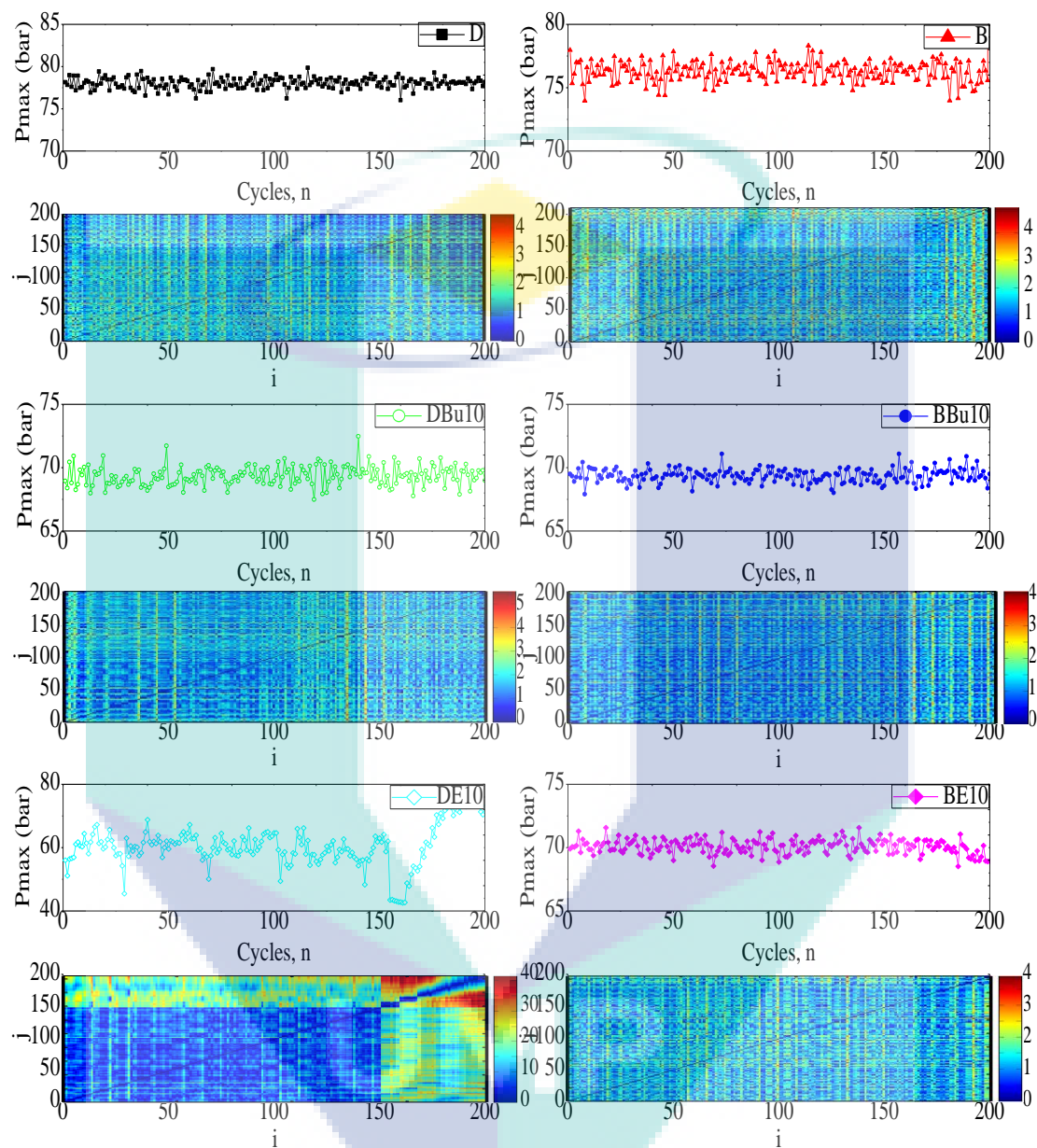

Figure 4.24   Time series of peak cylinder pressure cyclic variation values, P_{max} (i) and RP with a full load, 100% at 1700 rpm

The corresponding RP patterns for the examined peak cylinder pressure, P_{max} time series for all six fuels with full load for the crankshaft speed of 1700 rpm are shown in Figure 4.24. Here, due to a large number of points (720 points) per cycle, only peak cylinder pressure of all measured point is used. Note that the blue points found in Figure 4.27 indicate the highly correlated regions (close to each other) while the red region is

associated with the non-correlated parts of P_{max} (i) and P_{max} (j) series. Compared with the RP pattern for D as a reference, it is observed that the RPs of the P_{max} values for all fuels are inconsistent with that of pure random characteristic whose RP describes an invariable distribution (all blue regions) in the i, j coordinates. Those RPs are more similar to chaotic processes whose RP is characterised of red-yellow-green-blue regions at this state. Also, RP has characteristics of regular periodic oscillations in which the RP is composed of only blue regions. By visual inspection, patterns in RPs for all fuels change rapidly with the increasing cycle numbers at constant engine speed under full load. Furthermore, there are some regularities in the cycle number sequence that indicate the stability of the engine operation.

Table 4.16   RQA parameter values for test fuels at full load, 100% (N=1700 rpm)

Test fuels	RQA Parameters values	Values
	DET	LAM
D	7.579	0.470
B	5.607	0
BBu10	14.659	0.729
DBu10	4.799	2.104
BE10	11.143	1.173
DE10	0.024	0

Table 4.16 lists the summary of the corresponding RQA analysis for all six fuels tested with the similar operating condition. Note that the same fixed recurrence rate RR=0.5 is used in all fuels. As expected larger DET value for BBu10 is observed for a more stable work of the engine operation. The same argument can be applied to LAM. Structure of deterministic recurrence are linked with these RQA parameters which affirm that BBu10 has more deterministic nature compared to that of other fuels. Also, longer maximal length of diagonal L_{MAX} is observed for BBu10 compared to that of other fuels. Larger values of DET and LAM are also observed with D, B, BE10 and DBu10 fuels. On the other hand, the additional fuel, DE10 is characterised by the smallest values of DET and LAM, which indicate irregularities or less regular dynamics in the time series. These RQA parameters also lead to the conclusion that DE10 experiences less deterministic nature; in other words, more chaotic combustion in the time series. These

results are parallel with the results obtained by Longwic et al. (2009a) and Ding et al. (2015).

4.5.3 Effects of Engine Loads on P_{max} at Engine Speed, N=2300 rpm

Cylinder pressure data are collected over 200 cycles for three different engine loads particularly zero, partial and full engine load with the rotational speed of 2300 rpm. Then, the cylinder pressure data are used to obtain the P_{max} values over the entire engine cycles. Measurements are made with a sampling frequency of 1024 times per combustion cycle. Results from the measured P_{max} time series for engine speed, N=2300 rpm are shown in Section 4.4.3. These P_{max} values served as the single observable variable with a function of time series to be computed using scripts in Matlab into a two-dimensional topological pattern representing the multidimensional system behaviour using recurrence plot (RP) analysis. Moreover, it is convenient to use the P_{max} values to study the engine cyclic variability for the test fuels (Pham et al., 2014; Sen et al., 2010).

The time series of the P_{max} values were plotted and analysed using the RP analysis and presented in Figure 4.25 as a vibrant two-dimensional graphical RP representations. As shown in the figure, different colour codes from blue to red at the coordinates (i, j) characterised the distance between the points in the state space. Note that the points that are closer to each other in the state space are composed of the blue colour code, and the points that are located far from each other are regarded as the red colour code. The presence of different colour codes in RP patterns justifies either irregularity (chaotic) or regular (stable) dynamical of the time series (Chen & Yang, 2012a). Compared with D as a reference fuel, it is observed that the RPs of the peak cylinder pressure, P_{max} time series for all fuels are inconsistent with that of the uniform distribution (all blue regions). In Figure 4.25, DE10 consists mainly of blue regions on the upper-left and lower-left corners, indicating periodic oscillations or regular dynamic process (uniform distribution) in the time series. Periodic behaviours are also observed in B and BBu10. Conversely, there are extensive red regions in the RP patterns for D and BE10 consist which characterise larger periodic oscillations and irregularities in the P_{max} time series. These characterisations affirm higher cyclic variations of the P_{max} in the engine operation, whereas similar results are obtained by Ding et al. (2015).

Figure 4.25　　Time series of peak cylinder pressure cyclic variation values, P_{max} (i) and RP for all six fuels with zero load, 0% at 2300 rpm

The summary of the corresponding RQA results is presented in Table 4.17. In all fuels considered here the same fixed recurrence rate RR= 0.5 is used. Note that the values of DET and LAM for DE10 are the largest among all fuels, which affirm the deterministic nature of the periodic oscillations. These quantitative values are consistent with the qualitative RP pattern for DE10 with the presence of mainly blue regions (more deterministic nature) in the time series. On the other hand, the other periodic cases for DBu10 and BE10 are characterised by smaller values of DET and LAM, which indicate

higher regular dynamics or lower deterministic nature in the time series. Compared to the summary of RQA results in Table 4.13 and Table 4., when the engine load is held constant at zero load (0%), by changing the engine speeds from low speed to high speed, it is observed there is a simultaneous increase in all of RQA parameters for all fuels. These quantitative results can indicate that operating conditions of higher speeds and low load rate produce a stable condition to the engine.

Table 4.17   RQA parameter values for test fuels at zero load, 0% (N=2300 rpm)

Test fuels	RQA Parameters val-	Values
	DET	LAM
D	16.441	8.309
B	76.871	46.925
BBu10	4.205	0
DBu10	1.829	0
BE10	1.960	8.182
DE10	193.395	99.914

To assess the nonlinear dynamical system behaviour characteristics using different fuels, the P_{max} values were analysed using the RP, then presented in Figure 4.26 in the form of multi-coloured two-dimensional graphical representations. Here, due to a large number of points (720 points) per cycle in the fuel combustion cycle, only the peak points of all measured points represent the peak cylinder. Interestingly, the RP patterns can be used to represent both dynamical and non-dynamical changes in combustion cycle-to-cycle variations. Therefore, the highly correlated regions or periodic changes are represented by the red regions while the blue regions are associated with the highly deterministic nature of the peak cylinder fluctuations. In Figure 4.26, larger red point regions which represent higher dynamical fluctuations are observed with DE10 and BE10 blends as compared to other fuels. This is mainly due to the fuel combustion that influences the peak cylinder at specific engine speed.
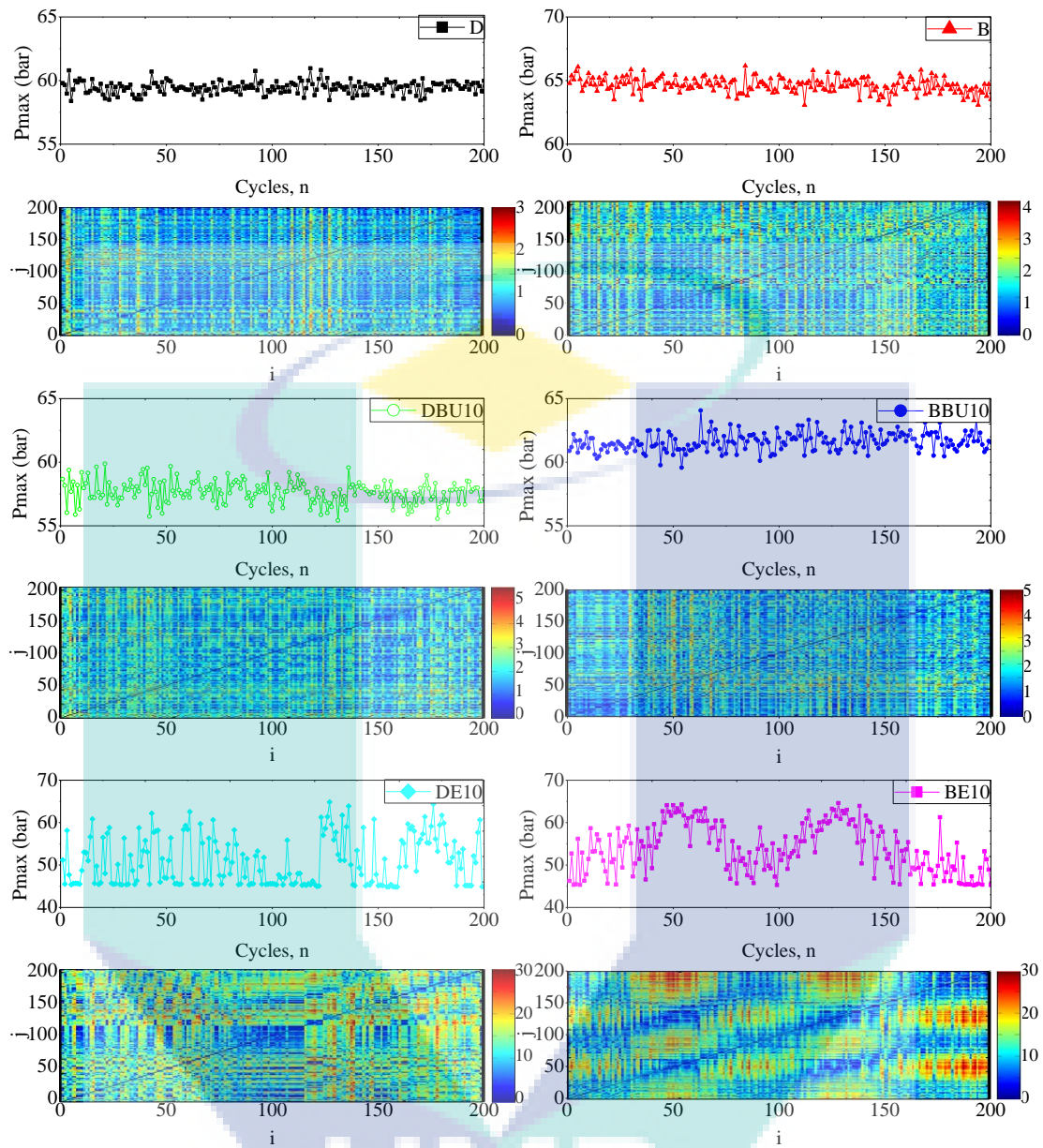
Figure 4.26   Time series of peak cylinder pressure cyclic variation values, P_{max} (i) and RP with partial load, 50% at 2300 rpm

The basic deterministic patterns of any RP consist of vertical and horizontal lines can be expressed into numbers known as RQA (Zbilut et al., 2002). In the frame of RQA, dynamics of the system or in the time series can be possibly identified. The summary of the corresponding quantitative RQA parameters for all six fuels can be found in Table 4.18. Note that DET and LAM are the corresponding ratios of points in diagonal and vertical lines (Marwan & Kurths, 2004). As expected the values of DET and LAM for B and D are larger for more stable works in the engine operation as similar patterns shown

in Figure 4.26. These quantities are connected to the structure of the deterministic recurrence, or in other words, the points are located close to each other in the state space (Yang et al., 2011). The different situation can be observed for BE10 and DE10 where the values of DET and LAM are smaller compared to others. These values represent the RP figures which indicate irregularity variations of the examined P_{max} values in the time series that cause higher cyclic variations for the examined fuels.

Table 4.18   RQA parameter values for test fuels at partial load, 50% (N=2300 rpm)

Test fuels	RQA Parameters values	Values
	DET	LAM
D	21.359	2.781
B	23.355	6.536
BBu10	4.8111	1.111
DBu10	3.9321	0
BE10	0.9622	0
DE10	0.4633	0

In the case of the P_{max} values at the rotational speed of 2300 rpm under full engine load, the RP analysis in the form of multi-dimensional graphical representations for all six fuels over 200 consecutive cycles are compared in Figure 4.27. It is seen from the figure that the recurrence plot analysis consists of different pixels whose colours are corresponding to the different magnitude of the P_{max} data values in a two-dimensional array. As shown in Figure 4.27, the distance between points is presented as a colour code at the coordinates of the recurrence plot. The points located close to each other are represented by the blue colour, and if the points are located farther apart, the colour code is red. Therefore by visible observation, it is noticeable that BE10 and DE10 have a clear presence of red vertical lines that indicate larger periodical irregularities occurred in the time series, whereas higher cyclic variation are observed. Most of the red vertical lines for BE10 and DE10 occurred at the coordinate, i=100. On the other hand, periodic behaviours are also observed in DBu10 and BBu10 with smaller red regions shown in the figure. These red regions indicate the presence of a trend or other irregularities in the time series. Also, these qualitative results also indicate variations of the much larger period, however longer time series is required to confirm that conclusion.
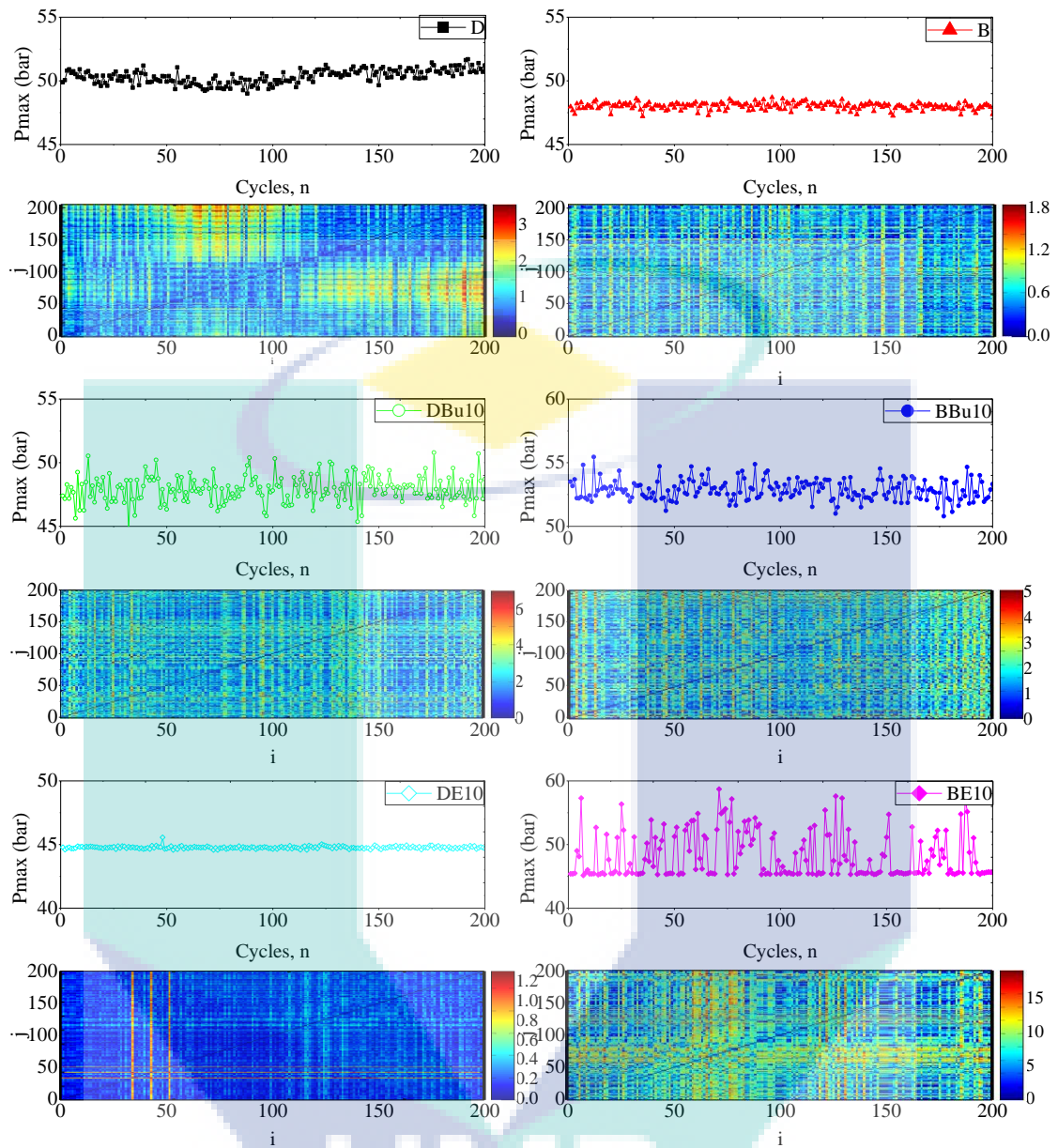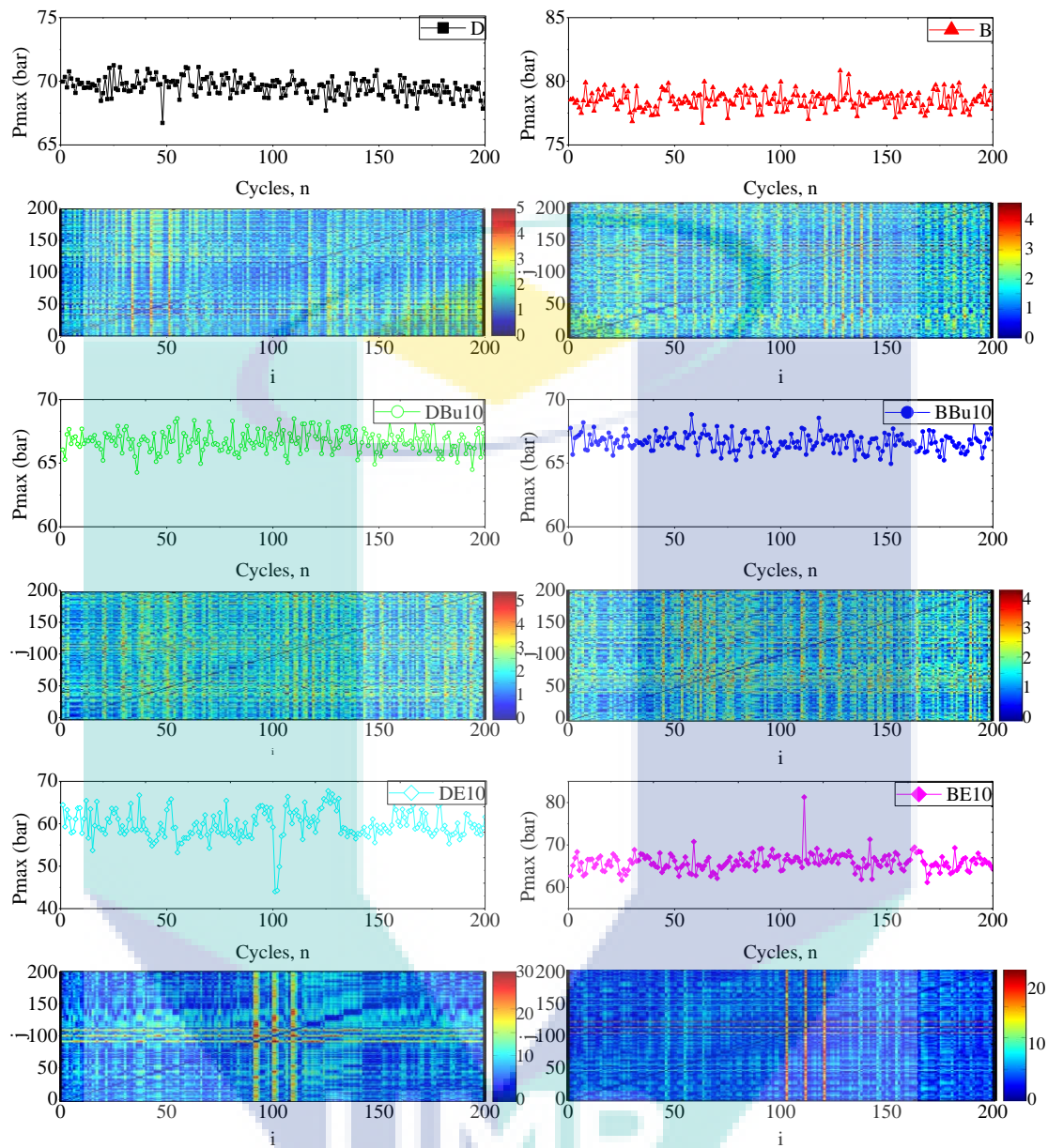
Figure 4.27   Time series of peak cylinder pressure cyclic variation values, P_{max} (i) and RP with a full load, 100% at 2300 rpm

Next, the results of corresponding parameters in RQA analysis are presented in Table 4.19. Here, the same fixed recurrence rate RR = 0.5 is used in all fuels. Note that the values of DET and LAM for B are the largest among all the fuels, followed by D and BBu10. These quantitative parameters confirm the deterministic nature or the points are closer to each other of the time series in the combustion cycle. Thus, more deterministic nature represents lower cyclic variation occurring in the engine operation. Interestingly

the other fuels; DE10 and BE10 blends are characterised by smaller values of DET and LAM, which indicate more dynamical irregularities. This could also be associated with the chaotic combustion nature due to the presence of ethanol in the blend fuels. Compared to D and B fuels, when the engine is maintained to a constant speed, by changing the engine loads from zero and partial to full load, simultaneous decrease is observed for all the quantitative RQA parameters. The maximum values for DET and LAM are obtained at 2300 rpm and 0% load rate.

Table 4.19   RQA parameter values for test fuels at full load, 100% (N=2300 rpm)

Test fuels	RQA Parameters Values	
	DET	LAM
D	6.154	0.290
B	10.24	6.903
BBu10	6.878	1.641
DBu10	3.599	1.155
BE10	0.333	0
DE10	0.107	0

The current study aimed to determine the effects of various engine loads and speeds with regards different fuel properties of the test fuels to the analysis of peak cylinder pressure, P_{max} using RP and RQA. The results of this investigation show that higher occurrence of P_{max} was observed for butanol blends for all operating conditions compared to than that of ethanol blends. The evidence from this study suggests that the engine was more stable running with butanol blends when operating at higher engine loads and speeds. The analysis of RP and RQA undertaken here, has extended the knowledge on the combustion characteristics of alcohol with regards higher occurrence of the peak cylinder pressure, P_{max} between test fuels and strong correlation with the fuel properties.

CHAPTER 5

CONCLUSION AND REMOMMENDATIONS

5.1   Introduction

The objective of this section is to provide at comprehensive outline from the results presented in the thesis. The brief details were justified to escalate the knowledge on the close correlation of the test fuels properties dealing with the combustion and the engine cyclic variations of mineral diesel (D), palm biodiesel (B), butanol (BBu10 and DBu10) and ethanol (BE10 and DE10) blends. Thus, this chapter summarises the conclusions composed of the presented results in Chapter 4 and proposes some recommendations for future work in significant areas.

5.2   Summary of Findings

Butanol and ethanol blends conform the ASTM D7467 blended fuel standard requirements which have been regulated as fuel for a standard diesel engine. The effects of various load rates of zero (0%), partial (50%) and full (100%) loads with three consecutive engine speeds; 1100 rpm, 1700 rpm and 2300 rpm were observed on the combustion and engine cyclic variations. The main findings and conclusions are discussed comprehensively in this section.

The fuel properties of butanol and ethanol blends were determined to confirm the ASTM D7647 blended fuel standard specifications. There were six different fuels were used for the fuel properties analysis. D and B acted as reference fuels; then both fuels

were blended with two short-chain alcohols; butanol and ethanol at 10% by volume. Both reference fuels; D and B were used for comparison with other test fuels, butanol and ethanol blends. D is a neat mineral diesel that complies with the recent standard of pure diesel, whereas B is designated for neat biodiesel originating from palm oil methyl ester (POME). These blends produced a series of test fuels; BBu10, BE10, DBu10 and DE10. The objective of the fuel properties analysis for the test fuels was to assess the close relationship of the alcohols on the combustion and cyclic variations.

The properties of butanol and ethanol blends were assessed by examining the effect of alcohols on the butanol and ethanol blends. The measured fuel properties include kinematic viscosity, density, Cetane number and calorific value. The results for the measured fuel properties have been discussed briefly in Section 0. Since butanol and ethanol had been blended with D and B, there were some significant impacts observed on the characteristics of the measured fuel properties that could influence the engine characteristics. A statistically significant decrease in the density of B was achieved by blending the butanol and ethanol at 10% by volume. It was observed that the density of BE10 and BE10 were 2.5% and 2.3% lower, respectively than B due to the effect of blending with alcohol. Alcohol is used to lower the density of the biodiesel in previous research works. Thus, the kinematic viscosity for BE10 and BE10 were 2.5% and 2.3% lower than B, with similar effect to density occurring.

Since butanol and ethanol are directly blended with D and B, the heating values for the test fuels were significantly reduced. The measured calorific values for BBu10 and BE10 were 16.5% and 17.9% lower than D and 1.6% and 3.1% lower than B. However, the calorific values for DBu10 and DE10 were 2.8% and 4.1% lower than D, however increased by 12.1% and 10.8% when compared to B. Improvement in the Cetane number was observed with the use of alcohol with 10% by volume increases, for example, the Cetane number for BBu10 and BE10 blends. Therefore, it can be concluded in this study that addition of butanol and and ethanol to B have improved the fuel properties of the fuel blends.

Butanol and ethanol blends are the primary subjects for further investigation in this study. Both butanol and ethanol were blended into D and B in 10% by volume to form the fraction of 10/90 fuel blends designated as BBu10, DBu10, BE10 and DE10,

respectively. Then, as for the combustion analysis, the combustion parameters taken into account for further fuel evaluations were in-cylinder pressure and HRR.

Further investigation was conducted on the engine combustion, and its parameters include in-cylinder pressure and HRR profiles when operated with increasing engine load at zero load, partial load and full load with 1100 rpm, 1700 rpm and 2300 rpm. For all six fuels, there was a significant increase of cylinder pressure with increasing engine loads from zero load and partial load to full load condition at increasing engine speeds. Also, B produced comparable peak cylinder pressure profiles concerning D corresponding to the increases in engine loads and speeds. However, lower peak cylinder pressure was observed for both biodiesel-alcohol and diesel-alcohol blends especially DE10 for all engine loads and speeds compared to that of D and B. On the other hand, further analysis on the HRR profiles was also conducted to evaluate the test fuel combustion at different engine speeds and loads. Since fuel blends have higher oxygenated content, the HRR was found to increase at higher engine loads, which improved the fuel combustion.

In this research work, the engine cyclic variations from the peak cylinder pressure time series were analysed on different test fuels at different engine test conditions. There were two kinds of analysis performed on engine cyclic variability; firstly, statistical analysis involving mean, maximum and minimum values, secondly, the COV. This COV was used to calculate and evaluate the effects of the test fuels particularly butanol (BBu10 and DBu10) and ethanol (BE10 and DE10) blends. The COV values for the corresponding test fuels at different test conditions were obtained from the calculation in MS Excel. There was a significant variation of COV values observed during the cycles when the load was applied to the engine. Moreover, as the applied load and engine speed increased, COV for the test fuels decreased simultaneously.

Several factors are identified which affect the values of COV at the test engine operating condition. By adding the alcohols; butanol and ethanol at 10% by volume, the values of COV for the butanol and ethanol blends tended to decrease due to the different chemical compositions, higher flash point, and low volatility of the alcohol blends. These observed properties mainly influence the characteristics of the fuel combustion which lead to a higher variation of COV with higher instabilities. B fuel produced the lowest

values of COV among all test fuels for all test engine operating condition because B has possessed higher Cetane number and oxygen content. These regular factors contribute to smoother engine operation with the combustion improvement and less engine cyclic variability. Hence, emission characteristics could be improved. It can be concluded from the study that the COV value has an increasing trend in the presence of ethanol in B and D fuels. Also, the COV values are found to be higher for ethanol blends compared to that of butanol blends. Also, The COV values show a diminishing trend according to an increment in the engine speed for each fuel. Lastly, an increase in cyclic variations of ethanol and butanol blends at low engine speed (1100 rpm) is higher than that of high engine speed (2300 rpm).

In this study, engine testing with all six fuels covering the different engine loads and engine speeds had been carried out. A licensed version of Matlab software was used to perform the scripts of RP and RQA using the data values of peak cylinder pressure, P_{max} in the time series of 200 consecutive cycles. These qualitative and quantitative methods were used to analyse the peak cylinder pressure, P_{max} cyclic variations and the deterministic dynamics of the combustion instability in a diesel engine using those fuels. In RP, different colour codes compose the occurrence of the points located between each other for the values of peak cylinder pressure time series at different operating conditions. Therefore, the RP patterns qualitatively indicate that depending on the engine speeds and load rates, the peak cylinder pressure, P_{max} cyclic variations exhibit different types of behaviour ranging from periodic oscillations to intermittent variations.

RP analysis exhibits that the red regions/lines of RP identified the presence of some irregularities or nonstationarity in the data values of the peak cylinder pressure, P_{max} time series and the blue regions/lines specify the existence of some determinism and periodic fluctuations in the combustion period. Therefore, the RPs of peak cylinder pressure, P_{max} time series for all six fuels are more similar to chaotic processes whose RPs are composed of red and blue regions for all operating conditions. The decreasing percentage of red regions with the increase of engine speeds and load rates indicate that the engine exhibits more stable and periodic fluctuations during the combustion period. To accomplish a qualitative RP analysis, a quantitative approach needs to be considered. Therefore, the RQA analysis has been introduced to identify the lengths of vertical, V_{MAX} or diagonal, L_{MAX} lines. In particular, the RQA parameters are used to quantify the peak

cylinder pressure, P_{max} variations in relatively short time series from the results of RP. The measure of RQA parameters indicates chaotic processes are characterised from the combustion process of a diesel engine at lower engine speed and load rates, while some determinism factors are observed during the engine operation with higher engine speed and load rates. It can be concluded from the study that cyclic variations of peak cylinder values, P_{max} of all test fuels could be interpreted into the graphical visualisation of RPs qualitatively and computed into RQA quantitatively. Also, higher recurrence points are observed for B fuel compared to that of butanol and ethanol blends, which shows more engine stability is obtained at all operating conditions.

The novel contributions of this research work are summarised as follows:

a) Engine performance, combustion and cyclic variability of the test diesel engine were evaluated as significant indicators to determine the suitability of the test fuels for further engine operation.

b) The effects of butanol and ethanol blends on engine cyclic variability were evaluated using the COV of peak cylinder pressure, P_{max} (COV_{Pmax}) values to characterise the engine cyclic variability from low load and low speed to high load and high speed.

c) The use of RP analysis and RQA is a novel analysis in the peak cylinder pressure, P_{max} time series for the further cyclic combustion analysis.

Further work from this would be to develop more information and results on alcohol blends characteristics of engine performance, combustion and emission characteristics. Correspondingly, the use of butanol and ethanol blends can be encouraged to replace current fossilized fuels in the future. Hence, several recommendations are identified and proposed for further work involving biofuels. The present study can lead to the following recommended future work:

- Different types of alcohol

This research work can be proposed for another type of alcohol including pentanol, propanol, acetone, and methanol. The characteristics of the engine such as performance, combustion, cyclic variation and emissions can be compared with previous research works using butanol and ethanol as well as the reference fuels in this study; D and B.

- Engine map modelling and optimisation

To determine how well the fuel burns during combustion, the engine map optimisation is proposed for further investigation of the characteristics of the performance, combustion, emissions and cyclic variation. Thus, artificial neural network (ANN) and response surface method (RSM) are available software that is mainly designed for optimisation and prediction on how well the engine operates with higher efficiency.

- Fuel injection pressure (FIP) sensor installation

This work had included a pressure transducer attached to the cylinder head for the engine cylinder pressure measurement. However, since the study involves different types of fuel with different psychochemical properties characteristics, it is suggested in the future that a fuel injection pressure sensor be attached to the fuel injector to measure the fuel pressure simultaneously as the fuel injected into the cylinder. This further study on the fuel combustion parameters especially cyclic variations would be more significant due to the sensor attachment.

- Simulation versus experiments

Engine testing provides insight measurable values to the quality data of the test fuels. However, engine testing application faces several undesirable parameters including humidity, working temperature and friction that could affect the reliability and consistency of the particular data as well as requiring high costs to set up and utilise. Utilisation of engine simulation software such as GT-Power and Ricardo Wave could provide more reliable and consistency of the data due to the controlled environment.

- Test at higher alcohol proportion

In this research work, two types of alcohol; namely butanol and ethanol are blended in 10% by volume with D and B as butanol (BBu10 and DBu10), and ethanol (BE10 and DE10) blends tested with a single cylinder diesel engine. This research work focuses only 10% by volume for the alcohol to be blended with the reference fuels and does not cover a wide range of alcohol blending percentages. This research work could, therefore, be extended to similar engine tests using higher alcohol proportions.
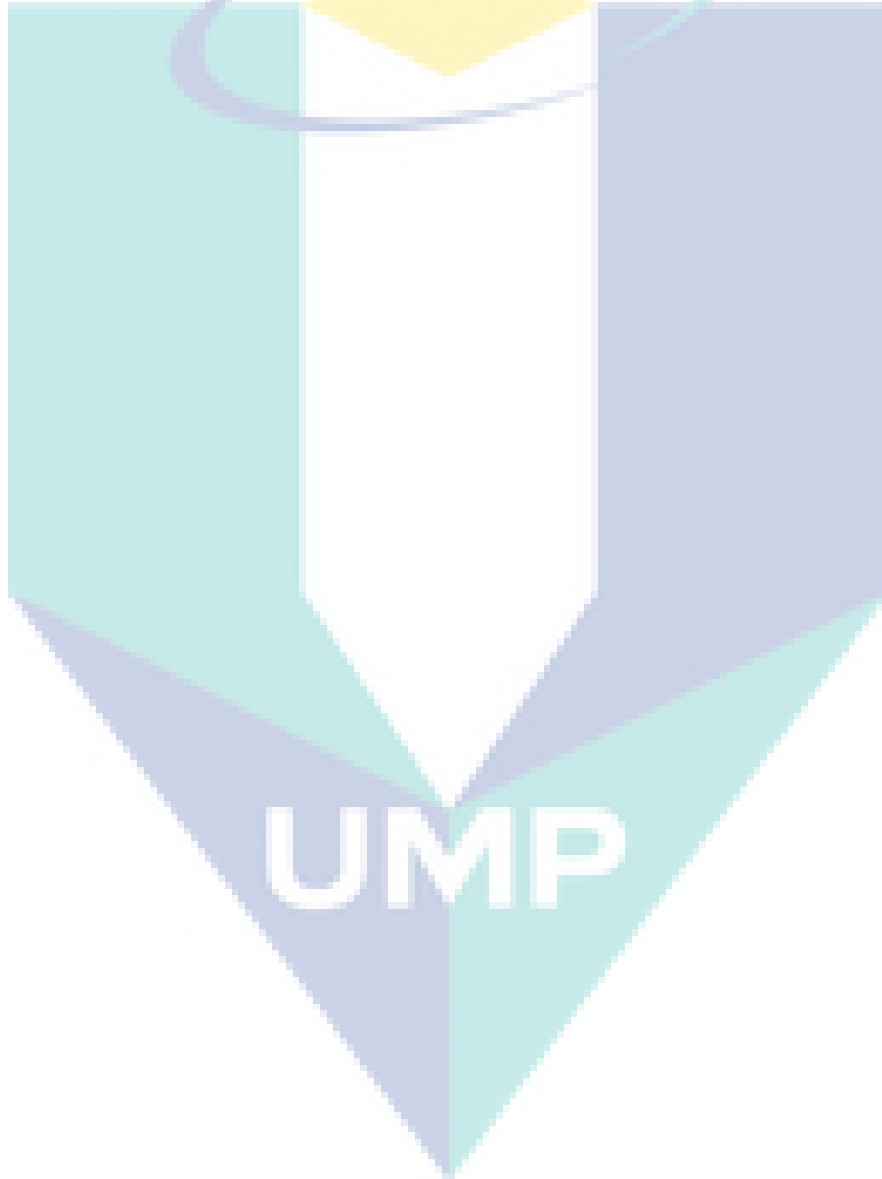
REFERENCES

Abu-Hamdeh, N. H., & Alnefaie, K. A. (2015). A comparative study of almond and palm oils as two bio-diesel fuels for diesel engine in terms of emissions and performance. *Fuel*, *150*(0), 318–324. http://doi.org/http://dx.doi.org/10.1016/j.fuel.2015.02.040

Aceves-Fernandez, M. A., Carlos Pedraza-Ortega, J., Sotomayor-Olmedo, A., Ramos-Arreguin, J. M., Emilio Vargas-Soto, J., & Tovar-Arriaga, S. (2014). Analysis of Key Features of Non-Linear Behaviour Using Recurrence Quantification. Case Study: Urban Airborne Pollution at Mexico City. *Environmental Modeling & Assessment*, *19*(2), 139–152. http://doi.org/10.1007/s10666-013-9381-3

Acharya, B., Guru, P. S., & Dash, S. (2016). Tween-80-n-butanol/isobutanol-(Diesel + Kerosene)-Water microemulsions - Phase behavior and fuel applications. *Fuel*, *171*, 87–93. http://doi.org/10.1016/j.fuel.2015.12.013

Adewale, P., Dumont, M.-J., & Ngadi, M. (2015). Recent trends of biodiesel production from animal fat wastes and associated production techniques. *Renewable and Sustainable Energy Reviews*, *45*, 574–588. http://doi.org/10.1016/j.rser.2015.02.039

Agarwal, A. K., Dhar, A., Gupta, J. G., Kim, W. I., Choi, K., Lee, C. S., & Park, S. (2015). Effect of fuel injection pressure and injection timing of Karanja biodiesel blends on fuel spray, engine performance, emissions and combustion characteristics. *Energy Conversion and Management*, *91*, 302–314. http://doi.org/10.1016/j.enconman.2014.12.004

Al Awad, A. S., Selim, M. Y. E., Zeibak, A. F., & Moussa, R. (2014). Jojoba ethyl ester production and properties of ethanol blends. *Fuel*, *124*, 73–75. http://doi.org/10.1016/j.fuel.2014.01.106

Alexa, O., Ilie, C. O., Marinescu, M., Vilau, R., & Grosu, D. (2015). Recurrence plot for parameters analysing of internal combustion engine. *IOP Conference Series: Materials Science and Engineering*, *95*, 12121. http://doi.org/10.1088/1757-899X/95/1/012121

Ali, O. M., Ali, O. M., Mamat, R., Abdullah, N. R., & Abdullah, A. A. (2015). Analysis of Blended Fuel Properties and Engine Cyclic Variations with Ethanol Additive Analysis of Blended Fuel Properties and Engine Cyclic Variations with Ethanol Additive, (April). http://doi.org/10.1166/jbmb.2015.1505

Ali, O. M., Mamat, R., Abdullah, N. R., & Abdullah, A. (2015). Analysis of Blended Fuel Properties and Engine Cyclic Variations with Ethanol Additive. *Journal of Biobased Materials and Bioenergy*, *9*, 108–141.

Ali, O. M., Mamat, R., Abdullah, N. R., & Abdullah, A. A. (2016). Analysis of blended fuel properties and engine performance with palm biodiesel–diesel blended fuel. *Renewable Energy*, *86*, 59–67. http://doi.org/10.1016/j.renene.2015.07.103

Ali, O. M., Mamat, R., Masjuki, H. H., & Abdullah, A. A. (2016). Analysis of blended fuel properties and cycle-to-cycle variation in a diesel engine with a diethyl ether additive. *Energy Conversion and Management*, *108*, 511–519. http://doi.org/http://dx.doi.org/10.1016/j.enconman.2015.11.035

Ali, O. M., Mamat, R., Masjuki, H. H., & Abdullah, A. A. (2016). Analysis of blended fuel properties and cycle-to-cycle variation in a diesel engine with a diethyl ether additive. *Energy Conversion and Management*, *108*, 511–519. http://doi.org/10.1016/j.enconman.2015.11.035

Ali, O. M., Mamat, R., Masjuki, H. H., & Adam, A. (2016). Analysis of blended fuel properties and cycle-to-cycle variation in a diesel engine with a diethyl ether additive. *Energy Conversion and Management*, *108*, 511–519. http://doi.org/10.1016/j.enconman.2015.11.035

Alonso-Pippo, W., Luengo, C. A., Alonsoamador Morales Alberteris, L., García del Pino, G., & Duvoisin, S. (2013). Practical implementation of liquid biofuels: The transferability of the Brazilian experiences. *Energy Policy*, *60*, 70–80. http://doi.org/10.1016/j.enpol.2013.04.038

Alptekin, E., Canakci, M., & Sanli, H. (2014). Biodiesel production from vegetable oil and waste animal fats in a pilot plant. *Waste Management*, *34*(11), 2146–2154. http://doi.org/10.1016/j.wasman.2014.07.019

An, H., Yang, W. M., & Li, J. (2015). Numerical modeling on a diesel engine fueled by biodiesel–methanol blends. *Energy Conversion and Management*, *93*(0), 100–108. http://doi.org/http://dx.doi.org/10.1016/j.enconman.2015.01.009

An, H., Yang, W. M., Li, J., & Zhou, D. Z. (2015). Modeling study of oxygenated fuels on diesel combustion : Effects of oxygen concentration , cetane number and C / H ratio, *90*, 261–271. http://doi.org/10.1016/j.enconman.2014.11.031

Andwari, A. M., Aziz, A. A., Said, M. F. M., & Latiff, Z. A. (2014). Experimental investigation of the influence of internal and external EGR on the combustion characteristics of a controlled auto-ignition two-stroke cycle engine. *Applied Energy*, *134*, 1–10. http://doi.org/10.1016/j.apenergy.2014.08.006

Angelovi, M., Tká, Z., & Jablonický, J. (2014). Determination Model for Cetane Number of Biodiesel at Different Fatty Acid Composition : a Review, *47*(1), 365–371.

Antunes, F. A. F., Chandel, A. K., Brumano, L. P., Terán Hilares, R., Peres, G. F. D., Ayabe, L. E. S., … Da Silva, S. S. (2017). A novel process intensification strategy for second-generation ethanol production from sugarcane bagasse in fluidized bed reactor. *Renewable Energy*, 6–13. http://doi.org/10.1016/j.renene.2017.06.004

ASTM International. ASTM D6751-15ce1- Standard Specification for Biodiesel Fuel Blend Stock (B100) for Middle Distillate Fuels (2015). West Conshohocken, PA. http://doi.org/10.1520/D6751-15CE01

Atkins, R. D. (2009). *An Introduction to Engine Testing and Development*. *SAE International*. http://doi.org/10.4271/R-344

Atmanli, A. (2016a). Comparative analyses of diesel-waste oil biodiesel and propanol, n-butanol or 1-pentanol blends in a diesel engine. *Fuel*, *176*, 209–215. http://doi.org/10.1016/j.fuel.2016.02.076

Atmanli, A. (2016b). Effects of a cetane improver on fuel properties and engine characteristics of a diesel engine fueled with the blends of diesel, hazelnut oil and higher carbon alcohol. *Fuel*, *172*, 209–217. http://doi.org/10.1016/j.fuel.2016.01.013

Atmanli, A., Ileri, E., & Yilmaz, N. (2016). Optimization of diesel-butanol-vegetable oil blend ratios based on engine operating parameters. *Energy*, *96*, 569–580. http://doi.org/10.1016/j.energy.2015.12.091

Atmanli, A., Ileri, E., & Yüksel, B. (2015). Effects of higher ratios of n-butanol addition to diesel-vegetable oil blends on performance and exhaust emissions of a diesel engine. *Journal of the Energy Institute*, *88*(3). http://doi.org/10.1016/j.joei.2014.09.008

Attia, A. M. A., & Hassaneen, A. E. (2016). Influence of diesel fuel blended with biodiesel produced from waste cooking oil on diesel engine performance. *Fuel*, *167*, 316–328. http://doi.org/10.1016/j.fuel.2015.11.064

Aurélio, M., Lagnier, B., Ferreira, G., Guilherme, L., Lamare, A., Murta, S., … Freitas, V. De. (2017). Comparative study of NOx emissions of biodiesel-diesel blends from soybean , palm and waste frying oils using methyl and ethyl transesterification routes. *Fuel*, *194*(2017), 144–156. http://doi.org/10.1016/j.fuel.2016.12.084

Awad, O. I., Mamat, R., Ali, O. M., Yusri, I. M., Abdullah, A. A., Yusop, A. F., & Noor, M. M. (2016). The effect of adding fusel oil to diesel on the performance and the emissions characteristics in a single cylinder CI engine. *Journal of the Energy Institute*. http://doi.org/10.1016/j.joei.2016.04.004

Aydin, S., Sayin, C., & Aydin, H. (2015). Investigation of the usability of biodiesel obtained from residual frying oil in a diesel engine with thermal barrier coating. *Applied Thermal Engineering*, *80*(0), 212–219. http://doi.org/http://dx.doi.org/10.1016/j.applthermaleng.2015.01.061

Azimov, U., Tomita, E., & Kawahara, N. (2013). Combustion-and-exhaust-emission-characteristics-of-diesel-micro-pilot-ignited-dual-fuel-engine. http://doi.org/10.5772/54613

Aziz, M. A., Yusop, A. F., Mat Yasin, M. H., Hamidi, M. A., Alias, A., Hussin, H., & Hamri, S. (2017). Study of alcohol fuel of butanol and ethanol effect on the compression ignition (CI) engine performance, combustion and emission characteristic. In *IOP Conference Series: Materials Science and Engineering* (Vol. 257). http://doi.org/10.1088/1757-899X/257/1/012079

Badday, A. S., Abdullah, A. Z., Lee, K. T., & Khayoon, M. S. (2012). Intensification of biodiesel production via ultrasonic-assisted process: A critical review on fundamentals and recent development. *Renewable and Sustainable Energy Reviews*, *16*(7), 4574–4587. http://doi.org/10.1016/j.rser.2012.04.057

Bae, C., & Kim, J. (2017). Alternative fuels for internal combustion engines. *Proceedings of the Combustion Institute*, *36*(3). http://doi.org/10.1016/j.proci.2016.09.009

Bair, S. (2014). The pressure and temperature dependence of volume and viscosity of four Diesel fuels. *Fuel*, *135*, 112–119. http://doi.org/10.1016/j.fuel.2014.06.035

Baklanov, A., Molina, L. T., & Gauss, M. (2016). Megacities, air quality and climate. *Atmospheric Environment*, *126*, 235–249. http://doi.org/10.1016/j.atmosenv.2015.11.059

Balamurugan, T., & Nalini, R. (2014). Experimental investigation on performance , combustion and emission characteristics of four stroke diesel engine using diesel blended with alcohol as fuel. *Energy*, *78*, 356–363. http://doi.org/10.1016/j.energy.2014.10.020

Ball, J. K. (1999). *Cycle-by-cycle variation in spark ignition internal combustion engines*. University of Oxford.

Bär, F., Hopf, H., Knorr, M., Schröder, O., & Krahl, J. (2016). Effect of hydrazides as fuel additives for biodiesel and biodiesel blends on NOx formation. *Fuel*, *180*, 278–283. http://doi.org/10.1016/j.fuel.2016.04.028

Barik, D., & Murugan, S. (2014). Simultaneous reduction of NOx and smoke in a dual fuel di diesel engine. *Energy Conversion and Management*, *84*(x), 217–226. http://doi.org/10.1016/j.enconman.2014.04.042

Barrios, C. C., Domínguez-Sáez, A., Martín, C., & Álvarez, P. (2014). Effects of animal fat based biodiesel on a TDI diesel engine performance, combustion characteristics and particle number and size distribution emissions. *Fuel*, *117*, *Part*(0), 618–623. http://doi.org/http://dx.doi.org/10.1016/j.fuel.2013.09.037

Barrios, C. C., Martín, C., Domínguez-Sáez, A., Álvarez, P., Pujadas, M., & Casanova, J. (2014). Effects of the addition of oxygenated fuels as additives on combustion characteristics and particle number and size distribution emissions of a TDI diesel engine. *Fuel*, *132*(0), 93–100. http://doi.org/http://dx.doi.org/10.1016/j.fuel.2014.04.071

Barros, S. D. T., Coelho, A. V., Lachter, E. R., San Gil, R. A. S., Dahmouche, K., Pais da Silva, M. I., & Souza, A. L. F. (2013). Esterification of lauric acid with butanol over mesoporous materials. *Renewable Energy*, *50*(October 2016), 585–589. http://doi.org/10.1016/j.renene.2012.06.059

Bedoya, I. D., Saxena, S., Cadavid, F. J., Dibble, R. W., & Wissink, M. (2012). Experimental evaluation of strategies to increase the operating range of a biogas-fueled HCCI engine for power generation. *Applied Energy*, *97*, 618–629. http://doi.org/10.1016/j.apenergy.2012.01.008

Bergthorson, J. M., & Thomson, M. J. (2015). A review of the combustion and emissions properties of advanced transportation biofuels and their impact on existing and future engines. *Renewable and Sustainable Energy Reviews*, *42*, 1393–1417. http://doi.org/10.1016/j.rser.2014.10.034

Bharathiraja, B., Chakravarthy, M., Kumar, R. R., Yuvaraj, D., Jayamuthunagai, J., Kumar, R. P., & Palani, S. (2014). Biodiesel production using chemical and biological methods – A review of process , catalyst , acyl acceptor , source and process variables. *Renewable and Sustainable Energy Reviews*, *38*, 368–382. http://doi.org/10.1016/j.rser.2014.05.084

Bharathiraja, B., Chakravarthy, M., Ranjith Kumar, R., Yogendran, D., Yuvaraj, D., Jayamuthunagai, J., … Palani, S. (2015). Aquatic biomass (algae) as a future feed stock for bio-refineries: A review on cultivation, processing and products. *Renewable and Sustainable Energy Reviews*, *47*, 635–653. http://doi.org/10.1016/j.rser.2015.03.047

Bhuiya, M. M. K., Rasul, M. G., Khan, M. M. K., Ashwath, N., & Azad, A. K. (2015). Prospects of 2nd generation biodiesel as a sustainable fuel—Part: 1 selection of feedstocks, oil extraction techniques and conversion technologies. *Renewable and Sustainable Energy Reviews*, *55*, 1109–1128. http://doi.org/10.1016/j.rser.2015.04.163

Bhuiya, M. M. K., Rasul, M. G., Khan, M. M. K., Ashwath, N., Azad, A. K., & Hazrat, M. A. (2016a). Prospects of 2nd generation biodiesel as a sustainable fuel – Part 2: Properties, performance and emission characteristics. *Renewable and Sustainable Energy Reviews*, *55*, 1129–1146. http://doi.org/http://dx.doi.org/10.1016/j.rser.2015.09.086

Bhuiya, M. M. K., Rasul, M. G., Khan, M. M. K., Ashwath, N., Azad, A. K., & Hazrat, M. A. (2016b). Prospects of 2nd generation biodiesel as a sustainable fuel – Part 2: Properties, performance and emission characteristics. *Renewable and Sustainable Energy Reviews*, *55*, 1129–1146. http://doi.org/10.1016/j.rser.2015.09.086

Bradley, E., & Kantz, H. (2015). Nonlinear time-series analysis revisited. *Chaos*, *25*(9). http://doi.org/10.1063/1.4917289

Brady, R. N. (2013). *Reference Module in Earth Systems and Environmental Sciences*. *Reference Module in Earth Systems and Environmental Sciences*. Elsevier. http://doi.org/10.1016/B978-0-12-409548-9.01056-3

Breeze, P. (2014). *Power Generation Technologies*. *Power Generation Technologies*. Elsevier. http://doi.org/10.1016/B978-0-08-098330-1.00005-3

British Petroleum. (2016). BP energy outlook 2016. *British Petroleum*, *53*(9), 98. http://doi.org/10.1017/CBO9781107415324.004

Bueno, A. V, Velásquez, J. A., & Milanez, L. F. (2012). Internal Combustion Engine Indicating Measurements. In *Applied Measurement Systems*. Intechopen. Retrieved from http://www.intechopen.com/books/applied-measurement-systems/internal-combustion-engine- indicating-measurements

Can, Ö., Öztürk, E., Solmaz, H., Aksoy, F., Çinar, C., & Yücesu, H. S. (2016). Combined effects of soybean biodiesel fuel addition and EGR application on the combustion and exhaust emissions in a diesel engine. *Applied Thermal Engineering*, *95*, 115–124. http://doi.org/http://dx.doi.org/10.1016/j.applthermaleng.2015.11.056

Ceviz, M. A., Çavuşoǵlu, B., Kaya, F., & İ. Volkan Őner. (2011). Determination of cycle number for real in-cylinder pressure cycle analysis in internal combustion engines. *Energy*, *36*(5), 2465–2472. http://doi.org/10.1016/j.energy.2011.01.038

Ceviz, M. A., Sen, A. K., Küleri, A. K., & Öner, I. V. (2012). Engine performance, exhaust emissions, and cyclic variations in a lean-burn SI engine fueled by gasoline–hydrogen blends. *Applied Thermal Engineering*, *36*, 314–324.

Chandrashekar, T. K., & Antony, a J. (2005). Simple Models for Cyclic Variations Spark Ignition Engines. *Energy Conversion and Resources*, *2005*(3), 185–193. http://doi.org/10.1115/IMECE2005-79678

Chauhan, B. S., Singh, R. K., Cho, H. M., & Lim, H. C. (2016). Practice of diesel fuel blends using alternative fuels: A review. *Renewable and Sustainable Energy Reviews*, *59*, 1358–1368. http://doi.org/http://dx.doi.org/10.1016/j.rser.2016.01.062

Chen, T., Zhao, H., Xie, H., & He, B. (2015). Analysis of cyclic variations during mode switching between spark ignition and controlled auto-ignition combustion operations. *International Journal of Engine Research*, *16*(3), 356–365.

Chen, Y., Dong, G., Mack, J. H., Butt, R. H., Chen, J., & Dibble, R. W. (2016). Cyclic variations and prior-cycle effects of ion current sensing in an HCCI engine : A time-series analysis. *Applied Energy*, *168*, 628–635. http://doi.org/10.1016/j.apenergy.2016.01.126

Chen, Y., & Yang, H. (2012a). Multiscale recurrence analysis of long-term nonlinear and nonstationary time series. *Chaos, Solitons and Fractals*, *45*(7), 978–987. http://doi.org/10.1016/j.chaos.2012.03.013

Chen, Y., & Yang, H. (2012b). Multiscale recurrence analysis of long-term nonlinear and nonstationary time series. *Chaos, Solitons and Fractals*, *45*(7), 978–987. http://doi.org/10.1016/j.chaos.2012.03.013

Chen, Y., & Yang, H. (2012c). Self-organized neural network for the quality control of 12-lead ECG signals. *Physiological Measurement*, *33*(9), 1399–1418. http://doi.org/10.1088/0967-3334/33/9/1399

Chen, Z., Yao, C., Yao, A., Dou, Z., Wang, B., Wei, H., … Shi, J. (2017). The impact of methanol injecting position on cylinder-to-cylinder variation in a diesel methanol dual fuel engine. *Fuel*, *191*(92), 150–163. http://doi.org/10.1016/j.fuel.2016.11.072

Cheung, C. S., Man, X. J., Fong, K. W., & Tsang, O. K. (2015). Effect of Waste Cooking Oil Biodiesel on the Emissions of a Diesel Engine. *Energy Procedia*, *66*(0), 93–96. http://doi.org/http://dx.doi.org/10.1016/j.egypro.2015.02.050

Chiatti, G., Chiavola, O., Palmieri, F., & Piolo, A. (2015). Diagnostic methodology for internal combustion diesel engines via noise radiation. *Energy Conversion and Management*, *89*, 34–42. http://doi.org/10.1016/j.enconman.2014.09.055

Choi, M., Song, J., & Park, S. (2016). Modeling of the fuel injection and combustion process in a CNG direct injection engine. *Fuel*, *179*, 168–178. http://doi.org/10.1016/j.fuel.2016.03.099

Chong, C. T., Ng, J.-H., Ahmad, S., & Rajoo, S. (2015a). Oxygenated palm biodiesel: Ignition, combustion and emissions quantification in a light-duty diesel engine. *Energy Conversion and Management*, *101*, 317–325. http://doi.org/10.1016/j.enconman.2015.05.058

Chong, C. T., Ng, J.-H., Ahmad, S., & Rajoo, S. (2015b). Oxygenated palm biodiesel: Ignition, combustion and emissions quantification in a light-duty diesel engine. *Energy Conversion and Management*, *101*(0), 317–325. http://doi.org/http://dx.doi.org/10.1016/j.enconman.2015.05.058

Chuepeng, S., Srisuwan, S., & Tongroon, M. (2016). Lean hydrous and anhydrous bioethanol combustion in spark ignition engine at idle. *Energy Conversion and Management*, *128*, 1–11. http://doi.org/10.1016/j.enconman.2016.09.059

Ciriminna, R., Pina, C. Della, Rossi, M., & Pagliaro, M. (2014). Understanding the glycerol market. *European Journal of Lipid Science and Technology*, *116*(10), 1432–1439. http://doi.org/10.1002/ejlt.201400229

Claros Garcia, J. C., & Von Sperling, E. (2017). Greenhouse gas emissions from sugar cane ethanol: Estimate considering current different production scenarios in Minas Gerais, Brazil. *Renewable and Sustainable Energy Reviews*, *72*(December 2016), 1033–1049. http://doi.org/10.1016/j.rser.2017.01.046

Constantin-Ovidiu, I., Octavian, A., Lespezeanu, I., Marinescu, M., & Grosu, D. (2017). Recurrence plot analysis to study parameters of a gasoline engine. *Applied Mechanics and Materials*, *823*, 323–328. http://doi.org/10.4028/www.scientific.net/AMM.823.323

Corach, J., Sorichetti, P. A., & Romano, S. D. (2015). Electrical and ultrasonic properties of vegetable oils and biodiesel. *Fuel*, *139*, 466–471. http://doi.org/10.1016/j.fuel.2014.09.026

Crago, C. L., Khanna, M., Barton, J., Giuliani, E., & Amaral, W. (2010). Competitiveness of Brazilian sugarcane ethanol compared to US corn ethanol. *Energy Policy*, *38*(11), 7404–7415. http://doi.org/10.1016/j.enpol.2010.08.016

D'Agosto, M. de A., Ribeiro, S. K., & de Souza, C. D. R. (2013). Opportunity to reduce greenhouse gas by the use of alternative fuels and technologies in urban public transport in Brazil. *Current Opinion in Environmental Sustainability*, *5*(2), 177–183. http://doi.org/10.1016/j.cosust.2013.03.003

D'Ambrosio, S., Ferrari, A., & Galleani, L. (2015). In-cylinder pressure-based direct techniques and time frequency analysis for combustion diagnostics in IC engines. *Energy Conversion and Management*, *99*, 299–312. http://doi.org/10.1016/j.enconman.2015.03.080

Datta, A., & Mandal, B. K. (2016a). A comprehensive review of biodiesel as an alternative fuel for compression ignition engine. *Renewable and Sustainable Energy Reviews*. http://doi.org/10.1016/j.rser.2015.12.170

Datta, A., & Mandal, B. K. (2016b). Impact of alcohol addition to diesel on the performance combustion and emissions of a compression ignition engine. *Applied Thermal Engineering*, *98*(JANUARY), 670–682. http://doi.org/10.1016/j.applthermaleng.2015.12.047

Deb, M., Sastry, G. R. K., Bose, P. K., & Banerjee, R. (2015). An experimental study on combustion, performance and emission analysis of a single cylinder, 4-stroke DI-diesel engine using hydrogen in dual fuel mode of operation. *International Journal of Hydrogen Energy*, *40*(27), 8586–8598. http://doi.org/http://dx.doi.org/10.1016/j.ijhydene.2015.04.125

Diederichs, G. W., Ali Mandegari, M., Farzad, S., & Görgens, J. F. (2016). Techno-economic comparison of biojet fuel production from lignocellulose, vegetable oil and sugar cane juice. *Bioresource Technology*, *216*, 331–339. http://doi.org/10.1016/j.biortech.2016.05.090

Ding, S., Yang, L., Song, E., & Ma, X. (2015). Investigations on In-Cylinder Pressure Cycle-to-Cycle Variations in a Diesel Engine by Recurrence Analysis. *SAE Technical Paper*, (April 2015). http://doi.org/10.4271/2015-01-0875

Dong, S., Cheng, X., Ou, B., Liu, T., & Wang, Z. (2016). Experimental and numerical investigations on the cyclic variability of an ethanol/diesel dual-fuel engine. *Fuel*, *186*, 665–673. http://doi.org/10.1016/j.fuel.2016.09.027

Eckmann, J.-P., Kamphorst, S. O., & Ruelle, D. (1987). Recurrence Plots of Dynamical Systems. *Europhysics Letters (EPL)*, *4*(9), 973–977. http://doi.org/10.1209/0295-5075/4/9/004

ENVIRON Australia. (2014). Reducing Emissions from Non-road Diesel Engines, 135. Retrieved from http://www.epa.nsw.gov.au/resources/air/140586NonrdDiesInfoRpt.pdf

European Standards. CSN EN 14214+A1-Liquid petroleum products - Fatty acid methyl esters (FAME) for use in diesel engines and heating applications - Requirements and test methods (2013). Retrieved from https://www.en-standard.eu/csn-en-14214-a1-liquid-petroleum-products-fatty-acid-methyl-esters-fame-for-use-in-diesel-engines-and-heating-applications-requirements-and-test-methods/

Fahd, M. E. A., Wenming, Y., Lee, P. S., Chou, S. K., & Yap, C. R. (2013). Experimental investigation of the performance and emission characteristics of direct injection diesel engine by water emulsion diesel under varying engine load condition. *Applied Energy*, *102*, 1042–1049. http://doi.org/10.1016/j.apenergy.2012.06.041

Fathi, M., Jahanian, O., & Shahbakhti, M. (2017). Modeling and controller design architecture for cycle-by-cycle combustion control of homogeneous charge compression ignition (HCCI) engines – A comprehensive review. *Energy Conversion and Management*, *139*, 1–19. http://doi.org/10.1016/j.enconman.2017.02.038

Fayyazbakhsh, A., & Pirouzfar, V. (2016). Investigating the influence of additives-fuel on diesel engine performance and emissions: Analytical modeling and experimental validation. *Fuel*, *171*, 167–177. http://doi.org/10.1016/j.fuel.2015.12.028

Feng, H., Zhang, J., Liu, D., An, M., Zhang, W., & Zhang, X. (2017). Development of a reduced n-butanol mechanism with combined reduction methods. *Fuel*, *187*, 403–416. http://doi.org/10.1016/j.fuel.2016.09.073

Finney, C. E. A., Kaul, B. C., Daw, C. S., Wagner, R. M., Edwards, K. D., & Green, J. B. (2015). A review of deterministic effects in cyclic variability of internal combustion engines. *International Journal of Engine Research*, 1–21. Retrieved from https://www.osti.gov/pages/servlets/purl/1265479

Focus Applied Technologies. (2017). Product Specifications. Retrieved from http://www.focusappliedtechnologies.com/

Fournier, S., Simon, G., & Seers, P. (2016). Evaluation of low concentrations of ethanol, butanol, BE, and ABE blended with gasoline in a direct-injection, spark-ignition engine. *Fuel*, *181*, 396–407. http://doi.org/10.1016/j.fuel.2016.04.135

Galloni, E. (2009a). Analyses about parameters that affect cyclic variation in a spark ignition engine. *Applied Thermal Engineering*, *29*(5–6), 1131–1137. http://doi.org/10.1016/j.applthermaleng.2008.06.001

Galloni, E. (2009b). Analyses about parameters that affect cyclic variation in a spark ignition engine. *Applied Thermal Engineering*, *29*(5–6), 1131–1137. http://doi.org/10.1016/j.applthermaleng.2008.06.001

Galloni, E., Fontana, G., Staccone, S., & Scala, F. (2016). Performance analyses of a spark-ignition engine firing with gasoline-butanol blends at partial load operation. *Energy Conversion and Management*, *110*, 319–326. http://doi.org/10.1016/j.enconman.2015.12.038

Gandure, J., Ketlogetswe, C., & Temu, A. (2014). Fuel properties of biodiesel produced from selected plant kernel oils indigenous to Botswana: A comparative analysis. *Renewable Energy*, *68*, 414–420. http://doi.org/10.1016/j.renene.2014.02.035

Ge, H., Reitz, R. D., & Willems, W. (2008). Modeling the Effects of In-Cylinder Flows on HSDI Diesel Engine Performance and Emissions, *2008*(724), 776–790.

Geacai, S., Iulian, O., & Nita, I. (2015). Measurement, correlation and prediction of biodiesel blends viscosity. *Fuel*, *143*, 268–274. http://doi.org/10.1016/j.fuel.2014.11.041

Ghadikolaei, M. A. (2016). Effect of alcohol blend and fumigation on regulated and unregulated emissions of IC engines — A review. *Renewable and Sustainable Energy Reviews*, *57*, 1440–1495. http://doi.org/10.1016/j.rser.2015.12.128

Gharehghani, A., Mirsalim, M., & Hosseini, R. (2017). Effects of waste fish oil biodiesel on diesel engine combustion characteristics and emission. *Renewable Energy*, *101*, 930–936. http://doi.org/10.1016/j.renene.2016.09.045

Ghazimirsaied, A., & Koch, C. R. (2012). Controlling cyclic combustion timing variations using a symbol-statistics predictive approach in an HCCI engine. *Applied Energy*, *92*, 133–146. http://doi.org/10.1016/j.apenergy.2011.09.018

Giakoumis, E. G., Rakopoulos, C. D., Dimaratos, A. M., & Rakopoulos, D. C. (2013). Exhaust emissions with ethanol or n-butanol diesel fuel blends during transient operation: A review. *Renewable and Sustainable Energy Reviews*, *17*, 170–190. http://doi.org/10.1016/j.rser.2012.09.017

Gomez, A., Soriano, J. A., & Armas, O. (2016). Evaluation of sooting tendency of different oxygenated and paraffinic fuels blended with diesel fuel. *Fuel*, *184*(x), 536–543. http://doi.org/10.1016/j.fuel.2016.07.049

Gómez, A., Soriano, J. A., & Armas, O. (2016). Evaluation of sooting tendency of different oxygenated and paraffinic fuels blended with diesel fuel. *Fuel*, *184*(x), 536–543. http://doi.org/10.1016/j.fuel.2016.07.049

Gomez Montoya, J. P., Amell, A. A., & Olsen, D. B. (2016). Prediction and measurement of the critical compression ratio and methane number for blends of biogas with methane, propane and hydrogen. *Fuel*, *186*, 168–175. http://doi.org/10.1016/j.fuel.2016.08.064

Guardiola, C., Olmeda, P., Pla, B., & Bares, P. (2017). In-cylinder pressure based model for exhaust temperature estimation in internal combustion engines. *Applied Thermal Engineering*, *115*, 212–220. http://doi.org/10.1016/j.applthermaleng.2016.12.092

Gülüm, M., & Bilgin, A. (2015). Density, flash point and heating value variations of corn oil biodiesel–diesel fuel blends. *Fuel Processing Technology*, *134*, 456–464. http://doi.org/http://dx.doi.org/10.1016/j.fuproc.2015.02.026

Gürbüz, H., Akçay, İ. H., & Buran, D. (2014). An investigation on effect of in-cylinder swirl flow on performance, combustion and cyclic variations in hydrogen fuelled spark ignition engine. *Journal of the Energy Institute*, *87*(1), 1–10.

Gurgen, S., Unver, B., & Altin, İ. (2017). Experimental investigation on cyclic variability, engine performance and exhaust emissions in a diesel engine using alcohol-diesel fuel blends. *Thermal Science*, *21*(1 Part B), 581–589. http://doi.org/10.2298/TSCI161020306G

Gürgen, S., Ünver, B., & Altın, İ. (2018). Prediction of cyclic variability in a diesel engine fueled with n-butanol and diesel fuel blends using artificial neural network. *Renewable Energy*, *117*, 538–544. http://doi.org/10.1016/j.renene.2017.10.101

He, B.-Q. (2016). Advances in emission characteristics of diesel engines using different biodiesel fuels. *Renewable and Sustainable Energy Reviews*, *60*, 570–586. http://doi.org/http://dx.doi.org/10.1016/j.rser.2016.01.093

Heywood, J. B. (1988). *Internal Combustion Engine Fundamentals*. McGraw-Hill Education.

Holman, J. P. (1994). *Experimental methods for engineers*. *Experimental Thermal and Fluid Science* (8th ed., Vol. 9). McGraw-Hill Education. http://doi.org/10.1016/0894-1777(94)90118-X

Hönig, V., Kotek, M., & Mařík, J. (2014). Use of butanol as a fuel for internal combustion engines. *Agronomy Research*, *12*(2), 333–340.

Huang, M., Gowdagiri, S., Cesari, X. M., & Oehlschlaeger, M. A. (2016). Diesel engine CFD simulations: Influence of fuel variability on ignition delay. *Fuel*, *181*, 170–177. http://doi.org/10.1016/j.fuel.2016.04.137

Iannuzzi, S. E., & Valentino, G. (2014). Comparative behavior of gasoline e diesel / butanol e diesel blends and injection strategy management on performance and emissions of a light duty diesel engine. *Energy*, *71*, 321–331. http://doi.org/10.1016/j.energy.2014.04.065

Ibrahim, A. (2016). Performance and combustion characteristics of a diesel engine fuelled by butanol–biodiesel–diesel blends. *Applied Thermal Engineering*, *103*, 651–659. http://doi.org/10.1016/j.applthermaleng.2016.04.144

Imdadul, H. K., Masjuki, H. H., Kalam, M. A., Zulkifli, N. W. M., Alabdulkarem, A., Kamruzzaman, M., & Rashed, M. M. (2016). A comparative study of C4 and C5 alcohol treated diesel–biodiesel blends in terms of diesel engine performance and exhaust emission. *Fuel*, *179*, 281–288. http://doi.org/10.1016/j.fuel.2016.04.003

Imdadul, H. K., Masjuki, H. H., Kalam, M. A., Zulkifli, N. W. M., Alabdulkarem, A., Rashed, M. M., & Ashraful, A. M. (2016). Influences of ignition improver additive on ternary (diesel-biodiesel-higher alcohol) blends thermal stability and diesel engine performance. *Energy Conversion and Management*, *123*, 252–264. http://doi.org/10.1016/j.enconman.2016.06.040

Imdadul, H. K., Masjuki, H. H., Kalam, M. A., Zulkifli, N. W. M., Alabdulkarem, A., Rashed, M. M., … How, H. G. (2016). Higher alcohol – biodiesel – diesel blends : An approach for improving the performance , emission , and combustion of a light-duty diesel engine. *Energy Conversion and Management*, *111*, 174–185. http://doi.org/10.1016/j.enconman.2015.12.066

Imran, A., Varman, M., Masjuki, H. H., & Kalam, M. A. (2013). Review on alcohol fumigation on diesel engine: A viable alternative dual fuel technology for satisfactory engine performance and reduction of environment concerning emission. *Renewable and Sustainable Energy Reviews*, *26*, 739–751. http://doi.org/10.1016/j.rser.2013.05.070

Ipci, D., & Karabulut, H. (2016). Thermodynamic and dynamic modeling of a single cylinder four stroke diesel engine. *Applied Mathematical Modelling*, *40*(5–6), 3925–3937. http://doi.org/10.1016/j.apm.2015.10.046

Issariyakul, T., & Dalai, A. K. (2014). Biodiesel from vegetable oils. *Renewable and Sustainable Energy Reviews*, *31*, 446–471. http://doi.org/10.1016/j.rser.2013.11.001

Jaat, N., Khalid, A., Sapit, A., Rhaodah, A., Basharie, M., & Fawzi, M. (2016). The influences of injection pressure and ambient temperature on ignition delay and emission. *ARPN Journal of Engineering and Applied Sciences*, *11*(12), 7522–7528.

Janakiraman, V. M., Nguyen, X., & Assanis, D. (2013). Nonlinear identification of a gasoline HCCI engine using neural networks coupled with principal component analysis. *Applied Soft Computing Journal*, *13*(5), 2375–2389. http://doi.org/10.1016/j.asoc.2013.01.006

J V Maizel, J., & Lenk, R. P. (1981). Enhanced graphic matrix analysis of nucleic acid and protein sequences. *Proc Natl Acad Sci U S A.*, *78*(12), 7665–7669. Retrieved from https://www.ncbi.nlm.nih.gov/pmc/articles/PMC349330/pdf/pnas00663-0458.pdf

Ji, C., Zhang, B., & Wang, S. (2013). Enhancing the performance of a spark-ignition methanol engine with hydrogen addition. *International Journal of Hydrogen Energy*, *38*(18), 7490–7498. http://doi.org/10.1016/j.ijhydene.2013.04.001

Ji, S., Lan, X., Cheng, Y., Zhao, X., Li, X., & Wang, F. (2016). Cyclic variation of large-bore multi point injection engine fuelled by natural gas with different types of injection systems. *Applied Thermal Engineering*, *102*, 1241–1249. http://doi.org/10.1016/j.applthermaleng.2016.03.082

Jiang, Y., Liu, J., Jiang, W., Yang, Y., & Yang, S. (2015). Current status and prospects of industrial bio-production of n-butanol in China. *Biotechnology Advances*, *33*(7), 1493–1501. http://doi.org/10.1016/j.biotechadv.2014.10.007

Jie, L., Shu-Ting, S., & Jun-Chan, Z. (2013). Comparison study of typical algorithms for reconstructing time series from the recurrence plot of dynamical systems. *Chinese Physics B*, *22*(1), 10505. http://doi.org/10.1088/1674-1056/22/1/010505

Johansson, B., Neij, H., Aid,n, M., & Juhlin, G. (1995). Investigations of the Influence of Mixture Preparation on Cyclic Variations in a SI-Engine, Using Laser Induced Fluorescence. *SAE Technical Paper*, (412). http://doi.org/10.4271/950108

Johnson, F. X., & Silveira, S. (2014). Pioneer countries in the transition to alternative transport fuels: Comparison of ethanol programmes and policies in Brazil, Malawi and Sweden. *Environmental Innovation and Societal Transitions*, *11*, 1–24. http://doi.org/10.1016/j.eist.2013.08.001

Johnson, T. V. (2015). Review of Vehicular Emissions Trends. *SAE Int. J. Engines*, *8*(3), 1152–1167. http://doi.org/10.4271/2015-01-0993

Jose, T. K., & Anand, K. (2016). Effects of biodiesel composition on its long term storage stability. *Fuel*, *177*, 190–196. http://doi.org/10.1016/j.fuel.2016.03.007

Josiński, H., Michalczuk, A., Świtoński, A., Szczęsna, A., & Wojciechowski, K. (2016). Recurrence Plots and Recurrence Quantification Analysis of Human Motion Data, *180014*, 1–4. http://doi.org/10.1063/1.4951961

Jung, D., & Iida, N. (2017). Thermal and chemical effects of the in-cylinder charge at IVC on cycle-to-cycle variations of DME HCCI combustion with combustion-phasing retard by external and rebreathed EGR. *Applied Thermal Engineering*, *113*, 132–149. http://doi.org/10.1016/j.applthermaleng.2016.11.011

Kaimal, V. K., & Vijayabalan, P. (2015). A detailed study of combustion characteristics of a DI diesel engine using waste plastic oil and its blends. *Energy Conversion and Management*, *105*, 951–956. http://doi.org/10.1016/j.enconman.2015.08.043

Karavalakis, G., Stournas, S., Ampatzoglou, D., Bakeas, E., & Spanos, A. (2010). Regulated and Unregulated Emissions of a Euro 4 SUV Operated with Diesel and Soy-based Biodiesel Blends. *SAE International Journal of Fuels and Lubricants*, *2*(2), 115–131. http://doi.org/10.4271/2009-01-2690

Karvountzis-Kontakiotis, A. (2015). *Impact of the cycle-to-cycle variation of an internal combustion engine to gaseous pollutants emissions*.

Kegl, B., Kegl, M., & Pehan, S. (2013). *Green Diesel Engines* (Vol. 12). http://doi.org/10.1007/978-1-4471-5325-2

Keskinen, J.-P., Vuorinen, V., & Kaario, O. (2016). Nonlinear time series analysis from large eddy simulation of an internal combustion engine. *International Journal of Heat and Fluid Flow*, *57*, 79–90. http://doi.org/10.1016/j.ijheatfluidflow.2015.11.009

Khandal SV, B. N., Chandrashekar TK, R. L., TK, C., & NR, B. (2015). Alcohol (Ethanol and Diethyl Ethyl Ether)-Diesel Blended Fuels for Diesel Engine Applications-A Feasible Solution. *Advances in Automobile Engineering*, *4*(1), 1–8. http://doi.org/10.4172/2167-7670.1000117

Knothe, G., & Razon, L. F. (2017). Biodiesel fuels. *Progress in Energy and Combustion Science*. http://doi.org/10.1016/j.pecs.2016.08.001

Kříž, R. (2014). Finding Chaos in Finnish GDP. *International Journal of Automation and Computing*, *11*(3), 231–240. http://doi.org/10.1007/s11633-014-0785-6

Krutof, A., & Hawboldt, K. (2016). Blends of pyrolysis oil, petroleum, and other bio-based fuels: A review. *Renewable and Sustainable Energy Reviews*, *59*, 406–419. http://doi.org/10.1016/j.rser.2015.12.304

Kugiumtzis, D., & Tsimpiris, A. (2010). Measures of Analysis of Time Series (MATS): A MATLAB Toolkit for Computation of Multiple Measures on Time Series Data Bases. *Journal of Statistical Software*, *33*(5).

Kujawska, A., Kujawski, J., Bryjak, M., & Kujawski, W. (2015). ABE fermentation products recovery methods - A review. *Renewable and Sustainable Energy Reviews*, *48*(August 2015), 648–661. http://doi.org/10.1016/j.rser.2015.04.028

Kumar, B. R., & Saravanan, S. (2016). Use of higher alcohol biofuels in diesel engines : A review. *Renewable and Sustainable Energy Reviews*, *60*, 84–115. http://doi.org/10.1016/j.rser.2016.01.085

Kumar, M., & Sharma, M. P. (2016). Selection of potential oils for biodiesel production. *Renewable and Sustainable Energy Reviews*, *56*, 1129–1138. http://doi.org/10.1016/j.rser.2015.12.032

Kumar, S., Cho, J. H., Park, J., & Moon, I. (2013). Advances in diesel–alcohol blends and their effects on the performance and emissions of diesel engines. *Renewable and Sustainable Energy Reviews*, *22*, 46–72. http://doi.org/10.1016/j.rser.2013.01.017

Kumar, S., & Kumar Chauhan, M. (2013). Numerical modeling of compression ignition engine: A review. *Renewable and Sustainable Energy Reviews*, *19*, 517–530. http://doi.org/10.1016/j.rser.2012.11.043

Kurkijärvi, A., Lehtonen, J., & Linnekoski, J. (2014). Novel dual extraction process for acetone-butanol-ethanol fermentation. *Separation and Purification Technology*, *124*, 18–25. http://doi.org/10.1016/j.seppur.2014.01.007

Kuszewski, H., Jaworski, A., Ustrzycki, A., Lejda, K., Balawender, K., & Woś, P. (2017). Use of the constant volume combustion chamber to examine the properties of autoignition and derived cetane number of mixtures of diesel fuel and ethanol. *Fuel*, *200*, 564–575. http://doi.org/10.1016/j.fuel.2017.04.021

Kyrtatos, P., Brückner, C., & Boulouchos, K. (2016). Cycle-to-cycle variations in diesel engines. *Applied Energy*, *171*, 120–132. http://doi.org/10.1016/j.apenergy.2016.03.015

Kyrtatos, P., Zivolic, A., Brückner, C., & Boulouchos, K. (2017). Cycle-to-cycle variations of NO emissions in diesel engines under long ignition delay conditions. *Combustion and Flame*, *178*, 82–96. http://doi.org/10.1016/j.combustflame.2016.12.025

Labeckas, G., Slavinskas, S., & Mažeika, M. (2014a). The effect of ethanol-diesel-biodiesel blends on combustion, performance and emissions of a direct injection diesel engine. *Energy Conversion and Management*, *79*(2014), 698–720. http://doi.org/10.1016/j.enconman.2013.12.064

Labeckas, G., Slavinskas, S., & Mažeika, M. (2014b). The effect of ethanol–diesel–biodiesel blends on combustion, performance and emissions of a direct injection diesel engine. *Energy Conversion and Management*, *79*, 698–720. http://doi.org/10.1016/j.enconman.2013.12.064

Lahane, S., & Subramanian, K. A. (2014). Impact of nozzle holes configuration on fuel spray, wall impingement and NOx emission of a diesel engine for biodiesel–diesel blend (B20). *Applied Thermal Engineering*, *64*(1–2), 307–314. http://doi.org/http://dx.doi.org/10.1016/j.applthermaleng.2013.12.048

Lahane, S., & Subramanian, K. A. (2015). Effect of different percentages of biodiesel–diesel blends on injection, spray, combustion, performance, and emission characteristics of a diesel engine. *Fuel*, *139*(0), 537–545. http://doi.org/http://dx.doi.org/10.1016/j.fuel.2014.09.036

Lapuerta, M., Rodríguez-Fernández, J., & García-Contreras, R. (2015). Effect of a glycerol-derived advanced biofuel -FAGE (fatty acid formal glycerol ester)- on the emissions of a diesel engine tested under the New European Driving Cycle. *Energy*, *93*, 568–579. http://doi.org/10.1016/j.energy.2015.09.070

Lapuerta, M., Rodríguez-Fernandez, J., García-Contreras, R., & Bogarra, M. (2015). Molecular interactions in blends of alcohols with diesel fuels: Effect on stability and distillation. *Fuel*, *139*, 171–179. http://doi.org/10.1016/j.fuel.2014.08.055

Lee, S., & Kim, T. Y. (2015). Feasibility study of using wood pyrolysis oil-ethanol blended fuel with diesel pilot injection in a diesel engine. *Fuel*, *162*, 65–73. http://doi.org/10.1016/j.fuel.2015.08.049

Li, J., Chen, X., Qi, B., Luo, J., Zhang, Y., Su, Y., & Wan, Y. (2014). Efficient production of acetone-butanol-ethanol (ABE) from cassava by a fermentation-pervaporation coupled process. *Bioresource Technology*, *169*(October 2014), 251–257. http://doi.org/10.1016/j.biortech.2014.06.102

Li, R., Wang, Z., Ni, P., Zhao, Y., Li, M., & Li, L. (2014a). Effects of cetane number improvers on the performance of diesel engine fuelled with methanol/biodiesel blend. *Fuel*, *128*(0), 180–187. http://doi.org/http://dx.doi.org/10.1016/j.fuel.2014.03.011

Li, R., Wang, Z., Ni, P., Zhao, Y., Li, M., & Li, L. (2014b). Effects of cetane number improvers on the performance of diesel engine fuelled with methanol/biodiesel blend. *Fuel*, *128*, 180–187. http://doi.org/10.1016/j.fuel.2014.03.011

Li, Y., Jia, M., Chang, Y., Xie, M., & Reitz, R. D. (2016). Towards a comprehensive understanding of the influence of fuel properties on the combustion characteristics of a RCCI (reactivity controlled compression ignition) engine. *Energy*, *99*(x), 69–82. http://doi.org/10.1016/j.energy.2016.01.056

Li, Y., Jia, M., Liu, Y., & Xie, M. (2013). Numerical study on the combustion and emission characteristics of a methanol/diesel reactivity controlled compression ignition (RCCI) engine. *Applied Energy*, *106*, 184–197. http://doi.org/10.1016/j.apenergy.2013.01.058

Li, Y., Meng, L., Nithyanandan, K., Lee, T. H., Lin, Y., & Lee, C. F. (2016). Combustion, performance and emissions characteristics of a spark-ignition engine fueled with isopropanol- n -butanol-ethanol and gasoline blends. *Fuel*, *184*, 864–872. http://doi.org/10.1016/j.fuel.2016.07.063

Lim, C., Lee, J., Hong, J., Song, C., Han, J., & Cha, J. S. (2014). Evaluation of regulated and unregulated emissions from a diesel powered vehicle fueled with diesel/biodiesel blends in Korea. *Energy*, *77*, 533–541. http://doi.org/10.1016/j.energy.2014.09.040

Litak, G., & Longwic, R. (2009a). Analysis of repeatability of diesel engine acceleration. *Applied Thermal Engineering*, *29*(17–18), 3574–3578. http://doi.org/10.1016/j.applthermaleng.2009.06.015

Litak, G., & Longwic, R. (2009b). Analysis of repeatability of Diesel engine acceleration. *Applied Thermal Engineering*, *29*(17–18), 3574–3578. http://doi.org/10.1016/j.applthermaleng.2009.06.015

Liu, C., Huang, Y., Wang, X., Tai, Y., Liu, L., Sun, C., & Liu, H. (2018). Emergy analysis for transportation fuels produced from corn stover in China. *Journal of Cleaner Production*, *174*, 213–225. http://doi.org/10.1016/j.jclepro.2017.10.306

Liu, H., Hu, B., & Jin, C. (2016). Effects of different alcohols additives on solubility of hydrous ethanol / diesel fuel blends. *Fuel*, *184*, 440–448.

Liu, H., Li, S., Zheng, Z., Xu, J., & Yao, M. (2013). Effects of n-butanol, 2-butanol, and methyl octynoate addition to diesel fuel on combustion and emissions over a wide range of exhaust gas recirculation (EGR) rates. *Applied Energy*, *112*. http://doi.org/10.1016/j.apenergy.2013.06.023

Liu, K., Li, Y., Yang, J., Deng, B., Feng, R., & Huang, Y. (2018). Comprehensive study of key operating parameters on combustion characteristics of butanol-gasoline blends in a high speed SI engine. *Applied Energy*, *212*(November 2017), 13–32. http://doi.org/10.1016/j.apenergy.2017.12.011

Longwic, R., Litak, G., & Sen, A. K. (2009a). Recurrence plots for diesel engine variability tests. *Zeitschrift Für Naturforschung*, *64a*(1–2), 96–102.

Longwic, R., Litak, G., & Sen, A. K. (2009b). Recurrence Plots for Diesel Engine Variability Tests, (8), 96–102.

López, A. F., Cadrazco, M., Agudelo, A. F., Corredor, L. A., Vélez, J. A., & Agudelo, J. R. (2015a). Impact of n-butanol and hydrous ethanol fumigation on the performance and pollutant emissions of an automotive diesel engine. *Fuel*, *153*(0), 483–491. http://doi.org/http://dx.doi.org/10.1016/j.fuel.2015.03.022

López, A. F., Cadrazco, M., Agudelo, A. F., Corredor, L. A., Vélez, J. A., & Agudelo, J. R. (2015b). Impact of n-butanol and hydrous ethanol fumigation on the performance and pollutant emissions of an automotive diesel engine. *Fuel*, *153*, 483–491. http://doi.org/10.1016/j.fuel.2015.03.022

López, A. F., Cadrazco, M., Agudelo, A. F., Corredor, L. A., Vélez, J. A., & Agudelo, J. R. (2015c). Impact of n-butanol and hydrous ethanol fumigation on the performance and pollutant emissions of an automotive diesel engine. *Fuel*, *153*, 483–491. http://doi.org/http://dx.doi.org/10.1016/j.fuel.2015.03.022

Lounici, M. S., Benbellil, M. A., Loubar, K., Niculescu, D. C., & Tazerout, M. (2017). Knock characterization and development of a new knock indicator for dual-fuel engines. *Energy*, *141*, 2351–2361. http://doi.org/10.1016/j.energy.2017.11.138

Ma, F., Zhao, C., Zhang, F., Zhao, Z., Zhang, Z., Xie, Z., & Wang, H. (2015). An experimental investigation on the combustion and heat release characteristics of an opposed-piston folded-cranktrain diesel engine. *Energies*, *8*(7), 6365–6381. http://doi.org/10.3390/en8076365

Maghbouli, A., Yang, W., An, H., Li, J., & Shafee, S. (2015). Effects of injection strategies and fuel injector configuration on combustion and emission characteristics of a D.I. diesel engine fueled by bio-diesel. *Renewable Energy*, *76*(0), 687–698. http://doi.org/http://dx.doi.org/10.1016/j.renene.2014.11.092

Maity, S. K. (2015). Opportunities, recent trends and challenges of integrated biorefinery: Part II. *Renewable and Sustainable Energy Reviews*, *43*, 1446–1466. http://doi.org/10.1016/j.rser.2014.08.075

Man, X., Tang, C., Zhang, J., Zhang, Y., Pan, L., Huang, Z., & Law, C. K. (2014). An experimental and kinetic modeling study of n -propanol and i -propanol ignition at high temperatures. *Combustion and Flame*, *161*(3), 644–656. http://doi.org/10.1016/j.combustflame.2013.08.003

Mansor, M. R. A., Abbood, M. M., & Mohamad, T. I. (2017). The influence of varying hydrogen-methane-diesel mixture ratio on the combustion characteristics and emissions of a direct injection diesel engine. *Fuel*, *190*, 281–291. http://doi.org/10.1016/j.fuel.2016.11.010

Maroteaux, F., & Saad, C. (2015). Combined mean value engine model and crank angle resolved in-cylinder modeling with NOx emissions model for real-time Diesel engine simulations at high engine speed. *Energy*. http://doi.org/10.1016/j.energy.2015.05.072

Martínez, G., Sánchez, N., Encinar, J. M., & González, J. F. (2014). Fuel properties of biodiesel from vegetable oils and oil mixtures. Influence of methyl esters distribution. *Biomass and Bioenergy*, *63*, 22–32. http://doi.org/10.1016/j.biombioe.2014.01.034

Martyr, A. J., & Plint, M. A. (2007). *Engine Testing: Theory and Practice* (3rd ed.). Butterworth-Heinemann. Retrieved from http://www.sciencedirect.com/science/book/9780080969497

Marwan, N. (2006). *Encouters with neighbours*. *Communications*.

Marwan, N. (2011). How to avoid potential pitfalls in recurrence plot based data analysis. *International Journal of Bifurcation and Chaos*, *21*(4), 1003–1017. http://doi.org/10.1142/S0218127411029008

Marwan, N., Carmen Romano, M., Thiel, M., & Kurths, J. (2007). Recurrence plots for the analysis of complex systems. *Physics Reports*, *438*(5–6), 237–329. http://doi.org/10.1016/j.physrep.2006.11.001

Marwan, N., & Kurths, J. (2004). Line Structures in Recurrence Plots, (February 2008). http://doi.org/10.1016/j.physleta.2004.12.056

Marwan, N., & Kurths, J. (2005). Line structures in recurrence plots. *Physics Letters, Section A: General, Atomic and Solid State Physics*, *336*(4–5), 349–357. http://doi.org/10.1016/j.physleta.2004.12.056

Marwan, N., & Meinke, A. (2002). Extended Recurrence Plot Analysis and its Application to ERP Data. *International Journal Of Bifurcation And Chaos*, *14*(2), 21. http://doi.org/10.1142/S0218127404009454

Marwan, N., Wessel, N., Stepan, H., & Kurths, J. (2010). Recurrence Based Complex Network Analysis of Cardiovascular Variability Data to Predict Pre-Eclampsia . *Proceedings of the International Symposium on Nonlinear Theory and Its Applications (NOLTA2010), Krakow*, (6170), 585–588.

Maunula, T. (2013). NOX Reduction with the Combinations on LNT and SCR in Diesel Applications. *(No. 2013-24-0161). SAE Technical Paper*, (x), 195–206. http://doi.org/10.4271/2013-24-0161

Maurya, R. K., & Agarwal, A. K. (2012). Statistical analysis of the cyclic variations of heat release parameters in HCCI combustion of methanol and gasoline. *Applied Energy*, *89*(1), 228–236.

Maurya, R. K., & Akhil, N. (2016). Numerical investigation of ethanol fuelled HCCI engine using stochastic reactor model . Part 1 : Development of a new reduced ethanol oxidation mechanism. *Energy Conversion and Management*, *118*, 44–54. http://doi.org/10.1016/j.enconman.2016.03.076

Maurya, R. K., Saxena, M. R., & Akhil, N. (2016). Experimental investigation of cyclic variation in a diesele engine using wavelets. *Advances in Intelligent Systems and Computing*, *384*(April), 247–257. http://doi.org/10.1007/978-3-319-23036-8

Maurya, R., Saxena, M., & Akhil, N. (2016). Experimental Investigation of Cyclic Variation in a Diesel Engine Using Wavelets. In S. Berretti, S. M. Thampi, & P. R. Srivastava (Eds.), *Intelligent Systems Technologies and Applications SE - 21* (Vol. 384, pp. 247–257). Springer International Publishing. http://doi.org/10.1007/978-3-319-23036-8_21

Mhalsekar, S. ., Rao, S. ., & Gangadharan, K. . (2010). Investigation on feasibility of recurrence quantification analysis for detecting flank wear in face milling. *International Journal of Engineering, Science and Technology*, *2*(5), 23–38. http://doi.org/10.4314/ijest.v2i5.60098

Mirzajanzadeh, M., Tabatabaei, M., Ardjmand, M., Rashidi, A., Ghobadian, B., Barkhi, M., & Pazouki, M. (2015). A novel soluble nano-catalysts in diesel–biodiesel fuel blends to improve diesel engines performance and reduce exhaust emissions. *Fuel*, *139*(0), 374–382. http://doi.org/http://dx.doi.org/10.1016/j.fuel.2014.09.008

Mo, J., Tang, C., Li, J., Guan, L., & Huang, Z. (2016). Experimental investigation on the effect of n-butanol blending on spray characteristics of soybean biodiesel in a common-rail fuel injection system. *Fuel*, *182*, 391–401. http://doi.org/10.1016/j.fuel.2016.05.109

Mofijur, M., Rasul, M. G., & Hyde, J. (2015). Recent developments on internal combustion engine performance and emissions fuelled with biodiesel-diesel-ethanol blends. *Procedia Engineering*, *105*(0), 658–664. http://doi.org/http://dx.doi.org/10.1016/j.proeng.2015.05.045

Mofijur, M., Rasul, M. G., Hyde, J., Azad, A. K., Mamat, R., & Bhuiya, M. M. K. (2016). Role of biofuel and their binary (diesel-biodiesel) and ternary (ethanol-biodiesel-diesel) blends on internal combustion engines emission reduction. *Renewable and Sustainable Energy Reviews*, *53*, 265–278. http://doi.org/10.1016/j.rser.2015.08.046

Mohebbi, M., Ghassemian, H., & Asl, B. M. (2011). Structures of the Recurrence Plot of Heart Rate Variability Signal as a Tool for Predicting the Onset of Paroxysmal Atrial Fibrillation. *Journal of Medical Signals and Sensors*, *1*(2), 113–121. Retrieved from http://www.ncbi.nlm.nih.gov/pmc/articles/PMC3342624/

Monirul, I. M., Masjuki, H. H., Kalam, M. A., Mosarof, M. H., Zulkifli, N. W. M., Teoh, Y. H., & How, H. G. (2016). Assessment of performance, emission and combustion characteristics of palm, jatropha and Calophyllum inophyllum biodiesel blends. *Fuel*. http://doi.org/10.1016/j.fuel.2016.05.010

Moon, S., Tsujimura, T., Oguma, M., Chen, Z., Huang, Z., & Saitou, T. (2013). Mixture condition, combustion and sooting characteristics of ethanol-diesel blends in diffusion flames under various injection and ambient conditions. *Fuel*, *113*, 128–139. http://doi.org/10.1016/j.fuel.2013.05.060

Morone, A., & Pandey, R. A. (2014). Lignocellulosic biobutanol production: Gridlocks and potential remedies. *Renewable and Sustainable Energy Reviews*, *37*, 21–35. http://doi.org/10.1016/j.rser.2014.05.009

Mosarof, M. H., Kalam, M. A., Masjuki, H. H., Ashraful, A. M., Rashed, M. M., Imdadul, H. K., & Monirul, I. M. (2015). Implementation of palm biodiesel based on economic aspects, performance, emission, and wear characteristics. *Energy Conversion and Management*. http://doi.org/10.1016/j.enconman.2015.08.020

Moxey, B. G., Cairns, A., & Zhao, H. (2016). A comparison of butanol and ethanol flame development in an optical spark ignition engine. *Fuel*, *170*, 27–38. http://doi.org/10.1016/j.fuel.2015.12.008

Murcak, A., Haşımoğlu, C., Çevik, I., Karabektas, M., & Ergen, G. (2013). Effects of ethanol-diesel blends to performance of a DI diesel engine for different injection timings. *Fuel*, *109*, 582–587. http://doi.org/10.1016/j.fuel.2013.03.014

Najafabadi, I., & Dynamics, D. (2017). Analyzing of in-Cylinder Flow Structures and Cyclic Variations of Partially Premix Combustion in a Light.

Nalgundwar, A., Paul, B., & Sharma, S. K. (2016). Comparison of performance and emissions characteristics of di CI engine fueled with dual biodiesel blends of palm and jatropha. *Fuel*, *173*(2016), 172–179. http://doi.org/10.1016/j.fuel.2016.01.022

Naser, N., Yang, S. Y., Kalghatgi, G., & Chung, S. H. (2017). Relating the octane numbers of fuels to ignition delay times measured in an ignition quality tester (IQT). *Fuel*, *187*, 117–127. http://doi.org/10.1016/j.fuel.2016.09.013

Ndaba, B., Chiyanzu, I., & Marx, S. (2015). N-Butanol derived from biochemical and chemical routes: A review. *Biotechnology Reports*, *8*, 1–9. http://doi.org/10.1016/j.btre.2015.08.001

Ng, J., Kiat, H., & Gan, S. (2012). Characterisation of engine-out responses from a light-duty diesel engine fuelled with palm methyl ester (PME). *Applied Energy*, *90*(1), 58–67. http://doi.org/10.1016/j.apenergy.2011.01.028

Nithyanandan, K., Zhang, J., Li, Y., Wu, H., Lee, T. H., Lin, Y., & Lee, C. F. F. (2016). Improved SI engine efficiency using Acetone-Butanol-Ethanol (ABE). *Fuel*, *174*, 333–343. http://doi.org/10.1016/j.fuel.2016.01.001

Nor, W., Wan, M., Mamat, R., Masjuki, H. H., & Naja, G. (2015). Effects of biodiesel from different feedstocks on engine performance and emissions : A review, *51*, 585–602. http://doi.org/10.1016/j.rser.2015.06.031

Ogunkoya, D., Roberts, W. L., Fang, T., & Thapaliya, N. (2015). Investigation of the effects of renewable diesel fuels on engine performance, combustion, and emissions. *Fuel*, *140*, 541–554. http://doi.org/10.1016/j.fuel.2014.09.061

Optrand Inc. (2017). AutoPSI- pressure sensor. Retrieved April 4, 2017, from http://www.optrand.com/

Ouyang, G., Zhu, X., Ju, Z., & Liu, H. (2014). Dynamical characteristics of surface EMG signals of hand grasps via recurrence plot. *IEEE Journal of Biomedical and Health Informatics*, *18*(1), 257–265. http://doi.org/10.1109/JBHI.2013.2261311

Paiva, E. M., Rohwedder, J. J. R., Pasquini, C., Pimentel, M. F., & Pereira, C. F. (2015). Quantification of biodiesel and adulteration with vegetable oils in diesel/biodiesel blends using portable near-infrared spectrometer. *Fuel*, *160*, 57–63. http://doi.org/10.1016/j.fuel.2015.07.067

Palash, S. M., Kalam, M. A., Masjuki, H. H., Masum, B. M., Rizwanul Fattah, I. M., & Mofijur, M. (2013). Impacts of biodiesel combustion on NOx emissions and their reduction approaches. *Renewable and Sustainable Energy Reviews*, *23*, 473–490. http://doi.org/10.1016/j.rser.2013.03.003

Pan, J., Shu, G., & Wei, H. (2014). Research on in-cylinder pressure oscillation characteristic during knocking combustion in spark-ignition engine. *Fuel*, *120*, 150–157. http://doi.org/10.1016/j.fuel.2013.11.054

Park, S. H., & Lee, C. S. (2013). Combustion performance and emission reduction characteristics of automotive DME engine system. *Progress in Energy and Combustion Science*. http://doi.org/10.1016/j.pecs.2012.10.002

Parthasarathi, R., Gowri, S., & Saravanan, C. G. (2014). Effects of ethanol-diesel emulsions on the performance, combustion and emission characteristics of di diesel engine. *American Journal of Applied Sciences*, *11*(4), 592–600. http://doi.org/10.3844/ajassp.2014.592.600

Pearson, R. J., & Turner, J. W. G. (2014). *Alternative Fuels and Advanced Vehicle Technologies for Improved Environmental Performance*. *Alternative Fuels and Advanced Vehicle Technologies for Improved Environmental Performance*. Elsevier. http://doi.org/10.1533/9780857097422.1.19

Pham, P. X., Bodisco, T. A., Ristovski, Z. D., Brown, R. J., & Masri, A. R. (2014). The influence of fatty acid methyl ester profiles on inter-cycle variability in a heavy duty compression ignition engine. *Fuel*, *116*, 140–150. http://doi.org/10.1016/j.fuel.2013.07.100

Phoon, L. Y., Hashim, H., Mat, R., & Mustaffa, A. A. (2016). Flash point prediction of tailor-made green diesel blends containing B5 palm oil biodiesel and alcohol. *Fuel*, *175*, 287–293. http://doi.org/10.1016/j.fuel.2016.02.027

Phuong X. Pham, Bodisco, T. A., Ristovski, Z. D., Brown, R. J., & Masri, A. R. (2014). The influence of fatty acid methyl ester profiles on inter-cycle variability in a heavy duty compression ignition engine. *Fuel*, (January 2014). http://doi.org/10.1016/j.fuel.2013.07.100

Pinzi, S., Rounce, P., Herreros, J. M., Tsolakis, A., & Pilar Dorado, M. (2013). The effect of biodiesel fatty acid composition on combustion and diesel engine exhaust emissions. *Fuel*, *104*(0), 170–182. http://doi.org/http://dx.doi.org/10.1016/j.fuel.2012.08.056

Porpatham, E., Ramesh, A., & Nagalingam, B. (2012). Effect of compression ratio on the performance and combustion of a biogas fuelled spark ignition engine. *Fuel*, *95*, 247–256. http://doi.org/10.1016/j.fuel.2011.10.059

Prakash, R., Singh, R. K., & Murugan, S. (2013). Experimental investigation on a diesel engine fueled with bio-oil derived from waste wood–biodiesel emulsions. *Energy*, *55*, 610–618. http://doi.org/10.1016/j.energy.2013.03.085

Rajesh Kumar, B., & Saravanan, S. (2016). Effects of iso-butanol/diesel and n-pentanol/diesel blends on performance and emissions of a di diesel engine under premixed LTC (low temperature combustion) mode. *Fuel*, *170*, 49–59. http://doi.org/10.1016/j.fuel.2015.12.029

Rakopoulos, C. D., Giakoumis, E. G., & Rakopoulos, D. C. (2008). Study of the short-term cylinder wall temperature oscillations during transient operation of a turbo-charged diesel engine with various insulation schemes. *International Journal of Engine Research*, *9*(3), 177–193. http://doi.org/10.1243/14680874JER00608

Rakopoulos, D. C., Rakopoulos, C. D., & Giakoumis, E. G. (2010a). Experimental-stochastic investigation of the combustion cyclic variability in HSDI diesel engine using ethanol – diesel fuel blends, *87*(2008), 1478–1491. http://doi.org/10.1016/j.fuel.2007.08.012

Rakopoulos, D. C., Rakopoulos, C. D., & Giakoumis, E. G. (2010b). Experimental-stochastic investigation of the combustion cyclic variability in HSDI diesel engine using ethanol – diesel fuel blends, (2007). http://doi.org/10.1016/j.fuel.2007.08.012

Rakopoulos, D. C., Rakopoulos, C. D., & Giakoumis, E. G. (2015). Impact of properties of vegetable oil, bio-diesel, ethanol and n-butanol on the combustion and emissions of turbocharged HDDI diesel engine operating under steady and transient conditions. *Fuel*, *156*(0), 1–19. http://doi.org/http://dx.doi.org/10.1016/j.fuel.2015.04.021

Rakopoulos, D. C., Rakopoulos, C. D., & Giakoumis, E. G. (2015). Impact of properties of vegetable oil, bio-diesel, ethanol and n-butanol on the combustion and emissions of turbocharged HDDI diesel engine operating under steady and transient conditions. *Fuel*, *156*, 1–19. http://doi.org/10.1016/j.fuel.2015.04.021

Rakopoulos, D. C., Rakopoulos, C. D., & Kyritsis, D. C. (2016). Butanol or DEE blends with either straight vegetable oil or biodiesel excluding fossil fuel: Comparative effects on diesel engine combustion attributes, cyclic variability and regulated emissions trade-off. *Energy*, *115*, *Part*, 314–325. http://doi.org/http://dx.doi.org/10.1016/j.energy.2016.09.022

Ramalingam, S., Govindasamy, M., Ezhulumalai, M., & Kaliyaperumal, A. (2016). Effect of leaf extract from Pongamia pinnata on the oxidation stability, performance and emission characteristics of calophyllum biodiesel. *Fuel*, *180*(2016), 263–269. http://doi.org/10.1016/j.fuel.2016.04.046

Ramírez, A. I., Aggarwal, S. K., Som, S., Rutter, T. P., & Longman, D. E. (2014). Effects of blending a heavy alcohol (C20H40O with diesel in a heavy-duty compression-ignition engine. *Fuel*, *136*, 89–102. http://doi.org/10.1016/j.fuel.2014.06.039

Reitz, R. D. (1997). Reciprocating Internal Combustion Engines. *Thermodynamics: Principles and Practice*, 390–392. http://doi.org/10.1016/B978-0-444-63373-6.00016-2

Renó, M. L. G., Olmo, O. A. del, Palacio, J. C. E., Lora, E. E. S., & Venturini, O. J. (2014). Sugarcane biorefineries: Case studies applied to the Brazilian sugar–alcohol industry. *Energy Conversion and Management*, *86*, 981–991. http://doi.org/10.1016/j.enconman.2014.06.031

Reyes, M., Melgar, A., Pérez, A., & Giménez, B. (2013). Study of the cycle-to-cycle variations of an internal combustion engine fuelled with natural gas/hydrogen blends from the diagnosis of combustion pressure. *International Journal of Hydrogen Energy*, *38*(35), 15477–15487. http://doi.org/10.1016/j.ijhydene.2013.09.071

SAE International. (2004). SAE J1349 Surface Vehicle Standard Engine Power Test Code-Spark Ignition and Compression Ignition-Net Power Rating. SAE International.

Şahin, Z., Durgun, O., & Aksu, O. N. (2015). Experimental investigation of n-butanol/diesel fuel blends and n-butanol fumigation – Evaluation of engine performance, exhaust emissions, heat release and flammability analysis. *Energy Conversion and Management*, *103*, 778–789. http://doi.org/10.1016/j.enconman.2015.06.089

Sakthivel, G., Nagarajan, G., Ilangkumaran, M., & Gaikwad, A. B. (2014). Comparative analysis of performance, emission and combustion parameters of diesel engine fuelled with ethyl ester of fish oil and its diesel blends. *Fuel*, *132*, 116–124. http://doi.org/10.1016/j.fuel.2014.04.059

Sakthivel, R., Ramesh, K., Purnachandran, R., & Mohamed Shameer, P. (2018). A review on the properties, performance and emission aspects of the third generation biodiesels. *Renewable and Sustainable Energy Reviews*, *82*(5), 2970–2992. http://doi.org/10.1016/j.rser.2017.10.037

Saleh, H. E., & Selim, M. Y. E. (2017). Improving the performance and emission characteristics of a diesel engine fueled by jojoba methyl ester-diesel-ethanol ternary blends. *Fuel*, *207*, 690–701. http://doi.org/10.1016/j.fuel.2017.06.072

Sandeep, P. P., Nithin, D. B., Jeevan, M., Marwin, D., & Umashankar, K. S. (2016). Detection of Bearing Damage Through Recurrence Quantification Analysis, 322–326.

Sarathy, S. M., Oßwald, P., Hansen, N., & Kohse-Höinghaus, K. (2014). Alcohol combustion chemistry. *Progress in Energy and Combustion Science*, *44*, 40–102. http://doi.org/10.1016/j.pecs.2014.04.003

Sathiyamoorthi, R., & Sankaranarayanan, G. (2017). The effects of using ethanol as additive on the combustion and emissions of a direct injection diesel engine fuelled with neat lemongrass oil-diesel fuel blend. *Renewable Energy*, *101*, 747–756. http://doi.org/10.1016/j.renene.2016.09.044

Saxena, M. R., & Maurya, R. K. (2016). Effect of butanol blends on nano particle emissions from a stationary conventional diesel engine. *Aerosol and Air Quality Research*, *16*(9), 2255–2266. http://doi.org/10.4209/aaqr.2016.04.0144

Schifter, I., González, U., & González-Macías, C. (2016). Effects of ethanol, ethyl-tert-butyl ether and dimethyl-carbonate blends with gasoline on SI engine. *Fuel*, *183*, 253–261. http://doi.org/10.1016/j.fuel.2016.06.051

Sehatpour, M.-H., Kazemi, A., & Sehatpour, H. (2017). Evaluation of alternative fuels for light-duty vehicles in Iran using a multi-criteria approach. *Renewable and Sustainable Energy Reviews*, *72*(October 2016), 295–310. http://doi.org/10.1016/j.rser.2017.01.067

Sen, A. K., Litak, G., Edwards, K. D., Finney, C. E. A., Daw, C. S., & Wagner, R. M. (2011). Characteristics of cyclic heat release variability in the transition from spark ignition to HCCI in a gasoline engine. *Applied Energy*, *88*(5), 1649–1655. http://doi.org/10.1016/j.apenergy.2010.11.040

Sen, A. K., Litak, G., Taccani, R., & Radu, R. (2008). Wavelet analysis of cycle-to-cycle pressure variations in an internal combustion engine. *Chaos, Solitons & Fractals*, *38*(3), 886–893. http://doi.org/10.1016/j.chaos.2007.01.041

Sen, A. K., Litak, G., Yao, B.-F., & Li, G.-X. (2010). Analysis of pressure fluctuations in a natural gas engine under lean burn conditions. *Applied Thermal Engineering*, *30*(6–7), 776–779. http://doi.org/10.1016/j.applthermaleng.2009.11.002

Sen, A. K., Longwic, R., Litak, G., & Górski, K. (2008). Analysis of cycle-to-cycle pressure oscillations in a diesel engine. *Mechanical Systems and Signal Processing*, *22*(2), 362–373. http://doi.org/10.1016/j.ymssp.2007.07.015

Sen, A. K., Medina, A., Curto-Risso, P. L., & Calvo Hernández, A. (2014). Effect of ethanol addition on cyclic variability in a simulated spark ignition gasoline engine. *Meccanica*, *49*(10), 2285–2297. http://doi.org/10.1007/s11012-014-9974-1

Sen, A. K., Zheng, J., & Huang, Z. (2011). Dynamics of cycle-to-cycle variations in a natural gas direct-injection spark-ignition engine. *Applied Energy*, *88*(7), 2324–2334.

Senthil, R., Sivakumar, E., & Silambarasan, R. (2015). Effect of butanol addition on performance and emission characteristics of a DI diesel engine fueled with pongamiaethanol blend. *International Journal of ChemTech Research*, *8*(2), 459–467.

Serrano, L., Lopes, M., Pires, N., Ribeiro, I., Cascão, P., Tarelho, L., … Borrego, C. (2015). Evaluation on effects of using low biodiesel blends in a EURO 5 passenger vehicle equipped with a common-rail diesel engine. *Applied Energy*, *146*, 230–238. http://doi.org/10.1016/j.apenergy.2015.01.063

Serras-Pereira, J., Aleiferis, P. G., Walmsley, H. L., Davies, T. J., & Cracknell, R. F. (2013). Heat flux characteristics of spray wall impingement with ethanol, butanol, iso-octane, gasoline and E10 fuels. *International Journal of Heat and Fluid Flow*, *44*, 662–683. http://doi.org/10.1016/j.ijheatfluidflow.2013.09.010

Shaafi, T., & Velraj, R. (2015). Influence of alumina nanoparticles, ethanol and isopropanol blend as additive with diesel–soybean biodiesel blend fuel: Combustion, engine performance and emissions. *Renewable Energy*, *80*, 655–663. http://doi.org/10.1016/j.renene.2015.02.042

Shahir, V. K., Jawahar, C. P., & Suresh, P. R. (2015). Comparative study of diesel and biodiesel on CI engine with emphasis to emissions—A review. *Renewable and Sustainable Energy Reviews*, *45*, 686–697. http://doi.org/10.1016/j.rser.2015.02.042

Shehata, M. S. (2010). Cylinder pressure, performance parameters, heat release, specific heats ratio and duration of combustion for spark ignition engine. *Energy*, *35*(12), 4710–4725. http://doi.org/10.1016/j.energy.2010.09.027

Shivapuji, A. M., & Dasappa, S. (2014). In-cylinder investigations and analysis of a SI gas engine fuelled with H2 and CO rich syngas fuel: Sensitivity analysis of combustion descriptors for engine diagnostics and control. *International Journal of Hydrogen Energy*, *39*(28), 15786–15802. http://doi.org/10.1016/j.ijhydene.2014.07.122

Sindhu, R., Amba, G., Rao, P., & Murthy, K. M. (2014). Thermodynamic Modelling of Diesel Engine Processes for Predicting Engine Performance. *International Journal of Applied Engineering and Technology*, *4*(2), 2277–212.

Singh, B., & Bharti, N. (2015). Software tools for heart rate variability analysis. *International Journal of Recent Scientific Research*, *6*(4), 3501–3506.

Soltau, J. P. (1960). Cylinder pressure variations in petrol engines. *Proceedings of the Institution of Mechanical Engineers: Automobile Division*, *14*(1). Retrieved from https://doi.org/10.1243/PIME_AUTO_1960_000_014_02

Sparavigna, A. C. (2014). Recurrence Plots from Altimetry Data of Some Lakes in Africa Original. *International Journal of Sciences*, *3*(July 2014). http://doi.org/10.18483/ijSci.534

Srirangan, K., Akawi, L., Moo-Young, M., & Chou, C. P. (2012). Towards sustainable production of clean energy carriers from biomass resources. *Applied Energy*, *100*, 172–186. http://doi.org/10.1016/j.apenergy.2012.05.012

Storch, M., Hinrichsen, F., Wensing, M., Will, S., & Zigan, L. (2015). The effect of ethanol blending on mixture formation , combustion and soot emission studied in an optical DISI engine. *Applied Energy*, *156*, 783–792. http://doi.org/10.1016/j.apenergy.2015.06.030

Strozzi, F., Zaldívar, J.-M., & Zbilut, J. P. (2002). Application of nonlinear time series analysis techniques to high-frequency currency exchange data. *Physica A: Statistical Mechanics and Its Applications*, *312*, 520–538. http://doi.org/10.1016/S0378-4371(02)00846-4

Suganya, T., Varman, M., Masjuki, H. H., & Renganathan, S. (2016). Macroalgae and microalgae as a potential source for commercial applications along with biofuels production: A biorefinery approach. *Renewable and Sustainable Energy Reviews*, *55*, 909–941. http://doi.org/10.1016/j.rser.2015.11.026

Suh, H. K., & Lee, C. S. (2016). A review on atomization and exhaust emissions of a biodiesel-fueled compression ignition engine. *Renewable and Sustainable Energy Reviews*, *58*, 1601–1620. http://doi.org/http://dx.doi.org/10.1016/j.rser.2015.12.329

Sun, J., Bittle, J. A., & Jacobs, T. J. (2013). Cyclic Variability in Diesel/Gasoline Dual-Fuel Combustion on a Medium-Duty Diesel Engine. In *ASME 2013 Internal Combustion Engine Division Fall Technical Conference* (p. V001T03A011-V001T03A011). American Society of Mechanical Engineers.

Sun, Y., Ponnusamy, S., Muppaneni, T., Reddy, H. K., Wang, J., Zeng, Z., & Deng, S. (2015). Transesterification of camelina sativa oil with supercritical alcohol mixtures. *Energy Conversion and Management*, *101*, 402–409. http://doi.org/10.1016/j.enconman.2015.05.056

Szulczyk, K. R. (2010). Which is a better transportation fuel–butanol or ethanol? *Int J Energy Environ*, *1*(3), 501–512.

Tadano, Y. S., Borillo, G. C., Godoi, A. F. L., Cichon, A., Silva, T. O. B., Valebona, F. B., … Godoi, R. H. M. (2014). Gaseous emissions from a heavy-duty engine equipped with SCR aftertreatment system and fuelled with diesel and biodiesel: Assessment of pollutant dispersion and health risk. *Science of The Total Environment*, *500–501*(0), 64–71. http://doi.org/http://dx.doi.org/10.1016/j.scitotenv.2014.08.100

Taghizadeh-Alisaraei, A., & Rezaei-Asl, A. (2016). The effect of added ethanol to diesel fuel on performance, vibration, combustion and knocking of a CI engine. *Fuel*, *185*, 718–733. http://doi.org/10.1016/j.fuel.2016.08.041

Tang, S., LaDuke, G., Chien, W., & Frank, B. P. (2016). Impacts of biodiesel blends on PM2.5, particle number and size distribution, and elemental/organic carbon from nonroad diesel generators. *Fuel*, *172*, 11–19. http://doi.org/10.1016/j.fuel.2015.12.060

Tarabet, L., Loubar, K., Lounici, M. S., Khiari, K., Belmrabet, T., & Tazerout, M. (2014). Experimental investigation of DI diesel engine operating with eucalyptus biodiesel/natural gas under dual fuel mode. *Fuel*, *133*(0), 129–138. http://doi.org/http://dx.doi.org/10.1016/j.fuel.2014.05.008

The U.S. Environmental Protection Agency (EPA). (2016). 40 CFR Part 80 Amendments Related to: Tier 3 Motor Vehicle Emission and Fuel Standards.

Tily, R., & Brace, C. J. (2011). Analysis of cyclic variability in combustion in internal combustion engines using wavelets. *Proceedings of the Institution of Mechanical Engineers, Part D: Journal of Automobile Engineering*, *225*, 341–353. http://doi.org/10.1177/09544070JAUTO1723

Tošić, T., Graben, P., Sellers, K. K., Fröhlich, F., & Hutt, A. (2015). Dynamics analysis of neural univariate time series by recurrence plots. *BMC Neuroscience*, *16*(Suppl 1), P105. http://doi.org/10.1186/1471-2202-16-S1-P105

Tosun, E., Yilmaz, A. C., Ozcanli, M., & Aydin, K. (2014). Determination of effects of various alcohol additions into peanut methyl ester on performance and emission characteristics of a compression ignition engine. *Fuel*, *126*, 38–43. http://doi.org/10.1016/j.fuel.2014.02.037

Tse, H., Leung, C. W., & Cheung, C. S. (2015). Investigation on the combustion characteristics and particulate emissions from a diesel engine fueled with diesel-biodiesel-ethanol blends. *Energy*, *83*(0), 343–350. http://doi.org/http://dx.doi.org/10.1016/j.energy.2015.02.030

Tüccar, G., Özgür, T., & Aydın, K. (2014). Effect of diesel–microalgae biodiesel–butanol blends on performance and emissions of diesel engine. *Fuel*, *132*, 47–52. http://doi.org/10.1016/j.fuel.2014.04.074

Turkcan, A. (2018). Effects of high bioethanol proportion in the biodiesel-diesel blends in a CRDI engine. *Fuel*, *223*(October 2017), 53–62. http://doi.org/10.1016/j.fuel.2018.03.032

Tutak, W., Lukács, K., Szwaja, S., & Bereczky, Á. (2015). Alcohol-diesel fuel combustion in the compression ignition engine. *Fuel*, *154*. http://doi.org/10.1016/j.fuel.2015.03.071

Uribe, L. F. S., Fazanaro, F. I., Castellano, G., Suyama, R., Attux, R., Cardozo, E., & Soriano, D. C. (2014). Translational Recurrences. *Springer Proceedings in Mathematics and Statistics*, *103*, 95–107. http://doi.org/10.1007/978-3-319-09531-8

Uyumaz, A. (2018). Combustion, performance and emission characteristics of a DI diesel engine fueled with mustard oil biodiesel fuel blends at different engine loads. *Fuel*, *212*(October 2017), 256–267. http://doi.org/10.1016/j.fuel.2017.09.005

Vallinayagam, R., Vedharaj, S., Yang, W. M., Lee, P. S., Chua, K. J. E., & Chou, S. K. (2013). Combustion performance and emission characteristics study of pine oil in a diesel engine. *Energy*, *57*, 344–351. http://doi.org/10.1016/j.energy.2013.05.061

Vallinayagam, R., Vedharaj, S., Yang, W. M., Lee, P. S., Chua, K. J. E., & Chou, S. K. (2014). Pine oil-biodiesel blends: A double biofuel strategy to completely eliminate the use of diesel in a diesel engine. *Applied Energy*, *130*(2014), 466–473. http://doi.org/10.1016/j.apenergy.2013.11.025

Vallinayagam, R., Vedharaj, S., Yang, W. M., Raghavan, V., Saravanan, C. G., Lee, P. S., … Chou, S. K. (2014). Investigation of evaporation and engine characteristics of pine oil biofuel fumigated in the inlet manifold of a diesel engine. *Applied Energy*, *115*, 514–524. http://doi.org/10.1016/j.apenergy.2013.11.004

Vandeput, S. (2010). *Heart rate variability : linear and nonlinear analysis with applications in human physiology*. *University Dissertation*.

Verma, P., & Sharma, M. P. (2016). Review of process parameters for biodiesel production from different feedstocks. *Renewable and Sustainable Energy Reviews*, *62*, 1063–1071. http://doi.org/10.1016/j.rser.2016.04.054

Vinod Babu, V. B. M., Madhu Murthy, M. M. K., & Amba Prasad Rao, G. (2017). Butanol and pentanol: The promising biofuels for CI engines – A review. *Renewable and Sustainable Energy Reviews*. http://doi.org/10.1016/j.rser.2017.05.038

Vojtisek-Lom, M., Pechout, M., Dittrich, L., Beránek, V., Kotek, M., Schwarz, J., … Topinka, J. (2015). Polycyclic aromatic hydrocarbons (PAH) and their genotoxicity in exhaust emissions from a diesel engine during extended low-load operation on diesel and biodiesel fuels. *Atmospheric Environment*, *109*(0), 9–18. http://doi.org/http://dx.doi.org/10.1016/j.atmosenv.2015.02.077

Wan Ghazali, W. N. M., Mamat, R., Masjuki, H. H., & Najafi, G. (2015). Effects of biodiesel from different feedstocks on engine performance and emissions: A review. *Renewable and Sustainable Energy Reviews*, *51*, 585–602. http://doi.org/10.1016/j.rser.2015.06.031

Wang, X., Ge, Y., Yu, L., & Feng, X. (2013). Comparison of combustion characteristics and brake thermal efficiency of a heavy-duty diesel engine fueled with diesel and biodiesel at high altitude. *Fuel*, *107*, 852–858. http://doi.org/http://dx.doi.org/10.1016/j.fuel.2013.01.060

Wang, Y., Xiao, F., Zhao, Y., Li, D., & Lei, X. (2015). Study on cycle-by-cycle variations in a diesel engine with dimethyl ether as port premixing fuel. *Applied Energy*, *143*(x), 58–70. http://doi.org/10.1016/j.apenergy.2014.12.079

Wei, L., Yao, C., Wang, Q., Pan, W., & Han, G. (2015). Combustion and emission characteristics of a turbocharged diesel engine using high premixed ratio of methanol and diesel fuel. *Fuel*, *140*, 156–163. http://doi.org/10.1016/j.fuel.2014.09.070

Wendeker, M., Litak, G., Czarnigowski, J., & Szabelski, K. (2003). Nonperiodic Oscillations of Pressure in a Spark Ignition Engine. *International Journal of Bifurcation and Chaos in Applied Sciences and Engineering*, *14*(5), 6. http://doi.org/10.1142/S0218127404010084

Wood, B. M., Kirwan, K., Maggs, S., Meredith, J., & Coles, S. R. (2015). Study of combustion performance of biodiesel for potential application in motorsport. *Journal of Cleaner Production*, *93*, 167–173. http://doi.org/10.1016/j.jclepro.2014.12.091

Wu, H. (2013). Study of Spark Ignition Engine Combustion Model for the Analysis of Cyclic Variation and Combustion Stability at Lean Operating Conditions.

Wu, H., Nithyanandan, K., Zhou, N., Lee, T. H., Lee, C. F. F., & Zhang, C. (2015). Impacts of acetone on the spray combustion of Acetone-Butanol-Ethanol (ABE)-Diesel blends under low ambient temperature. *Fuel*, *142*, 109–116. http://doi.org/10.1016/j.fuel.2014.10.009

Xin, Z., Jian, X., Shizhuo, Z., Xiaosen, H., & Jianhua, L. (2013). The experimental study on cyclic variation in a spark ignited engine fueled with biogas and hydrogen blends. *International Journal of Hydrogen Energy*, 1–5. http://doi.org/10.1016/j.ijhydene.2013.01.097

Xu, M., Shang, P., & Lin, A. (2017). Multiscale recurrence quantification analysis of order recurrence plots, *469*, 381–389.

Yang, H. (2011). Multiscale recurrence quantification analysis of spatial cardiac vectorcardiogram signals. *IEEE Transactions on Biomedical Engineering*, *58*(2), 339–347. http://doi.org/10.1109/TBME.2010.2063704

Yang, H., Bukkapatnam, S. T. S., & Barajas, L. G. (2011). Local recurrence based performance prediction and prognostics in the nonlinear and nonstationary systems. *Pattern Recognition*, *44*(8), 1834–1840. http://doi.org/10.1016/j.patcog.2011.01.010

Yang, H., & Liu, G. (2013). Self-organized topology of recurrence-based complex networks. *Chaos*, *23*(4). http://doi.org/10.1063/1.4829877

Yang, L.-P., Song, E.-Z., Ding, S.-L., Brown, R. J., Marwan, N., & Ma, X.-Z. (2016). Analysis of the dynamic characteristics of combustion instabilities in a pre-mixed lean-burn natural gas engine. *Applied Energy*, *183*(October), 746–759. http://doi.org/10.1016/j.apenergy.2016.09.037

Yao, C., Geng, P., Yin, Z., Hu, J., Chen, D., & Ju, Y. (2016). Impacts of nozzle geometry on spray combustion of high pressure common rail injectors in a constant volume combustion chamber. *Fuel*, *179*, 235–245. http://doi.org/10.1016/j.fuel.2016.03.097

Yasin, M. H. M., Mamat, R., Abdullah, A. A., Abdullah, N. R., & Wyszynski, M. L. (2013). Cycle-to-Cycle Variations of a Diesel Engine Operating with Palm Biodiesel. *Journal of KONES Powertrain and Transport*, *20*(3).

Yilmaz, N., & Atmanli, A. (2017). Experimental assessment of a diesel engine fueled with diesel-biodiesel-1-pentanol blends. *Fuel*, *191*, 190–197. http://doi.org/10.1016/j.fuel.2016.11.065

Yilmaz, N., & Davis, S. M. (2016a). Polycyclic aromatic hydrocarbon (PAH) formation in a diesel engine fueled with diesel, biodiesel and biodiesel/n-butanol blends. *Fuel*, *181*, 729–740. http://doi.org/http://dx.doi.org/10.1016/j.fuel.2016.05.059

Yilmaz, N., & Davis, S. M. (2016b). Polycyclic aromatic hydrocarbon (PAH) formation in a diesel engine fueled with diesel, biodiesel and biodiesel/n-butanol blends. *Fuel*, *181*, 729–740. http://doi.org/10.1016/j.fuel.2016.05.059

Yilmaz, N., & Vigil, F. M. (2014). Potential use of a blend of diesel, biodiesel, alcohols and vegetable oil in compression ignition engines. *Fuel*, *124*(2014), 168–172. http://doi.org/10.1016/j.fuel.2014.01.075

You-cheng, S., Min, X., Yong, G., Yi, C., Lei, S., & Kang-yao, D. (2015). Effects of injection pressure, exhaust gas recirculation and intake pressure on the cycle-to-cycle variations of HCCI combustion. *Journal of the Energy Institute*, 1–9. http://doi.org/10.1016/j.joei.2015.01.017

Yu, S., Gao, T., Wang, M., Li, L., & Zheng, M. (2017). Ignition control for liquid dual-fuel combustion in compression ignition engines. *Fuel*, *197*, 583–595. http://doi.org/10.1016/j.fuel.2017.02.047

Yuan, M.-H., Chen, Y.-H., Chen, J.-H., & Luo, Y.-M. (2017). Dependence of cold filter plugging point on saturated fatty acid profile of biodiesel blends derived from different feedstocks. *Fuel*, *195*, 59–68. http://doi.org/10.1016/j.fuel.2017.01.054

Yusri, I. M., Mamat, R., Ali, O. M., Aziz, A., Akasyah, M., Kamarulzaman, M. K., … Mahmadul, H. M. (2016). The combustion of N-butanol-diesel fuel blends and its cycle to cycle variability in a modern common-rail diesel engine. *ARPN Journal of Engineering and Applied Sciences*, *11*(4), 2297–2301.

Žaglinskis, J., Lukács, K., & Bereczky. (2016). Comparison of properties of a compression ignition engine operating on diesel-biodiesel blend with methanol additive. *Fuel*, *170*, 245–253. http://doi.org/10.1016/j.fuel.2015.12.030

Zaharin, M. S. M., Abdullah, N. R., Najafi, G., Sharudin, H., & Yusaf, T. (2017). Effects of physicochemical properties of biodiesel fuel blends with alcohol on diesel engine performance and exhaust emissions: A review. *Renewable and Sustainable Energy Reviews*, *79*(March), 475–493. http://doi.org/10.1016/j.rser.2017.05.035

Zare, A., Nabi, M. N., Bodisco, T. A., Hossain, F. M., Rahman, M. M., Ristovski, Z. D., & Brown, R. J. (2016). The effect of triacetin as a fuel additive to waste cooking biodiesel on engine performance and exhaust emissions. *Fuel*, *182*(2), 640–649. http://doi.org/10.1016/j.fuel.2016.06.039

Zbilut, J. P., Thomasson, N., & Webber, C. L. (2002). Recurrence quantification analysis as a tool for nonlinear exploration of nonstationary cardiac signals. *Medical Engineering and Physics*, *24*(1), 53–60. http://doi.org/10.1016/S1350-4533(01)00112-6

Zhang, C., & Wu, H. (2016). Combustion characteristics and performance of a methanol fueled homogenous charge compression ignition (HCCI) engine. *Journal of the Energy Institute*, *89*(3), 346–353. http://doi.org/10.1016/j.joei.2015.03.005

Zhang, H. G., Han, X. J., Yao, B. F., & Li, G. X. (2013). Study on the effect of engine operation parameters on cyclic combustion variations and correlation coefficient between the pressure-related parameters of a CNG engine, *104*, 992–1002. http://doi.org/10.1016/j.apenergy.2012.11.043

Zhang, T., Jacobson, L., Björkholtz, C., Munch, K., & Denbratt, I. (2016). Effect of using butanol and octanol isomers on engine performance of steady state and cold start ability in different types of Diesel engines. *Fuel*, *184*, 708–717. http://doi.org/10.1016/j.fuel.2016.07.046

Zhang, T., Munch, K., & Denbratt, I. (2015). An Experimental Study on the Use of Butanol or Octanol Blends in a Heavy Duty Diesel Engine. *SAE International Journal of Fuels and Lubricants*, *8*(3), 2015-24–2491. http://doi.org/10.4271/2015-24-2491

Zhang, Z.-H., & Balasubramanian, R. (2014). Influence of butanol addition to diesel–biodiesel blend on engine performance and particulate emissions of a stationary diesel engine. *Applied Energy*, *119*(0), 530–536. http://doi.org/http://dx.doi.org/10.1016/j.apenergy.2014.01.043

Zhang, Z. H., Chua, S. M., & Balasubramanian, R. (2016). Comparative evaluation of the effect of butanol-diesel and pentanol-diesel blends on carbonaceous particulate

composition and particle number emissions from a diesel engine. *Fuel*, *176*, 40–47. http://doi.org/10.1016/j.fuel.2016.02.061

Zheng, Z., Li, C., Liu, H., Zhang, Y., Zhong, X., & Yao, M. (2015). Experimental study on diesel conventional and low temperature combustion by fueling four isomers of butanol. *Fuel*, *141*, 109–119. http://doi.org/10.1016/j.fuel.2014.10.053

Zhou, J. H., Cheung, C. S., & Leung, C. W. (2013). Combustion, performance and emissions of ULSD, PME and B50 fueled multi-cylinder diesel engine with naturally aspirated hydrogen. *International Journal of Hydrogen Energy*, *38*(34), 14837–14848. http://doi.org/10.1016/j.ijhydene.2013.08.128

Zhu, L., Xiao, Y., Cheung, C. S., Guan, C., & Huang, Z. (2016). Combustion, gaseous and particulate emission of a diesel engine fueled with n-pentanol (C5 alcohol) blended with waste cooking oil biodiesel. *Applied Thermal Engineering*, *102*, 73–79. http://doi.org/http://dx.doi.org/10.1016/j.applthermaleng.2016.03.145
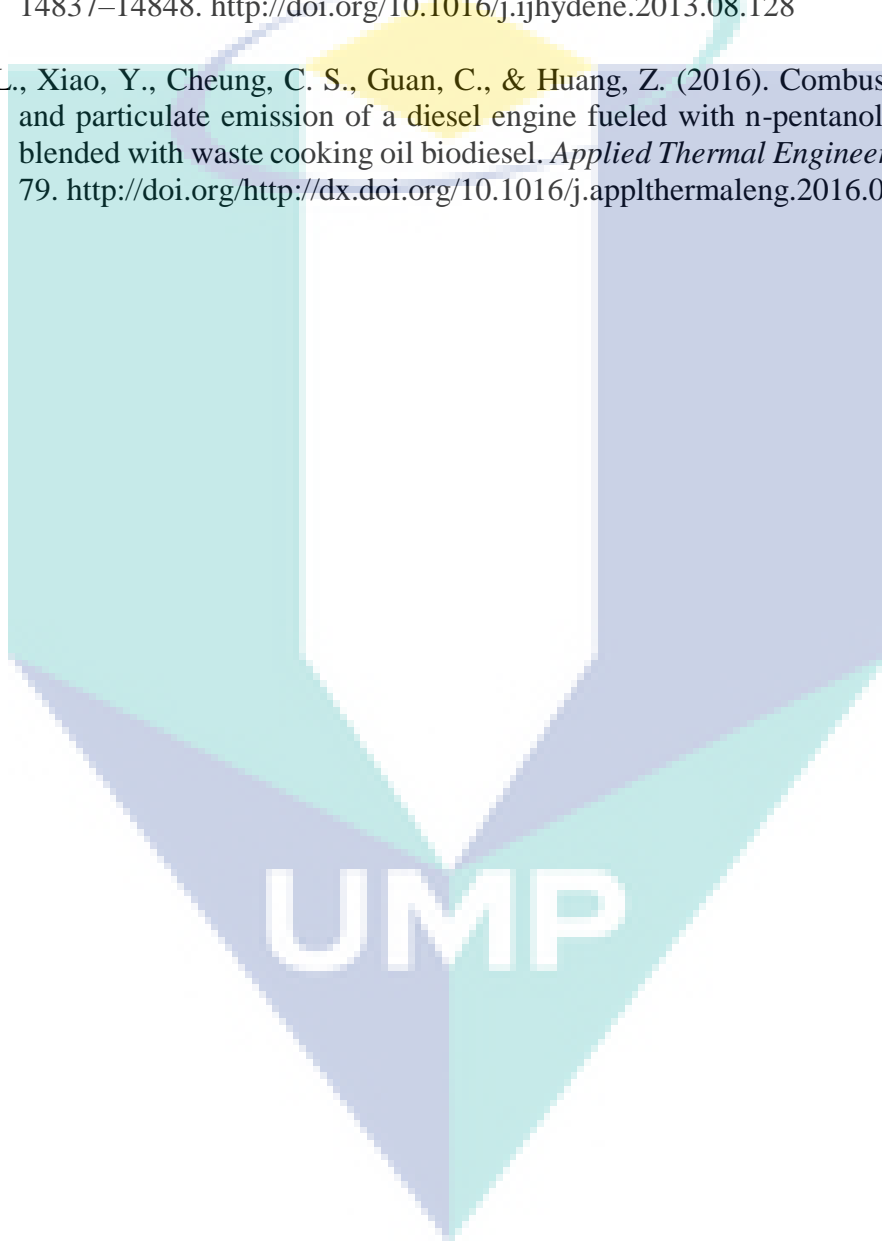
LIST OF PUBLICATIONS

A) International and National Journal & Proceedings

2018

1. **Mohd Hafizil Mat Yasin**, Rizalman Mamat, Abdul Adam Abdullah, Ahmad Fitri Yusop, Najmi Haziq Badrulhisham
   Comparison of the Cyclic Variation of a Diesel-Ethanol Blend in a Diesel Engine
   9th International Conference on Environmental Science and Technology (ICEST 2018)
   IOP Conf. Series: Earth and Environment Science 182 (2018) 012020
   ISSN:1755-1315
   Published online: 11 September 2018
   Publisher: IOP Publishing
   DOI: 10.1088/1755-1315/182/1/012020
   SCOPUS-indexed

2. **Mohd Hafizil Mat Yasin**, Rizalman Mamat, Ahmad Fitri Yusop, Abdul Adam Abdullah, Mohd Fahmi Othman, S.T Yusrizal, S.T Iqbal
   Cylinder Pressure Cyclic Variations in a Diesel Engine operating with Biodiesel-Alcohol Blend
   Energy Procedia
   Volume 142, December 2017, pages 303-308
   9th International Conference on Applied Energy, ICAE2017
   ISSN (Electronic Edition): 2261-236X
   Published online: 31 Jan 2018
   Publisher: Elsevier
   DOI: https://doi.org/10.1016/j.egypro.2017.12.048
   SCOPUS-indexed

2017

1. **Mohd Hafizil Mat Yasin**, Rizalman Mamat, G. Najafi, Obed Majeed Ali, Ahmad Fitri Yusop, Mohd Hafiz Ali,
   Potentials of palm oil as new feedstock oil for a global alternative fuel: A review
   Renewable Sustainable & Energy Reviews (RSER)
   Volume 7 (November 2017), pp. 1034-1049
   ISSN (Electronic Edition): 1364-0321
   Published online: 25 May 2017
   Publisher: Elsevier/Pergamon
   DOI: https://doi.org/10.1016/j.rser.2017.05.186
   ISI Q1 Journal with Impact Factor: 6.798
   5-Year Impact Factor:7.896

2. **Mohd Hafizil Mat Yasin**, Rizalman Mamat, Obed Majeed Ali, Ahmad Fitri Yusop, Mohd Adnin Hamidi, Muhammad Yusri Ismail, Muhammad Rasul, *Study of diesel engine performance with the exhaust gas recirculation (EGR) system fuelled with palm biodiesel*,
Energy Procedia
Volume 110 (2017), pp. 26-31
1st International Conference on Energy and Power (ICEP2016), 14-16 December 2016,
ISSN *(Electronic Edition):* 2261-236X
Published online: 22 April 2017
Publisher: Elsevier
DOI: https://doi.org/10.1016/j.egypro.2017.03.100
SCOPUS-indexed

3. **Mohd Hafizil Mat Yasin**, Rizalman Mamat, Obed Majeed Ali, Ahmad Fitri Yusop, Mohd Adnin Hamidi, Muhammad Yusri Ismail, Muhammad Rasul, *Study of diesel-biodiesel fuel properties and wavelet analysis on cyclic variations in a diesel engine*,
Energy Procedia
Volume 110 (2017) 498-503
1st International Conference on Energy and Power (ICEP2016), 14-16 December 2016,
ISSN (Electronic Edition): 2261-236X
Published online: 22 April 2017
Publisher: Elsevier
DOI: https://doi.org/10.1016/j.egypro.2017.03.175
SCOPUS-indexed

2016

1. **Mohd Hafizil Mat Yasin,** Rizalman Mamat,**,** Amir Aziz**,** Ahmad Fitri Yusop and Mohd Hafiz Ali, *Study of Fuel Inlet Temperature Variations on Palm Biodiesel Operating With A Diesel Engine,*
MATEC Web of Conferences, Volume 90
2nd International Conference on Automotive Innovation and Green Vehicle (AiGEV 2016)
ISSN *(Electronic* Edition): 2261-236X
Published online: 20 December 2016
Publisher: EDP Sciences - Web of Conferences
DOI: http://dx.doi.org/10.1051/matecconf/20179001079
SCOPUS-indexed

2015

1. **Mohd Hafizil Mat Yasin,** Rizalman Mamat,**,** Amir Aziz**,** Ahmad Fitri Yusop
    and Mohd Hafiz Ali,
    *Investigation on Combustion Parameters of Palm Biodiesel operating with a
    Diesel Engine*,
    Journal of Mechanical Engineering and Sciences (JMES),
    Volume 9. pp. 1714-1726.
    ISSN 2289-4659 (print); 2231- 8380 (online
    Publisher: Universiti Malaysia Pahang
    DOI: http://dx.doi.org/10.15282/jmes.9.2015.17.0165
    SCOPUS-indexed

2. **Mohd Hafizil Mat Yasin,** Rizalman Mamat, Ahmad Fitri Yusop, Perowansa
    Paruka, Talal Yusaf and Gholamhassan Najafi,
    *Effects of Exhaust Gas Recirculation (EGR) on a Diesel Engine fuelled with
    Palm Biodiesel*,
    Clean, Efficient and Affordable Energy for a Sustainable Future: The 7th
    International Conference on Applied Energy (ICAE2015)
    Energy Procedia,
    Volume 75, August 2015, Pages 30–36
    ISSN (Electronic Edition): 2261-236X
    Publisher: Elsevier
    DOI: 10.1016/j.egypro.2015.07.131
    SCOPUS-indexed

3. **Mohd Hafizil Mat Yasin,** Rizalman Mamat, Ahmad Fitri Yusop,
    Gholamhassan Najafi and Amir Aziz,
    *Comparative Study on Biodiesel-methanol-diesel Low Proportion Blends
    Operating with a Diesel Engine*,
    Clean, Efficient and Affordable Energy for a Sustainable Future: The 7th
    International Conference on Applied Energy (ICAE2015)
    Energy Procedia,
    Volume 75, August 2015, Pages 10–16
    ISSN (Electronic Edition): 2261-236X
    Publisher: Elsevier
    DOI:10.1016/j.egypro.2015.07.128
    SCOPUS-indexed

4. **Mohd Hafizil Mat Yasin,** Rizalman Mamat, Perowansa Paruka, Ahmad Fitri
    Yusop, Gholamhassan Najafi and Azri Alias,
    *Effect of Low Proportion Palm Biodiesel Blend on Performance, Combustion
    and Emission Characteristics of a Diesel Engine*,
    Clean, Efficient and Affordable Energy for a Sustainable Future: The 7th In-
    ternational Conference on Applied Energy (ICAE2015)

Energy Procedia,
Volume 75, August 2015, Pages 92–98
ISSN (Electronic Edition): 2261-236X
Publisher: Elsevier
DOI: 10.1016/j.egypro.2015.07.145
SCOPUS-indexed

5. **Mohd Hafizil Mat Yasin,** Perowansa Paruka, Rizalman Mamat, Mohd Hafiz Ali,
   Fundamental Study of Dual Fuel on Exhaust Gas Recirculation (EGR) operating with a Diesel Engine,
   Applied Mechanics and Materials
   Vols 773-774 (2015) pp 415-419
   ISSN: 1660-9336
   Publisher: Trans Tech Publications, Switzerland
   DOI: 10.4028/www.scientific.net/AMM.773-774.415
   SCOPUS-indexed

2014

1. **Mohd Hafizil Mat Yasin,** Rizalman Mamat, Abdul Mutalib Leman, Amir Khalid, Noreffendy Tamaldin,
   Experimental Investigation on Biodiesel-Ethanol-Diesel Blends Operating with a Diesel Engine,
   Applied Mechanics and Materials
   Vols. 465 – 466 (2014) Pages 221-225
   ISSN: 1660-9336
   Publisher: Trans Tech Publications, Switzerland
   DOI: 10.4028/www.scientific.net/AMM.465-466.221
   SCOPUS-indexed

2. **Mohd Hafizil Mat Yasin**, Talal Yusaf, Rizalman Mamat, K.V.Sharma, Ahmad Fitri Yusop,
   Characterization of a Diesel Engine operating with a Small Proportion of Methanol as a Fuel Additive in Biodiesel Blend
   Applied Energy
   Volume 114, February 2014, Pages 865 - 873
   ISSN: 0306-2619
   Publisher: Elsevier
   DOI: http://dx.doi.org/10.1016/j.apenergy.2013.06.012
   ISI Q1 Journal with Impact Factor: 5.613
   5-Year Impact Factor: 6.330

B) International and National Conference Papers

<u>2017</u>

1. **Mohd Hafizil Mat Yasin**, Rizalman Mamat, Abdul Adam Abdullah, Ahmad Fitri Yusop,
   Comparison of the Cyclic Variation of a Diesel-Ethanol Blend in a Diesel Engine
   The 2nd International Conference on Engineering Technology and Applied Science 2017, ICES 2017,
   2 December 2017, National Institute of Technology Malang, East Java, Indonesia
   National Institute of Technology Malang & Universiti Malaysia Pahang

2. **Mohd Hafizil Mat Yasin**, Rizalman Mamat, Ahmad Fitri Yusop, Abdul Adam Abdullah, Mohd Hafiz Ali, Mohd Fahmi Othman,
   Cylinder Pressure Cyclic Variations in a Diesel Engine operating with Biodiesel-Alcohol Blends
   9th International Conference on Applied Energy, ICAE2017,
   21-24 August 2017, Cardiff, UK
   The Applied Energy Innovation Institute

<u>2016</u>

1. **Mohd Hafizil Mat Yasin**, Rizalman Mamat, Obed Majeed Ali, Ahmad Fitri Yusop, Mohd Adnin Hamidi, Muhammad Yusri Ismail, Muhammad Rasul,
   Study Of Diesel-Biodiesel Fuel Properties And Wavelet Analysis On Cyclic Variations In A Diesell Engine,
   1st International Conference on Energy and Power, ICEP2016,
   14-16 December 2016, RMIT University, Melbourne, Australia
   RMIT Australia

2. **Mohd Hafizil Mat Yasin,** Rizalman Mamat,**,** Amir Aziz**,** Ahmad Fitri Yusop and Mohd Hafiz Ali,
   Study Of Fuel Inlet Temperature Variations On Palm Biodiesel Operating With A Diesel Engine
   2nd International Conference on Automotive Innovation and Green Energy Vehicle (*AIGEV* 2016),
   2th -3th August 2016, MAI Cyberjaya, Malaysia
   Universiti Malaysia Pahang and Automotive Engineering Center (AEC).

2015

1. **Mohd Hafizil Mat Yasin,** Rizalman Mamat,, Amir Aziz**,** Ahmad Fitri Yusop and Mohd Hafiz Ali,
   Investigation on Combustion Parameters of Palm Biodiesel operating with a Diesel Engine,
   3rd International Conference of Mechanical Engineering Research (*ICMER* 2015),
   18th -19th August 2015, Hotel Zenith Kuantan Pahang
   Universiti Malaysia Pahang

2. **Mohd Hafizil Mat Yasin,** Rizalman Mamat, Ahmad Fitri Yusop, Perowansa Paruka, Talal Yusaf and Gholamhassan Najafi,
   Effects of Exhaust Gas Recirculation (EGR) on a Diesel Engine fuelled with Palm Biodiesel,
   7th International Conference on Applied Energy 2015 (ICAE2015),
   28th – 31th March 2015, Abu Dhabi, UAE

3. **Mohd Hafizil Mat Yasin,** Rizalman Mamat, Ahmad Fitri Yusop, Gholamhassan Najafi and Amir Aziz,
   Comparative Study on Biodiesel-methanol-diesel Low Proportion Blends Operating with a Diesel Engine,
   7th International Conference on Applied Energy 2015 (ICAE2015),
   28th – 31th March 2015, Abu Dhabi, UAE

4. **Mohd Hafizil Mat Yasin,** Rizalman Mamat, Perowansa Paruka, Ahmad Fitri Yusop, Gholamhassan Najafi and Azri Alias,
   Effect of Low Proportion Palm Biodiesel Blend on Performance, Combustion and Emission Characteristics of a Diesel Engine,
   7th International Conference on Applied Energy 2015 (ICAE2015),
   28th – 31th March 2015, Abu Dhabi, UAE

APPENDIX A

RECURRENCE PLOT (RP)

```
clear all
close all
clc


ecg = load('MCP_B90BU10_1700_15.dat');

% mutual information test to determine the time delay
mutual(ecg);

% fnn test to determine the embedding dimension
out=false_nearest(ecg,1,10,8);
fnn = out(:,1:2);
figure('Position',[100 400 460 360]);
plt=plot(fnn(:,1),fnn(:,2),'o-','MarkerSize',8);
title('False nearest neighbor test','FontName','Times New
Roman','FontSize',16,'FontWeight','bold');
xlabel('dimension','FontName','Times New
Roman','FontSize',16,'FontWeight','bold');
ylabel('FNN','FontName','Times New
Roman','FontSize',16,'FontWeight','bold');
get(gcf,'CurrentAxes');
set(gca,'LineWidth',2,'FontName','Times New
Roman','FontSize',16,'FontWeight','bold');
grid on;

% phase space plot
y = phasespace(ecg,3,8);
figure('Position',[100 400 460 360]);
plot3(y(:,1),y(:,2),y(:,3),'.','LineWidth',2);
title('Max cylinder pressure time-delay embedding - state space
plot','FontName','Times New Roman','FontSize',20,'FontWeight','bold');
grid on;
set(gca,'CameraPosition',[25.919 27.36 13.854]);
xlabel('x(t)','FontName','Times New
Roman','FontSize',20,'FontWeight','bold');
ylabel('x(t+\tau)','FontName','Times New
Roman','FontSize',20,'FontWeight','bold');
zlabel('x(t+2\tau)','FontName','Times New
Roman','FontSize',20,'FontWeight','bold');
set(gca,'LineWidth',2,'FontName','Times New
Roman','FontSize',20,'FontWeight','bold');

% color recurrence plot
cerecurr_y(y);
recurdata = cerecurr_y(y);
```
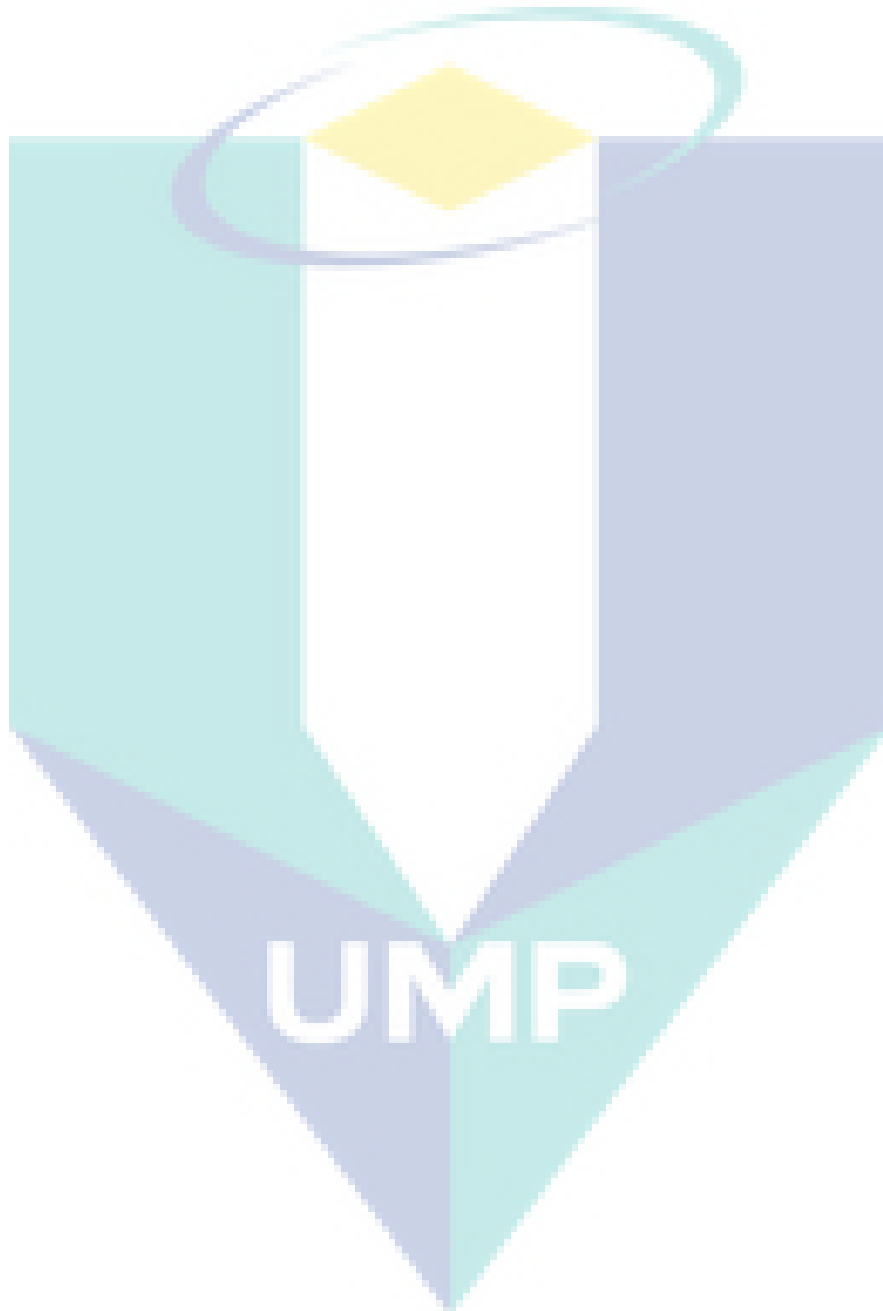
```
% black-white recurrence plot
tdrecurr_y(recurdata,0.5);
recurrpt = tdrecurr_y(recurdata,0.5);

%Recurrence quantification analysis
% rqa_stat - RQA statistics - [recrate DET LMAX ENT TND LAM TT]
rqa_stat = recurrqa_y(recurrpt)
```

APPENDIX B

CERECURR_Y.M

```matlab
function buffer = cerecurr_y(signal)
%This program produces a recurrence plot of the, possibly multivariate,
%data set. That means, for each point in the data set it looks for all
%points, such that the distance between these two points is smaller
%than a given size in a given embedding space.

%input:
%signal: input time series
%dim - embedded dimension    1
%tau - delay of the vectors      1

%output:
%buffer - Matrix containing the pair distances.

%example:
%t=sin(-pi:pi/100:10*pi);
%cerecurr_y(t,2,1);

len = length(signal);
N = len;
Y = signal;
buffer=zeros(N);

%h = waitbar(0,'Please wait...');
for i=1:N
    %waitbar(i/N);
    x0=i;
    for j=i:N
        y0=j;
        % Calculate the euclidean distance
        distance = norm(Y(i,:)-Y(j,:));
        % Store the minimum distance between the two points
        buffer(x0,y0) = distance;
        buffer(y0,x0) = distance;
    end
end
%close(h);

rmin=min(min(buffer));
rmax=max(max(buffer));

%%%%%%%%%%%%%%%%%%%%%%%%%%%%%%%%%%%%%%%
if nargout == 0
    figure('Position',[100 400 460 360]);
    imagesc(buffer);
    colormap Jet;
    colorbar;
```
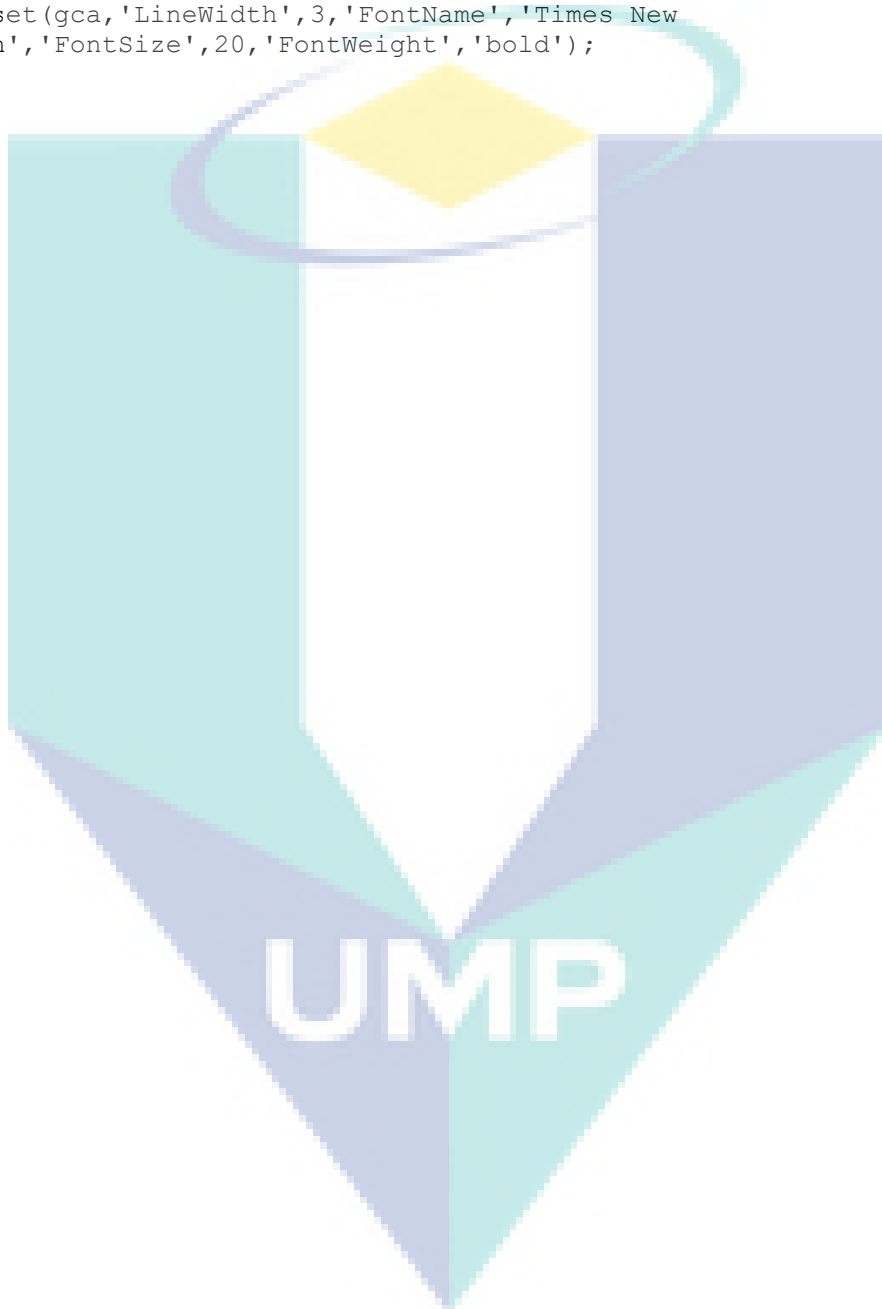
189

```
    axis image;
    xlabel('i','FontName','Times New
Roman','FontSize',20,'FontWeight','bold');
    ylabel('j','FontName','Times New
Roman','FontSize',20,'FontWeight','bold');
    title('Recurrence Plot','FontName','Times New
Roman','FontSize',20,'FontWeight','bold');
    get(gcf,'CurrentAxes');
    set(gca,'YDir','normal')
    set(gca,'LineWidth',3,'FontName','Times New
Roman','FontSize',20,'FontWeight','bold');
end
```

FALSE NEAREST NEIGHBOUR (FNN)

```matlab
function out = false_nearest(signal,mindim,maxdim,tau,rt,eps0)
%Determines the fraction of false nearest neighbors.
%signal: input time series
%mindim - minimal dimension of the delay vectors     1
%maxdim - maximal dimension of the delay vectors     5
%tau - delay of the vectors      1
%rt - ratio factor   10.0

if nargin<2 | isempty(mindim)
  mindim = 1;
end
if nargin<3 | isempty(maxdim)
  maxdim = 5;
end
if nargin<4 | isempty(tau)
  tau = 1;
end
if nargin<5 | isempty(rt)
  rt = 10;
end
if nargin<6 | isempty(eps0)
  eps0=1/200;
end

minimum = min(signal);
maximum = max(signal);
interval = maximum-minimum;
len = length(signal);
BOX = 1024;
ibox = BOX-1;
theiler = 0;
global aveps vareps variance box list toolarge

for i = 1:1:len
    signal(i) =(signal(i)- minimum)/interval;
end
av = mean(signal);
variance = std(signal);



out = zeros(maxdim,4);

for dim = mindim:maxdim
    epsilon=eps0;
    toolarge=0;
    alldone=0;
    donesofar=0;
    aveps=0.0;
    vareps=0.0;
```

```
    for i=1:len
      nearest(i)=0;
    end

    fprintf('Start for dimension=%d\n',dim);

    while (~alldone && (epsilon < 2*variance/rt))
        alldone=1;
        make_box(signal,len-1,dim,tau,epsilon);
        for i=(dim-1)*tau+1:(len-1)
            if (~nearest(i))
nearest(i)=find_nearest(i,dim,tau,epsilon,signal,rt,theiler);
                alldone = bitand(alldone,nearest(i));
                donesofar = donesofar+nearest(i);
            end
        end

        fprintf('Found %d up to
epsilon=%d\n',donesofar,epsilon*interval);

        epsilon=epsilon*sqrt(2.0);
        if (~donesofar)
            eps0=epsilon;
        end
    end
    if (donesofar == 0)
      fprintf('Not enough points found!\n');
      fnn = 0;
    else
        aveps = aveps*(1/donesofar);
        vareps = vareps*(1/donesofar);
        fnn = toolarge/donesofar;
    end

    out(dim,:) = [dim fnn aveps vareps];

end


function y = find_nearest(n,dim,tau,eps,signal,rt,theiler)
global aveps vareps variance box list toolarge

element=0;
which= -1;
dx=0;
maxdx=0;
mindx=1.1;
factor=0;
ibox=1023;

x=bitand(ceil(signal(n-(dim-1)*tau)/eps),ibox);
if x==0
    x=1;
end
y=bitand(ceil(signal(n)/eps),ibox);
if y==0
    y=1;
```
192

```
end

for x1=x-1:x+1
    if x1==0
        continue
    end
    x2= bitand(x1,ibox);
    for y1=y-1:y+1
        if y1==0
            continue
        end
        element = box(x2,bitand(y1,ibox));
        while (element ~= -1)
            if (abs(element-n) > theiler)
                maxdx=abs(signal(n)-signal(element));
                for i=1:dim
                    i1=(i-1)*tau;
                    dx = abs(signal(n-i1)-signal(element-i1));
                    if (dx > maxdx)
                        maxdx=dx;
                    end
                end
                if ((maxdx < mindx) && (maxdx > 0.0))
                    which = element;
                    mindx = maxdx;
                end
            end
            element = list(element);
        end
    end
end

if ((which ~= -1) && (mindx <= eps) && (mindx <= variance/rt))
    aveps = aveps+mindx;
    vareps = vareps+mindx*mindx;
    factor=abs(signal(n+1)-signal(which+1))/mindx;
    if (factor > rt)
      toolarge=toolarge+1;
    end
    y = 1;
else
    y = 0;
end


function make_box(ser,l,dim,del,eps)
global box list
bs=1024;
ib=bs-1;

box = -ones(bs,bs);

for i=(dim-1)*del+1:l
    x = bitand(ceil(ser(i-(dim-1)*del)/eps),ib);
    if x==0
        x=1;
    end
```
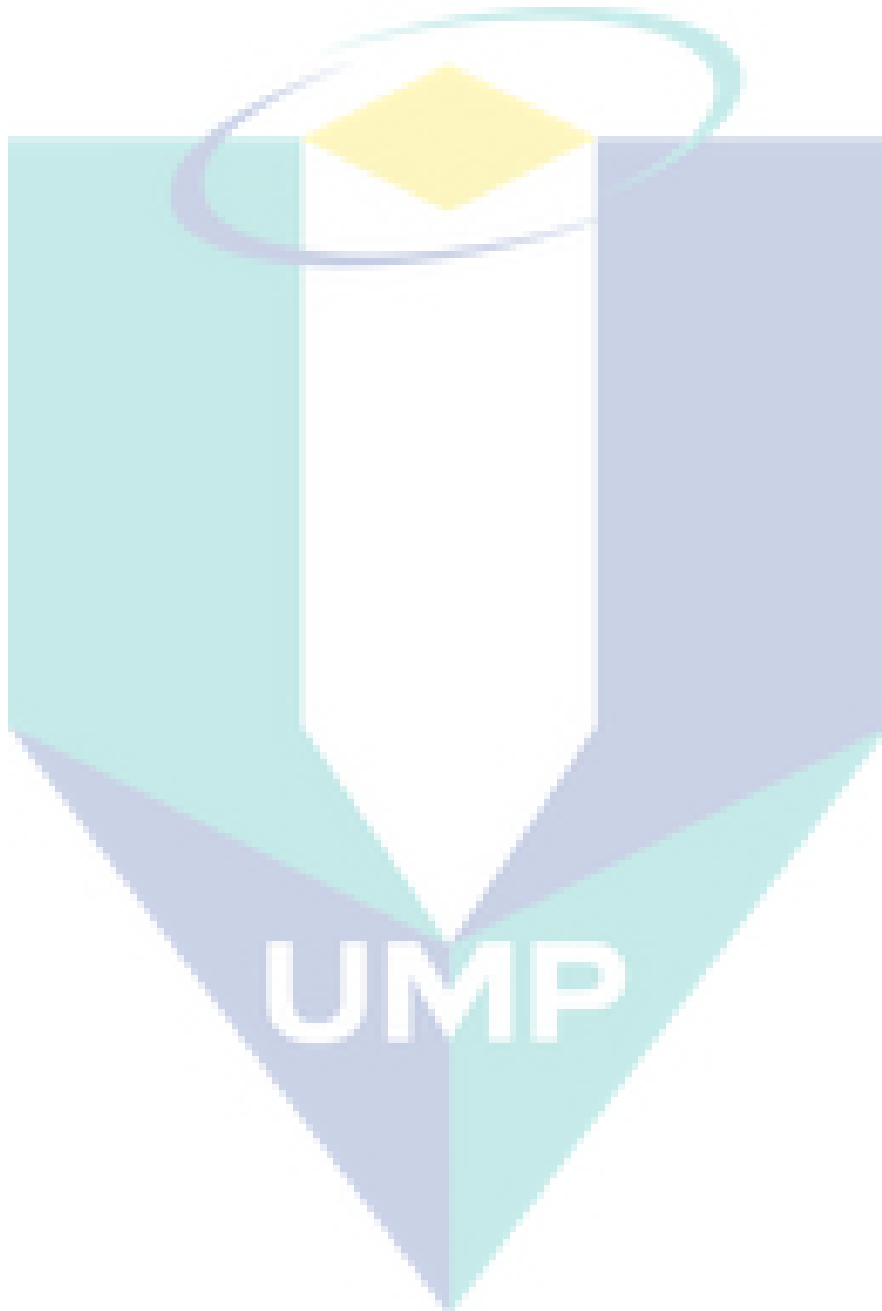
```
        y = bitand(ceil(ser(i)/eps),ib);
        if y==0
            y=1;
        end
        list(i)=box(x,y);
        box(x,y)=i;
end
```

APPENDIX D

FILTER SIGNAL

```
function filtersignal = fftfilter(ori_signal,lowband,highband)
%This is a program for bandpass filtering using FFT
%ori_signal: input time series
%lowband: low band
%highband: high band

%Note: It will be better for the length of input time series to be 2
power


fs=1000;
passband(1) = lowband;
passband(2) = highband;


N = length(ori_signal);
y = fft(ori_signal);


lowicut = round(passband(1)*N/fs);
lowmirror = N-lowicut+2;


highicut =  round(passband(2)*N/fs);
highmirror = N-highicut+2;


y([1:(lowicut-1) (lowmirror+1):end])=0;
y((highicut+1):(highmirror-1))=0;


filtersignal = ifft(y);
```

APPENDIX E

MUTUAL

```
function mi = mutual(signal,partitions,tau)
%Estimates the time delayed mutual information of the data set

%input: signal - input time series
%input: partitions - number of boxes for the partition
%input: tau - maximal time delay
%output: mi - mutual information from 0 to tau

av = mean(signal);
variance = var(signal);
minimum = min(signal);
maximum = max(signal);
interval = maximum-minimum;
len = length(signal);

if nargin<2 | isempty(partitions)
  partitions = 16;
end
if nargin<3 | isempty(tau)
  tau = 20;
end

for i = 1:1:len
    signal(i) =(signal(i)- minimum)/interval;
end

for i = 1:1:len
    if signal(i) > 0
        array(i) = ceil(signal(i)*partitions);
    else
        array(i) = 1;
    end
end

shannon = make_cond_entropy(0,array,len,partitions);

if (tau >= len)
    tau=len-1;
end

for i = 0:1:tau
    mi(i+1) = make_cond_entropy(i,array,len,partitions);
end


if nargout == 0
    figure('Position',[50 100 150 200]);
    plot(0:1:tau,mi,'o-','MarkerSize',5);
```

196

```matlab
    title('Mutual Information Test (first local
minimum)','FontName','Times New
Roman','FontSize',20,'FontWeight','bold');
    xlabel('Delay (sampling time)','FontName','Times New
Roman','FontSize',20,'FontWeight','bold');
    ylabel('Mutual Information','FontName','Times New
Roman','FontSize',20,'FontWeight','bold');
    get(gcf,'CurrentAxes');
    set(gca,'FontName','Times New
Roman','FontSize',20,'FontWeight','bold');
    grid on;
end


function mi = make_cond_entropy(t,array,len,partitions)

hi=0;
hii=0;
count=0;
hpi=0;
hpj=0;
pij=0;
cond_ent=0.0;


h2 = zeros(partitions,partitions);

for i = 1:1:partitions
    h1(i)=0;
    h11(i)=0;
end

for i=1:1:len
    if i > t
        hii = array(i);
        hi = array(i-t);
        h1(hi) = h1(hi)+1;
        h11(hii) = h11(hii)+1;
        h2(hi,hii) = h2(hi,hii)+1;
        count = count+1;
    end
end

norm=1.0/double(count);
cond_ent=0.0;

for i=1:1:partitions
    hpi = double(h1(i))*norm;
    if hpi > 0.0
        for j = 1:1:partitions
            hpj = double(h11(j))*norm;
            if hpj > 0.0
                pij = double(h2(i,j))*norm;
                if (pij > 0.0)
                    cond_ent = cond_ent + pij*log(pij/hpj/hpi);
                end
            end
        end
    end
```
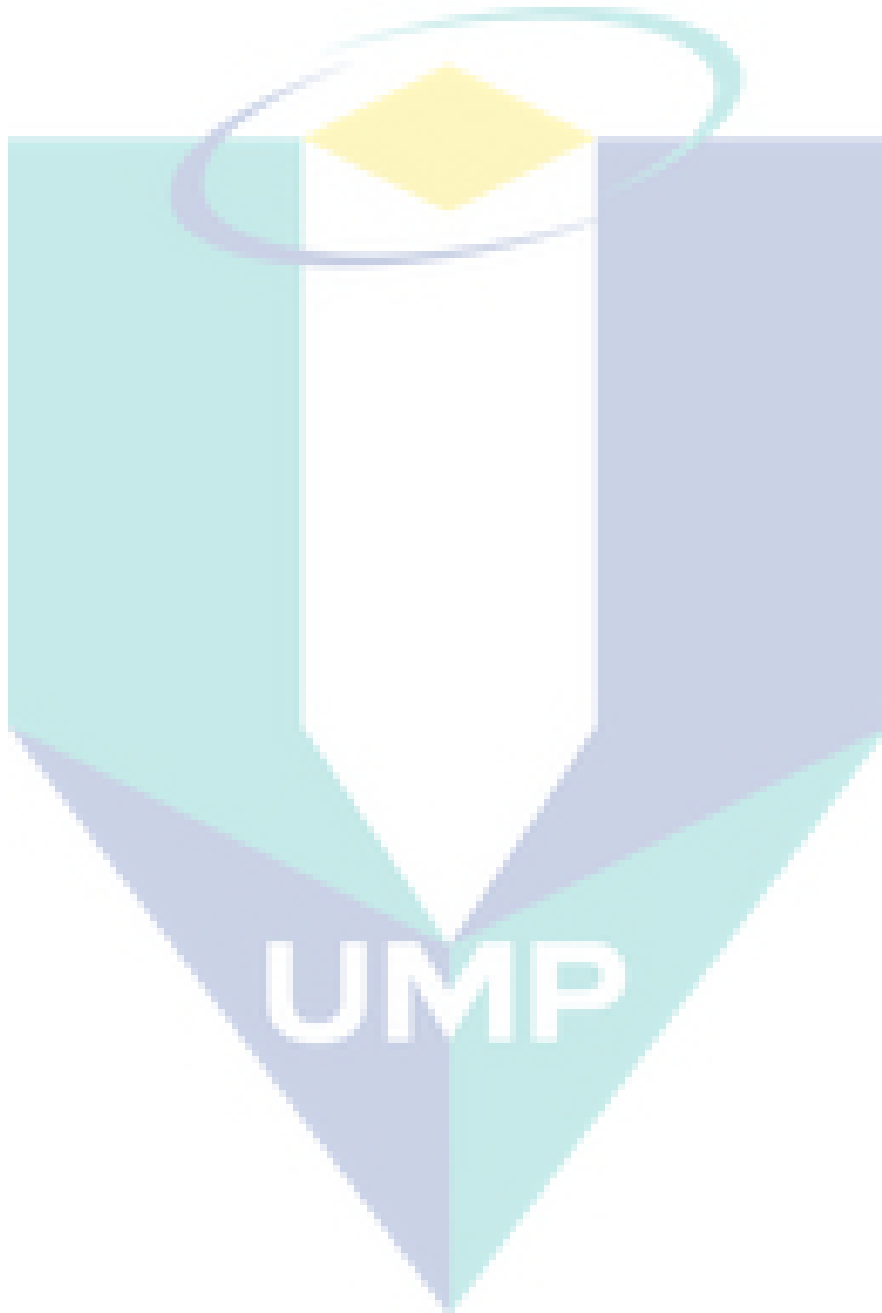
```
end

mi = cond_ent;
```

APPENDIX F

PHASE SPACE

```matlab
function [ Y ] = phasespace(signal,dim,tau)
%signal: input time series
%tau: time delay
%Y: delay embedding matrix(T*dim)

N = length(signal);
% Total points on phase space
T=N-(dim-1)*tau;
% Initialize the phase space
Y=zeros(T,dim);

for i=1:T
    Y(i,:)= signal(i+(dim-1)*tau-sort((0:dim-1),'descend')*tau)';
end


sizeY=size(Y,2);


if nargout == 0
    if sizeY == 2
        plot(Y(:,1),Y(:,2));
        xlabel('y1','FontName','Times New
Roman','FontSize',20,'FontWeight','bold');
        ylabel('y2','FontName','Times New
Roman','FontSize',20,'FontWeight','bold');
        get(gcf,'CurrentAxes');
        set(gca,'FontName','Times New
Roman','FontSize',20,'FontWeight','bold');
        grid on;
    else
        plot3(Y(:,1),Y(:,2),Y(:,3));
        xlabel('y1','FontName','Times New
Roman','FontSize',20,'FontWeight','bold');
        ylabel('y2','FontName','Times New
Roman','FontSize',20,'FontWeight','bold');
        zlabel('y3','FontName','Times New
Roman','FontSize',20,'FontWeight','bold');
        get(gcf,'CurrentAxes');
        set(gca,'FontName','Times New
Roman','FontSize',20,'FontWeight','bold');
        grid on;
    end
end
```

RQA STAT

```
function rqa_stat = recurrqa_y(recurrpt,linepara)
% This program calculate the RQA statistics for a recurrence plot.
% input:
% recurrpt - recurrence point matrix D(xi,xj)- N by 2 matrix
% For e.g, it should be:
% 1 1
% 1 2
% 1 10
% 1 80
% 6 9
% ...
% linepara - the minimal limit of vert and Horzt line pattern, default
= 2
% output:
% rqa_stat - RQA statistics - [recrate DET LMAX ENT TND LAM TT];


if nargin<2 || isempty(linepara)
    linepara = 2;
end

W=max(recurrpt(:,1));
matrixsize=size(recurrpt);
if matrixsize(2)~=2
    fprintf('Please provide the right recurrence point matrix! Thank
you!');
end

ptdiff = diff(recurrpt,1,2);
indices = find(ptdiff);
duprecurr = recurrpt(indices,:);
recurrpt = duprecurr;
clear duprecurr;

if isempty(recurrpt)
    rqa_stat = zeros(1,6);
else
    recrate=100*length(recurrpt)/(W*(W-1)/2);
    recurrpt = sortrows(recurrpt,1);
    recurrpt = horzcat(recurrpt,recurrpt(:,2)-recurrpt(:,1));
    recurrpt = sortrows(recurrpt,3);

    %%%%%%%%%%%%%%%%%%%%%%%%%%%%%%%%%%%%%%
    % Horizorntal Line Structure Search
    %%%%%%%%%%%%%%%%%%%%%%%%%%%%%%%%%%%%%%
    k=1;
    j=1;
    [row,col]=size(recurrpt);
    for i=1:row-1
        if recurrpt(i,3)==recurrpt(i+1,3)
            s{k}(j)=recurrpt(i,1);
```

```matlab
            displace(k)=recurrpt(i,3);
            j=j+1;
            if i==length(recurrpt)-1
                s{k}(j)=recurrpt(i+1,1);
            end
        else
            s{k}(j)=recurrpt(i,1);
            j=1;
            k=k+1;
        end
end


k=1;
diag = [];
len=1;
for i=1:length(s)
    for j=1:length(s{i})-1
        if s{i}(j)+1==s{i}(j+1)
            len=len+1;
        else
            diag(k)=len;
            disp(k)=displace(i);
            k=k+1;
            len=1;
        end
        if j==length(s{i})-1
            diag(k)=len;
            disp(k)=displace(i);
            k=k+1;
            len=1;
        end
    end
end

%TND=(disp')\(diag');
if isempty(diag);diag = 0; end

%Entropy Calculation
diag=diag(find(diag>linepara));
vect = diag(:);
region = max(vect) - min(vect) + 1;
freq = hist (vect, region);
prob = freq / sum (freq);
nonz = prob (find (prob));
ENT = sum (nonz .* (-log2 (nonz)));


DET = 100*sum(diag)/length(recurrpt);
LMAX = max(diag);



%%%%%%%%%%%%%%%%%%%%%%%%%%%%%%%%%%%%%%
% Vertical Line Structure Search
%%%%%%%%%%%%%%%%%%%%%%%%%%%%%%%%%%%%%%
clear s;
recurrpt = sortrows(recurrpt,1);
k=1;
j=1;
for i=1:row-1
    if recurrpt(i,1)==recurrpt(i+1,1)
        s{k}(j)=recurrpt(i,2);
```

```
            j=j+1;
            if i==length(recurrpt)-1
                s{k}(j)=recurrpt(i+1,2);
            end
        else
            s{k}(j)=recurrpt(i,2);
            j=1;
            k=k+1;
        end
    end

    k=1;
    len=1;
    vert = [];
    for i=1:length(s)
        for j=1:length(s{i})-1
            if s{i}(j)+1==s{i}(j+1)
                len=len+1;
            else
                vert(k)=len;
                k=k+1;
                len=1;
            end
            if j==length(s{i})-1
                vert(k)=len;
                k=k+1;
                len=1;
            end
        end
    end
    if isempty(vert); vert = 0; end

    vert=vert(find(vert>linepara));
    LAM = 100*sum(vert)/length(recurrpt);
    TT = mean(vert);

    if isempty(DET)||isnan(DET);DET = 0; end
    if isempty(LMAX)||isnan(LMAX);LMAX = 0; end
    if isempty(ENT)||isnan(ENT);ENT = 0; end
    if isempty(LAM)||isnan(LAM);LAM = 0; end
    if isempty(TT)||isnan(TT);TT = 0; end

    rqa_stat=[recrate DET LMAX ENT LAM TT];
    %rqa_stat=[recrate DET LMAX ENT TND LAM TT];
end
```

APPENDIX H

RESCALE DATA

```
function [signal,interval] = rescale_data(signal)
% This program rescale the input signal in the [0,1] interval.
min_signal = min(signal);
max_signal = max(signal);
interval = max_signal-min_signal;
len = length(signal);
if interval~=0
    for i = 1:1:len
        signal(i) =(signal(i)- min_signal)/interval;
    end
else
    fprintf('rescale_data: data interval is zero. It makes no sense to
continue. Exiting!');
end
```

APPENDIX I

THRESHOLD RECURRENCE PLOT

```
function x = tdrecurr_y(cbuffer,thrhd)
%This program produces a threshold recurrence plot of the, possibly
multivariate,
%data set. That means, for each point in the data set it looks for all
%points, such that the distance between these two points is smaller
%than a given size in a given embedding space.
%
%input:
%cbuffer: the recurrence matrix
%thrhd: threshold value for the recurrence matrix
%
%output:
%x - Vector containing the coordinate of recurrence points.

[m,n] = size(cbuffer);
[i,j] = find(cbuffer<=thrhd);
x=[i j];

if nargout == 0
    figure('Position',[100 400 460 360]);
    plot(x(:,1),x(:,2),'k.','MarkerSize',3);
    xlim([0,m]);
    ylim([0,n]);
    xlabel('i','FontName','Times New
Roman','FontSize',20,'FontWeight','bold');
    ylabel('j','FontName','Times New
Roman','FontSize',20,'FontWeight','bold');
    title('Recurrence Plot','FontName','Times New
Roman','FontSize',20,'FontWeight','bold');
    get(gcf,'CurrentAxes');
    set(gca,'LineWidth',2,'FontName','Times New
Roman','FontSize',20,'FontWeight','bold');
    %grid on;
en
```